Temperature Sensitive Hydrogels
for Protein Delivery
and Tissue Engineering

Roberta Censi

2010

Temperature Sensitive Hydrogels for Protein Delivery and Tissue Engineering

Temperatuurgevoelige Hydrogelen voor Eiwitafgifte en Tissue-Engineering
(met een samenvatting in het Nederlands)

Idrogeli Sensibili alla Temperatura per il Rilascio di Proteine e l'Ingegneria Tissutale
(con un riassunto in Italiano)

Proefschrift

ter verkrijging van de graad van doctor aan de Universiteit Utrecht op gezag van de rector magnificus, prof.dr. J.C. Stoof, ingevolge het besluit van het college voor promoties in het openbaar te verdedigen op
maandag 22 november 2010 des middags te 2.30 uur

door

Roberta Censi

geboren op 7 april 1980, Fermo, Italië

Promotoren: Prof. dr. ir. W. E. Hennink
Prof. dr. P. Di Martino

Co-promotoren: Dr. ir. T. Vermonden
Dr. C. F. van Nostrum

The ambitious climbs high and perilous stairs
and never cares how to come down;
the desire of rising
hath swallowed up his fear of a fall.

Thomas Adams

Alla mia famiglia ed a Romano

Table of Contents

Chapter 1

General Introduction

1.1 Biomaterials in medicine

Biomaterials are referred to as any substance (other than a drug) or combination of substances, synthetic or natural in origin, which can be used for any period of time, as a whole or as a part of a system which treats, augments, or replaces any tissue, organ, or function of the body (National Institutes of Health (NIH)). Their use allowed progress in diagnostic methods as well as in the regeneration of diseased tissues and organs and in the delivery of active ingredients to the right place at the right time and dose.(1-3)

Biomaterials comprise polymers, ceramics, composites and metals and have been used for many years in medical applications. It is estimated that over 40.000 pharmaceutical formulations, 8.000 medical devices and 2.500 diagnostic products that employ biomaterials are in current clinical practice.(1) In spite of their widespread use in medicine, many biomaterials lack some required properties to be used in biological systems and consequently their properties have to be further optimized to match the therapeutic need of the patients. Particularly, hydrophilic polymers in the form of cross-linked networks, known as hydrogels, are a class of biomaterials that have demonstrated great potential for pharmaceutical and biomedical applications.(4)

1.2 Hydrogels

Hydrogels are water-swollen polymeric materials able to maintain a distinct three-dimensional structure.(5-6) They were the first biomaterials designed for clinical use in the early 1950s, when Otto Wichterle and Drahoslav Lím initiated a research program aimed to the development of hydrogels for soft contact lenses.(7) The fortunate use of hydrogels in ophthalmology, which translated, besides contact lenses, also in glaucoma microcapillary drains (8) and fillings for the restoration of detached retina,(9) was the driving force towards the exploration of many other biomedical applications. Indeed, hydrogels extended their use to coverings for perforated ear drums,(10) implants for plastic surgery,(11) drug delivery depots,(12-15) etc. Amazingly, after 60 years, hydrogels are still inspiring the scientific community and progress in this field has moved forward at an impressive pace. Nowadays, novel synthetic methods for the design of gel-forming polymers and molecular biology have encompassed traditional chemical methods, resulting in self-assembling and environmentally sensitive hydrogels with controlled degradability and mechanical properties. Hydrogels have been applied, in addition to traditional areas, also to the delivery of biotechnologically derived drugs (proteins and peptides), tissue engineering, microfluidics and nanotechnology.

The success of hydrogels originates from their well known biocompatibility mainly due to their high water content and soft nature. These properties render hydrogels similar to biological tissues and consequently minimize cell adherence and inflammation once injected or implanted in the body.(16-21) Furthermore, their water absorbing capacity facilitates the accommodation of cells or hydrophilic molecules such as protein and peptides within the polymeric network.(22-25)

In order to ensure the clinical successes of hydrogels, several requirements, overviewed in **Figure 1**, need to be fulfilled. Besides biocompatibility, the biomaterial must be biodegradable (via chemical or enzymatic pathways), meaning that the hydrogel, after having served its biomedical function, is expected to degrade into soluble biocompatible products that can be metabolized and/or eliminated via renal filtration. In this way, surgical removal of the gel can be avoided. Additionally, ease of production and formulation, stability of the polymer and of the encapsulated drug, cytocompatibility, efficacy and flexibility, and minimally invasive administration are desirable characteristics (Figure 1).
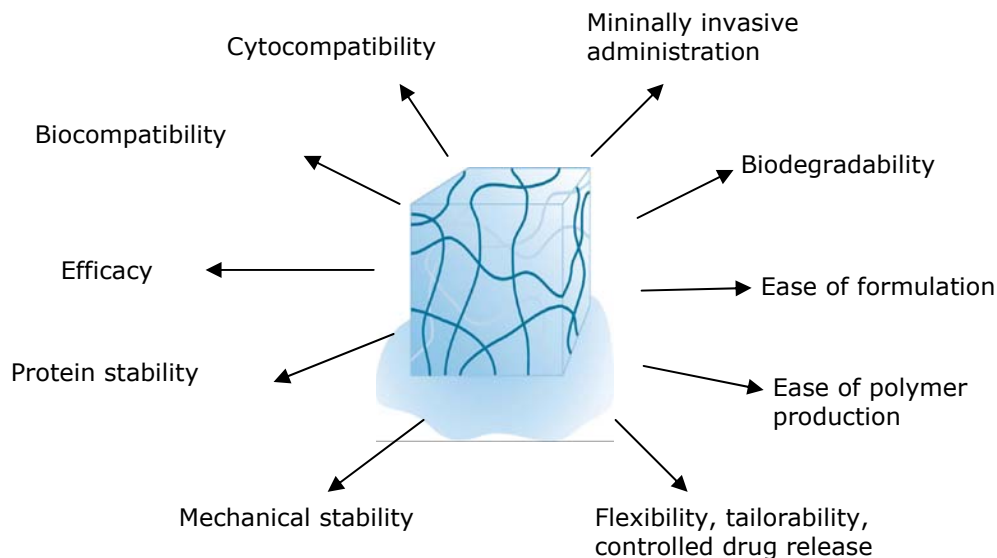
Figure1. Overview of the ideal characteristics of a hydrogel for biomedical and pharmaceutical applications

1.2.1   Polymers for the design of hydrogels

1.2.1a   Polymer architectures

Hydrogels are composed of polymers with different architectures (block copolymers, branched polymers, multi-arm polymers), as depicted in **Figure 2**. Based on the polymer topology, a large variety of different assemblies can be generated and peculiar hydrogel properties, such as mesh size, mechanical strength etc. can be tailored by changing the polymer design and thus by the hierarchical polymer organization.
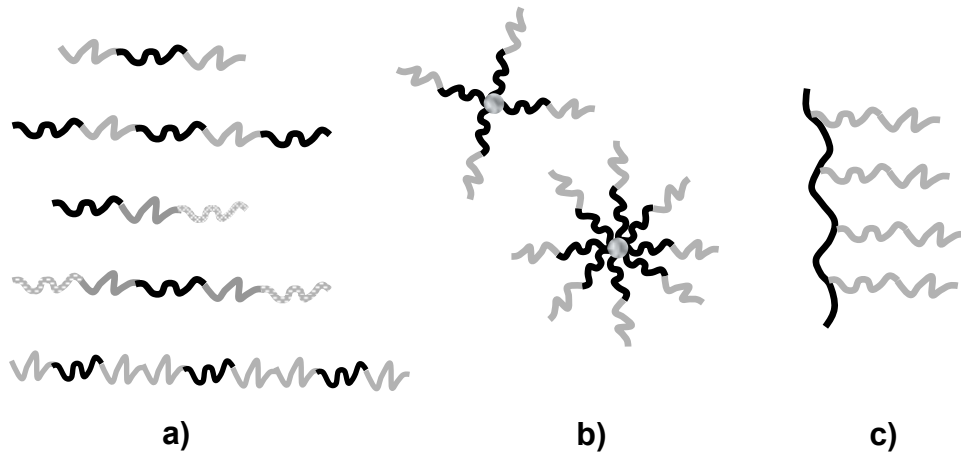
Figure 2. Macromolecular topologies of amphiphilic polymers capable to form self-assembled networks, a) linear block copolymers, b) star shape copolymers, c) graft copolymers.

1.2.1b   Natural, synthetic and hybrid hydrogels

Polymeric hydrogels can be based on natural or synthetic polymers as well as on combinations of these two. Examples of natural polymers are polysaccharides like hyaluronic acid, alginate, dextran, chitin/chitosan (26-35) and proteins like collagen, gelatin and fibrin.(36-39) Although natural polymers possess inherent biocompatibility, their use is also associated with a number of drawbacks, such as limitations in their production and purification from organisms, large batch-to-batch variation and contaminations that can possibly cause infections or immunogenicity. Moreover, their poor flexibility allows tailoring of the hydrogel properties only to a limited extent. With this respect synthetic polymers have distinct advantages. Examples of synthetic materials that have commonly been used to design hydrogels are poly(ethylene glycol) (PEG),(40) poly(2-hydroxypropyl methacrylamide) p(HPMAm),(41) poly(hydroxyethylmethacrylate) p(HEMA),(42) poly(vinyl alcohol) (PVA),(43) and poly((meth)acrylic acid) (p(M)AA).(44) **Figure 3** shows the chemical structures of the most commonly used synthetic and natural polymers.
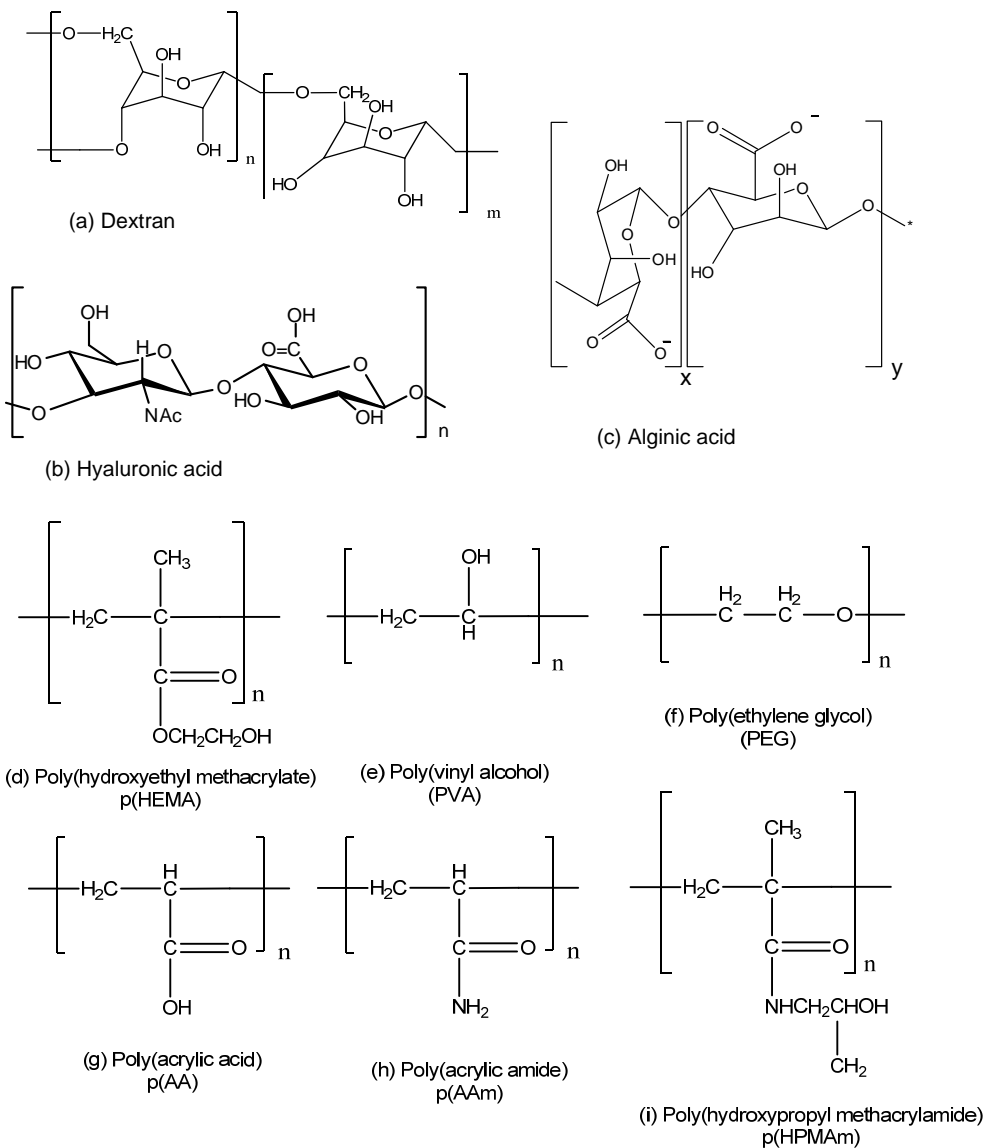
Figure 3. Chemical structures of natural ((a), (b) and (c)) and synthetic polymers ((d), (e), (f), (g), (h) and (i))

Of all synthetic polymers, PEG has gained the most interest in the biomedical field due to its appealing properties. PEG is a highly hydrophilic, biocompatible and low immunogenic polymer, it has protein-resistant properties,(19, 45-46) and is excreted up to a molecular weight of 50 kDa by the kidneys.(47) A number of PEG-based pharmaceutical products has been approved by the American Food and Drug Administration (FDA).(5) PEG lends itself to a

broad range of chemical modifications for the preparation of cross-linked polymeric networks in aqueous medium.(48) For instance, PEG functionalized with cyclodextrins or cholesterol has been used for the formation of supramolecularly self-assembled hydrogels for protein release applications.(40) Similarly, PEG has been used as building bock for the synthesis of copolymers with biodegradable aliphatic polyesters, such as polylactide (PLA),(49) poly(D,L-lactide-*co*-glycolide) (PLGA),(50) poly(ε-caprolactone) (PCL),(51) or polyphosphazenes.(52) Thermosensitive triblock copolymers of PEG and p(HPMAm) derivatives have been likewise designed for the preparation of injectable hydrogels.(53) P(HPMAm) is another hydrophilic and biocompatible synthetic polymer, currently under evaluation in a number of clinical trials, that has been used from the early 1970s to date in numerous applications, ranging from drug-polymer conjugates for cancer therapy to copolymers for network formation.(54)

Finally, hybrid hydrogels are composed of natural and synthetic polymers in an effort to exploit the advantageous properties of both systems.

1.2.2   Cross-linking methods

The above described (natural or synthetic) polymers share their high affinity for water and in order to prevent their dissolution in this medium they have to be crosslinked by either physical and/or chemical methods, yielding hydrogels.(55-56) Physical cross-linking relies on non-permanent reversible bonds based on hydrophobic interactions,(57-58) hydrogen bonding,(59) stereocomplexation,(60) inclusion complexation (61) or ionic interactions.(62) Thermosensitive polymers have been widely used for the preparation of physical hydrogels assembled by hydrophobic interaction between polymer chains at body temperature. Physical cross-linking is particularly appealing for biomedical applications as it allows minimally invasive administration of the hydrogel, which is formed *in situ* upon injection. However, a general drawback of physical hydrogels is their limited stability, and therefore, when mechanical strength and long-term stability are required, chemically cross-linking methods are preferred.

Chemical cross-linking leads to permanent covalent bonds that can be accomplished by a wide variety of chemical reactions, like e.g. radical polymerization,(23, 63-64) enzyme mediated polymerization,(65) click chemistry,(66-68) and Michael addition,(69-78).

Some of these covalent cross-linking methods can be used for the design of *in situ* gelling systems. To this end, the absence of leachable toxic compounds possibly needed for the polymerization is a strict requisite. The combination of physical and chemical cross-linking has been often applied for the preparation of hydrogels. Dual cross-linking comprises immediate physical gelation upon administration and subsequent structural stabilization of the hydrogel by covalent bonding. In this way, the initial physical gelation at the site of injection avoids premature dissolution of the hydrogel and the subsequent chemical cross-linking confers

stability to the network. Michael addition and photopolymerization are examples of chemical cross-linking reactions suitable for *in situ* gelation.(23, 78)

1.2.3 Thermo-gelling hydrogels

Thermosensitive polymers belong to the class of stimuli-responsive materials, also known as "smart", "intelligent" or "environmentally sensitive".(6, 79-80) Thermo-responsive polymers exhibit differences in solubility in aqueous medium in response to temperature changes. The temperature at which they undergo this transition is commonly referred to as the lower critical solution temperature (LCST). Below the LCST, the polymers are soluble in aqueous medium, whereas above the LCST, they are insoluble, due to hydrophobic interactions between the polymer chains. When thermosensitive and permanently hydrophilic polymers are combined (in form of block or graft copolymers), they are able to self-assemble above their LCST, forming a hydrogel structure. Polymers with LCST between room and body temperature can be used for the preparation of injectable hydrogels. In **Figure 4** the self-assembly mechanism of a thermosensitive triblock copolymer is depicted.

1.2.4 Photopolymerization

Photopolymerization is a type of radical polymerization that allows the formation of chemical cross-links between (meth)acrylate ((M)AA) bearing polymer chains. This type of reaction is initiated by a photoinitiator that decomposes and generates radicals in response to UV or visible light. A number of photoinitiators is available, with Irgacure 2959 being the most widely used for biomedical applications, as it has been demonstrated to be biocompatible at low dosage.(81) Photopolymerization is suitable for *in situ* gel formation as, potentially, it can be implemented by means of laparoscopy or transdermal illumination in case of subcutaneously injected depot systems.(81-82) The photocuring process is fast, taking usually only seconds to minutes to complete, can be conducted at room or body temperature without the use of organic solvents and offers the advantage of spatial and temporal control.(42, 83-84) Photopolymerization has been applied for the chemical cross-linking of degradable hydrogels, used for both tissue engineering and protein delivery applications.(85-86) Hubbell *et al.* were the first to introduce the use of *in situ* photopolymerizable hydrogels. The polymer they used was composed of a PEG middle block, flanked with acrylate modified oligo(α-hydroxy acids).(87) The systems showed rapid hydrogel formation upon irradiation with visible light in the presence of a suitable photoinitiator. This stable photopolymerized hydrogel, used as drug delivery depot, released a model protein, bovine serum albumin (BSA), for up to two months and, in tissue engineering application, it was effective in preventing scar adhesion formation after pelvic surgery in animal models.(85, 87) Additionally, it was shown that these gels did prevent surface-induced thrombosis and

reduced long-term intimal thickening when applied as a mechanical barrier on severely injured arteries.(88)
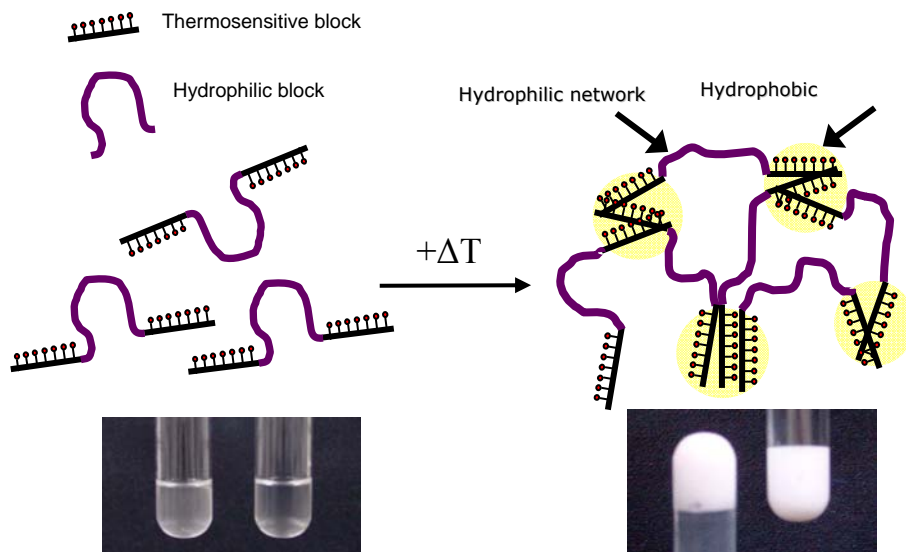
Figure 4. Self-assembly of a thermosensitive linear triblock copolymer composed of two outer thermosensitive blocks and an inner hydrophilic block yielding in the formation of a hydrogel above the LCST of the thermosensitive block.

This seminal work inspired other scientists, who developed a variety of other photopolymerizable polymers, such as (meth)acrylated linear and multi-arm PEGs,(89) methacrylated dextrans,(90) methacrylated dextran-hydroxyethyl methacrylate (dex-HEMA),(91) methacrylated eight-arm PEG-poly(lactic acid) (PEG-PLA) star block copolymers.(92)

1.2.5   Michael addition reaction

The Michael addition reaction is a versatile synthetic methodology for the efficient coupling of electron poor olefins (e.g. acrylates) with a vast array of nucleophiles (e.g. amines, thiols) and is a widely applied synthetic method for the preparation of polymeric networks for multiple applications.(93-94) The main reasons for its wide applicability are the possibility to use this cross-linking method for *in-situ* gel formation and the existence of commercially available functional oligomers including PEG diacrylates and numerous oligomeric diamines such as Jeffamine®. Michael addition reaction occurs at physiological conditions without the need for (toxic) catalysts.(69, 95-97) Because of this advantageous property, Michael addition reaction has been successfully applied for the

preparation of a number of hydrogels for biomedical applications,(69-74, 76-77) reviewed by Mather *et al*. (98) To give an example, Hubbell *et al*. studied protein drug delivery using Michael addition hydrogel networks from eight-arm PEG octaacrylate with dithiothreitol.(99) The protein drug human growth hormone (hGH), which suffers from rapid clearance, was entrapped into these hydrogels. The crosslink density of the networks, which influenced the drug diffusion, was controlled by the use of different molecular weights of PEG octaacrylate.

1.3   Applications of hydrogels

1.3.1   Protein delivery

Advances in molecular biology and biotechnology have resulted in the mass production of protein therapeutics. However, several obstacles remain before these compounds can be turned into medicines capable for the treatment of patients. The challenge of releasing these drugs at the right time, at the right site and in the right dose, can be potentially faced by advanced drug delivery systems like hydrogels.

The added value of hydrogels for protein delivery is improved safety, efficacy, convenience, and patient compliance. The rationale behind the use of hydrogels as drug delivery systems is that they can be administered in a minimally invasive manner, the encapsulated protein is released in a controlled fashion over an extended period of time, while remaining protected from rapid clearance due to enzymatic and/or chemical degradation (**Figure 5**). In this way, both the drug dosage and the number of administrations are decreased.
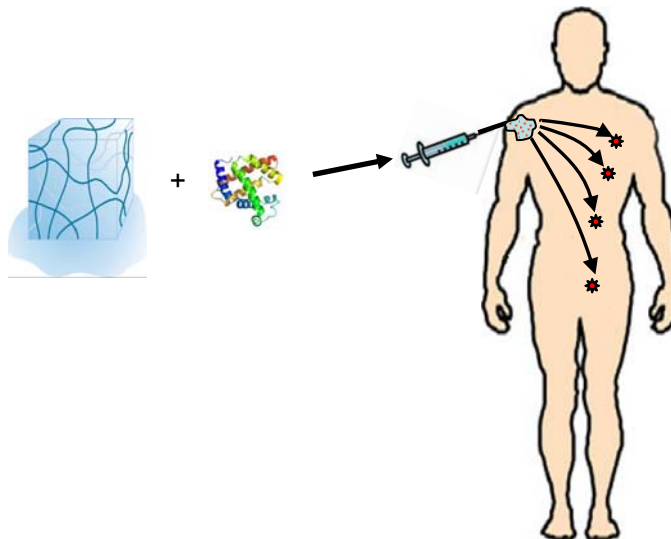

Figure 5. Schematic of the concept of controlled protein delivery using injectable hydrogel

1.3.2   Tissue engineering

The field of tissue engineering started to develop 15-20 years in response to the ever-increasing need for donor organs and tissues.Tissue engineering involves the regeneration of artificial organs or tissues using three dimensional matrices, referred to as scaffolds, in combination with cells and biologically active compounds (i.e. growth factors). The matrices used for engineering of soft tissues are mostly based on hydrogels, because their porosity and natural tissue resemblance make these three-dimensional networks an amenable environment for cells survival and differentiation. Moreover, the hydrogel diffusivity enhances the exchange of nutrients and the elimination of cell metabolites.(86, 100-102)

By tissue engineering, ideally, patient-derived cells can be cultured *in vitro*, mixed with hydrogel matrix to form a three-dimensional scaffold, fabricated by simple molding technique or more advanced bioprinting procedures (see section 3.2.1).(103-105) The obtained graft is subsequently implanted in the body, where the biomaterial is expected to support cell survival and differentiation and, in time, when new tissue is formed, to gradually degrade into biocompatible products that can be metabolized or eliminated from the body by renal filtration (**Figure 6**). The use of synthetic polymers for the preparation of hydrogels for tissue engineering offers the possibility to functionalize them by appropriate chemistry with peptide sequences that can improve interaction with cells. Several hydrogels have been derivatized with adhesive peptides, such as RGD sequences to promote cell adhesion.(106-109)
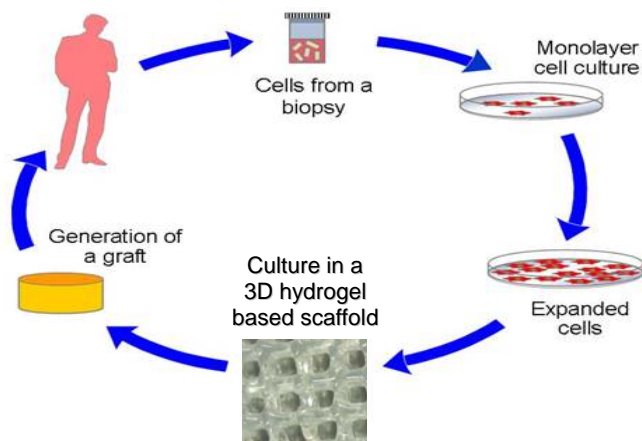
Figure 6. Schematic of the basic principles of tissue engineering by using hydrogels as extracellular matrix.

1.3.2a   Bioprinting

At present, scientists within the field of tissue regeneration are exploring novel and potential routes towards enhanced clinical outcomes of artificially engineered organs. Most tissues, such as bone, skin, liver, cartilage, exhibit a precise hierarchical cellular organization that highly influences the tissue functionality. Replicating the native structure in an artificial graft is of crucial importance for the restoration of tissue functions and represents the challenge tissue engineering is currently facing. A novel strategy to achieve this goal relies on bioprinting, a scaffold preparation technique based on computer aided layer-by-layer three-dimensional fiber deposition of cell-laden hydrogels **(Figure 7)**.(110-113) This rapid prototyping-derived technique allows the preparation of complex three dimensional scaffolds with biomimetical cell organization. Moreover, as compared to solid scaffolds, the highly porous micro/macroenvironment of bioprinted scaffolds is extremely beneficial for cell survival and differentiation, as metabolites, nutrients and oxygen diffusion can be accomplished.(114-118)
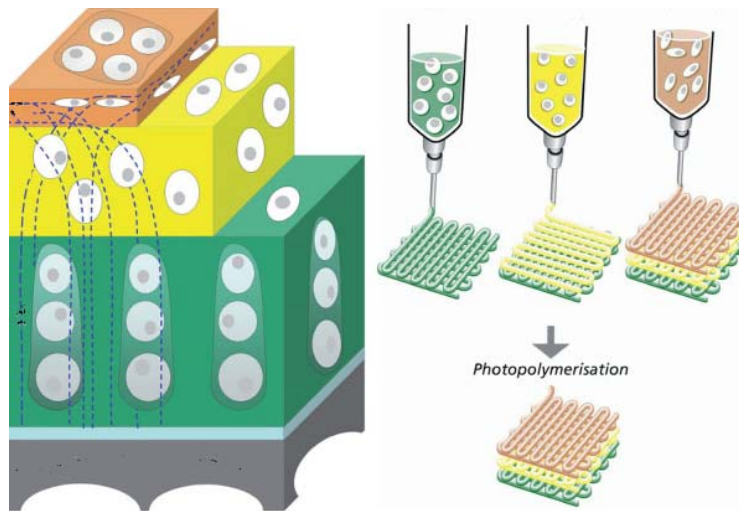
Figure 7. Schematic representation of a bioprinting technique procedure. Hydrogels can be loaded with different cell types and extruded according to a computer designed porous pattern. Hydrogel fibers are deposited to form a three-dimensional scaffold that recapitulates the physiological cell placement. Adapted from ref. (110)

1.4   Aim of the thesis

The aim of this thesis was to investigate the potential use of a novel biodegradable thermosensitive hydrogel, based on a triblock copolymer of (meth)acrylated poly(*N*-(2-hydroxypropyl) methacrylamide lactate) and poly(ethylene glycol); (p(HPMAm-lac)-PEG-p(HPMAm-lac)) (**Figure 8b**), as controlled protein delivery system and synthetic extracellular matrix for tissue engineering. P(HPMAm-lac) represents a novel class of biodegradable thermosensitive polymers, exhibiting LCST between room and body temperature, obtained by coupling lactate side chains to p(HPMAm) (**Figure 8a**).(41) By synthesizing an ABA architecture, where p(HPMAm-lac) are the thermosensitive A-blocks and PEG is the permanently hydrophilic B-block, a hydrogel is formed in response to a temperature change.(53) This visco-elastic network can be stabilized by additional chemical cross-links (i.e. by photopolymerization or Michael addition, see sections 1.2.4. and 1.2.5.) upon derivatization of the lactate side chains with (meth)acrylate groups, which form the central theme of this thesis (**Figure 8b**).(22)
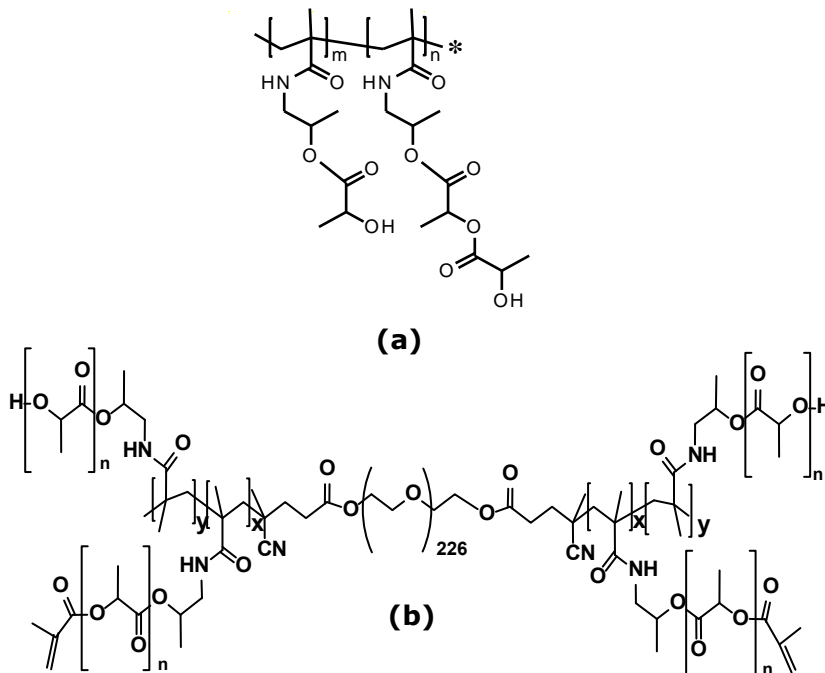
Figure 8.   Chemical structures of (a) p(HPMAm-lac) and (b) methacrylated p(HPMAm-lac)-PEG-p(HPMAm-lac)

In our approach an injectable hydrogel is prepared by thermo-gelling at 37 °C, and subsequently the structure of this physical three-dimensional network is stabilized by additional chemical cross-linking, that is implemented by means of photopolymerization or Michael addition with thiolated hyaluronic acid. Cells or proteins are mixed with the matrix prior to chemical cross-linking.

We aimed to evaluate whether proteins can be encapsulated in the hydrogel matrix and released in a controlled and tailorable fashion, retaining their native structure and biological activity. Additionally, different types of chemical cross-linking and the possibility to fine-tune the molecular design of the polymer in order to achieve modular mechanical, degradation and protein release behavior were explored. The potential of these hydrogels as bioprinted scaffolds for the regeneration of cartilage was also assessed. Finally, some insight into the hydrogel biocompatibility *in vivo* is provided.

1.5   Outline of the thesis

Chapter 2 gives a literature overview of currently developed hydrogel matrices for protein delivery. The general challenges towards protein delivery and the most relevant hydrogel systems designed to overcome them are reviewed and discussed. Particular emphasis is paid to biodegradable and injectable polymers. Release mechanisms are highlighted and possibilities for improvements are suggested.

Chapter 3 reports on the mechanical characterization, degradation and protein release behavior of photopolymerized thermosensitive hydrogels. Three model proteins are used (lysozyme, bovine serum albumin, immunoglobulin G) and their release mechanism is investigated. Assessment of protein stability, through the analysis of lysozyme secondary structure and biological activity is also studied.

Chapter 4 describes the possibility to fine-tune the macromolecular design of the photopolymerizable thermosensitive polymer by precise chemical synthesis and aims to demonstrate how the structure of the polymer affects the mechanical properties, degradation behavior and release kinetics. The morphology of the hydrogels is studied by confocal laser scanning microscopy and Fluorescence Recovery After Photobleaching (FRAP) is used to investigate its diffusivity (Supporting information Chapter 4 in Appendix B).

Chapter 5 explores a different type of chemical cross-linking method, other than photopolymerization. Thiolated hyaluronic acid (HA-SH) is synthesized and combined with the methacrylate bearing thermosensitive polymer bringing together advantageous properties of synthetic and natural materials. Michael addition reaction, occurring between thiols on HA-SH and (meth)acrylate groups on p(HPMAm-lac)-PEG-p(HPMAm-lac), is used as tissue and protein friendly cross-linking method for *in-situ* formation of a depot system. Characterization of the Michael addition reaction kinetics, as well as rheological analysis, degradation profiles and peptide release behavior of the formed hydrogels are reported.

In **chapter 6** the use of photopolymerized thermosensitive hydrogels for tissue engineering is examined. The suitability of the hydrogel for bioprinting purposes is studied and characterization of the rheological properties of solid and printed porous scaffolds is provided. In an effort to evaluate whether these porous scaffolds are suitable for the regeneration of cartilage, their stability in physiological buffer and chondrocyte compatibility are assessed.

Chapter 7 deals with the hydrogel biocompatibility *in vivo*. The effect of the network characteristics, with respect to cross-link density on tissue response is studied after subcutaneous implantation of the photopolymerized depot systems in Balb/c mice. Moreover, the degradation *in vivo* of the implanted hydrogels is investigated and correlated to *in vitro* behavior.

Finally, **chapter 8** summarizes the major findings of this thesis and outlines the potential applications and the future perspectives of the studied thermosensitive polymers.

References

1.   Langer R & Peppas NA (2003) Advances in Biomaterials, Drug Delivery, and Bionanotechnology. *AIChE Journal* 49(12):2990-3006.

2.   Peppas NA & Langer R (1994) New Challenges in Biomaterials. *Science* 263(5154):1715-1720.

3.   Langer R (2000) Biomaterials: Status, challenges, and perspectives. *AIChE Journal* 46(7):1286-1289.

4.   Peppas NA ed (1987) *Hydrogels in Medicine and Pharmacy* Boca Raton, FL).

5.   Peppas NA, Hilt JZ, Khademhosseini A, & Langer R (2006) Hydrogels in biology and medicine: From molecular principles to bionanotechnology. *Advanced Materials* 18(11):1345-1360.

6.   Kopeček J & Yang J (2007) Hydrogels as smart biomaterials. *Polymer International* 56(9):1078-1098.

7.   Wichterle O & Lim D (1960) Hydrophilic Gels for Biological Use. *Nature* 185(4706):117-118.

8.   Krejci L, Harrison R, & Wichterle O (1970) Hydroxyethyl Methacrylate Capillary Strip: Animal Trials With a New Glaucoma Drainage Device. *Archives of Ophthalmology* 84(1):76-82.

9.   Křístek AK, B.; Wichterle, O. (1966) *Kl Abl Augenheilk (German)* 149:219-227.

10.   Hubáček JW, O.; Kliment, K.; Hubáček, Jar.; Dušek, J. (1968) *J. Československá otolaryngologie (Czech)* 17:211-215.

11.   Voldřrich Z, Tománek Z, Vacík J, & Kopečcek J (1975) Long-term experience with poly(glycol monomethacrylate) gel in plastic operations of the nose. *Journal of Biomedical Materials Research* 9(6):675-685.

12.   Zentner GM, Cardinal JR, & Kim SW (1978) Progestin permeation through polymer membranes I: Diffusion studies on plasma-soaked membranes. *Journal of Pharmaceutical Sciences* 67(10):1347-1351.

13.   Majkus V, Horáková Z, Výmola F, & Štol M (1969) Employment of hydron polymer antibiotic vehicle in otolaryngology. *Journal of Biomedical Materials Research* 3(3):443-454.

14.   Davis BK (1972) Control of diabetes with polyacrylamide implants containing insulin. *Cellular and Molecular Life Sciences* 28(3):348-348.

15.   Hosaka S, Ozawa H, & Tanzawa H (1979) Controlled release of drugs from hydrogel matrices. *Journal of Applied Polymer Science* 23(7):2089-2098.

16.   Anderson JM & Langone JJ (1999) Issues and perspectives on the biocompatibility and immunotoxicity evaluation of implanted controlled release systems. *Journal of Controlled Release* 57(2):107-113.

17.   Cadée JA, Luyn MJAv, Brouwer LA, Plantinga JA, Wachem PBv, Groot CJd, Otter Wd, & Hennink WE (2000) *In vivo* biocompatibility of dextran-based hydrogels. *Journal of Biomedical Materials Research* 50(3):397-404.

18.   Gilding D (1981) *"Biodegradable polymers,"* in *Biocompatibility of implant materials* (CRC Press, Boca Raton, FL).

19.   Lee JH, Kopecek J, & Andrade JD (1989) Protein-resistant surfaces prepared by PEO-containing block copolymer surfactants. *Journal of Biomedical Materials Research* 23(3):351-368.

20.   Jiskoot W, van Schie R, Carstens M, & Schellekens H (2009) Immunological Risk of Injectable Drug Delivery Systems. *Pharmaceutical Research* 26(6):1303-1314.

21.   Kopecek J & Sprincl L (1974) Relationship between the structure and biocompatibility of hydrophilic gels. *Polimery w medycynie* 4(2):109-117.

22.   Vermonden T, Fedorovich NE, van Geemen D, Alblas J, van Nostrum CF, Dhert WJA, & Hennink WE (2008) Photopolymerized Thermosensitive Hydrogels: Synthesis, Degradation, and Cytocompatibility. *Biomacromolecules* 9(3):919-926.

23.   Censi R, Vermonden T, van Steenbergen MJ, Deschout H, Braeckmans K, De Smedt SC, van Nostrum CF, di Martino P, & Hennink WE (2009) Photopolymerized thermosensitive hydrogels for tailorable diffusion-controlled protein delivery. *Journal of Controlled Release* 140(3):230-236.

24.   Frokjaer S & Otzen DE (2005) Protein drug stability: a formulation challenge. *Nature Reviews Drug Discovery* 4(4):298-306

25.   Lutolf MP (2009) Biomaterials: Spotlight on hydrogels. *Nature Materials* 8(6):451-453.

26.   Kessler MW & Grande DA (2008) Tissue engineering and cartilage. *Organogenesis* 4(1):28-32.

27.   Möller S, Weisser J, Bischoff S, & Schnabelrauch M (2007) Dextran and hyaluronan methacrylate based hydrogels as matrices for soft tissue reconstruction. *Biomolecular Engineering* 24(5):496-504.

28.   Pereira RC, Scaranari M, Castagnola P, Grandizio M, Azevedo HS, Reis RL, Cancedda R, & Gentili C (2009) Novel injectable gel (system) as a vehicle for human articular chondrocytes in cartilage tissue regeneration. *Journal of Tissue Engineering and Regenerative Medicine* 3(2):97-106.

29.   Stoddart M, Grad S, Eglin D, & Alini M (2009) Cells and biomaterials in cartilage tissue engineering. *Regenerative Medicine* 4(1):81-98.

30.   Suri S & Schmidt CE (2010) Cell-laden hydrogel constructs of hyaluronic acid, collagen, and laminin for neural tissue engineering. *Tissue Engineering - Part A* 16(5):1703-1716.

31.   Tan H, Chu CR, Payne KA, & Marra KG (2009) Injectable in situ forming biodegradable chitosan-hyaluronic acid based hydrogels for cartilage tissue engineering. *Biomaterials* 30(13):2499-2506.

32.   Toh WS, Lee EH, Guo XM, Chan JKY, Yeow CH, Choo AB, & Cao T (2010) Cartilage repair using hyaluronan hydrogel-encapsulated human embryonic stem cell-derived chondrogenic cells. *Biomaterials* 31(27):6968-6980.

33.   Vanderhooft JL, Alcoutlabi M, Magda JJ, & Prestwich GD (2009) Rheological properties of cross-linked hyaluronan-gelatin hydrogels for tissue engineering. *Macromolecular Bioscience* 9(1):20-28.

34.   Pescosolido L, Miatto S, Di Meo C, Cencetti C, Coviello T, Alhaique F, & Matricardi P (2010) Injectable and in situ gelling hydrogels for modified protein release. *European Biophysics Journal* 39(6):903-909.

35.   Augst AD, Kong HJ, & Mooney DJ (2006) Alginate hydrogels as biomaterials. *Macromolecular Bioscience* 6(8):623-633.

36.   Basavaraj KH, Navya MA, Johnsy G, Siddaramaiah, & Rashmi R (2010) Biopolymers as transdermal drug delivery systems in dermatology therapy. *Critical Reviews in Therapeutic Drug Carrier Systems* 27(2):155-185.

37.   Helary C, Bataille I, Abed A, Illoul C, Anglo A, Louedec L, Letourneur D, Meddahi-Pellé A, & Giraud-Guille MM (2010) Concentrated collagen hydrogels as dermal substitutes. *Biomaterials* 31(3):481-490.

38.   Hesse E, Hefferan TE, Tarara JE, Haasper C, Meller R, Krettek C, Lu L, & Yaszemski MJ (2010) Collagen type I hydrogel allows migration, proliferation, and osteogenic differentiation of rat bone marrow stromal cells. *Journal of Biomedical Materials Research - Part A* 94(2):442-449.

39.   Hunt NC & Grover LM (2010) Cell encapsulation using biopolymer gels for regenerative medicine. *Biotechnology Letters*:1-10.

40.   Van Manakker FD, Braeckmans K, Morabit NE, De Smedt SC, Van Nostrum CF, & Hennink WE (2009) Protein-release behavior of self-assembled PEG-ß-cyclodextrin/PEG- cholesterol hydrogels. *Advanced Functional Materials* 19(18):2992-3001.

41.   Soga O, van Nostrum CF, & Hennink WE (2004) Poly(N-(2-hydroxypropyl) Methacrylamide Mono/Di Lactate):â€‰ A New Class of Biodegradable Polymers with Tuneable Thermosensitivity. *Biomacromolecules* 5(3):818-821.

42.   Lu S & Anseth KS (1999) Photopolymerization of multilaminated poly(HEMA) hydrogels for controlled release. *Journal of Controlled Release* 57(3):291-300.

43.   Bourke S, Al-Khalili M, Briggs T, Michniak B, Kohn J, & Poole-Warren L (2003) A photo-crosslinked poly(vinyl alcohol) hydrogel growth factor release vehicle for wound healing applications. *AAPS Journal* 5(4):101-111.

44.   Serra L, Doménech J, & Peppas NA (2006) Drug transport mechanisms and release kinetics from molecularly designed poly(acrylic acid-g-ethylene glycol) hydrogels. *Biomaterials* 27(31):5440-5451.

45.   Drumheller PD & Hubbell JA (1995) Densely crosslinked polymer networks of poly(ethylene glycol) in trimethylolpropane triacrylate for cell-adhesion-resistant surfaces. *Journal of Biomedical Materials Research* 29(2):207-215.

24

46.   Du H, Chandaroy P, & Hui SW (1997) Grafted poly-(ethylene glycol) on lipid surfaces inhibits protein adsorption and cell adhesion. *Biochimica et Biophysica Acta (BBA) - Biomembranes* 1326(2):236-248.

47.   Yamaoka T, Tabata Y, & Ikada Y (1994) Distribution and tissue uptake of poly(ethylene glycol) with different molecular weights after intravenous administration to mice. *Journal of Pharmaceutical Sciences* 83(4):601-606.

48.   Lin CC & Anseth KS (2009) PEG hydrogels for the controlled release of biomolecules in regenerative medicine. *Pharmaceutical Research* 26(3):631-643.

49.   Jeong B, Bae YH, Lee DS, & Kim SW (1997) Biodegradable block copolymers as injectable drug-delivery systems. *Nature* 388(6645):860-862.

50.   Jeong B, Bae YH, & Kim SW (1999) Thermoreversible Gelation of PEG−PLGA−PEG Triblock Copolymer Aqueous Solutions. *Macromolecules* 32(21):7064-7069.

51.   Hyun H, Kim YH, Song IB, Lee JW, Kim MS, Khang G, Park K, & Lee HB (2007) In Vitro and in Vivo Release of Albumin Using a Biodegradable MPEG-PCL Diblock Copolymer as an in Situ Gel-Forming Carrier. *Biomacromolecules* 8(4):1093-1100.

52.   Lee BH & Song S-C (2004) Synthesis and Characterization of Biodegradable Thermosensitive Poly(organophosphazene) Gels. *Macromolecules* 37(12):4533-4537.

53.   Vermonden T, Besseling NAM, van Steenbergen MJ, & Hennink WE (2006) Rheological Studies of Thermosensitive Triblock Copolymer Hydrogels. *Langmuir* 22(24):10180-10184.

54.   Kopecek J & Kopecková P (2010) HPMA copolymers: Origins, early developments, present, and future. *Advanced Drug Delivery Reviews* 62(2):122-149.

55.   Van Tomme SR, Storm G, & Hennink WE (2008) In situ gelling hydrogels for pharmaceutical and biomedical applications. *International Journal of Pharmaceutics* 355(1-2):1-18.

56.   Hoffman AS (2002) Hydrogels for biomedical applications. *Advanced Drug Delivery Reviews* 54(1):3-12.

57.   Jeong B, Kim SW, & Bae YH (2002) Thermosensitive sol-gel reversible hydrogels. *Advanced Drug Delivery Reviews* 54(1):37-51.

58.   Klouda L & Mikos AG (2008) Thermoresponsive hydrogels in biomedical applications. *European Journal of Pharmaceutics and Biopharmaceutics* 68(1):34-45.

59.   Noro A, Nagata Y, Takano A, & Matsushita Y (2006) Diblock-type supramacromolecule via biocomplementary hydrogen bonding. *Biomacromolecules* 7(6):1696-1699.

60.   Hiemstra C, Zhong Z, Dijkstra PJ, & Feijen J (2005) Stereocomplex mediated gelation of PEG-(PLA)2 and PEG-(PLA) 8 block copolymers. *Macromolecular Symposia* 224:119-131.

61.   Van de Manakker F, Van der Pot M, Vermonden T, Van Nostrum CF, & Hennink WE (2008) Self-assembling hydrogels based on β-cyclodextrin/cholesterol inclusion complexes. *Macromolecules* 41(5):1766-1773.

62.   Kuo CK & Ma PX (2001) Ionically crosslinked alginate hydrogels as scaffolds for tissue engineering: Part 1. Structure, gelation rate and mechanical properties. *Biomaterials* 22(6):511-521.

63.   Burdick JA, Chung C, Jia X, Randolph MA, & Langer R (2004) Controlled Degradation and Mechanical Behavior of Photopolymerized Hyaluronic Acid Networks. *Biomacromolecules* 6(1):386-391.

64.   Tai H, Wang W, Vermonden T, Heath F, Hennink WE, Alexander C, Shakesheff KM, & Howdle SM (2009) Thermoresponsive and Photocrosslinkable PEGMEMA-PPGMA-EGDMA Copolymers from a One-Step ATRP Synthesis. *Biomacromolecules* 10(4):822-828.

65.   Ferreira L, Gil MH, Cabrita AMS, & Dordick JS (2005) Biocatalytic synthesis of highly ordered degradable dextran-based hydrogels. *Biomaterials* 26(23):4707-4716.

66.   Crescenzi V, Cornelio L, Di Meo C, Nardecchia S, & Lamanna R (2007) Novel Hydrogels via Click Chemistry: Synthesis and Potential Biomedical Applications. *Biomacromolecules* 8(6):1844-1850.

67.   DeForest CA, Polizzotti BD, & Anseth KS (2009) Sequential click reactions for synthesizing and patterning three-dimensional cell microenvironments. *Nature Materials* 8(8):659-664.

68. Malkoch M, Vestberg R, Gupta N, Mespouille L, Dubois P, Mason AF, Hedrick JL, Liao Q, Frank CW, Kingsbury K, & Hawker CJ (2006) Synthesis of well-defined hydrogel networks using Click chemistry. *Chemical Communications* (26):2774-2776.

69. Cellesi F, Weber W, Fussenegger M, Hubbell JA, & Tirelli N (2004) Towards a fully synthetic substitute of alginate: Optimization of a thermal gelation/chemical cross-linking scheme (ldquotandemrdquo gelation) for the production of beads and liquid-core capsules. *Biotechnology and Bioengineering* 88(6):740-749.

70. Elbert DL, Pratt AB, Lutolf MP, Halstenberg S, & Hubbell JA (2001) Protein delivery from materials formed by self-selective conjugate addition reactions. *Journal of Controlled Release* 76(1-2):11-25.

71. Ferruti P, Bianchi S, Ranucci E, Chiellini F, & Caruso V (2005) Novel poly(amido-amine)-based hydrogels as scaffolds for tissue engineering. *Macromolecular Bioscience* 5(7):613-622.

72. Ferruti P, Bianchi S, Ranucci E, Chiellini F, & Piras AM (2005) Novel Agmatine-Containing Poly(amidoamine) Hydrogels as Scaffolds for Tissue Engineering. *Biomacromolecules* 6(4):2229-2235.

73. Lutolf MP & Hubbell JA (2003) Synthesis and Physicochemical Characterization of End-Linked Poly(ethylene glycol)-co-peptide Hydrogels Formed by Michael-Type Addition. *Biomacromolecules* 4(3):713-722.

74. Lutolf MP, Tirelli N, Cerritelli S, Cavalli L, & Hubbell JA (2001) Systematic Modulation of Michael-Type Reactivity of Thiols through the Use of Charged Amino Acids. *Bioconjugate Chemistry* 12(6):1051-1056.

75. Mather BD, Viswanathan K, Miller KM, & Long TE (2006) Michael addition reactions in macromolecular design for emerging technologies. *Progress in Polymer Science* 31(5):487-531.

76. Rizzi SC & Hubbell JA (2005) Recombinant Protein-co-PEG Networks as Cell-Adhesive and Proteolytically Degradable Hydrogel Matrixes. Part I: Development and Physicochemical Characteristics. *Biomacromolecules* 6(3):1226-1238.

77. Vernon B, Tirelli N, Bächi T, Haldimann D, & Hubbell JA (2003) Water-borne, *In situ* crosslinked biomaterials from phase-segregated precursors. J*ournal of Biomedical Materials Research* 64A(3):447-456.

78. Censi R, Fieten PJ, di Martino P, Hennink WE, & Vermonden T (2010) In Situ Forming Hydrogels by Tandem Thermal Gelling and Michael Addition Reaction between Thermosensitive Triblock Copolymers and Thiolated Hyaluronan. *Macromolecules*.

79. Nguyen MK & Lee DS (2010) Injectable Biodegradable Hydrogels. *Macromolecular Bioscience* 10(6):563-579.

80. Klouda L & Mikos AG (2008) Thermoresponsive hydrogels in biomedical applications. *European Journal of Pharmaceutics and Biopharmaceutics* 68(1):34-45.

81. Bryant SJ, Nuttelman CR, & Anseth KS (2000) Cytocompatibility of UV and visible light photoinitiating systems on cultured NIH/3T3 fibroblasts in vitro. *Journal of Biomaterials Science Polymer Edition* 11:439-457.

82. Elisseeff J, Anseth K, Sims D, McIntosh W, Randolph M, & Langer R (1999) Transdermal photopolymerization for minimally invasive implantation. *Proceedings of the National Academy of Sciences of the United States of America* 96(6):3104-3107.

83. Ward JH & Peppas NA (2001) Preparation of controlled release systems by free-radical UV polymerizations in the presence of a drug. *Journal of Controlled Release* 71(2):183-192.

84. Royce Hynes S, McGregor LM, Ford Rauch M, & Lavik EB (2007) Photopolymerized poly(ethylene glycol)/poly(L-lysine) hydrogels for the delivery of neural progenitor cells. *Journal of Biomaterials Science, Polymer Edition* 18(8):1017-1030.

85. West JL & Hubbell JA (1995) Photopolymerized hydrogel materials for drug delivery applications. *Reactive Polymers* 25(2-3):139-147.

86. Nguyen KT & West JL (2002) Photopolymerizable hydrogels for tissue engineering applications. *Biomaterials* 23(22):4307-4314.

87. Sawhney AS, Pathak CP, & Hubbell JA (1993) Bioerodible hydrogels based on photopolymerized poly(ethylene glycol)-co-poly(.alpha.-hydroxy acid) diacrylate macromers. *Macromolecules* 26(4):581-587.

88.   Hill-West JL, Chowdhury SM, Slepian MJ, & Hubbell JA (1994) Inhibition of thrombosis and intimal thickening by in situ photopolymerization of thin hydrogel barriers. *Proceedings of the National Academy of Sciences of the United States of America* 91(13):5967-5971.

89.   Lin-Gibson S, Bencherif S, Cooper JA, Wetzel SJ, Antonucci JM, Vogel BM, Horkay F, & Washburn NR (2004) Synthesis and characterization of PEG Dimethacrylates and their hydrogels. *Biomacromolecules* 5(4):1280-1287.

90.   Kim SH, Won CY, & Chu CC (1999) Synthesis and characterization of dextran-based hydrogel prepared by photocrosslinking. *Carbohydrate Polymers* 40(3):183-190.

91.   Van Thienen TG, Horkay F, Braeckmans K, Stubbe BG, Demeester J, & De Smedt SC (2007) Influence of free chains on the swelling pressure of PEG-HEMA and dex-HEMA hydrogels. *International Journal of Pharmaceutics* 337(1-2):31-39.

92.   Hiemstra C, Zhou W, Zhong Z, Wouters M, & Feijen J (2007) Rapidly in situ forming biodegradable robust hydrogels by combining stereocomplexation and photopolymerization. *Journal of the American Chemical Society* 129(32):9918-9926.

93.   van Dijk M, Rijkers DTS, Liskamp RMJ, van Nostrum CF, & Hennink WE (2009) Synthesis and Applications of Biomedical and Pharmaceutical Polymers via Click Chemistry Methodologies. *Bioconjug. Chem.* 20(11):2001-2016.

94.   Robb SA, Lee BH, McLemore R, & Vernon BL (2007) Simultaneously Physically and Chemically Gelling Polymer System Utilizing a Poly(NIPAAm-co-cysteamine)-Based Copolymer. *Biomacromolecules* 8(7):2294-2300.

95.   Niu G, Zhang H, Song L, Cui X, Cao H, Zheng Y, Zhu S, Yang Z, & Yang H (2008) Thiol/Acrylate-Modified PEO-PPO-PEO Triblocks Used as Reactive and Thermosensitive Copolymers. *Biomacromolecules* 9(10):2621-2628.

96.   Peattie RA, Rieke ER, Hewett EM, Fisher RJ, Shu XZ, & Prestwich GD (2006) Dual growth factor-induced angiogenesis in vivo using hyaluronan hydrogel implants. *Biomaterials* 27(9):1868-1875.

97.   Hiemstra C, van der Aa LJ, Zhong Z, Dijkstra PJ, & Feijen J (2007) Rapidly in Situ-Forming Degradable Hydrogels from Dextran Thiols through Michael Addition. *Biomacromolecules* 8(5):1548-1556.

98.   Mather BD, Viswanathan K, Miller KM, & Long TE (2006) Michael addition reactions in macromolecular design for emerging technologies. *Progress in Polymer Science* 31(5):487-531.

99.   Van De Wetering P, Metters AT, Schoenmakers RG, & Hubbell JA (2005) Poly(ethylene glycol) hydrogels formed by conjugate addition with controllable swelling, degradation, and release of pharmaceutically active proteins. *Journal of Controlled Release* 102(3):619-627.

100.   Bell CL & Peppas NA (1996) Water, solute and protein diffusion in physiologically responsive hydrogels of poly(methacrylic acid-g-ethylene glycol). *Biomaterials* 17(12):1203-1218.

101.   Reinout S (2008) Smart biomaterials for tissue engineering of cartilage. *Injury* 39(1):77-87.

102.   Langer R (2000) Biomaterials in drug delivery and tissue engineering: One laboratory's experience. *Accounts of Chemical Research* 33(2):94-101.

103.   David V, Malay D, Tao X, Priya K, Sunil O, & Thomas B (2005) Advances in tissue engineering: Cell printing. *Journal of Thoracic and Cardiovascular Surgery* 129(2):470-472.

104.   Fedorovich NE, Alblas J, de Wijn JR, Hennink WE, Verbout AJ, & Dhert WJA (2007) Hydrogels as Extracellular Matrices for Skeletal Tissue Engineering: State-of-the-Art and Novel Application in Organ Printing. *Tissue Engineering* 13(8):1905-1925.

105.   Peltola SM, Melchels FPW, Grijpma DW, & Kellomäki M (2008) A review of rapid prototyping techniques for tissue engineering purposes. *Annals of Medicine* 40(4):268-280.

106.   Qiong Liu S, Tian Q, Wang L, Hedrick JL, Po Hui JH, Yan Yang Y, & Ee PLR (2010) Injectable biodegradable polyethylene glycol/ RGD peptide hybrid hydrogels for in vitro chondrogenesis of human mesenchymal stern cellsa. *Macromolecular Rapid Communications* 31(13):1148-1154.

107.   Guarnieri D, De Capua A, Ventre M, Borzacchiello A, Pedone C, Marasco D, Ruvo M, & Netti PA (2010) Covalently immobilized RGD gradient on PEG hydrogel scaffold influences cell migration parameters. *Acta Biomaterialia*.

108.   Yu J, Gu Y, Du KT, Mihardja S, Sievers RE, & Lee RJ (2009) The effect of injected RGD modified alginate on angiogenesis and left ventricular function in a chronic rat infarct model. *Biomaterials* 30(5):751-756.

109.   Herten M, Jung RE, Ferrari D, Rothamel D, Golubovic V, Molenberg A, Hämmerle CHF, Becker J, & Schwarz F (2009) Biodegradation of different synthetic hydrogels made of polyethylene glycol hydrogel/RGD-peptide modifications: An immunohistochemical study in rats. *Clinical Oral Implants Research* 20(2):116-125.

110.   Klein TJ, Rizzi SC, Reichert JC, Georgi N, Malda J, Schuurman W, Crawford RW, & Hutmacher DW (2009) Strategies for Zonal Cartilage Repair using Hydrogels. *Macromolecular Bioscience* 9(11):1049-1058.

111.   Fedorovich NE, De Wijn JR, Verbout AJ, Alblas J, & Dhert WJA (2008) Three-Dimensional Fiber Deposition of Cell-Laden, Viable, Patterned Constructs for Bone Tissue Printing. *Tissue Engineering* 14(1):127-133.

112.   Fedorovich NE, Swennen I, Girones J, Moroni L, van Blitterswijk CA, Schacht E, Alblas J, & Dhert WJA (2009) Evaluation of Photocrosslinked Lutrol Hydrogel for Tissue Printing Applications. *Biomacromolecules* 10(7):1689-1696.

113.   Mironov V, Visconti RP, Kasyanov V, Forgacs G, Drake CJ, & Markwald RR (2009) Organ printing: Tissue spheroids as building blocks. *Biomaterials* 30(12):2164-2174.

114.   El-Ayoubi R, DeGrandpre C, DiRaddo R, Yousefi A-M, & Lavigne P (2009) Design and Dynamic Culture of 3D-Scaffolds for Cartilage Tissue Engineering. *Journal of Biomaterials Applications* doi: 10.1177/0885328209355332.

115.   Hollister SJ (2005) Porous scaffold design for tissue engineering. *Nature Materi*als 4(7):518-524.

116.   Masood SH, Singh JP, & Morsi Y (2005) The design and manufacturing of porous scaffolds for tissue engineering using rapid prototyping. *The International Journal of Advanced Manufacturing Technology* 27(3):415-420.

117.   Moutos FT, Freed LE, & Guilak F (2007) A biomimetic three-dimensional woven composite scaffold for functional tissue engineering of cartilage. *Nature Materials* 6(2):162-167.

118.   Woodfield TBF, Malda J, de Wijn J, Péters F, Riesle J, & van Blitterswijk CA (2004) Design of porous scaffolds for cartilage tissue engineering using a three-dimensional fiber-deposition technique. *Biomaterials* 25(18):4149-4161.

Chapter 2

Hydrogels for Protein Delivery

Roberta Censi,[a,b] Tina Vermonden,[a] Piera Di Martino,[b] Wim E Hennink[a]

[a] Department of Pharmaceutics Utrecht Institute for Pharmaceutical Sciences (UIPS); Utrecht University; P.O. Box 80082, 3508 TB Utrecht, The Netherlands.

[b] Department of Chemical Sciences; Camerino University; via S. Agostino 1, 62032, Camerino (MC), Italy.

Abstract

Proteins are an important class of therapeutics. However, the drawbacks associated with their use, such as chemical, physical and enzymatic instability, poor bioavailability after oral administration and short half-life are limiting their widespread use as medicines. Therefore, there is a high need for advanced delivery systems, which are able to improve the therapeutic efficacy and reduce the side effects of proteins. Hydrogels represent a class of controlled release systems that hold important potential in protein delivery. Since their discovery in the early 1960s, rapid advances have been made in this field, allowing the design of injectable physically and/or chemically cross-linked polymeric networks with controllable polymer design, degradability, mechanical properties and release behavior. Smart hydrogels with responsive behavior to environmental stimuli were synthesized, allowing *in situ* gelation and on demand release of drugs. This chapter outlines the main injectable hydrogel systems developed to date and describes the most relevant cross-linking methods for *in situ* gelling. A special focus of the discussion is the use of hydrogels as protein controlled delivery systems, with respect to their release mechanisms, protein stability and methods to study protein release.

2.1. Introduction to Protein Delivery

2.1.1 Pharmaceutical proteins and delivery issues

Once a rarely used class of therapeutic agents, pharmaceutical proteins have increased remarkably in number and frequency of use since the introduction of the first recombinant protein therapeutic, human insulin 30 years ago.(1) With more than 130 FDA (US Food and Drug Administration) approved products and many more in development, protein therapeutics gained a significant role in almost every field of medicine, like cancer, inflammatory diseases, vaccines and diagnostics.(2) The increasing use of pharmaceutical proteins can be explained by their advantageous properties as compared to small-molecule drugs and the progress achieved in their production technologies. Indeed, proteins serve a highly specific and complex set of functions - i.e. catalysis of biochemical reactions, formation of membrane receptors and channels, transport of molecules within a cell or from one organ to another, intracellular and extracellular scaffolding support, etc. - that can hardly be reproduced by small synthetic compounds.

Importantly, with the advent of hybridoma and recombinant DNA technologies, the limitations associated with the extraction and purification of pharmaceutical proteins from animal sources were circumvented. Protein therapeutics have become mass-scale products, manufactured using bacteria, yeast, mammalian cells, and transgenic plants. These biotechnological routes yield proteins with improved safety profiles, being generally well tolerated and less immunogenic, as compared to animal-extracted proteins. Protein therapeutics derive their specificity and function from their amino-acid-based primary, secondary and tertiary structure. For example, somatostatin owes its biological activity to a characteristic hairpin-loop structure, which is present in both the 14 and 28 amino-acid active forms.(3) Since this discovery, the production of smaller therapeutically active synthetic analogues (i.e. the octapeptide octreotide), all sharing the hairpin loop pattern, became possible. However, the delicate three-dimensional structure of proteins is also a major limitation to the use of pharmaceutical proteins as they suffer from poor stability, due to proteolytic and chemical degradation as well as physical unfolding and aggregation.(4-6) This instability leads to loss of activity and often to elicitation of an immune response.(7-8) Because of their fragile nature, oral administration of proteins is a particularly challenging route due to the high proteolytic activity and low pH of the stomach, that destabilize and degrade the protein structure resulting in loss of biological activity. However, the capability to protect the active from the harsh conditions of the gastro-intestinal (GI) tract is not the only challenge. Bioavailability is another major issue associated with oral administration. The large molecular size of protein therapeutics makes their absorption through biological membranes difficult; consequently oral and transdermal administrations are ineffective. Therefore, to date protein drugs are almost without exception administered parenterally. But, because of the consistent first-pass hepatic

metabolism, the fast renal clearance and consequently the short half-lives of many proteins (i.e. growth hormone, insulin, oxytocin, paratyrhoid hormone, vasopressin have half-lives lower than 25 minutes), frequent injections or infusions, that limit patient's comfort, convenience and compliance, are required to obtain a therapeutic effect.(9) The mentioned drawbacks represent an immense challenge to modern medicine as they restrict the widespread acceptance and applications of proteins as therapeutics by patients and physicians, but also represent a tremendous opportunity for the drug delivery field. Among the approaches implemented to enhance protein's pharmacokinetic and pharmacodynamic properties, while preserving its native form and improving patient's compliance, scientists centered their focus mainly on the following strategies:

(a) Development of needle-free administration routes with high bioavailability, such as pulmonary, oral and nasal delivery (10-11)

(b) Extension of circulation time and masking immunogenicity of protein drugs by conjugation of the protein with macromolecules like poly(ethylene glycol) (PEG) or (polysialic acid)(12)

(c) Development of injectable controlled release delivery systems, including liposomes, polymeric micro and nano particles, and hydrogels.

Generally speaking, all these approaches, aim to achieve the following benefits:

(a) Maintaining plasma protein-drug concentration within the therapeutic window over an extended period of time

(b) Protecting the active from premature degradation

(c) Enhancing drug efficacy, while reducing side-effects

(d) Avoiding frequent administration and lowering drug dosage.

This chapter reviews injectable polymeric delivery systems used for the controlled release of pharmaceutical proteins, with special focus on hydrogels. In particular, we shortly overview the currently available technologies, which include lipid-based delivery systems, nano/microparticles and hydrogels, highlighting their rationale, characteristics and shortcomings in protein delivery. Hydrogels are more extensively described, from their general features to recent advances in synthesis and pharmaceutical applications. The discussion covers both physical and chemical cross-linking methods used for *in situ* gelling systems, environmentally responsive hydrogels and their use for protein release. Some limitations of hydrogels in protein delivery (burst and incomplete release) are also discussed and ways to tackle these are provided. Finally, emerging techniques to study release from hydrogels are illustrated.

2.1.2. Particulate protein delivery systems

2.1.2a. Microspheres and nanoparticles

Nanoparticle and microsphere-based drug delivery systems are advantageous because of their injectability and possibility to achieved prolonged release.(13) Biocompatibility and biodegradability are necessary criteria for selecting the drug carrier. A variety of synthetic and naturally occurring biodegradable polymers have been investigated in the past 30 years for the preparation of nano and microspheres.(13) A few examples of natural polymers used for the preparation of microparticles include chitosan, used for vaccination purposes (14), alginate-based microparticles for the pulsatile release of insulin(15) and polymerized serum albumin beads for vaccine delivery.(16) However, the development of polymer-based micro and nanospheres based on natural polymers has been overshadowed by the advances made in synthetic polymer technology. Among the synthetic polymers, aliphatic polyesters, polyanhydrides, polyorthoesters, polyphosphazenes and polyaminoacids are the most relevant representatives. Polyesters, in particular poly(lactic-*co*-glycolic acid) (PLGA), dominate the field with a number of marketed formulations (i.e. Lupron Depot®, Nutropin Depot®, Decapeptyl®, etc.),(17-18) because of the demonstrated biocompatibility and degradation into toxicologically acceptable products.(19) Despite the many advantages of PLGA microspheres, they also showed some inherent shortcomings, such as polymer hydrophobicity, acidic microenviroment during bioerosion,(20-21) leading to protein denaturation and aggregation,(22) burst and incomplete release.(23-25) Therefore, microparticle-based delivery systems are still awaiting major clinical successes and extensive research is being conducted to improve the current technology. For example, approaches to reduce the burst release and increase loading efficiency in microspheres comprise optimization of preparation method parameters (typically the double emulsion technique).(26-27) Furthermore, the synthesis of novel hydrophilic polymers, such as poly(lactic-*co*-hydroxymethyl glycolic acid) (PLHMGA) as an alternative to PLGA for the preparation of microspheres has been reported.(28-29) Protein and peptide delivery using nanoparticles is still in its infancy, but the interest in this field is increasing and some examples of nano-delivery systems for proteins have become available.

Early developments on nanoparticulate systems for protein delivery were reviewed by Couvreur *et al.*,(30) while more recent advances were discussed by Pinto Reis *et al*.(31) The major advantage of using this approach resides in the possibility to achieve site-specific release of the drug by passive or active targeting and, in contrast to microparticles, to accomplish intracellular protein delivery. Targeting drugs to the desired site of action would not only improve therapeutic efficiency but also permits a reduction in the dose of drug administered, thus minimizing unwanted toxic effects.

2.1.2b   Lipid-based delivery systems

Emulsions, liposomes and solid lipid nanoparticles are all examples of lipid-based delivery systems for proteins. Proteins and peptides can be incorporated in the internal phase of water-in-oil emulsions and delivered in a controlled fashion upon administration.(32-33) Some studies have demonstrated *in vivo* efficacy of these delivery systems, releasing e.g. aprotinin for a prolonged period of time (33) or inducing immune response upon oral-antigen delivery (34). Despite these encouraging results and the possibility to modify to some extent their release behavior (35) by varying disperse phase volume fraction, osmotic gradient and particle size, formulation and protein stability issues as well as low encapsulation efficiency, incomplete release and poor control over release kinetics limit the use of this technology as protein delivery system.

Liposomes, consisting of one or more phospholipid bilayers separated by internal aqueous compartments, are well established and extensively investigated particulate carrier systems that have been successfully employed for the controlled release and site specific drug delivery. With the possibility to vary their dimensions, composition, surface charge and structure, liposomes have demonstrated to be suitable for encapsulation of enzymes and proteins. An advantage of liposome-encapsulated enzymes/proteins is their potential ability to enter the cytoplasm or lysosomes of cells. In the past 20 years, extensive literature on their application for the release of encapsulated or surface-associated proteins and peptides,(36-37) has been published (reviewed by Torchilin (38)). Unlike emulsions, liposomes can be lyophilized and administered upon reconstitution(39-40) and they have shown to be able to protect therapeutics from degradation and to slowly release them when liposome destabilization takes place. However, difficulties to achieve tailorable controlled release by liposomal formulation along with the risk for opsonization in humans still represent obstacles for the use of liposomes as protein and peptide delivery systems.(41)

Finally, a novel class of particles (based on lipid components other than phospholipids), described for the first time by Müller et al(42) is solid lipid nano- and microparticles. Incorporation of proteins into solid lipid nano- and microparticles is relatively new and the work on the characterization of these delivery systems is rather scarce. Nevertheless, some examples of prolonged *in vitro* release and *in vivo* efficacy are available and allow concluding that these types of formulation hold potential as protein carriers.(43-46) However, optimization of the solid lipid particles formulation aimed to overcome burst and incomplete release, often observed with these types of delivery systems, is needed.(44, 47-48) Moreover the possibility to tailor drug release has not been investigated in detail yet.

2.1.3.   Hydrogels for sustained delivery, general features

Hydrogels are cross-linked networks of hydrophilic polymers, capable to retain large amounts of water yet remaining insoluble and maintaining their three-dimensional structure. Since their discovery and application in the biomedical field by Wichterle *et al.* in the early 1950s,(49) an immense number of hydrogels have been developed and they have been studied for a wide range of biomedical and pharmaceutical applications, including contact lenses,(50) tissue engineering,(51) diagnostics, drug delivery,(52-53) vascular prostheses,(54) coating for stents and catheters.(55) Polymers need to be physically and/or chemically cross-linked, in order to prevent their dissolution. Hydrogels can be prepared using degradable and non-degradable, natural and synthetic polymers and they can consist of homopolymers, copolymers, interpenetrating or double polymeric networks.(56-57)

Hydrogels are generally regarded as biocompatible materials because their high water content and soft nature render them similar to the natural extracellular matrix and minimize tissue irritation and cell adherence.(58) Furthermore, their porous structure, along with their water content, are extremely suitable properties to accommodate high loads of water-soluble compounds, like therapeutically active proteins and peptides, in a physiologically relevant setting, amenable to protein stability.

Unlike other delivery systems (microparticles, emulsions, *etc*.), where preparation conditions are sometimes detrimental to proteins (i.e. use of organic solvents and protein denaturating processes, like homogenization, exposure to interfaces, *etc.*), hydrogel preparation procedures are beneficial in preserving protein stability, as very mild conditions (aqueous environment, room temperature) are normally adopted.

All these unique properties of hydrogels have sparked increasing interest in their use as reservoir systems for proteins that are slowly released from the hydrogel matrix in a controlled fashion to maintain a therapeutic effective concentration of the protein drug in the surrounding tissues or in the circulation over an extended period.

Proteins can be physically incorporated in the hydrogel matrix and their release is governed by several mechanisms, such as diffusion, swelling or erosion or combination of two or more of these mechanisms. Hydrogels allow fine-tuning of the protein release by tailoring their cross-link density via changes in polymer architecture, concentration, molecular weight, or chemistry. Other strategies to tailor drug release from hydrogels exist and they rely on reversible protein-polymer interaction, or encapsulation of the protein in a second delivery system (e.g. micro- or nanoparticles) dispersed in the hydrogel network.

Preformed, macroscopic hydrogels have to be admistered by surgical intervention. This is costly and not convenient for the patient and therefore nowadays, attention is focused on injectable hydrogels that can be administered in a minimally invasive manner. Injectable hydrogels are characterized as clear polymer solutions prior to administration and turn into a visco-elastic system at the site of administration upon injection. They jellify in response to

external stimuli (like temperature, pH, ionic strength, solvent) or by means of other physical and chemical cross-linking methods (stereocomplexation, inclusion complexation, photopolymerization, Michael addition, *etc.*).

Moreover, by appropriate design of the polymeric material, biodegradability and bioresorption can be ensured. Biodegradation is defined as conversion of materials into less complex intermediates or end-products that can be eliminated from the body without harmful effects.(59) In general it can be accomplished via dissociation of the polymer chains or enzymatic and hydrolytic degradation pathways.

2.2. Cross-linking methods for *in situ* forming hydrogels

2.2.1. Physical cross-linking

Physical cross-linking between polymers can be obtained by using several non-covalent interactions, such as e.g. hydrophobic interactions, ionic interactions, hydrogen bonding, host-guest interactions or combinations of these. The most popular interactions for building physically cross-linked hydrogels are hydrophobic interactions, because they are strong interactions in aqueous environment and hydrogels can simply be prepared by using amphiphilic block copolymers. As amphiphilic polymer hydrogels will be discussed in more detail in the "Smart Hydrogel" section, this section will focus on more specific interactions that have been used recently to prepare hydrogels for protein delivery.

2.2.1a. Inclusion complexes

Inclusion complexes of cyclic β-cyclodextrins (βCD), which are cyclic oligosaccharides with an internal hydrophobic pocket, and complementary low molecular weight guest molecules have been used as a cross-linking method for the design of *in situ* gelling networks.(60) Yui *et al.* reviewed several aspects of supramolecular self-assembling systems based on rapidly responsive hydrogels from polymeric hosts and low molecular weight guests.(61) βCD and cholesterol end-functionalized star-shaped PEG polymers have been synthesized and used as gelators for the preparation of hydrogels aimed to protein delivery.(62-64) Upon hydration of a mixture of star PEG-βCD and star PEG-cholesterol, hydrogels are formed (**Figure 1**). The hydrogels are assembled by formation of β-CD/cholesterol inclusion complexes driven by hydrophobic and van der Waals interactions. The hydrogels exhibited thermosensitive behavior being completely reversible upon cooling and heating steps. In particular, at low temperature viscoelastic behavior, due to slow dynamics, was observed, while at higher temperatures a viscous system, due to a reduced number of βCD/cholesterol complexes and faster chain relaxation processes was obtained.(62) A study of hydrogels based on cholesterol and βCD modified PEGs of different architecture (linear, 4-arm star and 8-arm star) revealed

that the 8-arm star based mixtures yielded the strongest viscoelastic network.(63) The 8-arm star PEG based hydrogels were studied for protein release purposes; hydrogels based on PEG of different molecular weights were used to study the release of model proteins and a quantitative and nearly zero-order release of entrapped proteins was shown. The release was governed by surface erosion, which depended on the network swelling stresses and initial crosslink density of the gels.(65)
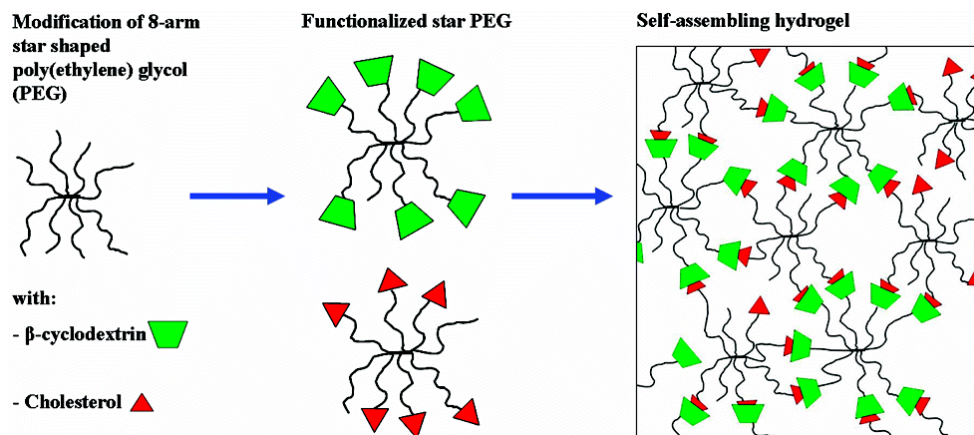

Figure 1. Self-assembling poly(ethylene glycol) hydrogel system based on inclusion complexes between β-cyclodextrin (β-CD) and cholesterol. Hydrogels are formed after hydration of a mixture of star-shaped 8-arm poly(ethylene glycol) (PEG) end-modified with β-CD groups and the same star-shaped PEG end-modified with cholesterol moieties. Reproduced from reference (62).

Other supramolecular-structured hydrogels, displaying a gel-sol phase transition, were prepared by inclusion complexation between poly(ethylene glycol) grafted dextrans and α-cyclodextrins (αCDs) in aqueous solution. The gel-sol transition was based on the supramolecular assembly and dissociation, and the transition was reversible and controllable by the polymer concentration and the PEG content of the graft copolymers as well as the ratio between the guest and host molecules. Thermosensitive behavior was also observed, as at high temperatures the network dissociated reversibly.(66) In order to add pH functionality to the described thermosensitive hydrogel based on inclusion complexes, poly(d-lysine) (PL), a cationic polymer, was grafted onto dextran and used for inclusion complexation with α-CDs. Transition from a phase-separated structure of hydrated dextrans and hydrophobically aggregated inclusion complexes in buffer solution at pH 10.0 (where the primary amine are deprotonated allowing the CDs to be threaded onto the PL chain) was observed. The hydrogels showed thermoreversible gel-sol transitions as well as pH-sensitive phase transitions.(67)

By utilizing the interaction of oligo(☐-CD) with dodecyl side chains modified poly(acrylic acid), systems that undergo gel-to-sol and sol-to-gel transitions were successfully constructed.(68)

2.2.1b.   Stereocomplexation

Stereocomplexation is defined as co-crystallization of two enantiomers. This physical interaction has been investigated as cross-linking method for the preparation of injectable hydrogels. The enantiomers mainly employed for the preparation of *in situ* forming hydrogels are poly(l-lactide) (PLLA) and poly(d-lactide) (PDLA), which combined in a 1:1 racemic mixture are able to form stereo-complex crystals. Other specialized reviews are focused on these stereocomplexed hydrogels, from their synthesis, to crystallization mechanism, degradation and general applications,(69-70) therefore just a few systems are discussed in this chapter. When PDLA and PLLA are coupled to hydrophilic polymers like dextran and mixed in an aqueous medium a hydrogel is formed. Proteins can be loaded in the hydrogels by dissolving them in the solution of the hydrogel precursors (**Figure 2**). This gelation mechanism was first described by De Jong *et al.* (71-72)
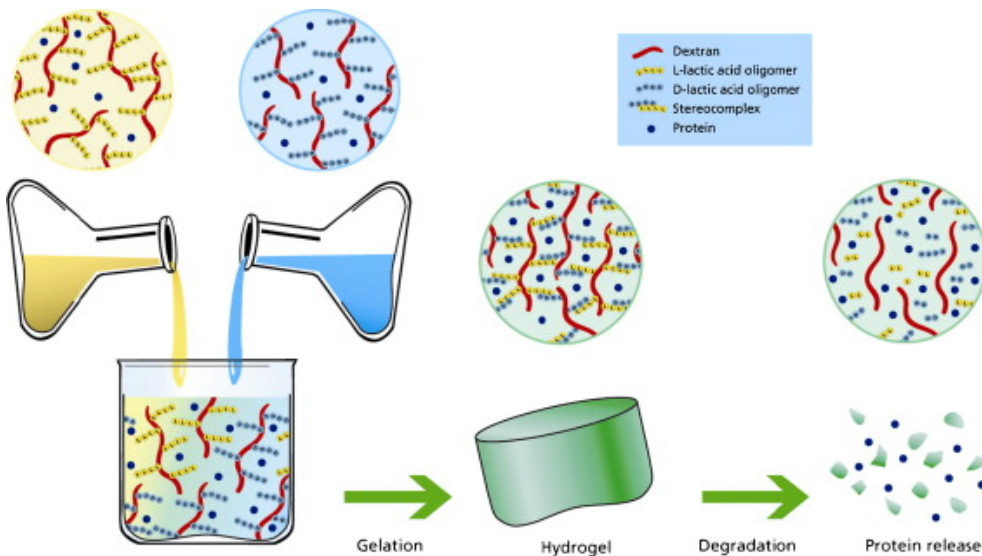
Figure 2. Schematic presentation of the self-assembling mechanism of stereocomplexed dextran hydrogel. Reproduced from reference.(71)

The application of these hydrogels as controlled drug delivery systems was described.(73) Model proteins (lysozyme and IgG) (73) as well as the therapeutically relevant proteins (recombinant human interleukin-2, rhIL-2) (52) from the dex-lactate hydrogels was studied *in vitro* and *in vivo*. Lysozyme was released from 30 wt% polymer hydrogels in 5 days by

diffusion, while the bigger protein IgG was released in 8 days by a combination of diffusion and swelling/degradation of the matrix. RhIL-2 was initially rapidly released *in vitro* and in a later stage a slower release was observed*. In vivo* studies were done by injecting intraperitoneally RhIL-2 loaded hydrogels into tumor bearing mice. Placebo hydrogels and RhIL-2 bolus injections were used as controls. The same therapeutic effect of one injection of RhIL-2 loaded hydrogels was achieved with 5 consecutive Rh-IL2 bolus injections. *In vivo* biocompatibility studies showed only a mild foreign body reaction, most likely due to degradation of the polymer.(74)

2.2.2.   Chemical cross-linking

Chemical cross-linking will yield covalent bonds between different polymer chains and the resulting hydrogel network is in general more resistant to mechanical forces than physically cross linked networks. Many coupling reactions can be used to obtain cross-linked polymers, especially "click chemistry"(75) and also "native chemical ligation" (76)are becoming more popular due to their ease of use and high conversion. However, in this section we focus on techniques that are used for *in situ* gelation and therefore most interesting for protein delivery at the moment.

2.2.2a.   Photopolymerization

Photopolymerization is a form of radical polymerization that allows the formation of *in situ* formed hydrogels by means of UV or visible light, in the presence of a photosensitive compound, called a photoinitiator. This chemical cross-linking reaction is initiated by the decomposition of the photoinitiator upon exposure to UV or visible light, leading to the formation of radicals. In the presence of hydrogel precursors, bearing polymerizable groups, such acrylate or methacrylate moieties, a gel is formed after UV/visible light irradiation. As these stimuli can be applied *in vivo* in a minimally invasive manner, by means of laparoscopic devices or cathethers or transdermal illumination, (77-78) photopolymerization is considered a suitable method for the preparation of *in situ* gelling viscoelastic systems. Since Hubbell *et al.* introduced this cross-linking method for the first time,(79) photopolymerization has been used for a number of biomedical applications, as it offers as series of advantages over other types of cross-linking methods. The photocuring process is fast, taking usually only seconds to minutes to complete, can be conducted at room or body temperature without the use of organic solvents and offers the advantage of spatial and temporal control.(80-82). In 2002, Nguyen *et al.* reviewed the photo-cross-linked hydrogels for potential tissue engineering application, describing the available photoinitiators and photopolymerizable compounds(51) and Van Tomme *et al.* provided a more recent update on the progress of photopolymerized hydrogel systems, as well as other types of *in situ* cross-linking methods.(83)

As mentioned, Hubbell *et al.* pioneered the field of photopolymerized hydrogels for biomedical applications, designing a polymer composed of a central PEG chain and lateral oligomeric blocks of a hydrolyzable α-hydroxy acid, or other degradable moiety. The hydrogel precursors were synthesized by reacting dihydroxy polyethylene glycol with D,L- lactide using stannous octoate as a catalyst. This polymer was then reacted with acryloyl chloride to connect an acrylate unit at each end. PEG molecular weight was varied to tune the permeability as well the physical properties of the hydrogel, while the length of the α-hydroxy acids modulated the degradation of the hydrogels. The photoinitiator 2,2-dimethoxy,2-phenyl acetophenone was dissolved in N-vinyl pyrrolidone and added to the polymeric precursors solution in the presence of proteins. It was observed that a rapid gelation of the solution occurred upon UV curing. The release of several proteins of different molecular weight was investigated (discussed in section 4.2.).(79, 84) One of the drawbacks of photopolymerization can be the possible degradation of the proteins during photopolymerization, as the UV light, as well as the developed radical species upon photoinitiator decomposition might be detrimental to the encapsulated therapeutic. However, it was demonstrated that UV light of selected wavelength and low intensity preserves protein stability.(78) Furthermore, several papers, where enzymes were encapsulated by photopolymerization in hydrogel networks, demonstrated that both the biological activity and the protein structure were retained.(84) Pescosolido *et al.* confirmed the protein compatible nature of photopolymerization by demonstrating that the enzymatic activity of horse radish peroxidase, encapsulated in and released from interpenetrating networks composed of ionically cross-linked Ca^{2+}-Alginate combined with photopolymerized methacrylated dextran, was preserved.(85) In a photopolymerized thermosensitive hydrogel based on methacrylated poly(*N*-(2-hydroxyl propyl) methacrylamide lactate)-PEG-poly(*N*-(2-hydroxyl propyl) methacrylamide lactate) (p(HPMAm-lac)-PEG-p(HPMAm-lac) it was demonstrated that lysozyme retained its enzymatic activity and secondary structure after photopolymerization and release. It was reasoned that the self-assembly mechanism of the hydrogel played a beneficial role in the stabilization of the protein. The hydrogel was prepared by dissolving polymer, photoinitiator and enzyme in aqueous medium and the resulting solution was heated to body temperature before photopolymerization to mimic the physiological situation. By this procedure, hydrophobic domains of self-assembled thermosensitive chains and hydrophilic PEG rich pores were formed. The hydrophobic photoinitiator has affinity for the hydrophobic domains, while the protein resides most likely in the hydrophilic PEG pores. The phase separation between the two species led the radical cross-linking reaction to be confined in the hydrophobic domains, minimizing potential damage to the protein, which is mainly present in the PEG-rich domains.(86) However, protein stability and photopolymerization is a controversial topic, where generalized principles cannot be applied and the protein stability must be assessed for each specific polymer, photoinitiator and protein therapeutic. For example, the same system developed by Hubbell *et al.*, which did not show detectable modification of encapsulated

proteins, adhered to surrounding cells when photopolymerized *in vivo*, most likely as a result of chemical reactions between polymer and extracellular proteins. In contrast, tissue adherence was not observed when the hydrogels were photopolymerized *ex vivo* and subsequently implanted.(87) The choice of the photoinitiator can also play a crucial role in the success of application of photopolymerizable systems in the field of tissue engineering and protein release. Besides protein stability, the cyto- and biocompatibility of the initiator used to carry out the polymerization has to be taken into account. Bryant *et al.* performed a comparative cytocompatibility study on several photoinitiating systems, including 2,2-dimethoxy-2-phenylacetophenone (Irgacure 651), 1-hydroxycyclohexyl phenyl ketone (Irgacure 184), 2-methyl-1-[4-(methylthio) phenyl]-2-(4-morpholinyl)-1-propanone (Irgacure 907), and 2-hydroxy-1-[4-hydroxyethoxy)phenyl]-2-methyl-1-propanone (Darocur 2959), camphorquinone (CQ) with ethyl 4-N,N-dimethylaminobenzoate (4EDMAB) and triethanolamine (TEA) and the photosensitizer isopropyl thioxanthone. Both UV and visible light were used and a fibroblast cell line, NIH/3T3, was exposed to the photoinitiators at varying concentrations from 0.01% (w/w) to 0.1% (w/w) and studied before and after exposure to the initiating light. The results demonstrated that at low photoinitiator concentrations (≤0.01% (w/w)), all photo-initiators were cytocompatible with the exception of CQ, Irgacure 651, and 4EDMAB. At low light intensity, Darocur 2959 at concentrations ≤0.05% (w/w) was among the most promising cytocompatible UV and visible light initiating systems, respectively.(78) More recently, Fedorovich *et al.* evaluated the effect of photopolymerization on stem cells embedded in hydrogels aimed for tissue engineering.(88) They analyzed the viability, proliferation and osteogenic differentiation of multipotent stromal cell (MSC) monolayers after exposure to UV-light in the presence of Darocur 2959. Apoptosis and osteogenic differentiation of encapsulated goat MSCs were studied in photopolymerized methacrylate-derivatized hyaluronic acid hydrogel and methacrylated hyperbranched polyglycerol gel. Adverse effects of photopolymerization on viability, proliferation and reentry into the cell cycle of the exposed cells in monolayers were observed, whereas the MSCs retained the ability to differentiate towards the osteogenic lineage. However, upon encapsulation in photopolymerizable hydrogels the viability of the embedded cells was unaffected by the photopolymerization conditions, while osteogenic differentiation depended on the type of hydrogel used, demonstrating in this case the protecting effect of hydrogels with respect to cells.

In contrast, Lin *et al.* showed that photopolymerization was the cause of the incomplete release of BSA from cross-linked PEG based networks because of grafting of the protein to the polymeric network during the gelation reaction. The fraction of immobilized protein decreased with increasing initial loading (**Figure 3**).(89) The covalent coupling between BSA and hydrogel precursors was studied recently by Valdebenito *et al.*, who demonstrated that BSA can act as chain transfer agent in radical reactions.(90)
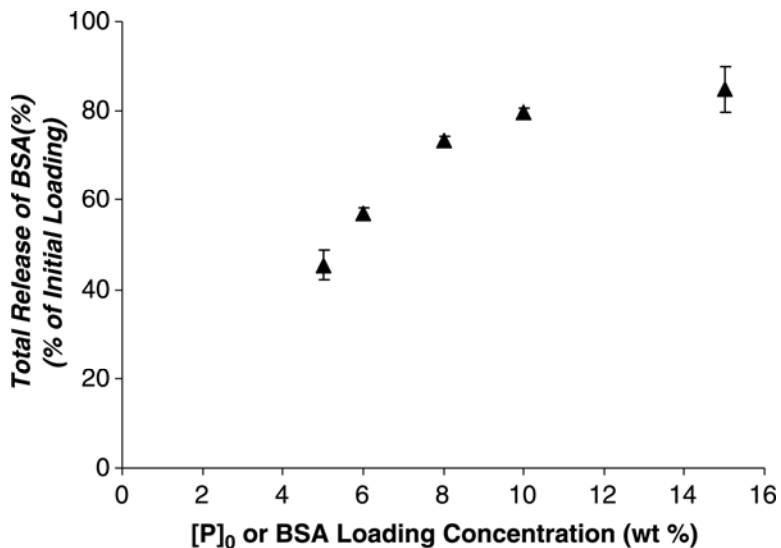
Figure 3. Effect of protein initial loading on total release of BSA from photopolymerized PEG based hydrogels. Reproduced from reference (89)

Another critical factor to be evaluated in photopolymerized hydrogels is their biodegradation. Although the polymer precursors are designed to be biodegradable, a third polymeric species is formed during polymerization, namely polyacrylic or polymethacrylic acid in case of acrylate and methacrylate bearing prepolymers, respectively. The solubility of these polyorganic acids, thus their possibility to be excreted by renal filtration, highly depends upon their molecular weight. Metters *et al.* carried out a detailed investigation of the bulk degradation phenomenon of photopolymerized hydrogels based on PEG and poly(lactic acid), previously developed by Hubbell and coworkers.(91) They developed a mathematical model, where the length of the molecular weight of the degradation products and, more in general, the kinetics of the bulk degradation phenomenon in chemically cross-linked matrices are predictable, allowing consequently a priori design of degrading hydrogels. They showed in a first and simpler model that the mass loss from the chemically cross-linked network depended on network parameters such as the number of cross-links per backbone chain and the mass fraction of the network contained in the backbone as opposed to the rest of the network. Model predictions versus degradation time also depended on reaction parameters such as the order of the hydrolysis reaction and the value of the kinetic rate constant.(92) An extension of this model to other aspects of the network degradation, where inclusion of partially reacted polymer and varying number of lactic acid repeating units were included and different polymerization conditions applied, was elaborated. This work allowed a more realistic representation of the bulk degradation of cross-linked hydrogels.(93)

Inspired by the work initiated by Hubbell, many other scientists designed photopolymerizable materials, such as acrylated 4-arm PEG, methacrylated dextran-HEMA, methacrylated dextran-HEMA-dimethylaminoethyl (dex-HEMA-DMAE), methacrylated eight-arm PEG-poly(lactic acid) (PEG-PLA) star block copolymers. Smeds and colleagues reported on the use of two methacrylate modified polysaccharides, alginate and hyaluronan, that, upon photopolymerization, formed viscoelastic gels for tissue engineering.(94) Similarly, Leach *et al.* reported on photocrosslinkable hyaluronic and PEG based hydrogels for protein delivery and tissue engineering.(95) Anseth *et al.* studied PEG and poly(vinyl alcohol)-based polymers, containing acrylate or methacrylate functionalities for the *in situ* generation of photopolymerized networks.(96)

2.2.2b.   Michael addition

While most of the addition reactions are carried out in organic solvent and using rather toxic chemicals, and therefore not suitable for *in situ* gelling systems, as all traces of unreacted compounds and solvents have to be removed, Michael addition reaction can be implemented to cross-link injectable hydrogels. This chemical reaction occurs in aqueous medium, room temperature and physiological pH, without need for toxic compounds and involves the addition of a nucleophile or activated olefin to a carbon-carbon double bond on alkenes. Michael addition reaction is recently emerging as an advantageous cross-linking method for biomedical applications, especially when thiol groups are used as Michael donor species. The benefits of this reaction derive from the high selectivity of Michael acceptors for thiols, as compared to amines.(97) This means that in the presence of proteins, either encapsulated in the hydrogels network or present on the cell surface, the hydrogel precursors hardly show cross-reactivity with amine groups of the therapeutic or present extracellular matrices where the hydrogel precursors are administered. Moreover, using Michael type addition, the formation of a polyacrylic or methacrylic acid of uncontrolled molecular weight is avoided, in contrast to photopolymerization, as 1 donor molecule reacts with only 1 acceptor molecule. Hubbell and coworkers introduced for the first time this type of reaction for the preparation of injectable matrices by reaction of PEG-dithiol with PEG-acrylates in aqueous medium at physiological pH and room temperature. Solid particles of bovine serum albumin were mixed with the gel precursor solution and, upon Michael addition curing, the protein-encapsulating hydrogels were formed in approximately 15 minutes. The different hydrogels reached equilibrium swelling in 24 hours and degraded in 5 to 25 days depending on the PEG functionality (PEG triacrylate degraded faster than PEG-octaacrylate). Albumin was released during 5–12 days and importantly, complete release of the protein was observed, demonstrating the self-selectivity of the Michael addition for the thiol-modified PEG, rather than for the disulfide bonds (S-S), free thiol (SH) or amine groups of the protein. It was reasoned that S-S and SH are normally located in hardly accessible pockets, limiting the

cross-reactivity of the protein with the hydrogel precursors.(98) In a subsequent study, Hubbell and coworkers used a similar approach to crosslink hydrogels by combining Michael addition donors such as pentaerythritol tetrakis 3'-mercaptopropionate (QT) and addition acceptors such as poly(ethylene glycol) diacrylate (PEGDA), pentaerythritol triacrylate (TA), and poly(propylene glycol) diacrylate (PPODA). The reactions were carried out both in phosphate buffer solutions of physiological pH and in emulsion to facilitate the dissolution of poorly water-soluble compounds. Gels were obtained in a time-scale between 5 and 10 minutes with complete conversion of thiols and acrylates, when the two species were combined in a 1:1 ratio. This indicated that side reactions, such as disulfide formation, are negligible on the time scale of the gelation. These crosslinked materials (at 75 wt% solid), showed compression moduli of 1.8 and 6.7 MPa and deformations up to 37%, depending on the preparation method (dispersion *vs* emulsion). In contrast to the highly water-swollen hydrogels designed for protein delivery, these materials exhibited much higher mechanical strength, they were therefore proposed for load-bearing applications, such as augmentation of collagenous or cartilaginous tissues.(99)

PEG bis(vinyl sulfone)s were used in combination with cysteine-functionalized recombinant proteins containing sequences for integrin receptor ligation for the preparation of cell-adhesive hydrogels aimed to tissue repair application. Non-degradable and degradable networks were designed, with the latter containing protease cleavable units.(100) The cross-linking kinetics of these hydrogels could be controlled by pH and the presence of charged amino acid residues in close proximity to the cysteine residue, which modulated the pK_a of the thiol group.(101) In a follow up paper, Hubbell *et al.* synthesized hydrogels comprising multiarm vinyl sulfone-terminated PEG, a monocysteine containing adhesion protein, and a bis(cysteine) metalloprotein substrate protein (MMP). These hydrogels were studied for tissue engineering purposes and both cells and vascular endothelial growth factor (VEGF$_{105}$) were encapsulated in the hydrogel. **Figure 4** shows the stepwise formation of the hydrogel containing the adhesion proteins and the MMP substrate proteins as well as the attack on the substrate protein by a metalloprotease.(102) Michael addition reaction was also used as a curing agent in hyaluronan hydrogels. Jin *et al.* showed that solutions of HA conjugates containing thiol functional groups (HA-SH) and PEG vinylsulfone (PEG-VS) macromers were cross-linked via Michael addition to form a 3D network under physiological conditions. Gelation times varied from 14 min to less than 1 min, depending on the molecular weights of HA-SH and PEG-VS, degree of substitution (DS) of HA-SH and total polymer concentration. Good chondrocyte viability and differentiation was shown in these gels.(103) A novel sustained release formulation for erythropoietin (EPO) was developed by Hahn *et al.* using hyaluronic acid (HA) hydrogels crosslinked by Michael addition. Adipic acid dihydrazide grafted HA (HA-ADH) was synthesized and subsequently converted into methacrylated HA (HA-MA) by reaction in water medium with methacrylic anhydride and subsequent isolation by ethanol precipitation. EPO was loaded into hydrogels during hydrogel preparation by reacting HA-MA

with two different cross-linkers, dithiothreitol (DTT) and thiols groups containing peptide linker. The gelation time was about 30 min and 180 min for peptide linker and DTT, respectively. The faster reaction kinetics of HA-MA with the peptide linker was ascribed to the positive charges of the amino acids adjacent to the thiol groups, which accelerated the Michael addition, as also observed by Lutolf *et al*.(104) Approximately 90% of EPO was released *in vitro* from both hydrogels degraded by hyaluronidase SD (HAse SD) and the kinetics showed a rapid phase of release during the first two days, followed by a slower phase for the next 7 days. *In vivo* release tests of EPO from HA-MA hydrogels crosslinked with the peptide linker confirmed an elevated plasma concentration of EPO for 7 days. (105-106)
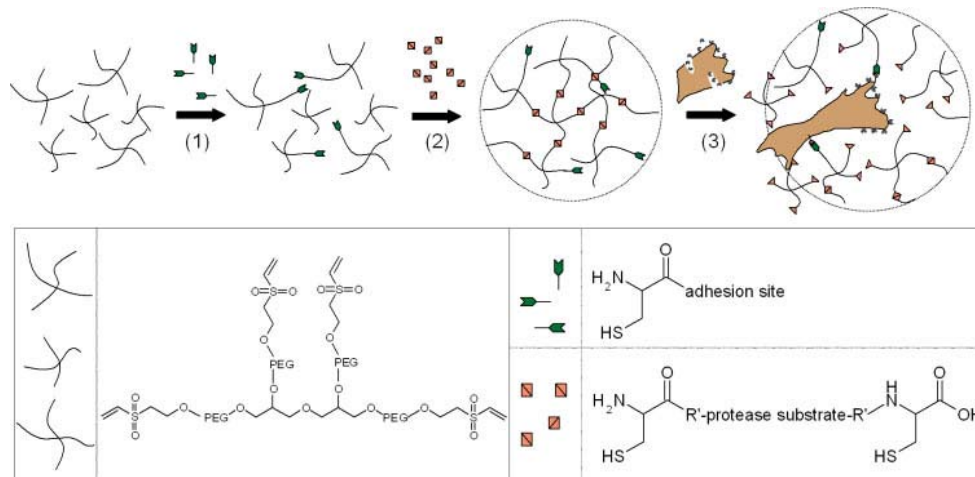

Figure 4. 1) Vinyl sulfone-functionalized PEGs were modified via Michael type addition reaction with mono-cysteine adhesion peptides and 2) bis-cysteine MMP substrate peptides was used to form gels from aqueous solutions in presence of cells and VEGF$_{105}$. 3) These elastic networks were designed to locally respond to protease activity at cell surface. Reproduced from (102)

Cellesi *et al.* have described the simultaneous thermal gelling and Michael addition cross-linking of linear and tetra-arm pluronic, which exhibits a reverse thermal gelation in water solutions at physiological temperature and pH for the design of a synthetic substitute of alginate. Pluronic was derivatized with thiol or electron poor olephins and when these two polymers were combined, a simultaneously thermally and chemically cross-linked hydrogel was formed. The thermal gelation at 37°C provides hardening kinetics similar to that of alginate. With slower kinetics, the chemical cross-linking then develops an irreversible and elastic gel structure, which in turn determines the transport/release properties of loaded compounds.(107) **Figure 5** shows the gelation chemistry of the described hydrogel. The hydrogels showed very high diffusivity(108) and these materials were also investigated for the preparation of beads and liquid core

hydrogel based nanoparticles for drug encapsulation.(109)
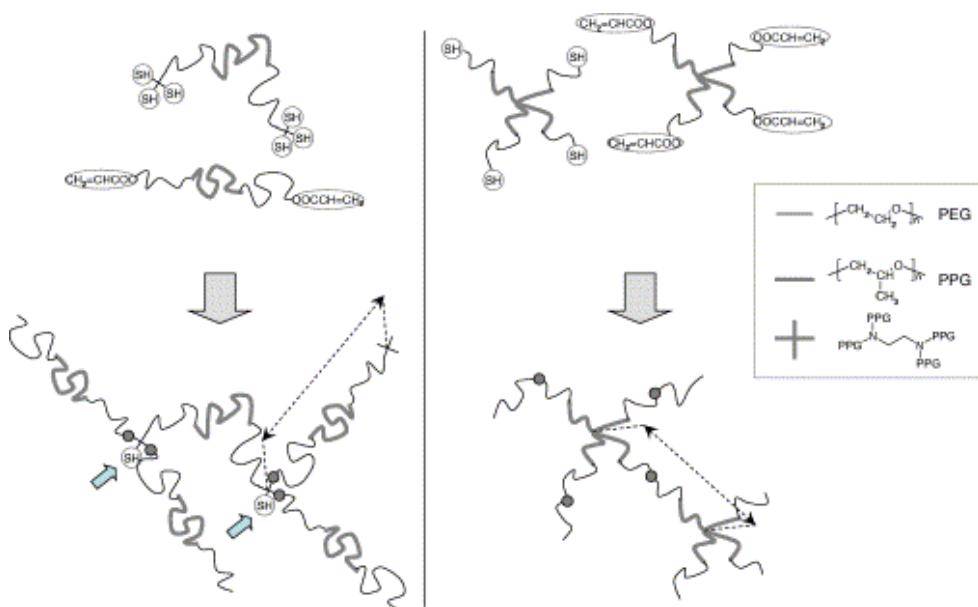
Figure 5. Linear (on the left) and tetramer (on the right) triblock copolymers of pluronic (PEG-PPG-PEG) were functionalized with two groups of clustered thiols or with two acrylates, respectively. Reproduced from reference (108).

Injectable physically and chemically cross-linked hydrogels using Michael addition were developed by Lee *et al*. A thermosensitive copolymer of *N*-isopropylacrylamide (NIPAAm) and hydroxyethyl methacrylate (HEMA) with an LCST of 32 °C was synthesized and converted to poly(NIPAAm-co-HEMA-acrylate)by reaction of some the hydroxyl groups with acryloyl chloride. When the obtained poly(NIPAAm-co-HEMA-acrylate) was mixed with pentaerythritol tetrakis 3-mercaptopropionate (QT) stoichiometrically in a 0.1 N PBS solution of pH 7.4 and 37 °C, a temperature-sensitive hydrogel was formed through the Michael-type addition reaction. The hydrogel had a low swelling and showed improved elastic properties at low frequency compared to the control physically crosslinked gels.(110) Later, Robb *et al.* copolymerized NIPAAm with *N*-acryloxysuccinimide (NASI) via free radical polymerization. The synthesized poly(NIPAAm-co-NASI) was further modified to obtain poly(NIPAAm-co-cysteamine) through a substitution reaction of NASI by the amine group of cysteamine. In addition to thermoresponsive physical gelling due to the presence of NIPAAm, this system also chemically gels via a Michael-type addition reaction when mixed with poly(ethylene glycol) diacrylate. The presence of both physical and chemical gelation resulted in material properties that are much improved in comparison to the corresponding physical

gels.(111-112) Similarly, poly(NIPAAm-*co*-PEG-acrylate) based hydrogels that simultaneously physically and chemically cross-linked (Michael addition) were developed by Vernon *et al*.(113) Very recently, Wang *et al*. described the preparation of thermosensitive Michael addition cross-linked injectable thiol- and vinyl-modified poly(*N*-isopropylacrylamide) (PNIPAAm)-based copolymer hydrogels for biomedical applications.(114)

2.3. Stimuli sensitive polymers for *in-situ* gelling systems

Stimuli sensitivity has been widely applied for the design of injectable *in-situ* forming hydrogels, with pH and temperature responsive systems being the most attractive biomaterials. In the past 10-15 years research has shifted its interest from the research area of implantable materials to the fast-developing field of injectable *in-situ* gelling systems. *In situ* forming hydrogels (**Figure 6**) exist as viscous but still liquid aqueous solutions prior to administration but abrupt turn into gels upon administration.(115-118) In contrast to permanent networks formed by chemical cross-linking, stimuli-sensitive hydrogels are transient physical networks that can be reversibly transformed into solutions by varying the environmental conditions. The advantages of these delivery systems, able to form macroscopic drug-encapsulating gels at the site of injection, include improved patient compliance, cost reduction compared to surgical intervention and ability to overcome all the limitations associated with drug post-loading techniques.
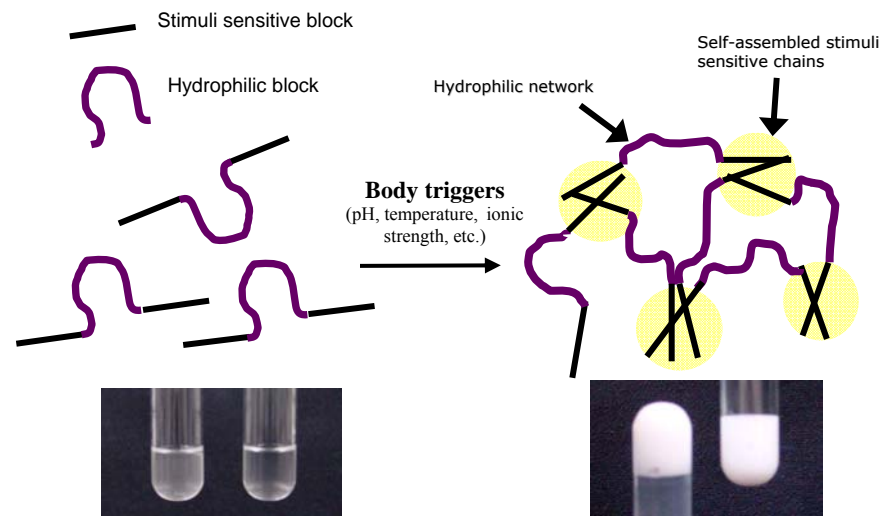

Figure 6. Self-assembly mechanism of stimuli sensitive hydrogels

2.3.1. Temperature sensitive hydrogels

Temperature is the most widely used stimulus in environmentally responsive hydrogels. Temperature-responsive polymers are characterized by a critical gelation temperature in aqueous solutions, where self-assembly of the polymer chains owing to hydrophobic interactions, thus phase separation is observed. Polymers can display Lower Critical Solution Temperature (LCST) or Upper Critical Solution Temperature (UCST), when the polymer solution is phase separated above or below a specific temperature, respectively. Thermosensitive behavior is generally viewed as a phenomenon governed by the balance of hydrophilic and hydrophobic moieties on the polymer chain.(119-120) Most of the polymers studied for biomedical applications exhibit LCST behavior, with a few exceptions, for example natural polymers like gelatin and polysaccharides like agarose or cellulose derivatives.(121-123) Only a few natural polymers display LCST behavior in the range between room and body temperature. Some cellulose derivatives (methyl and hydroxypropyl methylcellulose) at low concentrations (1-10 wt%) are liquid at low temperature, but jellify upon heating, however their gelation temperature is far above body temperature, representing a limitation of this material as *in-situ* gelling systems.(124) Chemical and/or physical modification can be adopted to lower the gelation temperature, for example by addition of NaCl or decreasing the hydroxypropyl molar substitution of hydroxypropyl methylcellulose.(124-125) However, no studies on protein release with these systems have been published to date. Chitosan has been reported by Chenite *et al.* to form a gel close to body temperature and at physiological pH when combined with glycerol phosphate disodium.(126) Bhattarai *et al.* developed a chitosan-PEG co-polymer (chitosan-*g*-PEG) injectable, thermoreversible gel that utilized intermolecular chitosan chain interactions for gelation. This hydrogel was used as a depot system for sustained protein release.(127) This type of thermosensitive gelation has also been observed in cellulose derivatives grafted with hydrophilic moieties.(128)

Synthetic polymers offer many more opportunities as compared to natural polymers for the design of injectable hydrogels. The most frequently studied synthetic thermsosensitive polymer for biomedical and pharmaceutical applications is poly(*N*-isopropylacrylamide) (PNIPAM), because its LCST in water is 32° C, thus suitable for *in-situ* gelling (**Figure 7**).(120) The incorporation of hydrophilic monomers in pNIPAM increases the LCST whereas more hydrophobic units decreases it.(129) Similar behavior was observed by Vermonden *et al.*, who reported a decrease in LCST of poly(hydroxylpropyl methacrylamide lactate) (pHPMAm-lac) upon introduction of hydrophobic methacrylate moieties in the polymer lactate side chains.(130) Similarly, the gelation behavior of poly(d,l-lactide-*co*-glycolide)–poly(ethylenglycol)–poly(d,l-lactide-*co*-glycolide) (PLGA-PEG-PLGA) was influenced by the hydrophobicity of end caps (hydroxy, acetyl, propionyl, and butanoyl groups); an increase in the hydrophobicity of the copolymer lowered the transition temperature.(131) The same finding was obtained with cholesterol end-capped star PEG-PLLA copolymers.(132)
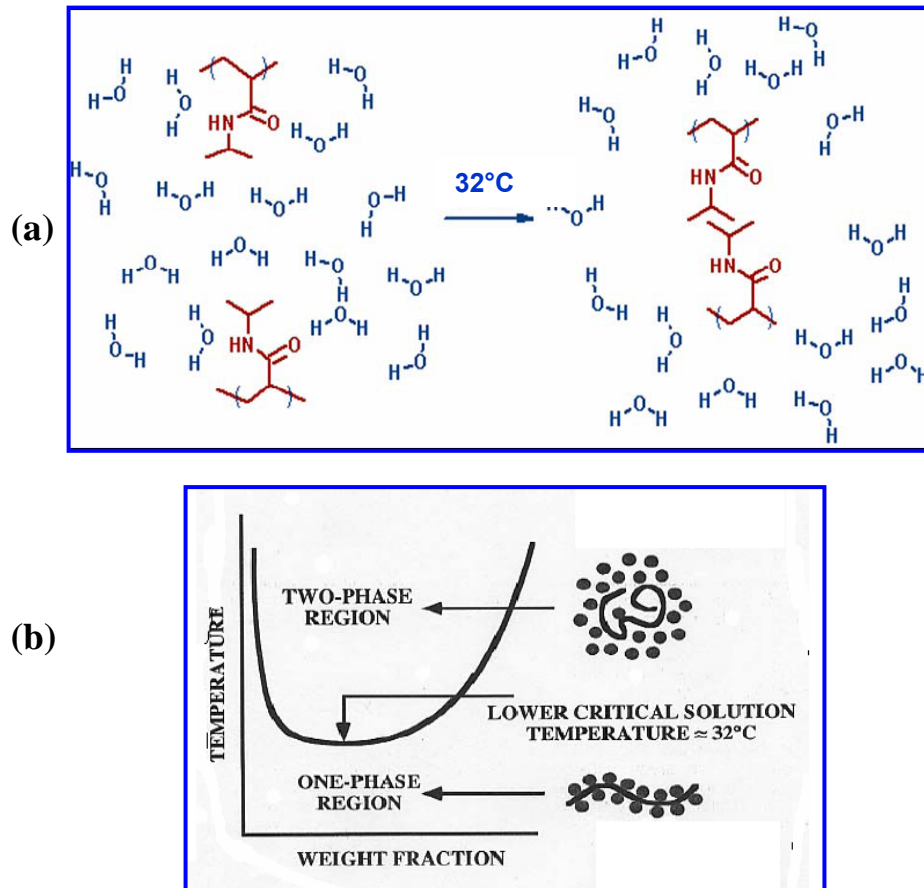
Figure 7. (a) Thermosensitive behavior of PNIPAM. Below its LCST (32 °C) the polymer is soluble in aqueous medium, because of hydrogen bond formation of the amides of the polymer and water molecules; above the LCST, the polymer becomes insoluble in medium, self-assembling by hydrophobic interaction.(b) Phase transition of PNIPAM as a function of temperature and polymer weight fraction.

Physically crosslinked PNIPAM-based hydrogels were described for the first time by Han *et al.*(133), who synthesized poly(N-isopropylacrylamide-co-acrylic acid) (p(NIPAM-*co*-AA)) to prepare thermosensitive matrices, that were used in follow-up studies for biomedical purposes, particularly as synthetic matrices in refillable bioartificial pancreas. Encapsulated Langeran islets showed good viability, and the cell-laden artificial matrices showed insulin release.(134-136). Similarly and more recently, p(NIPAM) networks were cross-linked using *N*, *N'*-methylenebisacrylamide (BIS) and used for bovine serum albumin (BSA) release studies *in vitro.* The release of the protein was not complete and a strong interaction between polymer and protein was proposed as the reason for the non-retrieved protein.(137) Kim *et*

al. described the use of pH/thermosensitive polymeric beads based on terpolymers of NIPAM, butyl methacrylate (BMA) and acrylic acid (AA) (pH-sensitive) to modulate release of insulin. A high loading efficiency was accomplished (90-95%) and while no release of insulin was observed at pH 2.0 and 37° C, the drug was released at physiological pH.(138) The release rate and mechanism depended on the molecular weight (MW) of the polymer: low MW terpolymers eroded very quickly and released insulin within 2 hours by an erosion mediated mechanism, while in case of high MW polymer, which had a better stability, the gels showed a release a insulin for 8 hours that was governed by swelling/diffusion.(138) As observed for many other thermally assembled polymers, the stability of such hydrogels is rather poor and represents a major limitation in the use of these materials for pharmaceutical purposes. Therefore, in recent years, strategies to improve the stability of thermosensitive networks by chemical cross-linking methods, suitable for *in-situ* gelling, have been exploited. Examples of such methods are photopolymerization or Michael Addition reaction discussed in sections 2.2.1 and 2.2.2, respectively.(108, 110-111, 130, 139-141)

PNIPAM-based hydrogels self-assembling in a thermoreversible fashion and displaying improved hydrophilicity, thus enhanced capability to retain water within the hydrogels matrix, were synthesized by grafting NIPAM to permanently hydrophilic polymers like poly(ethylenglycol) (PEG), for example via Ce^+/OH redox initiated free radical polymerization.(142-143) A series of polymers with different architectures were syntheszied (AB, BAB, $A(B)_4$, and $A(B)_8$ linear and star-shaped block copolymers with PEG as A block and PNIPAM as B block), and characterized for gelation mechanism and exploited for chondrocytes immobilization.(144) Several other copolymers of PNIPAM with poly(2-methacryloyloxyethyl phosphorylcholine) (PMPC) were synthesized and characterized.(145-146)

Other non-degradable thermosensitive polymers exhibiting hydrophilic-hydrophobic transition at temperatures close to body temperature are poly(vinyl ether)s (PVEs), their derivatives and copolymers (147) are excellently reviewed elsewhere(148) and are beyond the scope of this review as data on pharmaceutical and biomedical applications to date are lacking.

A series of polymers, namely Pluronic® (BASF), based on poly(ethylene oxide)-*b*-poly(propylene oxide)-*b*-poly(ethylene oxide) triblock copolymers (PEO–PPO–PEO), with varying PEO/PPO molecular weights and contents, exhibit LCST behavior below body temperature (149) and have been extensively investigated for their physical-chemical and thermodynamic properties, and pharmaceutical applications (150-153). Pluronics have been extensively used as *in-situ* forming drug delivery matrices and the possibility to prolong to some extent the drug pharmacokinetics by using Pluronic-based hydrogels was demonstrated. For example, similarly to NIPAM, monoamino-terminated Pluronic (mainly Poloxamer PF127) was coupled to poly(acrylic acid) (PAA) using dicyclohexyl carbodiimide (DCC) and graft copolymers of poly(acrylic acid)-*g*-Pluronic of different MW were synthesized via chain transfer reactions.(154) These graft copolymers gave improved gelation and mechanical properties as

compared to the corresponding Pluronic, due to the presence of pH-sensitive moieties (PAA), that affect ionization and chain expansion of the polymer. Pluronic-based copolymers were widely studied for the delivery of protein and peptide therapeutics, like insulin, interleukin-2, urease, epidermal growth factor, endothelial cell growth factor, etc. Sustained release over several hours was observed with possibility to tailor the release kinetics by polymer concentration or addition of excipients.(155-159) However, Pluronics, as well as pNIPAM, are not ideal biomaterials for *in vivo* applications. Besides toxicity issues, observed with Pluronics in intraocular implantation,(160) their main disadvantage is their non-biodegradability that makes surgical intervention necessary to remove the delivery system from the body after the drug has been released. In addition, weak mechanical strength and stability, as well as high permeability for entrapped compounds are further limitations associated with the use of these polymers. Some of the listed drawbacks were partially overcome; to mention, Cohn *et al.* copolymerized PEG and PPO segments using two synthetic pathways: 1) chain extension of native Pluronics with hexamethylene diisocyanate (HDI) and 2) covalent binding of PEG and PPO chains using phosgene as the connecting molecule. The multiblock copolymers synthesized displayed remarkably improved mechanical properties as compared to Pluronic, moreover an extension of the drug release time (release of RG-13577 up to 40 days) as compared to self-assembled Pluronic hydrogels.(161) However, biodegradability issues still exist.(162) Many block copolymers of Pluronics with polyesters (PLA and PCL) were also reported.(163-165)

The most advanced thermosensitive delivery systems for proteins rely on biodegradable polymers, which is very advantageous for *in-vivo* applications.

Biodegradable and biocompatible PEG/polyester block copolymer hydrogels, initiated by Kim and coworkers,(166) were introduced in 1990s as a novel class of biodegradable thermosensitive matrices. ABA-type PEG–poly(l-lactide)–PEG triblock copolymers (PEG–PLLA–PEG) were first synthesized by ring-opening polymerization of l-lactide (LLA) using the monomethoxy PEG (MPEG) as macroinitiator; then the PEG–PLLA–PEG triblock copolymers were obtained by coupling MPEG–PLLA using hexamethylene diisocyanate (HMDI). These polymers exhibited UCST, therefore the drug loaded hydrogels were prepared at 45° C and then gelation is induced by lowering the temperature below 37 ° C. The release of fluorescein isothiocyanate (FITC) labeled dextran was studied and it was demonstrated that 12 days sustained release was achieved for 35 wt% hydrogels. Formulations of lower polymer content showed burst release that could be decreased by increasing the polymer concentration. Also a series of star-shaped PLLA–PEG block copolymers were synthesized by coupling star PLLA with monocarboxy-MPEG using DCC coupling reaction.(167) The main disadvantages of this system are the long degradation time due to PLLA crystallinity and the need for high temperatures for the preparation of the hydrogels, as the polymer exhibit UCST behavior. Under these conditions the structure of labile protein molecules, along with their activity might be affected.

The next generation of PEG/polyesters hydrogels were based on PEG-PLGA-PEG triblock copolymers.(168) These materials displayed both LCST and UCST behavior and were processable avoiding the use of high temperatures to dissolve the polymer. The hydrogel stability upon subcutaneous injection *in vivo* was demonstrated using rat models and one month stable matrices were obtained.(169) TGF-β1 was loaded into these hydrogels and used as a reservoir for controlled drug release aimed for wound healing purposes.(170) Significantly high levels of re-epithelialization, cell proliferation and collagen organization were observed. The sustained release of synthetic drugs like ketoprofen and spirolactone was also studied from PEG-PLGA-PEG hydrogels(171), as well as release of insulin, porcine growth hormone and glycosylated granulocyte colony stimulating factor (*in vitro* and *in vivo*).(172-173) Taken together, all these studies confirmed an improved stability and capability to release drugs over an extended period of time (weeks) as compared to Pluronics formulations. More detailed overviews of the characterics and efficacy of this type of copolymers can be found in other reviews.(148, 151)

Several other thermosensitive copolymers of PEG with aliphatic polyesters were synthesized and applied for drug delivery. Some examples are AB, ABA, BAB copolymers of PEG with caprolactone (PCL) and δ-valerolactone (PVL).(174-177) The *in vitro* and *in vivo* release of fluorescein isothiocyanate-labeled bovine serum albumin (BSA-FITC) was studied from PEG-PCL diblock copolymers gels and compared to Pluronic gels, demonstrating longer in vivo stability of PEG-PCL hydrogels and enhanced capability to provide sustained protein release over 10 days, as compared to Pluronic gels, where destabilization and drug release within 3 days was observed.(178-179)

Mikos *et al.* proposed the synthesis of PEG-based triblock copolymers consisting of poly(propylene fumarate) (PPF) as middle block.(180) Compared to other PEG copolymers, the use of PPF has the advantage of having unsaturated double bonds, suitable for stabilization of the hydrogels by chemical cross-linking of the hydrogels. Biodegradable multiblock amphiphilic and thermosensitive poly(ether ester urethane)s consisting of poly-[(R)-3-hydroxybutyratel (PHB), poly(ethylene glycol) (PEG), and poly(propylene glycol) (PPG) blocks were synthesized by Loh *et al*. Their aqueous solutions were found to undergo a reversible sol-gel transition by micellar packing upon temperature changes at very low copolymer concentrations (2-5 wt%) and the authors envisioned that these systems are suitable for protein delivery.(181), Recently Pluronic analogs, containing middle blocks of poly(hexamethylene adipate) (PHA), poly(ethylene adipate) (PEA), and poly(ethylene succinate) (PESc) instead of PPO were synthesized. Because of the hydrophobic nature of PHA and PEA, strong hydrophobic interactions and micellization occurred, leading to formation of hydrogels only at high concentrations, while the more hydrophilic PESs showed gelation at low concentrations.(182) A general drawback of some of these polyester-based copolymers is their very long degradation time (i.e. PCL degrades in vivo in 2 to 4 years(183)), that leads to

polymer accumulation in the body for long periods, limiting the use of these materials for chronic diseases, where controlled delivery systems need to be administered repeatedly.

In 2004, Hennink *et al.* introduced a new class of thermosensitive and biodegradable polymers based on pHPMAm-lac that displays tunable LCST behavior from ~ 10 to 60° C by simply changing the length of the lactate side chains.(184) The polymer biodegradability is ensured by the presence of hydrolytically sensitive ester bonds in the lactate side chains. When the terminal lactate group is cleaved by hydrolysis, the resulting polymer becomes water-soluble and can be eliminated by renal filtration, as long as its molecular weight is lower than the renal cutoff.(185) These thermosensitive polymers have been coupled to PEG by free radical polymerization using a PEG macroinitiator and yielding a copolymer with ABA triblock architecture, consisting of inner PEG B-block flanked by outer p(HPMAm-lac) A-blocks. These polymers are suitable for the preparation of *in-situ* gelling systems, (186) whose mechanical properties and degradation behavior were improved by combining thermal self-assembly with photopolymerization upon polymer derivatization with methacrylate moieties.(130) As described in chapters 3 and 4, the chemically stabilized hydrogels were suitable as controlled protein delivery, where model proteins were released according to diffusion governed kinetics, easily tailorable from 1 week to 2 months by changing polymer molecular weight, concentration and degree of derivatization with methacrylate groups.(86, 187-188) The potential of this thermosensitive hydrogel for tissue engineering was assessed by demonstrating good viability and differentiation of human Mesenchymal Stem Cells (hMSCs).(187) It was further demonstrated that by randomly copolymerizing p(HPMAm-dilactate) and NIPAM, a biodegradable thermosensitive polymer was yielded.(141)

Emerging thermosensitive hydrogels in the field of protein delivery are also biodegradable polyphosphazenes, consisting of a hydrophilic PEG block and hydrophobic amino acids or a peptide block (L-isoleucine ethyl ester (IleOEt), D,L-leucine ethyl ester (LeuOEt), L-valine ethyl ester (ValOEt), or di-, tri-,and oligo-peptides in the side groups.(189-191) Hydrogels were formed by intermolecular association of hydrophobic peptide chains and when PEG was coupled to di-, tri-,and oligo-peptides as side groups, hydrogels of higher mechanical strength were obtained as compared to PEG-IlaOEt polymer gels. Polymers containing depsipeptide (GlyGlycOEt) showed faster hydrolytical degradation because of the generation of carboxylic acid groups that made the polymers more hydrophilic, resulting in sustained release FITC-dextran and human serum albumin *in vitro* for about 2 weeks. The authors also studied strategies to decrease the burst release from polyphosphazene hydrogels by addition of chitosan that due to its positive charge retained negatively charged proteins like BSA, gelatin type B (GB20), and FITC-BSA within the hydrogel network (192) Application of these hydrogels as extracellular matrix for artificial pancreas was investigated.(193)

Finally, polypeptides are important biodegradable and biocompatible polymers having a variety of conformations, such as α-helix, β-sheet, and random coil and they lend themselves for the synthesis of building blocks for the preparation of thermosensitive hydrogels with

potential biomedical applications. Tirrell *et al.* introduced a polymer consisting of leucine zipper terminated protein flanking a central, flexible, water-soluble polyelectrolyte segment. Formation of coiled-coil aggregates of the terminal domains in near-neutral aqueous solutions triggers formation of a three-dimensional polymer network, with the polyelectrolyte segment retaining solvent and preventing precipitation of the chain.(194) Kopeček *et al.* reported a hybrid hydrogel system assembled from water-soluble synthetic polymers and a coiled-coil protein-folding motif. These hydrogels underwent temperature-induced collapse owing to the cooperative conformational transition of the coiled-coil protein domain.(195) Shortly later, amphiphilic diblock copolypeptide that assembles into a gel both by supramolecular and thermal association were reported by Nowak *et al.*(196) Jeong *et al.* developed L/DL poly(alanine) (PA) end-capped poly(propylene glycol)-poly(ethylene glycol)-poly(propylene glycol) (PLX) (PA-PLX-PA) polymers that in aqueous solutions underwent a sol-to-gel transition at increasing temperature by increase in β-sheet content of PA and dehydration of PLX. This system was stable *in vivo* for over 15 days.(197) Physically crosslinked poly(amino acid) hydrogels, formed by a sol-gel transition of amphiphilic poly(N-substituted α/β-asparagine)s in an aqueous solution was described by Tacheuchi *et al.*(198) while recently Jeong *et al.* described amphiphilic polymers consisting of the hydrophilic poly(N-vinyl pyrrolidone) (PVP) block and a hydrophobic poly(alanine) (PA) block that formed micelles in water which aggregated as the temperature increased to yield gels. They demonstrated the use of PVP as an alternative to PEG to design reverse thermo-gelling biomaterials.(199)

2.3.2. pH sensitive polymers

Due to the specific pH range occurring at physiological, pathological or sub-cellular sites such as stomach, intestine, endosome/lysosome, tumor sites etc. pH is another very important stimulus used for the design of *in-situ* gelling hydrogels.

Suitable polymers for this purpose are those bearing weak polyelectrolyte (polyacid, polybase) or polyampholyte sequences. pH sensitive polymers rely on the protonation/deprotonation equilibrium which depends on the pK_a of the acidic and/or basic moieties present in the polymer. Therefore, a pH sensitive polymer can be charged (yielding a swollen state) or uncharged (hydrophobic/collapsed state) depending on the environmental pH.

Hydrogels comprising poly(methyl methacrylate) (PMAA) grafted to PEG (P(MAA-*g*-EG)) showing pH sensitivity due to complex formation and dissociation, have been used as drug-delivery carriers for salmon calcitonin.(200-201) Recently, hydrogels that assembled at physiological pH were synthesized by grafting hydrophobic palmitoyl sequences to a biodegradable chitosan backbone. Hydrogelation was controlled by the degree of *N*-palmitoyl substitution and the pH. A 15% derivatized chitosan of 1 wt % concentration in aqueous system showed gelation upon increasing pH from 6 to 7.5, due to a transition from local

micelles to interconnected nanodomains. An *in vivo* study showed the actual formation of a gel at the site of injection, demonstrating potential for biomedical applications.(202)

2.3.3. *pH/temperature sensitive hydrogels*

PH/temperature-sensitive copolymer hydrogels are prepared by introducing pH-sensitive moieties in a temperature-sensitive polymer. A pH/thermo-sensitive ABA copolymer was obtained by introducing carboxylic acid groups end groups into of PLGA–PEG–PLGA triblock copolymers. Although the non-modified triblock copolymer did not exhibit gelation upon increase of temperature, the carboxyl-capped PLGA–PEG–PLGA led to four states (sol, gel, precipitate, and turbid sol) depending on pH and temperature.(203)

PH- and temperature-sensitive multiblock poly(ester amino urethane)s were synthesized by coupling poly(amino urethane) (PAU) through a condensation reaction to PCL-PEG-PCL triblock copolymers to yield multiblock copolymers (PCL-PEG-PCL-PAU)$_n$. The incorporation of the ionizable PAU segments in the macromolecule induced pH sensitivity due to the tertiary amine moieties. Thus below pH 6.9 the polymer is in a sol state in aqueous solution up to 60 °C due to of the electrostatic repulsion of the piperazine groups. In contrast, at physiological pH (pH 7.4) the solution displays a sol–gel transition upon increasing temperature to 37°C. The formation of the free-standing gel depended on the formation of interconnected micelles. The formation of a gel was assessed *in vivo* (204) and injectable poly(amidoamine)-poly(ethylene glycol)-poly(amidoamine) triblock copolymer hydrogels exhibiting pH and temperature sensitivity were designed for bioadhesive applications. The dual responsiveness depended upon the poly(amidoamine) outer blocks which turned from a hydrophilic into hydrophobic state upon increasing pH and/or temperature. At low pH a sol was observed up to 60 °C, while above pH 7.0 the micelles bridged, leading to the formation of a gel. *In vivo* experiments showed that upon subcutaneous injection of 12.5 wt % copolymer solution a white gel was obtained after one minute.(205)

A thermosensitive triblock copolymer composed of poly(ε-caprolactone-*co*-lactic acid)-PEG-poly(ε-caprolactone-*co*-lactic acid) (PCLA-PEG-PCLA) was synthesized by ring opening polymerization using ε-caprolacton (CL), lactide (LA) and PEG as macroinitiator. Separately, carboxylic acid terminated sulfamethazine oligomers (OSMs) were polymerized by chain transfer polymerization and coupled to terminal hydroxyl groups of the triblock copolymer, yielding a pentablock copolymer (OSMs-PCLA-PEG-PCLA-OSMs). The synthesized polymer solution showed a reversible sol-gel transition by a small pH change in the range of pH 7.4-8.0 and also by a temperature change in the region of body temperature, forming a gel at 37 °C, pH 7.4 (**Figure 8**). The block copolymers OSM−PCLA−PEG−PCLA did not form a gel at pH 8.0 in the tested temperature range (from 4 to 60 °C) because the hydrophobic interaction between PCLA−OSM blocks is perturbed by the ionized sulfonamide group of the OSM block. As the pH is decreased, most of the OSM is deionized, restoring the hydrophobic interaction

between PCLA−OSM blocks and forming a gel. By exploiting both pH and thermosensitive functionalities of the polymer, it was possible to broaden the gel window and obtain a sol between 10 and 70 °C at pH 8.0. It is clear that this solution could be injected without concerns for premature gelation in the needle and, once in the body, the physiological pH triggered the gel formation. PCLA-PEG-PCLA gels showed a drop of pH (from 7.4 to 2.2), whereas the pentablock OSMs-PCLA-PEG-PCLA-OSMs showed the capability to buffer the pH, maintaining a value of 5.5. (206-207)

Figure 8. Schematic representation of the sol–gel mechanism of the pH/temperature sensitive block OSMs-PCLA-PEG-PCLA-OSMs copolymer solution. A) pH 7.4, 37 8C; B) pH 8.0, 37 °C; C) pH 7.4, 15 °C; D) pH 8.0, 15 °C. Reproduced from reference (206)

The same group synthesized diblock copolymer hydrogels based on a basic poly(β-aminoester) (PAE) coupled to MPEG. A gel-to-sol transition at pH >6.0 was observed, when the temperature was increased, as a result of micelle packing.(208)

Another dual responsive polymer is PAE-PCL-PEG-PCL-PAE pentablock copolymer, used for the release of insulin, was prepared by Michael addition polymerization of 4,4-trimethylene dipiperidine (TMDP), PCL-PEG-PCL diacrylate, and butane-1,4-diol diacrylate (BDA). Insulin, loaded into the hydrogels, formed complexes with the polymer lowering its LCST and acting as physical cross-links which was confirmed by the longer stability of the protein loaded hydrogels as compared with the placebo gels.(209)

2.3.4.   *Other stimuli responsive polymers*

2.3.4a.   Biomolecule sensitive hydrogels

On demand release of drugs is a widely explored and particularly relevant for the release of drugs that necessitate a more complex release profile able to mimic the physiological drug concentration (E.g. insulin or hormones). Glucose sensitive hydrogels are insulin reservoirs of polymeric networks that release the drug on demand, particularly when the glucose concentration exceeds a certain level. One strategy to achieve this goal relies on the use of pH responsive hydrogels entrapping glucose oxidase, catalase and insulin. As a pH sensitive moiety, *N*,*N*-dimethyl aminoethyl methacrylate (DMAEMA) is often used. This compound is a weak and has often been introduced into copolymer hydrogels to render them pH sensitive. When glucose diffuses into the hydrogels, it is converted to gluconic acid due to the action of glucose oxidase. The formed gluconic acid causes a pH drop, responsible for the protonation of DMAEMA and swelling of the hydrogel due to increased electrostatic chain repulsions, resulting in larger pores in the gels and release of insulin.(210) A similar approach was reported using a sulfonamide based glucose-responsive hydrogel.(211) In contrast, Kitano *et al.* proposed a poly(*N*-vinyl-2-pyrrolidone-*co*-phenylboronic acid) (p(NVP-PBA) as a chemically regulated delivery system for insulin. The diol moiety on PBA is involved in the glucose sensing mechanism and is responsible for the decrease in hydrogel stiffness with increasing glucose concentration followed by insulin release.(212) Brownlee *et al.* and Kim *et a*l. pioneered the field of glucose-sensitive hydrogels using lecitin, known for its ability to bind carbohydrates. They loaded the hydrogel composed of cross-linked concanavalin A (a lectin having 4 binding sites), complexed to a glycosylated insulin in a pouch of Durapore® membrane. In presence of glucose, its competitive binding with concanavalin A triggers the release of insulin.(213-214) Hydrogel systems sensing other biomolecules like antigens and proteins have been published as well; the reader is referred to more specialized reviews in which these systems are described and discussed. (215-216)

2.3.4b   Drug sensitive hydrogels

Recently, Weber *et al*. proposed a drug-sensing hydrogel based on gyrase sub-unit B, reversibly cross-linked by coumermycin and able to release VEGF upon addition of novobiocin. The polymer forming the hydrogel is based on polyacrylamide functionalized with nitrilotriacetic acid chelating a Ni^{2+} ion to which GyrB can bind through a hexahistidine sequence. Through a mechanism of drug displacement, the addition of novobicin causes the cross-links to be partly broken , resulting in opening of the network structure and release of VEGF.(217) Antigen-sensing polymers have also been developed for the preparation of hydrogels. Miyata *et al.* reported on an semi-IPN hydrogel composed of two polymeric chains,each of them bearing either an antigen (rabbit IgG) or its specific antibody (goat anti-rabbit IgG). The presence of free target antigen induces a change in hydrogel volume followed by the release of an encapsulated protein. They demonstrated that stepwise changes in antigen concentration can induce pulsatile permeation of a model protein (haemoglobin) through the network.(218)

2.3.4c   Ionic strength responsive hydrogels

In ionic strength responsive hydrogels the sol-gel transition is triggered by the salt concentration. To give an example, poly(NIPAAm-*co*-vinylimidazole) has been used to immobilize Cu (II) ions, and aimed to bind proteins. Upon increase of ionic strength the polymer chains collapse due to reduction of repulsive forces and increase in hydrophobic interactions, leading to precipitation of specifically bound proteins to metal ions. This system can be used for protein separation.(219)

2.3.4d   Other stimuli sensitive hydrogels

UV light has been used as a trigger for the (dis)assembly of hydrogels as well as for the release of encapsulated drugs. In order to design photosensitive hydrogels, a photochrome unit (e.g. azobenzene (AZOB)) has to be incorporated in the polymer structure. Azobenzene-modified polyacrylate with different spacers between the photochrome and the backbone was synthesized and BSA was combined with the polymer in aqueous medium. In the dilute regime, BSA/AZOB complexes are formed in equilibrium with unbound BSA and the affinity of the protein for the polymer depended on the length of the hydrophobic spacer and the presence of additional n-alkyl side groups. In the semidilute regime, physical cross-linking involving BSA greatly enhanced the strength of the hydrogel. In the two regimes, light was shown to modify the binding properties due to cis-trans isomerization of the azobenzene. Reversible release of BSA (by up to 80% of the protein) was obtained by exposure to UV.(220) When a ternary gel mixture of p(AA/C_{12}), α-CD, and 4,4'-azodibenzoic acid (ADA)

was irradiated with UV light, ADA isomerized from its trans to cis form , and the mixture underwent a gel-to-sol transition because α-CD formed inclusion complexes more favorably with C_{12} side chains than with *cis*-ADA. When subsequently the ternary sol mixture was irradiated with visible light, ADA isomerized back from cis to trans and the mixture underwent a sol-to-gel transition. Furthermore, these gel-to-sol and sol-to-gel transitions occurred repeatedly by repetitive irradiations of UV and visible light.(221)

Similarly, mixtures of polyacrylamide bearing pendant AZOB moieties and βCD derivatized poly(allylamine) leads to photoresponsive hydrogels.(222) Kwon *et al.* introduced a polymeric system, which rapidly changed from a solid into a liquid in response to small electric currents, by solubilization of the solid polymer complex upon decomposition into two water-soluble polymers. The system is based on poly(ethyloxazoline) that forms complexes with poly(acrylic acid) or poly(methacrylic acid) and modulated release of insulin was achieved with this polymeric system.(223) Magnetic field sensitive gels can be obtained by incorporating colloidal magnetic particles into cross-linked hydrogels.

2.4. Protein release

2.4.1. Background

As described in section 1, traditionally, protein therapeutics are administered parenterally upon reconstitution. The drug pharmacokinetics depend on the site of administration (i.v., s.c., i.m., etc.), the physico-chemical properties (solubility, molecular weight, isoelectric point, etc.) and the elimination rate (via hydrolytic or enzymatic degradation or simply by kidney excretion). Advanced controlled delivery systems aim to improve the unfavorable protein pharmacokinetics, enhancing their therapeutic effect. The fluctuating plasma drug concentrations observed with traditional repeated bolus injections are avoided by the use of controlled releasing hydrogels that are potentially able to maintain drug levels within the therapeutic window, overcoming risks associated with potentially toxic or ineffective drug concentrations.

Generally speaking, the main mechanisms governing the protein release from hydrogels are:

1. Diffusion
2. Swelling
3. Erosion/Degradation

Of course, the different release mechanisms can also coexist.(224) The release mechanism depends on the characteristics of the polymeric network and the protein. When the hydrogel pores are bigger than the hydrodynamic radius of the protein, diffusion is the driving mechanism for release, with a diffusion rate depending on the protein size. When instead the hydrogels pores are smaller than the protein radius, swelling or erosion/degradation (bulk or

surface) are needed for release. Deviation from this behavior is observed when the hydrogel is triggered to swell/shrink by a specific stimulus, as described in other sections of this chapter or when the polymer and protein interact via non-covalent interactions (i.e. electrostatic, hydrophobic interaction, *etc*.). The release of such hydrogels depends on the dissociation rate of the protein from the polymer.

2.4.2. Diffusion controlled release

Many of the gel matrices reported to date exhibite diffusion controlled release, following Higuchi's kinetics , implying that the release is proportional to the square root of time.(225)

The protein release profiles can be generally fine-tuned in order to meet their specific medical needs. One of the most commonly used methods to modulate release is tailoring the hydrogel cross-link density. In this respect, synthetic polymers offer several advantages as compared to their natural counterparts, as both the polymer architecture and its chemical structure can be easily modulated.

Hubbell *et al.* in his pioneering work on photopolymerized hydrogels based on PEG and α-hydroxy acid showed that the diffusivity of proteins in the hydrogels decreased with PEG molecular weight and protein release was governed by a combination of diffusion and degradation. It was reasoned that the PEG molecular weight determined the hydrogel mesh size.(84, 91) In the hydrogel studied by Censi *et al.* (described in chapter 3 and 4 of this thesis) a different polymer assembly was observed, as the hydrogel was cross-linked by a tandem method: hydrophobic interactions of the thermosensitive p(HPMAm-lac) chains, followed by subsequent photopolymerization. The PEG molecular weight was varied while the thermosensitive chain length was kept constant, implying that at body temperature the hydrogels of shorter PEG blocks had a greater hydrophobicity, as compared to analogues of longer PEG molecular weight. As a result, a more extensive phase separation with formation of bigger hydrophilic pores was observed for shorter polymers. The diffusivity of BSA was higher in hydrogels with higher porosity, which was confirmed by confocal laser microscopy studies (CLSM), that revealed the existence of bigger hydrophilic micropores in hydrogels of shorter PEGs. Differences in hydrogel inner structure were clearly visible. CLSM emerged in this work, as well as in the paper by Vermonden *et al.*,(188) as a powerful technique to investigate the hydrogel's inner structure, especially in systems where phase separation into hydrophilic and hydrophobic domains is observed.

2.4.3. Degradation controlled release

Stereocomplex PEG-(PLLA)$_8$/PEG-(PDLA)$_8$ based hydrogels that showed diffusion controlled release when loaded with lysozyme, released IgG (MW = 150 kDa) in 20 days with nearly zero order kinetics, meaning that the initial mesh size of the hydrogel was bigger than

LZM hydrodynamic radius and smaller than the one of IgG, which needed matrix degradation to be released. Similarly, the release of interleukin-2 (IL-2), investigated both *in vitro* and *in vivo*, showed degradation mediated kinetics for 10 days.(226)

Pluronics gels have been used to encapsulate and release proteins, such as insulin,(159) and IL-2.(227) In both studies zero order kinetics mechanism. However, the major shortcomings of these gels, as many other physical hydrogels, are their weak mechanical strength, rapid erosion, and fast release of the therapeutics from the gel networks.(153)

A constant rate of human insulin release over two weeks was observed *in vitro* from injectable PLGA-PEG-PLGA (ReGel) systems, but incomplete release was obtained.(173) This drawback was overcome by adding 0.2% (w/v) zinc, with 90% of the loaded insulin released. A similar study was conducted with the incretin hormone glucagon-like peptide-1 (GLP-1), which was released *in vitro* from ReGel for over five days. Extended zero order release to over two weeks without burst effect was observed using zinc complexed GLP-1.(228)

Another example of an insulin releasing hydrogel is based on PAE-PCL-PEG-PCL-PAE.(209) Insulin was loaded into the matrix, forming an ionically linked insulin-PAE complex. An *in vitro* study showed an almost zero order release for up to 20 days. *In vivo* efficacy of insulin loaded gels was also assessed by implanting them sc in healthy and STZ-induced diabetic rats. The insulin-release profile showed that insulin was maintained at a constant steady-state level for 15 days in healthy rats, and further demonstrated that insulin levels were controlled by the amount of insulin loaded into the copolymer and the copolymer concentration in the hydrogel. Blood glucose and plasma insulin levels of diabetic rats showed that efficacy of the delivery system for more than 1 week with a single injection. (229)

Surface eroding self-assembled hydrogels based on PEG/chol and PEG/β-CD, showing nearly zero release of lysozyme BSA and IgG were investigated by van de Manakker *et al.* Regardless of the polymer molecular weight the proteins were released *in vitro* in approximately 200 hours (**Figure 9**). The release however, could be tailored by the polymer content of the hydrogels.(65)

2.4.4. Enhancing protein release

Although significant progress has been achieved in the development of injectable biodegradable polymeric hydrogels, some challenges still remain. Initial burst or very fast release, which is observed in many protein releasing hydrogels both *in vitro* and *in vivo*, are limiting factors for many applications. *In vivo* burst release may be ascribed to the rate of gelation of injectable *in situ* gelling systems. When the sol-gel transition is not immediate, indeed, premature leakage of the protein in the surrounding tissue prior to complete gelation might occur. Burst or fast release can be also ascribed to hydrogel network defects or inhomogeneities as well as high diffusivity.

(a)

(b)
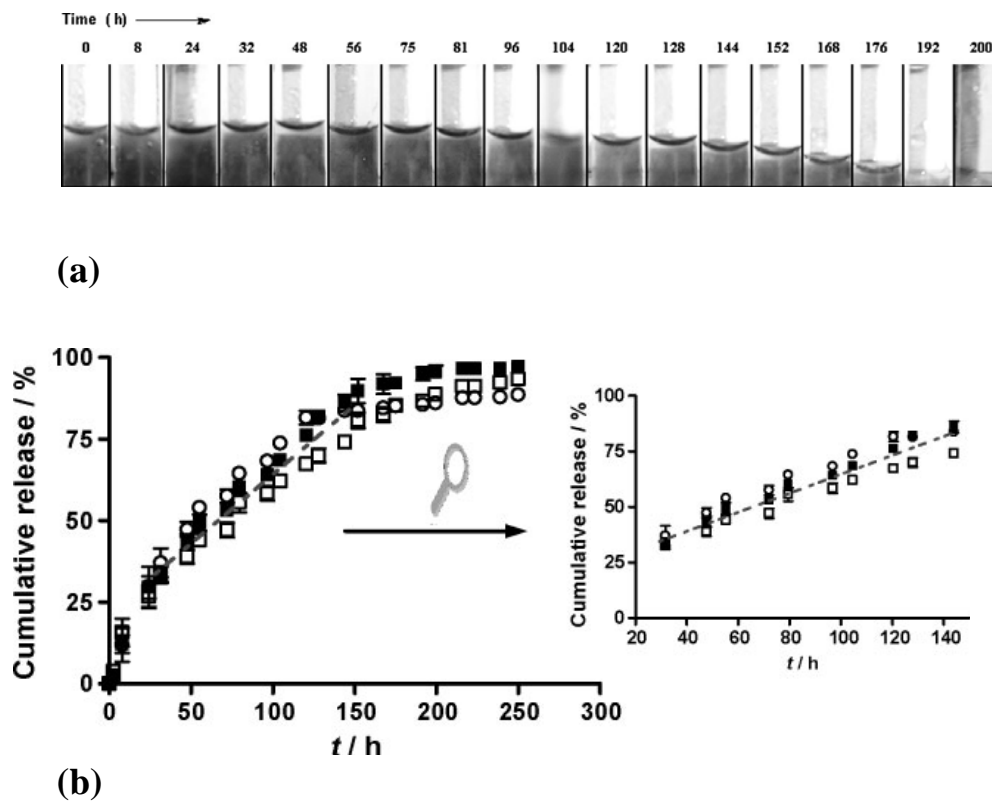
Figure 9. Surface eroding hydrogels composed of multiarm PEG-cyclodextrin/PEG-cholesterol inclusion complexes. (a) volume change in time of hydrogels loaded with dextran blue at physiological conditions (PBS, pH 7.4, 37 °C). (b) Almost zero order release kinetics of model proteins (lysozyme, BSA and IgG). Reproduced from reference (65)

Some approaches to improve hydrogel performances and overcoming burst and fast release have been proposed. Synthetic flexible polymers like the photopolymerizable thermosensitive p(HPMAm-lac)-PEG-p(HPMAm-lac) triblock, investigated by Censi *et al.* and described in section 5.2. and in chapter 3 and 4 of this thesis, showed the capability to tailor the protein release profiles by designing modular polymer structures and extend the release time according to the aimed pharmacokinetics of the drug.(187)

Another successful strategy is the introduction of functionalities in the polymer structure like charged groups or binding sites, which can prevent fast protein diffusion by polymer interaction. One example of such system has been already described in section 5.3. The release mechanism of proteins from PAE-PCL-PEG-PCL-PAE hydrogels depends on two

concomitant factors, the ionic interactions between partial positive charges in PAE blocks and negative charges in insulin and degradation of the PAE blocks.(229)

The RADA16 peptide, self-assembled by formation of β-sheet structures, first reported by Zhang (230) has been used to encapsulate and deliver several proteins for intramyocardial delivery. This peptide has also been used to deliver platelet-derived growth factor BB (PDGF-BB) (231), stromal cell-derived factor-1 (SDF-1) (232), and insulin-like growth factor I (IGF-I) (233) to decrease myocardial infarct. Also in this case, the slow and controlled release of the active proteins is due to the amphiphilic nature of the self-assembling peptide that give some interaction with loaded proteins which slows down diffusion and subsequent release kinetics.

Similarly, the release of FITC-albumin from polyphosphazene hydrogels was controlled using chitosan,(234) and was sustained over two months without an burst in the presence of chitosan, in contrast to the observed release over one month from gels without chitosan. The prolongation of release time was ascribed to the formation of an ionic complex between chitosan and FITC-albumin. The polyphosphazene hydrogel form Park *et al.* has also been used to entrap pancreatic islets,(235) which is an alternative way to overcome burst and uncontrolled release of insulin, as the protein release rate depends on the capability of cells to stay viable and produce the protein. In comparison with both rat islets entrapped in other hydrogels, and free islets, rat islets in the polyphosphazene hydrogel retained higher cell viability and showed insulin production, and consquently release of this protein from the gel for over a 28-day culture period. In a subsequent paper, polyphosphazene hydrogels were used to encapsulate hepatocytes as spheroids or single cells.(236) Over a 28-day culture period, the spheroid hepatocytes maintained a higher viability and produced albumin, whereas single hepatocytes showed lower levels of albumin secretion from the hydrogel.

An alternative approach to prevent burst release is the combination of two delivery systems in one composite matrix. For example, Leach *et al.* developed a photopolymerizable (PEG-)glycidyl methacrylate-hyaluronic acid ((PEG-)GMHA) that showed remarkable diffusivity, leading to fast release of BSA (approximately 60% within 6 hours). The release time could be prolonged to a certain extent by increasing the polymer concentration, but the longest duration of release (up to several weeks) was achieved by incorporating BSA-PLGA microparticles within the hydrogel matrix (**Figure 10**).(95) Undesired interactions between the loaded protein and the hydrogel matrix are often observed in *in situ* cross-linked matrices and sometimes leading to the incomplete release of the protein. Protein immobilization within the nondegradable networks via free-radical reaction, demonstrated by gel electrophoresis, was dependent on photoinitiator and initial protein concentration (**Figure 11**a and b). Lin *et al.* proposed a method for enhancing cumulative release of protein from photopolymerized poly(ethylene glycol) hydrogels by using a pseudo-specific protein ligand. A model was developed to predict the release behavior of BSA in the presence of the metal chelator iminodiacetic acid (IDA), used as an excipient to diminish protein-polymer interactions and thus enhance the release of BSA.
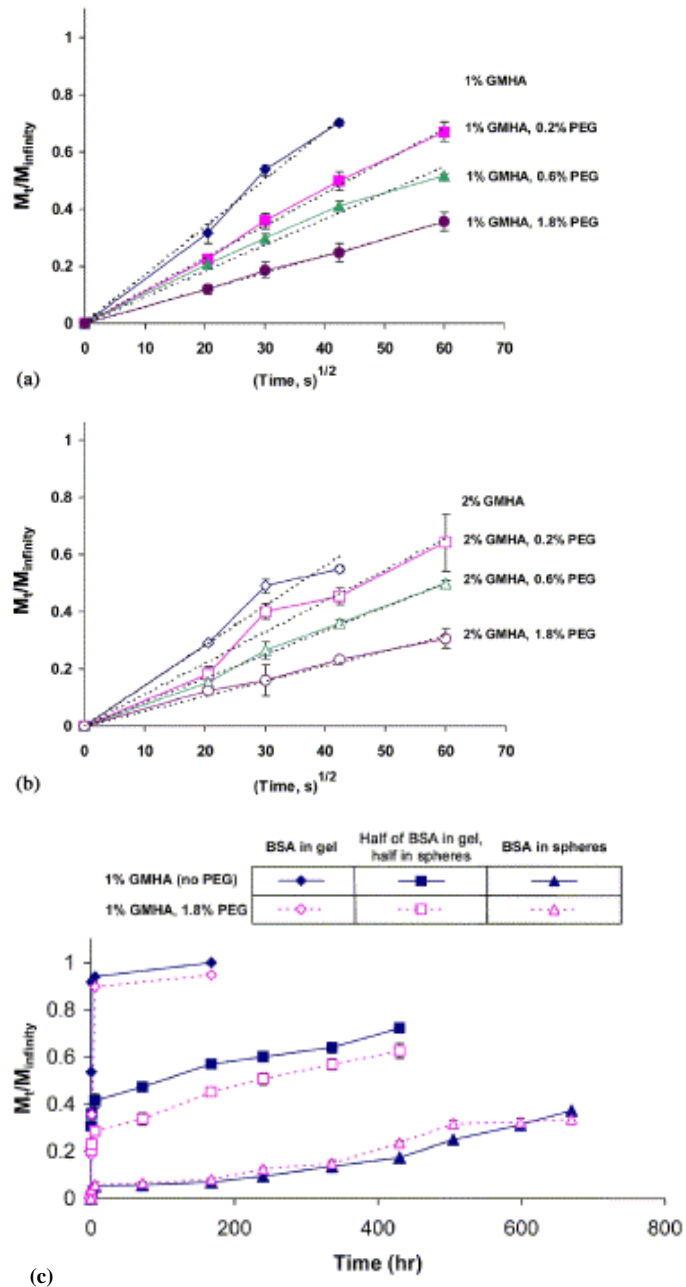
Figure 10. BSA release profiles from photo-cross-linked (PEG-)glycidyl methacrylate-hyaluronic acid hydrogels. The fast diffusive release of the protein from the hydrogels could be retarded by increasing PEG and GMHA concentration (a, b), while the incorporation of BSA encapsulating PLGA microparticles allowed extension of the release time up to several weeks (c). Reproduced from reference (95)

This model quantitatively predicts the improved release characteristics of BSA as ligand concentration and ligand affinity increase. Divalent metal ions such as copper, zinc, and nickel were also used synergistically with the IDA to evaluate the effect of ligand affinity on the extent of protein protection (Figure 11c).(89)

(a)

(b)

(c)
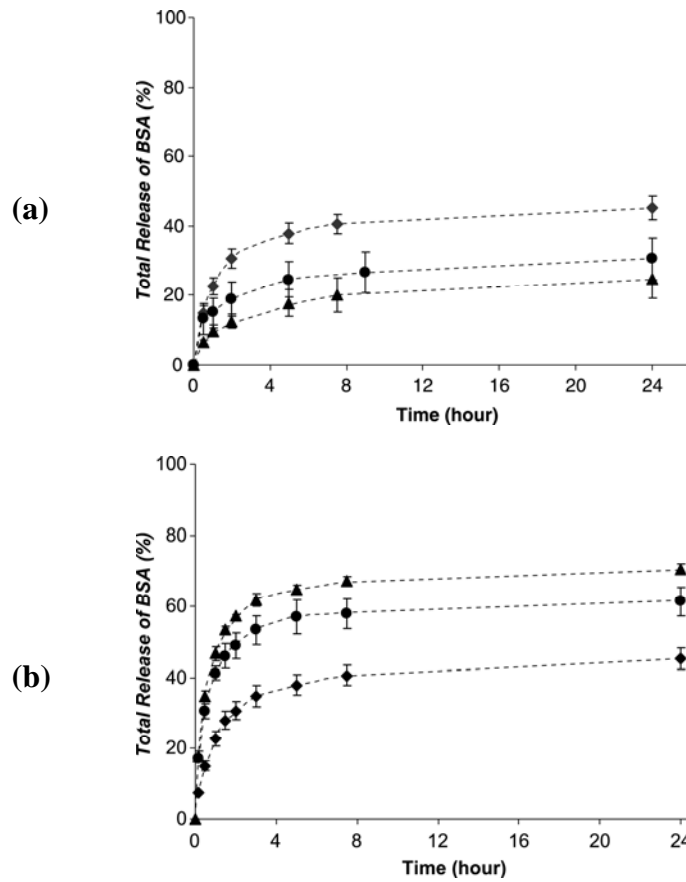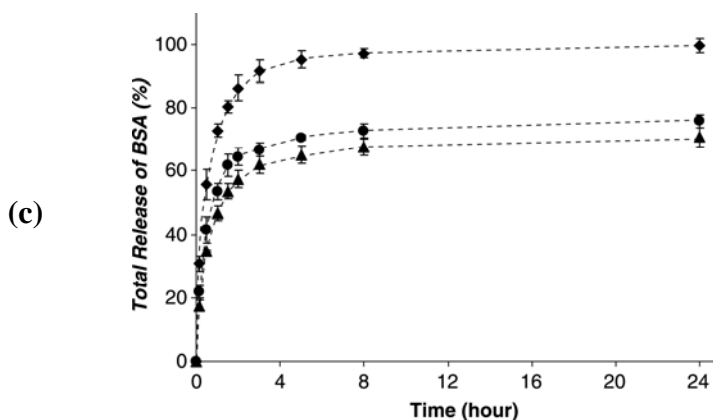
Figure 11. (a) The effect of photoinitiator concentration on BSA release. BSA release decreased with increasing photoinitiator concentration from 0.2 to 1 wt% **(b)**The effect of IDA concentration on BSA release at IDA/BSA molar ratio of 1 **(c)** Effect of Cu^{2+} concentration on BSA release. Molar ratio of IDA to BSA was kept at 1, while the molar ratio of Cu^{2+} ions to BSA were 1 (♦), 0.5 (●), and 0 (▲). Reproduced from reference (89)

2.4.5. Methods to measure release kinetics

The method generally applied to evaluate the release from gel based drug delivery systems relies on release studies. However, these experiments are time-consuming and sometimes poorly predictable because high variation among results can be observed depending on the method used for release studies *in vitro* (geometry of the dosage form, sampling method, volume of acceptor medium, swelling/degradation/erosion of the hydrogel matrix etc.). An emerging technique to investigate the mobility of molecules embedded in hydrogel matrices is analytical method named fluorescence recovery after photobleaching (FRAP).

FRAP experiments are performed on hydrogels loaded with fluorescently labeled protein, which is photobleached in small regions (typically 10-50 um^2) within the gel using an optical microscope equipped with a light source. After bleaching the probe molecules, the fluorescence intensity within the bleached region recovers due to diffusion of unbleached molecules from the surrounding and the diffusion coefficient of the protein in the matrix can then be calculated from the resulting recovery profiles.(237) FRAP experiments have already been used to evaluate the mobility of molecules in cells and biological tissues, for example, Braeckmans *et al.* explored the mobility of macromolecules in bulk three-dimensional biological materials, such as vitreous body isolated from bovine eyes and lung sputum expectorated by cystic fibrosis patients.(238) Recently, several research groups characterized hydrogel-based drug delivery systems by FRAP. Vermonden *et al*. synthesized a series of thermo-gelling p(HPMAm-lac)-PEG-p(HPMAm-lac) triblock copolymer hydrogels containing PEG's middle blocks of different molecular weight and used FRAP analysis to investigate how

macromolecular diffusion can be controlled according to polymer design, concentration and temperature. FITC-dextrans were used as fluorescent probe and the results revealed that its diffusivity decreased with increasing polymer concentration, temperature and PEG's molecular weight.(239) In another study, Branco *et al.* incorporated FITC-dextrans of different molecular weight in peptide based hydrogels, formed by peptide self-assembling in response to pH and ionic strength by formation of amphiphilic β-hairpin. Dextran mobility within and release from hydrogels of varying solid content was studied and it was found that the release was influenced by diffusion and charge interaction between dextran and peptide. Moreover the results observed in bulk release experiments correlated very well those obtained by FRAP. (240)

Similarly, the possibility to tailor the molecular architecture of galactomanna hydrogels as well as guar-drug conjugates to entrap and limit the diffusion of model drugs was researched by Burke *et al.* Also in this study FRAP experiments were a valuable tool to study to which extent the hydrogel matrix was able to restrict the drug mobility and a fast screening method to design formulations with extended release profiles.(241)

Kuijpers *et al.* performed parallel FRAP and bulk release studies to investigate the mobility of lysozyme in gelatin-chondroitin sulfate hydrogels containing 5, 10 and 20% of chondroitin sulfate. The results of lysozyme release experiments, which revealed that release was governed by diffusion and electrostatic interactions between the protein and the hydrogel matrix, were confirmed by FRAP analysis. These studies showed that the combination of chondroitin sulfate with cross-linked gelatin gels led to a significant increase in the lysozyme loading capacity of the gel and a prolonged release time (by charge interaction).(242)

A good correlation between FRAP and release data was found by Van Tomme *et al*. and Censi *et al.,* whose hydrogel systems (86, 187, 243) are described in others sections of this chapter. Surface eroding hydrogels, releasing the drug with zero order kinetics showed immobile proteins by FRAP.(65)

A more systematic comparative study between the measured diffusion coefficients by FRAP and the release kinetics was carried out recently by Brandl *et al* (**Figure 12**).(244) They used gels prepared by step-growth polymerization of PEG, loaded with FITC labeled dextrans.
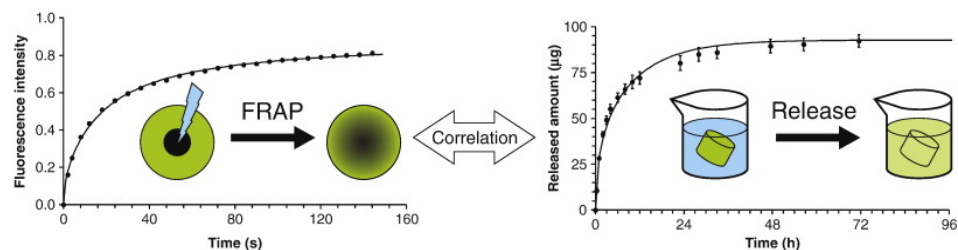

Figure 12. Schematic comparison between the classical approach of release study method and the FRAP technique.

The translational diffusion coefficients of the incorporated FITC-dextrans were measured by FRAP and pulsed field gradient NMR spectroscopy. Because the determined diffusion coefficients agreed well with those obtained from release studies, mechanical testing, FRAP, and pulsed field gradient NMR spectroscopy were proposed as alternatives to release experiments. However, although FRAP always reflects very well the relative differences in macromolecular diffusivity between hydrogels of different composition and cross-linking degree, the technique has some limitations. Quantitative correlation between the two techniques is not always possible as they rely on remarkably different setups. The time scales of FRAP and release experiments are totally different (FRAP monitors protein diffusivity for minutes while release experiments are performed over days or weeks), moreover FRAP experiments measure diffusion coefficient on a microscale level, unlike release experiments that provide data on the macrodiffusivity. Furthermore, swelling processes, often influencing the diffusion of entrapped molecules can occur only when the gel is exposed to aqueous medium in a release experiment setting; FRAP does not take swelling/matrix erosion into account. Thus, in our view, FRAP technique can be used as a complementary technique to release experiments to rapidly and qualitatively evaluate the potential of newly developed drug delivery systems for controlled release purposes.

2.4.6. Protein stability

The potential of drug delivery systems to enter the clinic and make an impact on patient's life strictly depends on their ability to release *active* proteins, besides providing their sustained release. Therefore, the assessment of protein stability needs to be implemented in the evaluation of hydrogel based delivery systems, in order to certify the pharmacological drug activity and the lack of immunogenicity. The stability of the protein has to be maintained during hydrogel preparation, storage and release.

The maintenance of protein's native structure still represents an issue for many hydrogel formulations, as very often incomplete release due to aggregation, chemical binding between protein and polymer, oxidation, deamidation, *etc.* might occur.(6)

As already mentioned, it was reported that BSA loaded in chemically cross-linked hydrogels by radical polymerization covalently coupled to the polymer, due to the role of BSA as chain transfer agent during the polymerization.(90)

A number of complementary techniques to evaluate the structural changes of proteins are available and several of those need to be combined in order to have full characterization of the protein stability. Liquid chromatography (HPLC, SEC) is one of the fundamental methods to investigate possible changes in the primary structure of the protein, including oxidation, deamidation, or the presence of (ir)reversible aggregates.

Other techniques of interest, aimed at characterizing structural changes are fourier transform infrared spectroscopy (FTIR), differential scanning calorimetry (DSC), fluorescence

spectroscopy, far and near circular dichroism (CD), *etc.* and they are reviewed in more specialized papers.(245)

2.5. Conclusions

Significant progress has been achieved in the development of injectable biodegradable polymeric hydrogels for protein delivery. In order to be eligible for clinical use, hydrogels must fulfill several requirements. They must be biocompatible, protein and cell friendly, biodegradable into excretable and non-harmful products and administered in an effective and minimally invasive manner. Importantly, they must exhibit mechanical properties and protein release behavior suitable for their specific application. Possibly, the tailorability of these properties is highly desirable. Advances in polymer chemistry allow the design of hydrogels of different topology and functionality, able to accomplish many of the demanded requisites. For example, stimuli sensitive hydrogels can modulate their behavior in response to environmental conditions (temperature, pH, ionic strength, biomolecules, drugs, *etc.*), being able to release proteins on demand or turn into a gel only upon parenteral administration. Besides stimuli sensitive hydrogels, other self-assembling systems lend themselves to be injectable, for instance stereo- or inclusion-complexed hydrogels. Chemical cross-linking can also be applied *in situ* as reaction like photopolymerization or Michael addition because these methods do not need toxic catalyst and can occur at physiological conditions (aqueous medium, pH 7.4, 37 °C). Polymer design at a molecular level allows the modulation of biodegradability, mechanical properties and release behavior in many advanced hydrogels. However, some challenges remain for achieving ideal characteristics. First of all, the parenteral administration of hydrogels must ensure *in vivo* rapid gelation and hydrogel stability during the release period, in order to avoid burst or unwanted rapid release of the drug; moreover needle clogging must be avoided. To this end, strategies comprising combinations of functionalities within a hydrogels have been applied. For instance, the combination of tandem cross-linking methods (thermosensitivity/photopolymerization, thermosensitivity/Michael addition) has been proposed as approach to achieve fast gelation and subsequent long-term stabilization of the releasing matrices. Combining thermo- and pH-sensitivity will avoid needle clogging for administration in deep sites in the body. Secondly, although the biodegradation of many hydrogels have been investigated *in vitro* and *in vivo*, the fate of the degradation products, in order to assess lack of accumulation, has been hardly studied. The release behavior of many hydrogels is still unsatisfactory and optimization is needed. Furthermore, the inflammatory reaction caused by the delivery system might be a potential limitation for their application, especially for chronic diseases treatments, where repeated administration of the depot system is envisioned. Analytical techniques and biological assays to characterize the stability of the released protein need to be implemented in order to ensure biological activity and lack of immunogenicity. Finally, although polymer

chemistry allowed the synthesis of biomaterials with appealing functionalities, sometimes translating these synthesis procedures into industrial mass-scale production can be challenging.

References

1. Goeddel DV, Kleid DG, & Bolivar F (1979) Expression in Escherichia coli of chemically synthesized genes for human insulin. *Proceedings of the National Academy of Sciences of the United States of America* 76(1):106-110.

2. Malik NN (2008) Drug discovery: past, present and future. *Drug Discovery Today* 13(21-22):909-912.

3. Holladay LA & Puett D (1976) Somatostatin conformation: evidence for a stable intramolecular structure from circular dichroism, diffusion, and sedimentation equilibrium. *Proceedings of the National Academy of Sciences of the United States of America* 73(4):1199-1202.

4. Manning MC, Patel K, & Borchardt RT (1989) Stability of Protein Pharmaceuticals. *Pharmaceutical Research* 6(11):903-918.

5. Manning M, Chou D, Murphy B, Payne R, & Katayama D (2010) Stability of Protein Pharmaceuticals: An Update. *Pharmaceutical Research* 27(4):544-575.

6. Wang W (1999) Instability, stabilization, and formulation of liquid protein pharmaceuticals. *International Journal of Pharmaceutics* 185(2):129-188.

7. Kaliyaperumal A & Jing S (2009) Immunogenicity assessment of therapeutic proteins and peptides. *Current Pharmaceutical Biotechnology* 10(4):352-358.

8. De Groot AS & Martin W (2009) Reducing risk, improving outcomes: Bioengineering less immunogenic protein therapeutics. *Clinical Immunology* 131(2):189-201.

9. Tang L, Persky AM, Hochhaus G, & Meibohm B (2004) Pharmacokinetic aspects of biotechnology products. *Journal of Pharmaceutical Sciences* 93(9):2184-2204.

10. Antosova Z, Mackova M, Kral V, & Macek T (2009) Therapeutic application of peptides and proteins: parenteral forever? *Trends in Biotechnology* 27(11):628-635.

11. Werle M, Makhlof A, & Takeuchi H (2009) Oral Protein Delivery: A Patent Review of Academic and Industrial Approaches. *Recent Patents on Drug Delivery & Formulation* 3:94-104.

12. Veronese FM & Harris JM (2002) Introduction and overview of peptide and protein pegylation. *Advanced Drug Delivery Reviews* 54(4):453-456.

13. Sinha VR & Trehan A (2003) Biodegradable microspheres for protein delivery. *Journal of Controlled Release* 90(3):261-280.

14. Jaganathan KS, Rao YUB, Singh P, Prabakaran D, Gupta S, Jain A, & Vyas SP (2005) Development of a single dose tetanus toxoid formulation based on polymeric microspheres: A comparative study of poly(D,L-lactic-co-glycolic acid) versus chitosan microspheres. *International Journal of Pharmaceutics* 294(1-2):23-32.

15. Saslawski O, Weingarten C, Benoit JP, & Couvreur P (1988) Magnetically responsive microspheres for the pulsed delivery of insulin. *Life Sciences* 42(16):1521-1528.

16. Martin MED, Dewar JB, & Newman JFE (1988) Polymerized serum albumin beads possessing slow release properties for use in vaccines. *Vaccine* 6(1):33-38.

17. Cleland JL, Johnson OL, Putney S, & Jones AJS (1997) Recombinant human growth hormone poly(lactic-co-glycolic acid) microsphere formulation development. *Advanced Drug Delivery Reviews* 28(1):71-84.

18. Okada H (1997) One- and three-month release injectable microspheres of the LH-RH superagonist leuprorelin acetate. *Advanced Drug Delivery Reviews* 28(1):43-70.

19. Anderson JM & Shive MS (1997) Biodegradation and biocompatibility of PLA and PLGA microspheres. *Advanced Drug Delivery Reviews* 28(1):5-24.

20. Shenderova A, Burke TG, & Schwendeman SP (1999) The acidic microclimate in poly(lactide-co-glycolide) microspheres stabilizes camptothecins. *Pharmaceutical Research* 16(2):241-243.

21. Fu K, Pack DW, Klibanov AM, & Langer R (2000) Visual evidence of acidic environment within degrading poly(lactic-co- glycolic acid) (PLGA) microspheres. *Pharmaceutical Research* 17(1):100-106.

22. Van De Weert M, Hennink WE, & Jiskoot W (2000) Protein instability in poly(lactic-co-glycolic acid) microparticles. *Pharmaceutical Research* 17(10):1159-1167.

23. Jiang G, Woo BH, Kang F, Singh J, & DeLuca PP (2002) Assessment of protein release kinetics, stability and protein polymer interaction of lysozyme encapsulated poly(D,L-lactide-co-glycolide) microspheres. *Journal of Controlled Release* 79(1-3):137-145.

24. Kim HK & Park TG (1999) Microencapsulation of human growth hormone within biodegradable polyester microspheres: Protein aggregation stability and incomplete release mechanism. *Biotechnology and Bioengineering* 65(6):659-667.

25. Yeo Y & Park K (2004) Control of encapsulation efficiency and initial burst in polymeric microparticle systems. *Archives of Pharmacal Research* 27(1):1-12.

26. Péan JM, Venier-Julienne MC, Boury F, Menei P, Denizot B, & Benoit JP (1998) NGF release from poly(D,L-lactide-co-glycolide) microspheres. Effect of some formulation parameters on encapsulated NGF stability. *Journal of Controlled Release* 56(1-3):175-187.

27. Péan JM, Venier-Julienne MC, Filmon R, Sergent M, Phan-Tan-Luu R, & Benoit JP (1998) Optimization of HSA and NGF encapsulation yields in PLGA microparticles. *International Journal of Pharmaceutics* 166(1):105-115.

28. Ghassemi AH, van Steenbergen MJ, Talsma H, van Nostrum CF, Jiskoot W, Crommelin DJA, & Hennink WE (2009) Preparation and characterization of protein loaded microspheres based on a hydroxylated aliphatic polyester, poly(lactic-co-hydroxymethyl glycolic acid). *Journal of Controlled Release* 138(1):57-63.

29. Ghassemi AH, van Steenbergen MJ, Talsma H, van Nostrum CF, Crommelin DJA, & Hennink WE (2010) Hydrophilic Polyester Microspheres: Effect of Molecular Weight and Copolymer Composition on Release of BSA. *Pharmaceutical Research*:1-10.

30. Couvreur P & Puisieux F (Nano- and microparticles for the delivery of polypeptides and proteins. *Advanced Drug Delivery Reviews* 10(2-3):141-162.

31. Pinto Reis C, Neufeld RJ, Ribeiro AJ, & Veiga F (2006) Nanoencapsulation II. Biomedical applications and current status of peptide and protein nanoparticulate delivery systems. *Nanomedicine: Nanotechnology, Biology and Medicine* 2(2):53-65.

32. Becher PE ed (1985) *Medical and Pharmaceutical application of emulsions* (Marcel Dekker, Inc., New York), Vol vol. 2, pp 159-238.

33. Bjerregaard S, Wulf-Andersen L, Stephens RW, Roge Lund L, Vermehren C, Söderberg I, & Frokjaer S (2001) Sustained elevated plasma aprotinin concentration in mice following intraperitoneal injections of w/o emulsions incorporating aprotinin. *Journal of Controlled Release* 71(1):87-98.

34. Masuda K, Horie K, Suzuki R, Yoshikawa T, & Hirano K (2003) Oral-antigen delivery via a water-in-oil emulsion system modulates the balance of the Th1/Th2 type response in oral tolerance. *Pharmaceutical Research* 20(1):130-134.

35. Bjerregaard S, Söderberg I, Vermehren C, & Frokjaer S (1999) Formulation and evaluation of release and swelling mechanism of a water- in-oil emulsion using factorial design. *International Journal of Pharmaceutics* 193(1):1-11.

36. Liang MT, Davies NM, & Toth I (2005) Encapsulation of lipopeptides within liposomes: Effect of number of lipid chains, chain length and method of liposome preparation. *International Journal of Pharmaceutics* 301(1-2):247-254.

37. Vyas SP, Rawat M, Rawat A, Mahor S, & Gupta PN (2006) Pegylated protein encapsulated multivesicular liposomes: A novel approach for sustained release of interferon α. *Drug Development and Industrial Pharmacy* 32(6):699-707.

38. Puri A, Loomis K, Smith B, Lee JH, Yavlovich A, Heldman E, & Blumenthal R (2009) Lipid-based nanoparticles as pharmaceutical drug carriers: From concepts to clinic. *Critical Reviews in Therapeutic Drug Carrier Systems* 26(6):523-580.

39. Stevens PJ & Lee RJ (2003) Formulation kit for liposomal doxorubicin composed of lyophilized liposomes. *Anticancer Research* 23(1 A):439-442.

40. Van Winden ECA & Crommelin DJA (1999) Short term stability of freeze-dried, lyoprotected liposomes. *Journal of Controlled Release* 58(1):69-86.

41. Yan X, Scherphof GL, & Kamps JAAM (2005) Liposome Opsonization. *Journal of Liposome Research* 15(1-2):109-139.

42. Muller RH, Mehnert W, Lucks JS, Schwarz C, Zur Muhlen A, Weyhers H, Freitas C, & Ruhl D (1995) Solid lipid nanoparticles (SLN) - An alternative colloidal carrier system for controlled drug delivery. *European Journal of Pharmaceutics and Biopharmaceutics* 41(1):62-69.

43. Del Curto MD, Chicco D, D'Antonio M, Ciolli V, Dannan H, D'Urso S, Neuteboom B, Pompili S, Schiesaro S, & Esposito P (2003) Lipid microparticles as sustained release system for a GnRH antagonist (Antide). *Journal of Controlled Release* 89(2):297-310.

44. Garcia-Fuentes M, Prego C, Torres D, & Alonso MJ (2005) A comparative study of the potential of solid triglyceride nanostructures coated with chitosan or poly(ethylene glycol) as carriers for oral calcitonin delivery. *European Journal of Pharmaceutical Sciences* 25(1):133-143.

45. Ribeiro Dos Santos I, Richard J, Pech B, Thies C, & Benoit JP (2002) Microencapsulation of protein particles within lipids using a novel supercritical fluid process. *International Journal of Pharmaceutics* 242(1-2):69-78.

46. Trotta M, Cavalli R, Carlotti ME, Battaglia L, & Debernardi F (2005) Solid lipid micro-particles carrying insulin formed by solvent-in-water emulsion-diffusion technique. *International Journal of Pharmaceutics* 288(2):281-288.

47. Reithmeier H, Herrmann J, & Göpferich A (2001) Lipid microparticles as a parenteral controlled release device for peptides. *Journal of Controlled Release* 73(2-3):339-350.

48. García-Fuentes M, Torres D, & Alonso MJ (2003) Design of lipid nanoparticles for the oral delivery of hydrophilic macromolecules. *Colloids and Surfaces B: Biointerfaces* 27(3/2):159-168.

49. Wichterle O & Lim D (1960) Hydrophilic Gels for Biological Use. *Nature* 185(4706):117-118.

50. Ritu A, Shailley J, Sumit M, Raja N, Usha Kaul R, & Dinesh Kumar M (2004) Efficacy of continuous wear PureVision contact lenses for therapeutic use. *Contact lens & anterior eye : the journal of the British Contact Lens Association* 27(1):39-43.

51. Nguyen KT & West JL (2002) Photopolymerizable hydrogels for tissue engineering applications. *Biomaterials* 23(22):4307-4314.

52. Bos GW, Jacobs JJL, Koten JW, Van Tomme S, Veldhuis T, van Nostrum CF, Den Otter W, & Hennink WE (2004) In situ crosslinked biodegradable hydrogels loaded with IL-2 are effective tools for local IL-2 therapy. *European Journal of Pharmaceutical Sciences* 21(4):561-567.

53. Nam K, Watanabe J, & Ishihara K (2004) Modeling of swelling and drug release behavior of spontaneously forming hydrogels composed of phospholipid polymers. *International Journal of Pharmaceutics* 275(1-2):259-269.

54. West JL & Hubbell JA (1996) Separation of the arterial wall from blood contact using hydrogel barriers reduces intimal thickening after balloon injury in the rat: The roles of medial and luminal factors in arterial healing. *Proceedings of the National Academy of Sciences of the United States of America* 93(23):13188-13193.

55. Denstedt JD, Reid G, & Sofer M (2000) Advances in ureteral stent technology. *World Journal of Urology* 18(4):237-242.

56. Hennink WE & Van Nostrum CF (2002) Novel crosslinking methods to design hydrogels. *Advanced Drug Delivery Reviews* 54(1):13-36.

57. Kopecek J (2007) Hydrogel biomaterials: A smart future? *Biomaterials* 28(34):5185-5192.

58. Park H & Park K (1996) Biocompatibility Issues of Implantable Drug Delivery Systems. *Pharmaceutical Research* 13(12):1770-1776.

59. Lenz R (1993) Biodegradable polymers. *Biopolymers I,* Advances in Polymer Science, eds Langer R & Peppas N (Springer Berlin / Heidelberg), Vol 107, pp 1-40.

60. Hashidzume A, Tomatsu I, & Harada A (2006) Interaction of cyclodextrins with side chains of water soluble polymers: A simple model for biological molecular recognition and its utilization for stimuli-responsive systems. *Polymer* 47(17):6011-6027.

61. Choi HS & Yui N (2006) Design of rapidly assembling supramolecular systems responsive to synchronized stimuli. *Progress in Polymer Science* 31(2):121-144.

62. van de Manakker F, van der Pot M, Vermonden T, van Nostrum CF, & Hennink WE (2008) Self-Assembling Hydrogels Based on β-Cyclodextrin/Cholesterol Inclusion Complexes. *Macromolecules* 41(5):1766-1773.

63. van de Manakker F, Vermonden T, el Morabit N, van Nostrum CF, & Hennink WE (2008) Rheological Behavior of Self-Assembling PEG-β-Cyclodextrin/PEG-Cholesterol Hydrogels. *Langmuir* 24(21):12559-12567.

64. Van De Manakker F, Kroon-Batenburg LMJ, Vermonden T, Van Nostrum CF, & Hennink WE (2009) Supramolecular hydrogels formed by β-cyclodextrin self-association and host-guest inclusion complexes. *Soft Matter* 6(1):187-194.

65. Van Manakker FD, Braeckmans K, Morabit NE, De Smedt SC, Van Nostrum CF, & Hennink WE (2009) Protein-release behavior of self-assembled PEG-ß-cyclodextrin/PEG- cholesterol hydrogels. *Advanced Functional Materials* 19(18):2992-3001.

66. Huh KM, Ooya T, Lee WK, Sasaki S, Kwon IC, Jeong SY, & Yui N (2001) Supramolecular-structured hydrogels showing a reversible phase transition by inclusion complexation between poly(ethylene glycol) grafted dextran and α-cyclodextrin. *Macromolecules* 34(25):8657-8662.

67. Choi HS, Yamamoto K, Ooya T, & Yui N (2005) Synthesis of poly(ε-lysine)-grafted dextrans and their pH- And thermosensitive hydrogelation with cyclodextrins. *A European Journal of Chemical Physics and Physical Chemistry 6(6):1081-1086.*

68. Tomatsu I, Hashidzume A, & Harada A (2005) Gel-to-Sol and Sol-to-Gel Transitions Utilizing the Interaction of α-Cyclodextrin with Dodecyl Side Chains Attached to a Poly(acrylic acid) Backbone. *Macromolecular Rapid Communications* 26(10):825-829.

69. Van Tomme SR, Storm G, & Hennink WE (2008) In situ gelling hydrogels for pharmaceutical and biomedical applications. *International Journal of Pharmaceutics* 355(1-2):1-18.

70. Tsuji H (2005) Poly(lactide) stereocomplexes: Formation, structure, properties, degradation, and applications. *Macromolecular Bioscience* 5(7):569-597.

71. De Jong SJ, De Smedt SC, Wahls MWC, Demeester J, Kettenes-van Den Bosch JJ, & Hennink WE (2000) Novel self-assembled hydrogels by stereocomplex formation in aqueous solution of enantiomeric lactic acid oligomers grafted to dextran. *Macromolecules* 33(10):3680-3686.

72. De Jong SJ, Van Nostrum CF, Kroon-Batenburg LMJ, Kettenes-van Den Bosch JJ, & Hennink WE (2002) Oligolactate-grafted dextran hydrogels: Detection of stereocomplex crosslinks by X-ray diffraction. *Journal of Applied Polymer Science* 86(2):289-293.

73. de Jong SJ, van Eerdenbrugh B, van Nostrum CF, Kettenes-van den Bosch JJ, & Hennink WE (2001) Physically crosslinked dextran hydrogels by stereocomplex formation of lactic acid oligomers: degradation and protein release behavior. *Journal of Controlled Release* 71(3):261-275.

74. Bos GW, Hennink WE, Brouwer LA, Den Otter W, Veldhuis TFJ, Van Nostrum CF, & Van Luyn MJA (2005) Tissue reactions of in situ formed dextran hydrogels crosslinked by stereocomplex formation after subcutaneous implantation in rats. *Biomaterials* 26(18):3901-3909.

75. van Dijk M, Rijkers DTS, Liskamp RMJ, van Nostrum CF, & Hennink WE (2009) Synthesis and Applications of Biomedical and Pharmaceutical Polymers via Click Chemistry Methodologies. *Bioconjugate Chemistry* 20(11):2001-2016.

76. Hu BH, Su J, & Messersmith PB (2009) Hydrogels cross-linked by native chemical ligation. *Biomacromolecules* 10(8):2194-2200.

77. Elisseeff J, Anseth K, Sims D, McIntosh W, Randolph M, & Langer R (1999) Transdermal photopolymerization for minimally invasive implantation. *Proceeding of the National Academy of Sciences of U.S.A.* 96(6):3104-3107.

78. Bryant SJ, Nuttelman CR, & Anseth KS (2000) Cytocompatibility of UV and visible light photoinitiating systems on cultured NIH/3T3 fibroblasts in vitro. *Journal of Biomaterials Science Polymer Edition* 11:439-457.

79. Sawhney AS, Pathak CP, & Hubbell JA (1993) Bioerodible hydrogels based on photopolymerized poly(ethylene glycol)-co-poly(.alpha.-hydroxy acid) diacrylate macromers. *Macromolecules* 26(4):581-587.

80. Lu S & Anseth KS (1999) Photopolymerization of multilaminated poly(HEMA) hydrogels for controlled release. *Journal of Controlled Release* 57(3):291-300.

81. Ward JH & Peppas NA (2001) Preparation of controlled release systems by free-radical UV polymerizations in the presence of a drug. *Journal of Controlled Release* 71(2):183-192.

82. Royce Hynes S, McGregor LM, Ford Rauch M, & Lavik EB (2007) Photopolymerized poly(ethylene glycol)/poly(L-lysine) hydrogels for the delivery of neural progenitor cells. *Journal of Biomaterials Science, Polymer Edition* 18(8):1017-1030.

83. Van Tomme SR, Storm G, & Hennink WE (2008) In situ gelling hydrogels for pharmaceutical and biomedical applications. *International Journal of Pharmaceutics* 355(1-2):1-18.

84.   West JL & Hubbell JA (1995) Photopolymerized hydrogel materials for drug delivery applications *Reactive Polymers* 25(2-3):139-147.

85.   Pescosolido L, Miatto S, Di Meo C, Cencetti C, Coviello T, Alhaique F, & Matricardi P (2010) Injectable and in situ gelling hydrogels for modified protein release. *European Biophysics Journal* 39(6):903-909.

86.   Censi R, Vermonden T, van Steenbergen MJ, Deschout H, Braeckmans K, De Smedt SC, van Nostrum CF, di Martino P, & Hennink WE (2009) Photopolymerized thermosensitive hydrogels for tailorable diffusion-controlled protein delivery. *Journal of Controlled Release* 140(3):230-236.

87.   Sawhney AS, Pathak CP, van Rensburg JJ, Dunn RC, & Hubbell JA (1994) Optimization of photopolymerized bioerodible hydrogel properties for adhesion prevention. *Journal of Biomedical Materials Research* 28(7):831-838.

88.   Fedorovich NE, Oudshoorn MH, van Geemen D, Hennink WE, Alblas J, & Dhert WJA (2009) The effect of photopolymerization on stem cells embedded in hydrogels. *Biomaterials* 30(3):344-353.

89.   Lin C-C & Metters A (2006) Enhanced Protein Delivery from Photopolymerized Hydrogels Using a Pseudospecific Metal Chelating Ligand. *Pharmaceutical Research* 23(3):614-622.

90.   Valdebenito A, Espinoza P, Lissi EA, & Encinas MV (2010) Bovine serum albumin as chain transfer agent in the acrylamide polymerization. Protein-polymer conjugates. *Polymer* 51(12):2503-2507.

91.   Sawhney AS, Pathak CP, & Hubbell JA (1993) Bioerodible hydrogels based on photopolymerized poly(ethylene glycol)-co-poly(α-hydroxy acid) diacrylate macromers. *Macromolecules* 26(4):581-587.

92.   Metters AT, Bowman CN, & Anseth KS (2000) A Statistical Kinetic Model for the Bulk Degradation of PLA-b-PEG-b-PLA Hydrogel Networks. *The Journal of Physical Chemistry B* 104(30):7043-7049.

93.   Metters AT, Anseth KS, & Bowman CN (2001) A Statistical Kinetic Model for the Bulk Degradation of PLA-b-PEG-b-PLA Hydrogel Networks: Incorporating Network Non-Idealities. *The Journal of Physical Chemistry B* 105(34):8069-8076.

94.   Smeds KA, Pfister-Serres A, Miki D, Dastgheib K, Inoue M, Hatchell DL, & Grinstaff MW (2001) Photocrosslinkable polysaccharides for in situ hydrogel formation. *Journal of Biomedical Materials Research* 55(2):254-255.

95.   Leach JB & Schmidt CE (2005) Characterization of protein release from photocrosslinkable hyaluronic acid-polyethylene glycol hydrogel tissue engineering scaffolds. *Biomaterials* 26(2):125-135.

96.   Anseth KS, Metters AT, Bryant SJ, Martens PJ, Elisseeff JH, & Bowman CN (2002) In situ forming degradable networks and their application in tissue engineering and drug delivery. *Journal of Controlled Release* 78(1-3):199-209.

97.   Friedman M, Cavins JF, & Wall JS (1965) Relative Nucleophilic Reactivities of Amino Groups and Mercaptide Ions in Addition Reactions with α,β-Unsaturated Compounds1,2. *Journal of the American Chemical Society* 87(16):3672-3682.

98.   Elbert DL, Pratt AB, Lutolf MP, Halstenberg S, & Hubbell JA (2001) Protein delivery from materials formed by self-selective conjugate addition reactions. *Journal of Controlled Release* 76(1-2):11-25.

99.   Vernon B, Tirelli N, Bächi T, Haldimann D, & Hubbell JA (2003) Water-borne, in situ crosslinked biomaterials from phase-segregated precursors. *Journal of Biomedical Materials Research - Part A* 64(3):447-456.

100.   Rizzi SC & Hubbell JA (2005) Recombinant protein-co-PEG networks as cell-adhesive and proteolytically degradable hydrogel matrixes. Part I: Development and physicochemical characteristics. *Biomacromolecules* 6(3):1226-1238.

101.   Lutolf MP & Hubbell JA (2003) Synthesis and Physicochemical Characterization of End-Linked Poly(ethylene glycol)-co-peptide Hydrogels Formed by Michael-Type Addition. *Biomacromolecules* 4(3):713-722.

102.   Lutolf M, Raeber G, Zisch A, Tirelli N, & Hubbell J (2003) Cell-Responsive Synthetic Hydrogels. *Advanced Materials* 15(11):888-892.

103.   Jin R, Moreira Teixeira LS, Krouwels A, Dijkstra PJ, van Blitterswijk CA, Karperien M, & Feijen J Synthesis and characterization of hyaluronic acid-poly(ethylene glycol) hydrogels via Michael addition: An injectable biomaterial for cartilage repair. *Acta Biomaterialia* 6(6):1968-   77.

104. Lutolf MP, Tirelli N, Cerritelli S, Cavalli L, & Hubbell JA (2001) Systematic Modulation of Michael-Type Reactivity of Thiols through the Use of Charged Amino Acids. *Bioconjugate Chemistry* 12(6):1051-1056.

105. Hahn SK, Oh EJ, Miyamoto H, & Shimobouji T (2006) Sustained release formulation of erythropoietin using hyaluronic acid hydrogels crosslinked by Michael addition. *International Journal of Pharmaceutics* 322(1-2):44-51.

106. Hahn SK, Park JK, Tomimatsu T, & Shimoboji T (2007) Synthesis and degradation test of hyaluronic acid hydrogels. *International Journal of Biological Macromolecules* 40(4):374-380.

107. Cellesi F, Tirelli N, & Hubbell JA (2002) Materials for cell encapsulation via a new tandem approach combining reverse thermal gelation and covalent crosslinking. *Macromolecular Chemistry and Physics* 203(10-11):1466-1472.

108. Cellesi F, Weber W, Fussenegger M, Hubbell JA, & Tirelli N (2004) Towards a fully synthetic substitute of alginate: Optimization of a thermal gelation/chemical cross-linking scheme (ldquotandemrdquo gelation) for the production of beads and liquid-core capsules. *Biotechnology and Bioengineering* 88(6):740-749.

109. Cellesi F, Weber W, Fussenegger M, Hubbell JA, & Tirelli N (2004) Towards a fully synthetic substitute of alginate: Optimization of a thermal gelation/chemical cross-linking scheme ("tandem" gelation) for the production of beads and liquid-core capsules. *Biotechnology and Bioengineering* 88(6):740-749.

110. Lee BH, West B, McLemore R, Pauken C, & Vernon BL (2006) In-Situ Injectable Physically and Chemically Gelling NIPAAm-Based Copolymer System for Embolization. *Biomacromolecules* 7(6):2059-2064.

111. Robb SA, Lee BH, McLemore R, & Vernon BL (2007) Simultaneously Physically and Chemically Gelling Polymer System Utilizing a Poly(NIPAAm-co-cysteamine)-Based Copolymer. *Biomacromolecules* 8(7):2294-2300.

112. McLemore R, Robb S, Lee B, Caplan M, & Vernon B (2009) Michael-Type Addition Reactions in NIPAAm-Cysteamine Copolymers Follow Second Order Rate Laws with Steric Hindrance. *Annals of Biomedical Engineering* 37(11):2416-2425.

113. Cheng V, Lee BH, Pauken C, & Vernon BL (2007) Poly(N-isopropylacrylamide-*co*-poly(ethylene glycol))-acrylate simultaneously physically and chemically gelling polymer systems. *Journal of Applied Polymer Science* 106(2):1201-1207.

114. Wang Z-C, Xu X-D, Chen C-S, Yun L, Song J-C, Zhang X-Z, & Zhuo R-X (2010) In Situ Formation of Thermosensitive PNIPAAm-Based Hydrogels by Michael-Type Addition Reaction. *ACS Applied Material & Interfaces*.

115. Gupta P, Vermani K, & Garg S (2002) Hydrogels: From controlled release to pH-responsive drug delivery. *Drug Discovery Today* 7(10):569-579.

116. Jeong B & Gutowska A (2002) Lessons from nature: Stimuli-responsive polymers and their biomedical applications. *Trends in Biotechnology* 20(7):305-311.

117. Klouda L & Mikos AG (2008) Thermoresponsive hydrogels in biomedical applications. *European Journal of Pharmaceutics and Biopharmaceutics* 68(1):34-45.

118. Tanaka T, Fillmore D, Sun S-T, Nishio I, Swislow G, & Shah A (1980) Phase Transitions in Ionic Gels. *Physical Review Letters* 45(20):1636.

119. Heskins M & Guillet JE (1968) Solution Properties of Poly(N-isopropylacrylamide). 2(8):1441 - 1455.

120. Schild HG (1992) Poly(N-isopropylacrylamide): Experiment, theory and application. *Progress in Polymer Science (Oxford)* 17(2):163-249.

121. Arnott S, Fulmer A, & Scott WE (1974) The agarose double helix and its function in agarose gel structure. *Journal of Molecular Biology* 90(2):269-284.

122. Rees DA & Welsh EJ (1977) Secondary and tertiary structure of polysaccharides in solutions and gels. *Angewandte Chemie - International Edition* 16(4):214-224.

123. Ball PGHaRC ed (1990) *Physical Network. Polymers and Gels* New York), pp 185–194.

124. Sarkar N (1979) Thermal gelation properties of methyl and hydroxypropyl methylcellulose *Journal of Applied Polymer Science* 24(4):1073-1087.

125.   Heymann E (1935) Studies on sol-gel transformations. I. The inverse sol-gel transformation of methylcellulose in water. *Transactions of the Faraday Society* 31:846-864.

126.   Chenite A, Chaput C, Wang D, Combes C, Buschmann MD, Hoemann CD, Leroux JC, Atkinson BL, Binette F, & Selmani A (2000) Novel injectable neutral solutions of chitosan form biodegradable gels in situ. *Biomaterials* 21(21):2155-2161.

127.   Bhattarai N, Ramay HR, Gunn J, Matsen FA, & Zhang M (2005) PEG-grafted chitosan as an injectable thermosensitive hydrogel for sustained protein release. *Journal of Controlled Release* 103(3):609-624.

128.   Peppas NA ed (1986) *Hydrogels in medicine and pharmacy*).

129.   Feil H, Bae YH, Feijen J, & Kim SW (1993) Effect of comonomer hydrophilicity and ionization on the lower critical solution temperature of N-isopropylacrylamide copolymers. *Macromolecules* 26(10):2496-2500.

130.   Vermonden T, Fedorovich NE, van Geemen D, Alblas J, van Nostrum CF, Dhert WJA, & Hennink WE (2008) Photopolymerized Thermosensitive Hydrogels: Synthesis, Degradation, and Cytocompatibility. *Biomacromolecules* 9(3):919-926.

131.   Yu L, Chang G, Zhang H, & Ding J (2007) Temperature-induced spontaneous sol-gel transitions of poly(D,L-lactic acid-co-glycolic acid)-b-poly(ethylene glycol)-b-poly(D,L-lactic acid-co-glycolic acid) triblock copolymers and their end-capped derivatives in water. *Journal of Polymer Science, Part A: Polymer Chemistry* 45(6):1122-1133.

132.   Nagahama K, Ouchi T, & Ohya Y (2008) Temperature-induced hydrogels through self-assembly of cholesterol- substituted star PEG-b-PLLA copolymers: An injectable scaffold for tissue engineering. *Advanced Functional Materials* 18(8):1220-1231.

133.   Han CK & Bae YH (1998) Inverse thermally-reversible gelation of aqueous N-isopropylacrylamide copolymer solutions. *Polymer* 39(13):2809-2814.

134.   Bae YH, Vernon B, Han CK, & Kim SW (1998) Extracellular matrix for a rechargeable cell delivery system. *Journal of Controlled Release* 53(1-3):249-258.

135.   Vernon B, Gutowska A, Kim SW, & Bae YH (1996) Thermally reversible polymer gels for biohybrid artificial pancreas. *Macromolecular Symposia* 109:155-167.

136.   Vernon B, Kim SW, & Bae YH (1999) Insulin release from islets of Langerhans entrapped in a poly(N-isopropylacrylamide-co-acrylic acid) polymer gel. *Journal of Biomaterials Science, Polymer Edition* 10(2):183-198.

137.   Wu J-Y, Liu S-Q, Heng PW-S, & Yang Y-Y (2005) Evaluating proteins release from, and their interactions with, thermosensitive poly (N-isopropylacrylamide) hydrogels. *Journal of Controlled Release* 102(2):361-372.

138.   Ramkissoon-Ganorkar C, Liu F, Baudyš M, & Kim SW (1999) Modulating insulin-release profile from pH/thermosensitive polymeric beads through polymer molecular weight. *Journal of Controlled Release* 59(3):287-298.

139.   Jeong KJ & Panitch A (2009) Interplay between Covalent and Physical Interactions within Environment Sensitive Hydrogels. *Biomacromolecules* 10(5):1090-1099.

140.   Niu G, Zhang H, Song L, Cui X, Cao H, Zheng Y, Zhu S, Yang Z, & Yang H (2008) Thiol/Acrylate-Modified PEO-PPO-PEO Triblocks Used as Reactive and Thermosensitive Copolymers. *Biomacromolecules* 9(10):2621-2628.

141.   Censi R, Fieten PJ, di Martino P, Hennink WE, & Vermonden T (2010) In Situ Forming Hydrogels by Tandem Thermal Gelling and Michael Addition Reaction between Thermosensitive Triblock Copolymers and Thiolated Hyaluronan. *Macromolecules*.

142.   Lin HH & Cheng YL (2001) In-situ thermoreversible gelation of block and star copolymers of poly(ethylene glycol) and poly(n-isopropylacrylamide) of varying architectures. *Macromolecules* 34(11):3710-3715.

143.   Topp MDC, Leunen IH, Dijkstra PJ, Tauer K, Schellenberg C, & Feijen J (2000) Quasi-living polymerization of N-isopropylacrylamide onto poly(ethylene glycol). *Macromolecules* 33(14):4986-4988.

144.   Kwon IK & Matsuda T (2006) Photo-iniferter-based thermoresponsive block copolymers composed of poly(ethylene glycol) and poly(N-isopropylacrylamide) and chondrocyte immobilization. *Biomaterials* 27(7):986-995.

145. Li C, Buurma NJ, Haq I, Turner C, Armes SP, Castelletto V, Hamley IW, & Lewis AL (2005) Synthesis and characterization of biocompatible, thermoresponsive ABC and ABA triblock copolymer gelators. *Langmuir* 21(24):11026-11033.

146. Li C, Tang Y, Armes SP, Morris CJ, Rose SF, Lloyd AW, & Lewis AL (2005) Synthesis and characterization of biocompatible thermo-responsive gelators based on ABA triblock copolymers. *Biomacromolecules* 6(2):994-999.

147. Aoshima S, Oda H, & Kobayashi E (1992) Synthesis of thermally-induced phase separating polymer with well-defined polymer structure by living cationic polymerization. I. Synthesis of poly(vinyl ether)s with oxyethylene units in the pendant and its phase separation behavior in-aqueous solution. *Journal of Polymer Science, Part A: Polymer Chemistry* 30(11):2407-2413.

148. He C, Kim SW, & Lee DS (2008) In situ gelling stimuli-sensitive block copolymer hydrogels for drug delivery. *Journal of Controlled Release* 127(3):189-207.

149. Mortensen K & Pedersen JS (1993) Structural study on the micelle formation of poly(ethylene oxide)-poly(propylene oxide)-poly(ethylene oxide) triblock copolymer in aqueous solution. *Macromolecules* 26(4):805-812.

150. Dumortier G, Grossiord JL, Agnely F, & Chaumeil JC (2006) A review of poloxamer 407 pharmaceutical and pharmacological characteristics. *Pharmaceutical Research* 23(12):2709-2728.

151. Jeong B, Kim SW, & Bae YH (2002) Thermosensitive sol-gel reversible hydrogels. *Advanced Drug Delivery Reviews* 54(1):37-51.

152. Alexandridis P & Alan Hatton T (1995) Poly(ethylene oxide)poly(propylene oxide)poly(ethylene oxide) block copolymer surfactants in aqueous solutions and at interfaces: thermodynamics, structure, dynamics, and modeling. *Colloids and Surfaces A: Physicochemical and Engineering Aspects* 96(1-2):1-46.

153. Ruel-Gariépy E & Leroux JC (2004) In situ-forming hydrogels - Review of temperature-sensitive systems. *European Journal of Pharmaceutics and Biopharmaceutics* 58(2):409-426.

154. Bromberg L (1998) Polyether-modified poly(acrylic acid): Synthesis and applications. *Industrial and Engineering Chemistry Research* 37(11):4267-4274.

155. Johnston TP, Punjabi MA, & Froelich CJ (1992) Sustained delivery of interleukin-2 from a poloxamer 407 gel matrix following intraperitoneal injection in mice. *Pharmaceutical Research* 9(3):425-434.

156. Fults KA & Johnston TP (1990) Sustained-release of urease from a poloxamer gel matrix. *Journal of Parenteral Science and Technology* 44(2):58-65.

157. Bhardwaj R & Blanchard J (1996) Controlled-release delivery system for the α-MSH analog Melanotan-I using poloxamer 407. *Journal of Pharmaceutical Sciences* 85(9):915-919.

158. Morishita M, Barichello JM, Takayama K, Chiba Y, Tokiwa S, & Nagai T (2001) Pluronic® F-127 gels incorporating highly purified unsaturated fatty acids for buccal delivery of insulin. *International Journal of Pharmaceutics* 212(2):289-293.

159. Barichello JM, Morishita M, Takayama K, & Nagai T (1999) Absorption of insulin from Pluronic F-127 gels following subcutaneous administration in rats. *International Journal of Pharmaceutics* 184(2):189-198.

160. Davidorf FH, Chambers RB, Kwon OW, Doyle W, Gresak P, & Frank SG (1990) Ocular toxicity of vitreal pluronic polyol F-127. *Retina* 10(4):297-300.

161. Cohn D, Sosnik A, & Levy A (2003) Improved reverse thermo-responsive polymeric systems. *Biomaterials* 24(21):3707-3714.

162. Ahn JS, Suh JM, Lee M, & Jeong B (2005) Slow eroding biodegradable multiblock poloxamer copolymers. *Polymer International* 54(5):842-847.

163. Xiong XY, Tam KC, & Gan LH (2005) Synthesis and thermal responsive properties of P(LA-b-EO-b-PO-b-EO-b-LA) block copolymers with short hydrophobic poly(lactic acid) (PLA) segments. *Polymer* 46(6):1841-1850.

164. Xiong XY, Tam KC, & Gan LH (2006) Synthesis and thermally responsive properties of novel pluronic F87/polycaprolactone (PCL) block copolymers with short pcl blocks. *Journal of Applied Polymer Science* 100(5):4163-4172.

165. Cohn D, Lando G, Sosnik A, Garty S, & Levi A (2006) PEO-PPO-PEO-based poly(ether ester urethane)s as degradable reverse thermo-responsive multiblock copolymers. *Biomaterials* 27(9):1718-1727.

166. Jeong B, Bae YH, Lee DS, & Kim SW (1997) Biodegradable block copolymers as injectable drug-delivery systems. *Nature* 388(6645):860-862.

167. Park SY, Han DK, & Kim SC (2001) Synthesis and characterization of star-shaped PLLA-PEO block copolymers with temperature-sensitive sol-gel transition behavior. *Macromolecules* 34(26):8821-8824.

168. Jeong B, Bae YH, & Kim SW (1999) Thermoreversible gelation of PEG-PLGA-PEG triblock copolymer aqueous solutions. *Macromolecules* 32(21):7064-7069.

169. Jeong B, Bae YH, & Kim SW (2000) In situ gelation of PEG-PLGA-PEG triblock copolymer aqueous solutions and degradation thereof. *Journal of Biomedical Materials Research* 50(2):171-177.

170. Lee PY, Li Z, & Huang L (2003) Thermosensitive Hydrogel as a Tgf-β1 Gene Delivery Vehicle Enhances Diabetic Wound Healing. *Pharmaceutical Research* 20(12):1995-2000.

171. Jeong B, Bae YH, & Kim SW (2000) Drug release from biodegradable injectable thermosensitive hydrogel of PEG-PLGA-PEG triblock copolymers. *Journal of Controlled Release* 63(1-2):155-163.

172. Zentner GM, Rathi R, Shih C, McRea JC, Seo MH, Oh H, Rhee BG, Mestecky J, Moldoveanu Z, Morgan M, & Weitman S (2001) Biodegradable block copolymers for delivery of proteins and water-insoluble drugs. *Journal of Controlled Release* 72(1-3):203-215.

173. Kim YJ, Choi S, Koh JJ, Lee M, Ko KS, & Kim SW (2001) Controlled Release of Insulin from Injectable Biodegradable Triblock Copolymer. *Pharmaceutical Research* 18(4):548-550.

174. Kim MS, Seo KSU, Khang C, Sun Cho H, & Lee HB (2004) Preparation of methoxy poly(ethylene glycol)/polyester diblock copolymers and examination of the gel-to-sol transition. *Journal of Polymer Science, Part A: Polymer Chemistry* 42(22):5784-5793.

175. Kim MS, Hyun H, Khang G, & Lee HB (2006) Preparation of thermosensitive diblock copolymers consisting of MPEG and polyesters. *Macromolecules* 39(9):3099-3102.

176. Yang J, Jia L, Hao Q, Li Y, Li Q, Fang Q, & Cao A (2005) New biodegradable amphiphilic block copolymers of ε-caprolactone and δ-valerolactone catalyzed by novel aluminum metal complexes: II. Micellization and solution to gel transition. *Macromolecular Bioscience* 5(9):896-903.

177. Bae SJ, Suh JM, Sohn YS, Bae YH, Kim SW, & Jeong B (2005) Thermogelling poly(caprolactone-6-ethylene glycol-b-caprolactone) aqueous solutions. *Macromolecules* 38(12):5260-5265.

178. Hyun H, Kim YH, Song IB, Lee JW, Kim MS, Khang G, Park K, & Lee HB (2007) In Vitro and in Vivo Release of Albumin Using a Biodegradable MPEG-PCL Diblock Copolymer as an in Situ Gel-Forming Carrier. *Biomacromolecules* 8(4):1093-1100.

179. Kim MS, Seo KS, Hyun H, Khang G, Cho SH, & Lee HB (2006) Controlled release of bovine serum albumin using MPEG-PCL diblock copolymers as implantable protein carriers. *Journal of Applied Polymer Science* 102(2):1561-1567.

180. Behravesh E, Shung AK, Jo S, & Mikos AG (2002) Synthesis and characterization of triblock copolymers of methoxy poly(ethylene glycol) and poly(propylene fumarate). *Biomacromolecules* 3(1):153-158.

181. Loh XJ, Goh SH, & Li J (2007) New biodegradable thermogelling copolymers having very low gelation concentrations. *Biomacromolecules* 8(2):585-593.

182. Song MJ, Lee DS, Ahn JH, Kim DJ, & Kim SC (2004) Thermosensitive Sol-Gel Transition Behaviors of Poly(ethylene oxide)/Aliphatic Polyester/Poly(ethylene oxide) Aqueous Solutions. *Journal of Polymer Science, Part A: Polymer Chemistry* 42(3):772-784.

183. Sun H, Mei L, Song C, Cui X, & Wang P (2006) The in vivo degradation, absorption and excretion of PCL-based implant. *Biomaterials* 27(9):1735-1740.

184. Soga O, van Nostrum CF, & Hennink WE (2004) Poly(N-(2-hydroxypropyl) Methacrylamide Mono/Di Lactate): A New Class of Biodegradable Polymers with Tuneable Thermosensitivity. *Biomacromolecules* 5(3):818-821.

185. Neradovic D, van Steenbergen MJ, Vansteelant L, Meijer YJ, van Nostrum CF, & Hennink WE (2003) Degradation Mechanism and Kinetics of Thermosensitive Polyacrylamides Containing Lactic Acid Side Chains. *Macromolecules* 36(20):7491-7498.

186. Vanderhooft JL, Alcoutlabi M, Magda JJ, & Prestwich GD (2009) Rheological Properties of Cross-Linked Hyaluronan-Gelatin Hydrogels for Tissue Engineering. *Macromolecular Bioscience* 9(1):20-28.

187. Censi R, Vermonden T, Deschout H, Braeckmans K, Di Martino P, De Smedt S, Van Nostrum C, & Hennink WE (2010) Photopolymerized Thermosensitive Poly(HPMAlactate)-PEG Based Hydrogels: Effect of Network Design on Mechanical Properties, Degradation and Release Behavior. *Biomacromolecules* In Press.

188. Vermonden T, Jena SS, Barriet D, Censi R, van der Gucht J, Hennink WE, & Siegel RA (2009) Macromolecular Diffusion in Self-Assembling Biodegradable Thermosensitive Hydrogels. *Macromolecules* 43(2):782-789.

189. Lee BH, Lee YM, Sohn YS, & Song SC (2002) A thermosensitive poly(organophosphazene) gel. *Macromolecules* 35(10):3876-3879.

190. Seong JY, Jun YJ, Jeong B, & Sohn YS (2005) New thermogelling poly(organophosphazenes) with methoxypoly(ethylene glycol) and oligopeptide as side groups. *Polymer* 46(14):5075-5081.

191. Lee BH & Song SC (2004) Synthesis and characterization of biodegradable thermosensitive poly(organophosphazene) gels. *Macromolecules* 37(12):4533-4537.

192. Kang GD & Song SC (2008) Effect of chitosan on the release of protein from thermosensitive poly(organophosphazene) hydrogels. *International Journal of Pharmaceutics* 349(1-2):188-195.

193. Park KH & Song SC (2005) A thermo-sensitive poly(organophosphazene) hydrogel used as an extracellular matrix for artificial pancreas. *Journal of Biomaterials Science, Polymer Edition* 16(11):1421-1431.

194. Petka WA, Harden JL, McGrath KP, Wirtz D, & Tirrell DA (1998) Reversible hydrogels from self-assembling artificial proteins. *Science* 281(5375):389-392.

195. Wang C, Stewart RJ, & Kopeček J (1999) Hybrid hydrogels assembled from synthetic polymers and coiled-coil protein domains. *Nature* 397(6718):417-420.

196. Nowak AP, Breedveld V, Pakstis L, Ozbas B, Pine DJ, Pochan D, & Deming TJ (2002) Rapidly recovering hydrogel scaffolds from self-assembling diblock copolypeptide amphiphiles. *Nature* 417(6887):424-428.

197. Oh HJ, Joo MK, Sohn YS, & Jeong B (2008) Secondary structure effect of polypeptide on reverse thermal gelation and degradation of L/DL-poly(alanine)-poloxamerL/DL-poly(alanine) copolymers. *Macromolecules* 41(21):8204-8209.

198. Takeuchi Y, Uyama H, Tomoshige N, Watanabe E, Tachibana Y, & Kobayashi S (2006) Injectable thermoreversible hydrogels based on amphiphilic poly(amino acid)s. *Journal of Polymer Science, Part A: Polymer Chemistry* 44(1):671-675.

199. Han JO, Joo MK, Jang JH, Park MH, & Jeong B (2009) PVPylated Poly(alanine) as a New Thermogelling Polymer. *Macromolecules* 42(17):6710-6715.

200. Bell CL & Peppas NA (1996) Water, solute and protein diffusion in physiologically responsive hydrogels of poly(methacrylic acid-g-ethylene glycol). *Biomaterials* 17(12):1203-1218.

201. Torres-Lugo M & Peppas NA (1999) Molecular Design and in Vitro Studies of Novel pH-Sensitive Hydrogels for the Oral Delivery of Calcitonin. *Macromolecules* 32(20):6646-6651.

202. Chiu Y-L, Chen M-C, Chen C-Y, Lee P-W, Mi F-L, Jeng US, Chen H-L, & Sung H-W (2009) Rapidly in situ forming hydrophobically-modified chitosan hydrogels via pH-responsive nanostructure transformation. *Soft Matter* 5(5):962-965.

203. Chang G, Yu L, Yang Z, & Ding J (2009) A delicate ionizable-group effect on self-assembly and thermogelling of amphiphilic block copolymers in water. *Polymer* 50(25):6111-6120.

204. Dayananda K, He C, & Lee DS (2008) In situ gelling aqueous solutions of pH- and temperature-sensitive poly(ester amino urethane)s. *Polymer* 49(21):4620-4625.

205. Nguyen MK, Park DK, & Lee DS (2009) Injectable Poly(amidoamine)-poly(ethylene glycol)-poly(amidoamine) Triblock Copolymer Hydrogel with Dual Sensitivities: pH and Temperature. *Biomacromolecules* 10(4):728-731.

206. Shim WS, Yoo JS, Bae YH, & Lee DS (2005) Novel injectable pH and temperature sensitive block copolymer hydrogel. *Biomacromolecules* 6(6):2930-2934.

207. Shim WS, Kim SW, & Lee DS (2006) Sulfonamide-based pH- and temperature-sensitive biodegradable block copolymer hydrogels. *Biomacromolecules* 7(6):1935-1941.

208. Joo JS, Kim, M.S., Lee, D.S. (2006) *Macromolecular Research* 14:117.

209. Huynh DP, Nguyen MK, Pi BS, Kim MS, Chae SY, Lee KC, Kim BS, Kim SW, & Lee DS (2008) Functionalized injectable hydrogels for controlled insulin delivery. *Biomaterials* 29(16):2527-2534.

210. Traitel T, Cohen Y, & Kost J (2000) Characterization of glucose-sensitive insulin release systems in simulated in vivo conditions. *Biomaterials* 21(16):1679-1687.

211. Kang SI & Bae YH (2003) A sulfonamide based glucose-responsive hydrogel with covalently immobilized glucose oxidase and catalase. *Journal of Controlled Release* 86(1):115-121.

212. Kitano S, Koyama Y, Kataoka K, Okano T, & Sakurai Y (1992) A novel drug delivery system utilizing a glucose responsive polymer complex between poly (vinyl alcohol) and poly(N-vinyl-2-pyrrolidone) with a phenylboronic acid moiety. *Journal of Controlled Release* 19(1-3):161-170.

213. Brownlee M & Cerami A (1979) A glucose-controlled insulin-delivery system: semisynthetic insulin bound to lectin. *Science* 206(4423):1190-1191.

214. Kim SW, Pai CM, Makino K, Seminoff LA, Holmberg DL, Gleeson JM, Wilson DE, & Mack EJ (1990) Self-regulated glycosylated insulin delivery. *Journal of Controlled Release* 11(1-3):193-201.

215. Miyata T, Uragami T, & Nakamae K (2002) Biomolecule-sensitive hydrogels. *Advanced Drug Delivery Reviews* 54(1):79-98.

216. Qiu Y & Park K (2001) Environment-sensitive hydrogels for drug delivery. *Advanced Drug Delivery Reviews* 53(3):321-339.

217. Ehrbar M, Schoenmakers R, Christen EH, Fussenegger M, & Weber W (2008) Drug-sensing hydrogels for the inducible release of biopharmaceuticals. *Nature Materials* 7(10):800-804.

218. Miyata T, Asami N, & Uragani T (1999) A reversibly antigen-responsive hydrogen. *Nature* 399(6738):766-768.

219. Irvin DJ, Goods SH, & Whinnery LL (2001) Direct measurement of extension and force in conductive polymer gel actuators. *Chemistry of Materials* 13(4):1143-1145.

220. Pouliquen G & Tribet C (2005) Light-Triggered Association of Bovine Serum Albumin and Azobenzene-Modified Poly(acrylic acid) in Dilute and Semidilute Solutions. *Macromolecules* 39(1):373-383.

221. Tomatsu I, Hashidzume A, & Harada A (2005) Photoresponsive Hydrogel System Using Molecular Recognition of α-Cyclodextrin. *Macromolecules* 38(12):5223-5227.

222. Takashima Y, Nakayama T, Miyauchi M, Kawaguchi Y, Yamaguchi H, & Harada A (2004) Complex Formation and Gelation between Copolymers Containing Pendant Azobenzene Groups and Cyclodextrin Polymers. *Chemistry Letters* 33(7):890-891.

223. Kwon IC, Bae YH, & Kim SW (1991) Electrically erodible polymer gel for controlled release of drugs. *Nature* 354(6351):291-293.

224. Peppas NA, Bures P, Leobandung W, & Ichikawa H (2000) Hydrogels in pharmaceutical formulations. *European Journal of Pharmaceutics and Biopharmaceutics* 50(1):27-46.

225. Korsmeyer RW & Peppa NA eds (1983) *Macromolecular and modeling aspects of swelling-controlled systems* (Marcel Dekker), pp 77-90.

226. Hiemstra C, Zhong Z, Van Tomme SR, van Steenbergen MJ, Jacobs JJL, Otter WD, Hennink WE, & Feijen J (2007) In vitro and in vivo protein delivery from in situ forming poly(ethylene glycol)-poly(lactide) hydrogels. *Journal of Controlled Release* 119(3):320-327.

227. Wang PL & Johnston TP (1995) Sustained-release interleukin-2 following intramuscular injection in rats. *International Journal of Pharmaceutics* 113(1):73-81.

228. Choi S, Baudys M, & Kim S (2004) Control of Blood Glucose by Novel GLP-1 Delivery Using Biodegradable Triblock Copolymer of PLGA-PEG-PLGA in Type 2 Diabetic Rats. *Pharmaceutical Research* 21(5):827-831.

229. Huynh DP, Im GJ, Chae SY, Lee KC, & Lee DS (2009) Controlled release of insulin from pH/temperature-sensitive injectable pentablock copolymer hydrogel. *Journal of Controlled Release* 137(1):20-24.

230. Zhang S, Holmes TC, DiPersio CM, Hynes RO, Su X, & Rich A (1995) Self-complementary oligopeptide matrices support mammalian cell attachment. *Biomaterials* 16(18):1385-1393.

231. Hsieh PCH, Davis ME, Gannon J, MacGillivray C, & Lee RT (2006) Controlled delivery of PDGF-BB for myocardial protection using injectable self-assembling peptide nanofibers. *Journal of Clinical Investigation* 116(1):237.

232.	Segers VFM, Tokunou T, Higgins LJ, MacGillivray C, Gannon J, & Lee RT (2007) Local Delivery of Protease-Resistant Stromal Cell Derived Factor-1 for Stem Cell Recruitment After Myocardial Infarction. *Circulation* 116(15):1683-1692.

233.	Davis ME, Hsieh PCH, Takahashi T, Song Q, Zhang S, Kamm RD, Grodzinsky AJ, Anversa P, & Lee RT (2006) Local myocardial insulin-like growth factor 1 (IGF-1) delivery with biotinylated peptide nanofibers improves cell therapy for myocardial infarction. *Proceedings of the National Academy of Sciences of the United States of America* 103(21):8155-8160.

234.	Kempe S, Metz H, Bastrop M, Hvilsom A, Contri RV, & Mäder K (2008) Characterization of thermosensitive chitosan-based hydrogels by rheology and electron paramagnetic resonance spectroscopy. *European Journal of Pharmaceutics and Biopharmaceutics* 68(1):26-33.

235.	Park K-H & Song S-C (2005) A thermo-sensitive poly(organophosphazene) hydrogel used as an extracellular matrix for artificial pancreas. *Journal of Biomaterials Science, Polymer Edition* 16:1421-1431.

236.	Park K-H & Song SC (2006) Morphology of spheroidal hepatocytes within injectable, biodegradable, and thermosensitive poly(organophosphazene) hydrogel as cell delivery vehicle. *Journal of Bioscience and Bioengineering* 101(3):238-242.

237.	De Smedt SC, Meyvis TKL, Demeester J, Van Oostveldt P, Blonk JCG, & Hennink WE (1997) Diffusion of macromolecules in dextran methacrylate solutions and gels as studied by confocal scanning laser microscopy. *Macromolecules* 30(17):4863-4870.

238.	Braeckmans K, Peeters L, Sanders NN, De Smedt SC, & Demeester J (2003) Three-dimensional fluorescence recovery after photobleaching with the confocal scanning laser microscope. *Biophysical Journal* 85(4):2240-2252.

239.	Tai H, Wang W, Vermonden T, Heath F, Hennink WE, Alexander C, Shakesheff KM, & Howdle SM (2009) Thermoresponsive and Photocrosslinkable PEGMEMA-PPGMA-EGDMA Copolymers from a One-Step ATRP Synthesis. *Biomacromolecules* 10(4):822-828.

240.	Branco MC, Pochan DJ, Wagner NJ, & Schneider JP (2009) Macromolecular diffusion and release from self-assembled β-hairpin peptide hydrogels. *Biomaterials* 30(7):1339-1347.

241.	Burke MD, Park JO, Srinivasarao M, & Khan SA (2005) A novel enzymatic technique for limiting drug mobility in a hydrogel matrix. *Journal of Controlled Release* 104(1):141-153.

242.	Kuijpers AJ, Engbers GHM, Meyvis TKL, de Smedt SSC, Demeester J, Krijgsveld J, Zaat SAJ, Dankert J, & Feijen J (2000) Combined Gelatin−Chondroitin Sulfate Hydrogels for Controlled Release of Cationic Antibacterial Proteins. *Macromolecules* 33(10):3705-3713.

243.	Van Tomme SR, De Geest BG, Braeckmans K, De Smedt SC, Siepmann F, Siepmann J, Van Nostrum CF, & Hennink WE (2005) Mobility of model proteins in hydrogels composed of oppositely charged dextran microspheres studied by protein release and fluorescence recovery after photobleaching. *Journal of Controlled Release* 110(1):67-78.

244.	Brandl F, Kastner F, Gschwind RM, Blunk T, Teßmar J, & Göpferich A (2010) Hydrogel-based drug delivery systems: Comparison of drug diffusivity and release kinetics. *Journal of Controlled Release* 142(2):221-228.

245.	Jorgensen L, Moeller EH, van de Weert M, Nielsen HM, & Frokjaer S (2006) Preparing and evaluating delivery systems for proteins. *European Journal of Pharmaceutical Sciences* 29(3-4):174-182.

Chapter 3

Photopolymerized Thermosensitive Hydrogels for Tailorable Diffusion-Controlled Protein Delivery

Roberta Censi,[a,b] Tina Vermonden,[a] Mies J. van Steenbergen,[a] Hendrik Deschout,[c] Kevin Braeckmans,[c] Stefaan C. De Smedt,[c] Cornelus F. van Nostrum,[a] Piera Di Martino,[b] Wim E. Hennink[a]

[a] Department of Pharmaceutics Utrecht Institute for Pharmaceutical Sciences (UIPS); Utrecht University; P.O. Box 80082, 3508 TB Utrecht, The Netherlands.

[b] Department of Chemical Sciences; Camerino University; via S. Agostino 1, 62032, Camerino (MC), Italy.

[c] Laboratory of General Biochemistry and Physical Chemistry, Department of Pharmaceutics, Ghent University, Harelbekestraat 72, B-9000, Ghent, Belgium

Abstract

In this paper the possibility to tailor degradation and protein release behavior of photopolymerized thermosensitive hydrogels is studied. The hydrogels consist of ABA triblock copolymer, in which the thermosensitive A-blocks are methacrylated poly(*N*-(2-hydroxypropyl) methacrylamide lactate)s and the B-block is poly(ethylene glycol) with molecular weight of 10 kDa. These hydrogels are prepared by using a combination of physical and chemical cross-linking methods. When a solution of a thermosensitive methacrylated p(HPMAm-lac)-PEG-p(HPMAm-lac) is heated above its cloud point a viscoelastic material is obtained, which can be stabilized by introducing covalent cross-links by photopolymerization. By varying the polymer concentration, hydrogels with different mechanical properties are formed, of which the cross-linking density, mesh size, swelling and degradation behavior can be tuned. It was demonstrated that the release rate of three model proteins (lysozyme, BSA and IgG, with hydrodynamic diameters ranging from 4.1 to 10.7 nm) depended on the protein size and hydrogel molecular weight between cross-links and was governed by Fickian diffusion. Importantly, the encapsulated proteins were quantitatively released and the secondary structure and the enzymatic activity of lysozyme were fully preserved demonstrating the protein friendly nature of the studied delivery system.

3.1   Introduction

The advent of the modern generation of biotherapeutics, such as peptides, proteins and DNA has resulted in a high need for suitable materials and technologies to deliver these biologicals (1). Hydrogels represent an important class of pharmaceutical delivery systems, aimed to overcome the major challenges associated with the formulation of biotherapeutic drugs, which are known for their problematic chemical and physical stability (2-4).

Hydrogels are polymeric networks that absorb large quantities of water while remaining insoluble in aqueous solution due to the presence of chemical and/or physical cross-links between the polymer chains. They are excellent materials for the release of biotherapeutics because they display advantageous physico-chemical properties by protecting these active compounds from premature degradation and by releasing them in a controlled manner (5-8). Hydrogels can be prepared from both natural and synthetic hydrophilic polymers, as well as from combinations thereof (9). Synthetic polymers are preferred over their natural counterparts because the risk of immune responses and viral and bacterial contaminations associated with the use of natural polymers can be circumvented. Importantly, synthetic polymers have well defined structures that can be modified to tailor the final properties of the systems. In this study a synthetic biodegradable polymer, exhibiting lower critical solution temperature (LCST) behavior in aqueous solution, was investigated that potentially can be used to design an injectable *in situ* forming hydrogel (10). The body temperature induced formation of a macroscopic gel at the site of injection offers several benefits including patient comfort, enhanced by the minimally invasive administration, and cost reduction when compared to a surgical intervention (11). Moreover, the use of LCST polymer-gels permits encapsulation of active compounds during network formations, overcoming complexities and limitations associated with post-loading technologies.

As the use of physical-crosslinked hydrogels is limited by their relative poor stability, in our approach the hydrogel network is formed by using a combination of physical and chemical cross-linking methods, as successfully applied in other systems (6, 12-13). To this end, association of the thermosensitive blocks above their cloud point at first induces physical gelation and subsequently UV-photopolymerization introduces chemical cross-links to improve the stability of the hydrogels. Photopolymerization can be applied in a minimally invasive manner, for example, using laparascopic devices, cathethers or transdermal illumination. Further, the photocuring process is fast, taking usually only seconds to minutes to complete, can be conducted at room or body temperature without the use of organic solvents and offers the advantage of spatial and temporal control (14-16). Photopolymerization has been applied for the chemical cross-linking of degradable hydrogels, used either for tissue engineering or protein delivery applications (17-20). The polymer used in this study, as depicted in **Figure 1**, has a triblock structure (ABA) with thermosensitive poly(*N*-(2-hydroxypropyl) methacrylamide

lactate) A-blocks that are partly modified with methacrylate moieties and a B-block of hydrophilic poly(ethylene glycol) with molecular weight of 10 kDa (21-22).
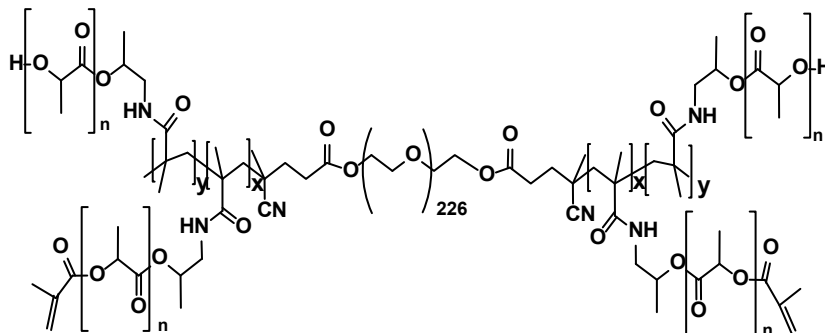

Figure 1. Chemical structure of ABA triblock copolymer consisting of partly methacrylated poly(N-(2-hydroxypropyl) methacrylamide lactate) and PEG 10000.

The p(HPMAm-lac) blocks are responsible for the thermosensitive behavior of the polymer whereas the methacrylate groups can be used for further chemical crosslinking of the hydrogel. Degradability is ensured by the presence of hydrolytically sensitive ester bonds in the lactate side chains of the polymer as well as in the ester bonds between PEG and thermo-blocks (23). This will eventually result in biocompatible degradation products, i.e. PEG, p(HPMAm), polymethacrylic acid and lactic acid, which can be either metabolized or eliminated through renal filtration.

We demonstrated that the cloud point of the polymer can be tuned by the average length of the lactate side chains (21). However, it was shown that this physically crosslinked gel had a limited stability in aqueous environment likely due to its fast swelling and subsequent dissolution. We also showed that the stability was substantially improved by introduction of covalent crosslinks in the hydrophobic domains upon UV polymerization of the methacrylate groups (24).

The aim of this work was to investigate the tailorability of the newly developed injectable thermosensitive hydrogels for protein release. Further, the structural integrity and biological activity of the released proteins was studied.

3.2. Materials and methods

3.2.1. Materials

Unless indicated otherwise, chemicals were obtained from Sigma Aldrich and were used as received. L-lactide was obtained from Purac Biochem BV (Gorinchem, The Netherlands) and Irgacure 2959 was obtained from Ciba Specialty Chemicals Inc. White egg chicken lysozyme

and 4,4′-azobis(4-cyanopentanoic acid) were obtained from Fluka Chemie AG (Buchs, Switzerland). HPMAm was obtained from Zentiva a. s. (Praha, Czech Republic). HPMAm-monolactate and HPMAm-dilactate were synthesized according to a previously reported method (25). Monoclonal human IgG1 (solution of 65mg/ml in 10mM sodium citrate solution, 5% (w/v) sucrose, pH 6) was provided by Biogen Idec Intl BV (The Netherlands).

3.2.2. ^{1}H NMR spectroscopy

^{1}H NMR (300 MHz) spectra were recorded on a Gemini 300 MHz spectrometer (Varian Associates Inc., NMR Instruments, Palo Alto, CA) using CDCl$_3$ and DMSO-d_6 as solvents. Chemical shifts were referred to the solvent peak.

3.2.3.   Synthesis of methacrylated triblock copolymer

ABA triblock copolymer of PEG 10 kDa as hydrophilic B-block and p(HPMAm-lac) as thermosensitive outer A-blocks with a feed ratio HPMAm-monolactate/HPMAm-dilactate of 50/50 was synthesized by free radical polymerization using (PEG-ABCPA)$_n$ as macroinitiator according to the method described by Vermonden et al. (22). The M_n of the polymer was determined by ^{1}H NMR and by GPC as described in section 2.3. Subsequently, methacrylic side groups at 10% of the available OH groups were introduced.The yield was 1.5 g (94%) and the degree of methacrylation (DM) 10 %, as determined by ^{1}H NMR in DMSO (24).

3.2.4.   Preparation of the empty and protein loaded hydrogels

Gels with a weight of 100 mg were prepared in cylindrical shaped glass vials (diameter of 5 mm) as follows. The polymer was dissolved at a concentration of 20, 25 or 35% (w/w) unless indicated otherwise in PBS buffer pH 7.4 (8.2 g/l NaCl; 3.1 g/l Na$_2$HPO$_4$.12H$_2$O; 0.3 g/l NaH$_2$PO$_4$, supplemented with 0.02% NaN$_3$). The samples were then kept at 4 ºC for 2 hours to fully dissolve the polymers. Next 20 μl of a concentrated Irgacure 2959 solution (25 mg/ml) in PBS buffer pH 7.4, was added to the polymer solution to get a final photoinitiator concentration of 0.05% (w/v). The prepared hydrogel was heated to 37 ºC in order to induce physical gelation of the polymer. A BluePoint lamp 4 (350-450 nm, Honle UV technology, light intensity of 450 mW/cm^2) was applied during 5 minutes for the photopolymerization of the hydrogels.

3.2.5.   Methacrylate conversion measurements

The gels prepared as described in section 2.6 were incubated at 37 ºC in 10 ml of 0.02 M NaOH for 30 minutes to dissolve the gels. Subsequently, 2 ml of 2 M acetic acid solution

was added. Samples treated the same way, but without the addition of photoinitiator and UV irradiation were used as controls. For detection of methacrylic acid, a Waters Acquity UPLC^{TM} system was used with a BEH C18 1.7μm, 2.1 × 50 mm column, equipped with a UV detector operating at 210 nm. The eluent used was 95/5/0.1% H_2O/acetonitrile/CF_3COOH. The flow rate was 0.5 ml/min and the column temperature was 50 °C.

3.2.6. *Hydrogel degradation studies*

Gels (100 mg, 20 and 35 % w/w) were prepared in cylindrical glass vials as described in section 2.6. The vials were transferred to a water bath of 37 °C and 0.9 ml of PBS buffer at pH 7.4 containing 0.02% NaN_3 was added on top of the gels. At regular intervals the weight of the gel was measured (W_t) upon removal of the excess of buffer to calculate the swelling ratio ($SR = W_t/W_0$) as ratio between weight of the gel at different time-points and initial gel weight (W_0). After each measurement 0.9 ml of fresh buffer was added and the vials stored again in the water bath at 37 °C.

3.2.7. *Rheological characterization of (non)-photopolymerized hydrogels*

Rheology analysis of the photopolymerized hydrogels was performed on an AR G-2 (TA-Instruments), which was equipped with UV lightguide connected to a BluePoint lamp 4 (350-450 nm, Honle UV technology, light intensity of 50 mW/cm^2). Gels were studied at 37 °C using a plate-plate geometry at 0.1% strain and 1 Hz frequency. The diameter of the geometry was 20 mm and the gap between the plates 300 μm. The polymer solution was applied between the two plates and heated from 4 to 37 °C and after 3 minutes the sample was UV irradiated for 5 minutes. From the storage modulus G', the molar weight between effective cross-links, M_c, was calculated using equation 1,

$$G' = \frac{\rho RT}{M_c} \qquad (1)$$

where ρ is the polymer concentration [g/m^3], R is the molar gas constant and T is the absolute temperature (26).

3.2.8. *Protein Release studies from photopolymerized hydrogels*

In vitro protein release from photopolymerized gels was studied using three model proteins, lysozyme, BSA and IgG, differing in molecular weight (Mw) and hydrodynamic diameter (d$_h$) (Mw$_{lysozyme}$ = 14000 g/mol; Mw$_{BSA}$ = 67000 g/mol; Mw$_{IgG}$ = 150000 g/mol; d$_h$ $_{lysozyme}$ = 4.1 nm (27); d$_h$ $_{BSA}$ = 7.2nm (27); d$_h$ $_{IgG}$ = 10.7 nm (28)). Twenty μl of a concentrated

protein solution (50 mg/ml) was added to 60 µl of a polymer solution in PBS pH 7.4, upon storage of the latter at 4 °C to allow homogeneous distribution of the protein in the hydrogel. Subsequently, 20 µl of Irgacure solution (25 mg/ml) was added to 80 µl of protein/polymer solution and the resulting solution was heated to 37 °C and photopolymerized in a cylindrical glass vial, as described in section 2.4. Next, 0.9 ml of PBS buffer pH 7.4 was applied on top of the gels and the vials were incubated in a shaking water bath at 37 °C. Samples of 0.15 ml were taken in time and replaced by an equal volume of fresh buffer. The concentration of lysozyme and BSA in the different samples was determined using an Acquity UPLC^{TM} with a BEH C18 1.7 µm, 2.1 × 50 mm column. An eluent gradient, from 0 to 100% of eluent A was used, where eluent A was 95/5/0.1% H_2O/acetonitrile/CF_3COOH and eluent B was 100/0.1% acetonitrile/CF_3COOH. The injection volumes of the samples were 5 µl, the flow rate 0.25 ml/min and detection was done at 210 nm. The concentration of IgG in the release samples was determined by GPC using a using a TSK Gek 3000 SWXL column (300 × 7.8 mm) with TSK Gel 3000 pre column (Tosoh Biosep, Stuttgart, Germany) and PBS pH 7.4 as eluent. The flow rate was 0.7 ml/min and detection was done at 280 nm. The column temperature was 40 °C and the injection volumes of samples were 40 µl.

3.2.9. *Fluorescence recovery after photobleaching (FRAP)*

The mobility of FITC-labeled BSA (obtained from Sigma Aldrich) in 20 and 35% (w/w) gels was studied with FRAP analysis. FITC-BSA (2 mg/ml) loaded gels were prepared as described in section 2.4. Prior to photopolymerization, a spatula tip of the mentioned hydrogels was placed between two objective glasses, separated by a 0.5 mm thick adhesive spacer (Secure-Seal Spacer, Molecular Probes, Leiden, The Netherlands). Next, the gel was photopolymerized using the same experimental conditions as described in section 2.4. Measurements were performed using a previously published FRAP method (29). FRAP experiments were carried out on a confocal scanner laser microscope (MRC1024 UV, Bio-Rad, Hemel Hempstead, UK) modified for bleaching arbitrary regions and. The 488-nm line of a 4W Ar-ion laser (Stabilite 2017; Spectra Physics, Darmstadt, Germany) was used for photobleaching and imaging. Uniform disks of 40 µm of diameter were bleached at high laser intensity for 200 ms and the recovery of fluorescence in that area was monitored during 60 s by using a strongly attenuated laser beam. The microscope was equipped with a 10× objective lens (CFI Plan Apochromat; Nikon, Badhoevedorp, The Netherlands). The local diffusion coefficient and immobile fraction were calculated from the experimental recovery curve by fitting of the appropriate FRAP model (29).

3.3. Results and Discussion

3.3.1. Synthesis and characterization of methacrylated triblock copolymers

A p(HPMAm-lac)-PEG-p(HPMAm-lac) triblock copolymer was synthesized by radical polymerization using a PEG macroinitiator with a yield of 84% (22). **Table 1** shows the characteristics of the synthesized polymer. The ratio of HPMAm-monolactate and HPMAm-dilactate (ML/DL) in the thermosensitive polymer was 55/45 as determined by NMR, which was close to the feed ratio of 50/50. The molecular weight M_n of the polymer was 52 kDa, as determined by ^{1}H-NMR; in detail, the M_n's of the PEG block and the p(HPMAm-lac) blocks were 10 kDa and 21 kDa, respectively. The polymer was functionalized using methacrylic anhydride and DMAP as catalyst in dry THF (**Figure 1**).

Table 1. Characteristics of triblock p(HPMAm-lac)-PEG-p(HPMAm-lac)

M_n (kDa)	PDI[b]	Yield (%)	Feed ratio ML/DL	Measured ratio ML/DL[a]	DM (%)[a]	CP (°C)[c]
52[a] 38.5[b]	1.4	84	50/50	55/45	0 10	29 21

[a] Determined by ^{1}H NMR
[b] Determined by GPC using PEG standards [21]
[c] Determined by SLS at 5 mg/ml in acetate buffer pH 5.0 [23].

^{1}H NMR showed that 10% of the hydroxyl groups on the lactate chains was methacrylated and the efficiency of methacrylation was about 40%. The molecular weight M_n determined by GPC using PEG standards was 38 kDa. It should be noted that GPC with PEG standards always provide lower M_n's for these kind of polymers compared to NMR data (21-22, 24). The M_n of the synthesized p(HPMAm-lac)-PEG-p(HPMAm-lac) triblock copolymer was similar to that before methacrylation, indicating that no premature polymerization of the methacrylate groups had occurred. The synthesized triblock copolymer had a rather narrow molecular weight distribution (the polydispersity index (PDI) was 1.4). The non-methacrylated triblock copolymer had a cloud point of 29 °C, which is in line with LCST-values found before for p(HPMAm-lac) with a ratio of HPMAm-monolactate/HPMAm-dilactate of 55/45 (21). A decrease in LCST to 21 °C was observed after methacrylation, which is caused by the increased hydrophobicity of the polymer.

3.3.2. Gel formation and rheological properties

A 35 % aqueous solution of p(HPMAm-lac)-PEG-p(HPMAm-lac) triblock copolymer had a gelation point of 31 °C (Appendix A, Figure 1SI), but these gels however had a limited

stability at 37 °C.(24) To stabilize the structure of the gels they were crosslinked by polymerization of the methacrylate groups upon UV-irradiation using Irgacure 2959 as photoinitiator, which was selected for its known biocompatibility (30). **Table 2** shows that methacrylate conversion was around 80% for the 35% formulation and even increased to around 95% for the 20% formulation. This might be due to the lower turbidity of the polymer gel at lower concentrations, which allows a more efficient penetration of the UV light into the gel.

Table 2. Methacrylate conversion and average molar weights between effective cross-links (M_c) for gels with 20, 25 and 35% w/w of polymer concentration at 37 °C.

Polymer concentration (% w/w)	Methacrylate conversion (%)	M_c (kDa)
20%	94±3	322 ± 22
25%	87±5	364 ± 19
35%	79±5	196 ± 12

Figure 2 shows that the storage modulus of the hydrogels rapidly and substantially increased upon UV irradiation. Subsequently, *G′* of the gels with lower polymer content reached almost a plateau level, whereas *G′* of the gel with 35% of polymer increased until the end of the 5 min UV curing. The storage moduli of the gels after the UV polymerization increased from 1600 to 4600 Pa with increasing polymer concentration from 20 to 35% (**Figure 3**), which in turn suggests a decrease of hydrogel molecular weight between cross-links with increasing solid content. *Tan δ* was similar for the three gels and had a value between 0.5 and 0.75.

In line with expectations, the 35% gels displayed a higher *G′* than the 25% gels, while the *G′* and *G′′* for the 20 and 25% hydrogels were about the same (Figure 2). This observation can likely be explained by the methacrylate conversion (Table 2), which shows a higher methacrylate conversion in the 20% hydrogel than for the 25% hydrogel and counterbalances the effect of the lower solid content of the gel. For the gel with 20% of polymer concentration, an absolute amount of $2.1 \pm 0.1*10^{-11}$ mol of methacrylate groups were converted and, similarly, $2.4 \pm 0.1*10^{-11}$ mol were calculated for the gel with 25% of polymer concentration. Whereas for 35% polymer hydrogels a higher amount of converted methacrylate groups was found ($3.1 \pm 0.2*10^{-11}$ mol), which explains the higher value of the storage modulus.

To further characterize the gel properties, the M_c was investigated (5, 31). As expected, the M_c values of the studied hydrogels, as determined from the storage moduli and calculated using equation (1), decrease with increasing polymer concentration (Table 2). This result

shows a similar tendency as was previously reported for dextran hydrogels (32-33). Furthermore, it can be observed that in the studied range of polymer concentrations, the M_c values of the gels are always higher than the molecular weight of the selected proteins.
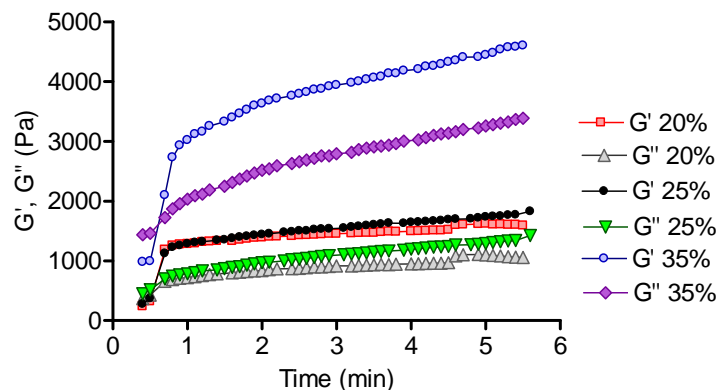

Figure 2. Storage modulus (G') and loss modulus (G'') of hydrogels with 20, 25 and 35% w/w of polymer concentration during the UV curing process. UV-illumination was done for 5 minutes and started at time 0.5 min.

3.3.3. Degradation behavior of the (non)-photopolymerized hydrogels

Swelling and degradation experiments (**Figure 3**) showed that non-photopolymerized gels at 35% of polymer concentration fully dissolved in around 100 hours at 37 ºC and pH 7.4.
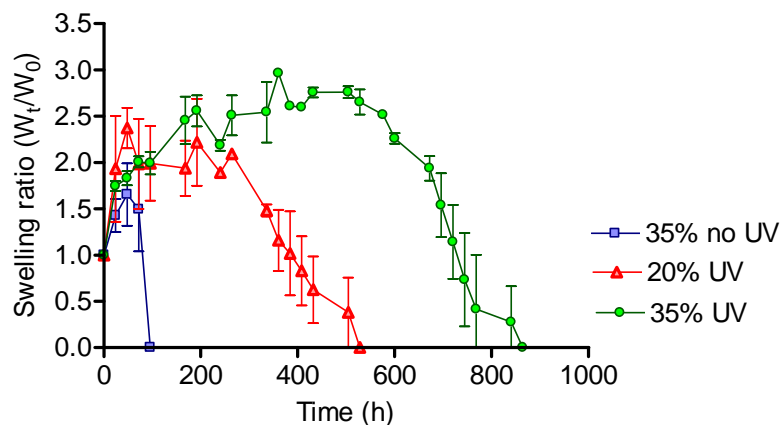

Figure 3. Swelling curves of photopolymerized hydrogels ((▲) 20 and (●) 35% (w/w)) and (■) non-photopolymerized 35% (w/w) hydrogel at 37 ºC, pH 7.4. Data are shown as average (n=2).

During incubation with buffer the gels absorb water, resulting in swelling stresses in the gel. When the strength of the swelling stresses becomes higher than that of hydrophobic interactions, which hold together the thermosensitive chains within hydrophobic domains, polymer dissociation occurs, eventually leading to its dissolution into the incubation buffer.

The chemically crosslinked the networks are able to resist the swelling stresses, improving the stability of the gels. Photopolymerized 35% hydrogels swelled to almost 3 times their initial weight within 360 hours and subsequently dissolved completely in about 850 hours. Hydrogels with 20% of polymer concentration reached a maximum swelling ratio just above 2.0 after 48 hours, and then dissolved in about 500 hours. As reported previously (21), the strong swelling is caused by hydrolysis of the lactate side chains at pH 7.4. When the lactate groups are cleaved, the network becomes more hydrophilic and consequently will absorb more water, resulting in an increased swelling ratio during the first days. The degradation of the hydrogels is due to hydrolysis of the ester groups connecting the methacrylate moieties and the polymer backbone. These connecting ester bonds are less sensitive for hydrolysis than those present in the non-derivatized units (34).

3.3.4. *In vitro protein release*

Proteins were easily loaded in the hydrogel network by mixing an aqueous protein solution and a polymer solution prior to heating and photopolymerization. The influence of protein molecular weights and of hydrogel composition on release was investigated. A continuous release of proteins from gels of both 20 and 35% of polymer content was observed and, importantly, a quantitative release was obtained for all proteins and hydrogel formulations (**Figure 4**), meaning that neither irreversible aggregation nor covalent bonding of protein to the polymer chains had occurred.

To further investigate the compatibility of the delivery system with the protein, preservation of the structure of the released protein was assessed for lysozyme. CD measurements revealed that there were no changes in the spectra of the released lysozyme when compared to native lysozyme (Appendix A, Figure 2SI). A bioactivity assay showed that the specific activity of released lysozyme was unaltered (Appendix A, Figure 3SI), when compared with that of the native protein. It can therefore be concluded that the structure of the released lysozyme was fully preserved, indicating that the preparation process of the photopolymerized gels is protein friendly. This may be due to the separation of the proteins that reside in the hydrophilic domains, from the site of polymerization that occurs in the hydrophobic domains of the hydrogels.Figure 4a shows that the complete release of lysozyme was obtained in 45 and 105 hours, while BSA (Figure 4b) was released in about 150 and 325 hours and IgG (Figure 4c) in 250 and 400 hours from hydrogels with 20 and 35% of polymer concentration, respectively. From this protein release behavior it can be concluded that the protein release kinetics can be tailored by changing the polymer concentration and that the

release is dependent on the protein size. Hydrogels with increasing polymer content display higher cross-link density, which leads to a smaller molecular weight between cross-links, as shown in Table 2, and thereby to a lower release rate,(35) which correlate very well with the hydrodynamic diameters and molecular weights of the selected proteins (IgG>BSA>Lysozyme).
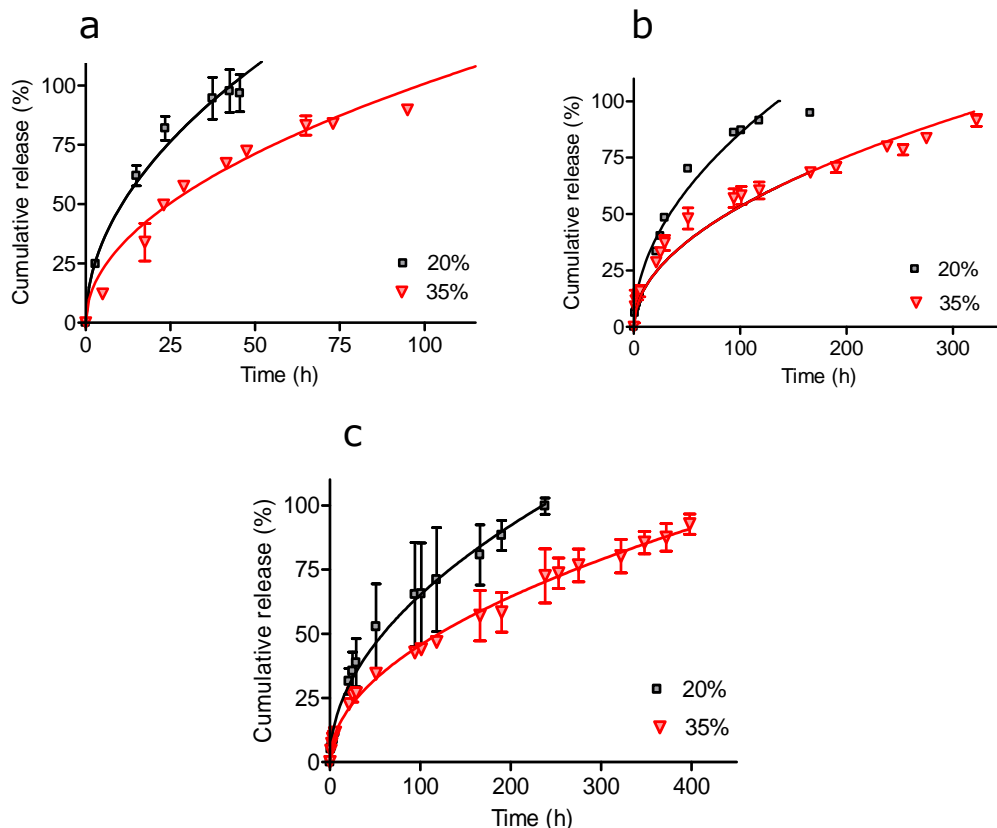

Figure 4. Cumulative protein release from hydrogels with (■) 20 and (▼) 35% (w/w) of polymer concentration as a function of time. (a) Lysozyme, (b) BSA, (c) IgG (n=3).

To gain more insight into the release mechanism, the experimental release data were fitted to the Ritger-Peppas equation (36-37):

$$M^t/M^\infty = kt^n \qquad\qquad (2)$$

where M^t/M^∞ represents the fractional release of the loaded protein, k is a kinetic constant, t is the release time and n is the diffusional exponent that can be related to the release mechanism of the entrapped molecules. If $n = 0.5$, the release is governed by Fickian

diffusion. If *n* = 1, molecules are released by surface erosion, while both mechanisms play a role in release if *n* has a value between 0.5 and 1. The experimental release curves fit to n-values of 0.5 for all the proteins; the cumulative release scaled linearly with the square root of time up to a cumulative release of 80-90% (**Figure 5**), meaning that the release displayed first order kinetics (38). These release profiles suggest a typical diffusion-controlled release of the loaded proteins (31, 39-40). A similar behavior was observed by Hiemstra et. al. in degradable dextran hydrogels, which showed a biphasic release of Lysozyme, BSA and IgG with an initial diffusion controlled phase, whereas basic fibroblast growth factor (bFGF) was quantitatively released by diffusion governed first order kinetics.(41) A diffusional controlled release implies that the hydrogel mesh size is bigger than the diameter of the investigated proteins, which indeed correspond to the calculated mesh sizes from the rheological data (Table 2). By comparing the slopes of the cumulative release versus square root of time plots, it can be noticed that, the release rate decreased with increasing protein size and polymer concentration, meaning that mobility of proteins is restricted by their size (42) and by the cross-linking density of the hydrogel.(35)
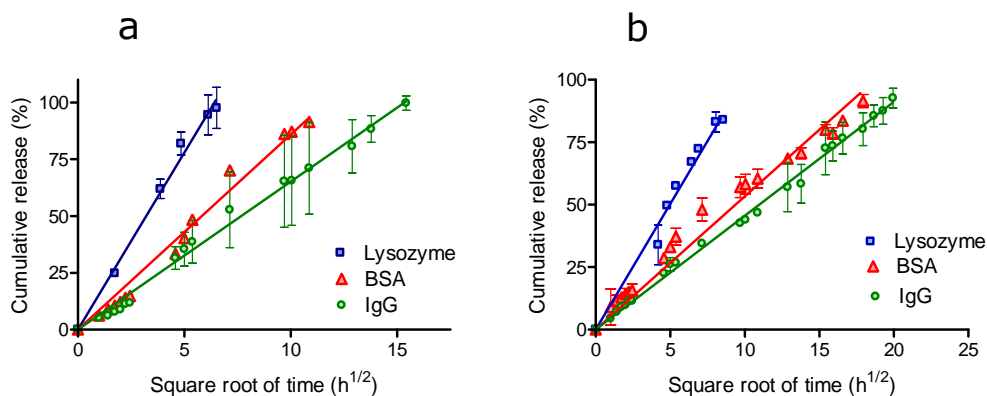

Figure 5. Cumulative release of the three model proteins ((■) lysozyme, (▲) BSA and (▼) IgG) from corresponding hydrogel formulations as a function of the square root of time. (a) 20% w/w polymer concentration; (b) 35% w/w polymer concentration.

Table 3 lists the calculated protein diffusion coefficients by the early-time approximation equation of Fick's second law (36):

$$M^t/M^\infty = 4(Dt/\pi\delta^2)^{1/2} \tag{3}$$

where M^t/M^∞ represents the fractional release of the entrapped protein, D is the diffusion coefficient, t is the release time and δ is the diffusional distance, equal to the thickness of the gel (4.5 and 4.0 mm for gels with 20 and 35% of polymer concentration respectively). As expected, the diffusion coefficients in the hydrogels decrease with increasing molecular weight

of the protein. It is further shown in line with expectations, that an increase of initial polymer concentration leads to lower diffusion coefficients of the proteins in the hydrogel matrices.

3.3.5.   Fluorescence recovery after photobleaching (FRAP)

To further investigate the protein mobility in the hydrogels containing 20 and 35% of polymer concentration, fluorescence recovery measurements after photobleaching (FRAP) were performed at 37 °C, using FITC-labeled BSA as model protein. After photobleaching of FITC-BSA in hydrogels with 20 and 35% (w/w) of polymer the fluorescence almost completely recovered within 60 seconds in both hydrogels, and consequently the mobile fractions values were close to 1 (**Table 4**).

Table 3. Diffusion coefficients (μm^2/sec) of lysozyme, BSA and IgG in water and hydrogels with 20 and 35% (w/w) of polymer concentration calculated by the early-time approximation equation of Fick's second law (n=3)

Protein	H_2O	Hydrogel 20% w/w	Hydrogel 35% w/w
Lysozyme	104[a]	24.8 ± 0.2	8.4 ± 0.1
BSA	59[b]	7.8 ± 0.1	2.3 ± 0.2
IgG	40[c]	4.6 ± 0.1	2.0 ± 0.3

[a] from reference (27)
[b] from reference (27)
[c] from reference (28)

Table 4. Diffusion coefficients and mobile fractions of FITC-BSA from hydrogels with increasing polymer concentrations

Polymer concentration (%)	D (μm^2/sec)	Mobile Fraction
0	59 [a]	N.A.
20	6.4 ± 1.1	0.89 ± 0.04
35	2.4 ± 0.2	0.94 ± 0.03

[a] from reference (27)

This means that almost the entire protein population is able to freely diffuse through the hydrogel network, and demonstrates in line with the release data, that the pores in the network are greater than the hydrodynamic diameter of BSA. Further, a mobile fraction of approx. 1 also shows that neither insoluble protein aggregates were present in the network, nor chemical protein-polymer coupling had occurred (e.g by Michael addition reaction between

 methacrylate groups of p(HPMAm-lac)-PEG-p(HPMAm-lac) triblock copolymer and lysine residues present in BSA) during the process of hydrogel formation.

The FRAP experiments also showed that the diffusion coefficient of FITC-BSA decreases with increasing polymer concentration, more precisely a 9 and 20 time decrease was observed in hydrogels with 20 and 35% of polymer concentration, respectively, as compared to the protein diffusion coefficient in water.

The calculated diffusion coefficients from the FRAP experiments are in excellent agreement with the values calculated from the release data (Table 3 and 4). Therefore, it can be concluded that the protein release was governed exclusively by diffusion and swelling/degradation of the matrix does not contribute to the release mechanism.

3.4. Conclusions

Chemically cross-linked p(HPMAm-lac)-PEG-p(HPMAm-lac) hydrogels were prepared by thermogelling combined with photopolymerization, which is a fast and simple crosslinking method that substantially improves the stability and the mechanical properties of hydrogels. Proteins were easily loaded into the hydrogels by mixing a concentrated protein solution with a polymer solution prior to heating and photopolymerization. They were quantitatively released with first order kinetics and therefore the release mechanism was governed by diffusion. The release kinetics of entrapped proteins can be tailored by the gel characteristics**.** Finally, the preservation of lysozyme structure and function upon release demonstrates the protein friendly nature of these hydrogels and their potential as biomaterials for controlled protein delivery.

References

1. Pavlou AK & Reichert JM (2004) Recombinant protein therapeutics success rates, market trends and values to 2010. *Nature Biotechnology* 22(12):1513-1519.

2. Wang W (1999) Instability, stabilization, and formulation of liquid protein pharmaceuticals. *International Journal of Pharmaceutics* 185(2):129-188.

3. Wang W (2000) Lyophilization and development of solid protein pharmaceuticals. *International Journal of Pharmaceutics* 203(1-2):1-60.

4. Frokjaer S & Otzen DE (2005) Protein drug stability: a formulation challenge. *Nature Reviews Drug Discovery* 4(4):298-306.

5. Peppas NA, Bures P, Leobandung W, & Ichikawa H (2000) Hydrogels in pharmaceutical formulations. *European Journal of Pharmaceutics and Biopharmaceutics* 50(1):27-46.

6. Hennink WE & van Nostrum CF (2002) Novel crosslinking methods to design hydrogels. *Advanced Drug Delivery Reviews* 54(1):13-36.

7. Hoffman AS (2002) Hydrogels for biomedical applications. *Adv. Drug Del. Rev.* 54(1):3-12.

8. Jeong B, Kim SW, & Bae YH (2002) Thermosensitive sol-gel reversible hydrogels. *Advanced Drug Delivery Reviews* 54(1):37-51.

9. Davis KA & Anseth KS (2002) Controlled release from crosslinked degradable networks. *Critical Reviews in Therapeutic Drug Carrier Systems* 19(4-5):385-423.

10. Kretlow JD, Klouda L, & Mikos AG (2007) Injectable matrices and scaffolds for drug delivery in tissue engineering. *Advanced Drug Delivery Reviews* 59(4-5):263-273.

11. Van Tomme SR, Storm G, & Hennink WE (2008) In situ gelling hydrogels for pharmaceutical and biomedical applications. *International Journal of Pharmaceutics* 355(1-2):1-18.

12. Martens PJ, Bowman CN, & Anseth KS (2004) Degradable networks formed from multi-functional poly(vinyl alcohol) macromers: comparison of results from a generalized bulk-degradation model for polymer networks and experimental data. *Polymer* 45(10):3377-3387.

13. van de Wetering P, Metters AT, Schoenmakers RG, & Hubbell JA (2005) Poly(ethylene glycol) hydrogels formed by conjugate addition with controllable swelling, degradation, and release of pharmaceutically active proteins. *Journal of Controlled Release* 102(3):619-627.

14. Lu S & Anseth KS (1999) Photopolymerization of multilaminated poly(HEMA) hydrogels for controlled release. *Journal of Controlled Release* 57(3):291-300.

15. Ward JH & Peppas NA (2001) Preparation of controlled release systems by free-radical UV polymerizations in the presence of a drug. *Journal of Controlled Release* 71(2):183-192.

16. West JL & Hubbell JA (1995) Photopolymerized hydrogel materials for drug delivery applications. *Reactive Polymers* 25:139-147.

17. Lin C-C & Metters A (2006) Enhanced Protein Delivery from Photopolymerized Hydrogels Using a Pseudospecific Metal Chelating Ligand. *Pharmaceutical Research* 23(3):614-622.

18. Kim B & Peppas NA (2003) Poly(ethylene glycol)-containing Hydrogels for Oral Protein Delivery Applications. *Biomedical Microdevices* 5(4):333-341.

19. Burdick JA, Mason MN, Hinman AD, Thorne K, & Anseth KS (2002) Delivery of osteoinductive growth factors from degradable PEG hydrogels influences osteoblast differentiation and mineralization. *Journal of Controlled Release* 83(1):53-63.

20. Hiemstra C, Zhou W, Zhong Z, Wouters M, & Feijen J (2007) Rapidly in Situ Forming Biodegradable Robust Hydrogels by Combining Stereocomplexation and Photopolymerization. *Journal of the American Chemical Society* 129(32):9918-9926.

21. Soga O, Van Nostrum CF, & Hennink WE (2004) Poly(*N*-(2-hydroxypropyl)methacylamide mono/di lactate): a new class of biodegradable polymers with tunable thermosensitivity. *Biomacromolecules* 5:818-821.

22. Vermonden T, Besseling NAM, van Steenbergen MJ, & Hennink WE (2006) Rheological Studies of Thermosensitive Triblock Copolymer Hydrogels. *Langmuir* 22(24):10180-10184.

23. Neradovic D, van Steenbergen MJ, Vansteelant L, Meijer YJ, van Nostrum CF, & Hennink WE (2003) Degradation Mechanism and Kinetics of Thermosensitive Polyacrylamides Containing Lactic Acid Side Chains. *Macromolecules* 36(20):7491-7498.

24. Vermonden T, Fedorovich NE, van Geemen D, Alblas J, van Nostrum CF, Dhert WJA, & Hennink WE (2008) Photopolymerized Thermosensitive Hydrogels: Synthesis, Degradation, and Cytocompatibility. *Biomacromolecules* 9(3):919-926.

25. Soga O, van Nostrum CF, Ramzi A, Visser T, Soulimani F, Frederik PM, Bomans PHH, & Hennink WE (2004) Physicochemical Characterization of Degradable Thermosensitive Polymeric Micelles. *Langmuir* 20(21):9388-9395.

26. Goodwin JW & Hughes RW (2000) *Rheology for chemists, an introduction* (The Royal Society of Chemistry, Cambridge).

27. Merrill EW, Dennison KA, & Sung C (1993) Partitioning and diffusion of solutes in hydrogels of poly(ethylene oxide). *Biomaterials* 14(15):1117-1126.

28. Burczak K, Fujisato T, Hatada M, & Ikada Y (1994) Protein permeation through poly(vinyl alcohol) hydrogel membranes. *Biomaterials* 15(3):231-238.

29. Braeckmans K, Peeters L, Sanders NN, Smedt SCD, & Demeester J (2003) Three-Dimensional Fluorescence Recovery after Photobleaching with the Confocal Scanning Laser Microscope *Biophysical Journal* 85(4):2240-2252.

30. Bryant SJ, Nuttelman CR, & Anseth KS (2000) Cytocompatibility of UV and visible light photoinitiating systems on cultured NIH/3T3 fibroblasts in vitro. *Journal of Biomaterials Science, Polymer Edition* 11:439-457.

31. Lin C-C & Metters AT (2006) Hydrogels in controlled release formulations: Network design and mathematical modeling. *Advanced Drug Delivery Reviews* 58(12-13):1379-1408.

32. Chung JT, Vlugt-Wensink KDF, Hennink WE, & Zhang Z (2005) Effect of polymerization conditions on the network properties of dex-HEMA microspheres and macro-hydrogels. *International Journal of Pharmaceutics* 288(1):51-61.

33. de Jong SJ, De Smedt SC, Demeester J, van Nostrum CF, Kettenes-van den Bosch JJ, & Hennink WE (2001) Biodegradable hydrogels based on stereocomplex formation between lactic acid oligomers grafted to dextran. *Journal of Controlled Release* 72(1-3):47-56.

34. Rijcken CJ, Snel CJ, Schiffelers RM, van Nostrum CF, & Hennink WE (2007) Hydrolysable core-crosslinked thermosensitive polymeric micelles: Synthesis, characterisation and in vivo studies. *Biomaterials* 28(36):5581-5593.

35. Lee F, Chung JE, & Kurisawa M (2009) An injectable hyaluronic acid-tyramine hydrogel system for protein delivery. *Journal of Controlled Release* 134(3):186-193.

36. Ritger PL & Peppas NA (1987) A simple equation for description of solute release II. Fickian and anomalous release from swellable devices. *Journal of Controlled Release* 5(1):37-42.

37. Serra L, Doménech J, & Peppas NA (2006) Drug transport mechanisms and release kinetics from molecularly designed poly(acrylic acid-g-ethylene glycol) hydrogels. *Biomaterials* 27(31):5440-5451.

38. Hiemstra C, Zhong Z, Van Tomme SR, van Steenbergen MJ, Jacobs JJL, Otter WD, Hennink WE, & Feijen J (2007) In vitro and in vivo protein delivery from in situ forming poly(ethylene glycol)-poly(lactide) hydrogels. *Journal of Controlled Release* 119(3):320-327.

39. Siepmann J & Peppas NA (2001) Modeling of drug release from delivery systems based on hydroxypropyl methylcellulose (HPMC). *Advanced Drug Delivery Reviews* 48(2-3):139-157.

40. Van Tomme SR, De Geest BG, Braeckmans K, De Smedt SC, Siepmann F, Siepmann J, van Nostrum CF, & Hennink WE (2005) Mobility of model proteins in hydrogels composed of oppositely charged dextran microspheres studied by protein release and fluorescence recovery after photobleaching. *Journal of Controlled Release* 110(1):67-78.

41. Hiemstra C, Zhong Z, van Steenbergen MJ, Hennink WE, & Feijen J (2007) Release of model proteins and basic fibroblast growth factor from in situ forming degradable dextran hydrogels. *Journal of Controlled Release* 122(1):71-78.

42. Koutsopoulos S, Unsworth LD, Nagai Y, & Zhang S (2009) Controlled release of functional proteins through designer self-assembling peptide nanofiber hydrogel scaffold. *Proceedings of the National Academy of Sciences U.S.A.* 106(12):4623-4628.

Chapter 4

Photopolymerized Thermosensitive Poly(HPMAlactate)-PEG Based Hydrogels: Effect of Network Design on Mechanical Properties, Degradation and Release Behavior

Roberta Censi,[a,b] Tina Vermonden,[a] Hendrik Deschout,[c] Kevin Braeckmans,[c] Piera di Martino,[a] Stefaan C. De Smedt,[c] Cornelus F. van Nostrum,[a] Wim E. Hennink[a]

[a] Department of Pharmaceutics Utrecht Institute for Pharmaceutical Sciences (UIPS); Utrecht University; P.O. Box 80082, 3508 TB Utrecht, The Netherlands.

[b] Department of Chemical Sciences; Camerino University; via S. Agostino 1, 62032, Camerino (MC), Italy.

[c] Laboratory of General Biochemistry and Physical Chemistry, Department of Pharmaceutics, Ghent University, Harelbekestraat 72, B-9000, Ghent, Belgium

Abstract

Photopolymerized thermosensitive A-B-A triblock copolymer hydrogels composed of poly(*N*-(2-hydroxypropyl)methacrylamide lactate) A-blocks, partly derivatized with methacrylate groups at different extent (10, 20 and 30%) and hydrophilic poly(ethylene glycol) B-blocks of different molecular weights (4, 10, 20kDa) were synthesized. The aim of the present study was to correlate the polymer architecture with the hydrogel properties, particularly rheological, swelling, degradation properties and release behavior. It was found that an increasing methacrylation extent and a decreasing PEG molecular weight resulted in increasing gel strength and cross-link density, which tailored the degradation profiles from 25 to more than 300 days. Polymers having small PEG-blocks showed a remarkable phase-separation into polymer- and water-rich domains as demonstrated by confocal microscopy. Depending on the hydrophobic domain density, the loaded protein resides in the hydrophilic pores or is partitioned into hydrophilic and hydrophobic domains and its release from these compartments is tailored by the extent of methacrylation and by PEG length, respectively. As the mechanical properties, degradation and release profiles can be fully controlled by polymer design and concentration, these hydrogels are suitable for controlled protein release.

4.1. Introduction

The design of a controlled drug delivery system is usually based on the drug's physicochemical and pharmacokinetic properties and aimed to prevent drug's rapid clearance, inducing a desired pharmacological response over a prolonged period of time and to obviate potentially harmful plasma peak concentrations, normally occurring upon bolus injection.(1-3) Despite the encouraging progress in the field of controlled drug delivery over the past decades, some important clinical needs are still unmet. Conventional delivery systems suffer from the limitation of minimal synchronization between the required time for therapeutically effective drug plasma concentrations and the actual drug release profile exhibited by the dosage form. These considerations have upraised the importance of drug delivery systems fulfilling the drug's therapeutical requirements and have shifted the focus of scientists towards the design of idealized drug formulations, wherein the required amount of active agent is made available at the desired time and site of action in the body.(4)

Hydrogels are three-dimensional networks of physically and/or chemically cross-linked polymers that imbibe large amounts of water, mimicking tissues and allowing encapsulation and release of biomolecules in a physiologically relevant setting and they have emerged as promising candidates in this respect.(5-7) Besides their ability to circumvent some of the complexities associated with the release of biotherapeutics from hydrophobic polymers (e.g. degradable copolymers of lactic and glycolic acid) such as protein denaturation(8),(9) and immunogenic response towards the entrapped protein,(10) they exhibit the capability to modify the pharmacological performance of various classes of drugs by precise modulation of their release in a sustained and tailorable fashion.(5) Amphiphilic block copolymers are a particular class of suitable hydrogel building blocks because of their ability to self-assemble, as well as flexibility of block copolymer chemistry, which allows the realization of well-defined molecular architectures of hydrogel networks, and thereby tailoring their macroscopic properties and drug release behavior. Moreover, another crucial functionality of synthetic block copolymer based hydrogels is their biodegradability.

Hydrogel networks composed of hydrophilic polymers such as poly(ethylene glycol) (PEG)(11-12) or poly(vinyl alcohol) (PVA)(13) are particularly suitable to carry out the above functions, as these materials possess physicochemical characteristics that closely mimic those of natural tissues. This characteristic is well suited for the design of "smart" biomaterials with tunable bioresponsive functions. Degradation and drug release kinetics in a given biological environment can be readily controlled by the polymer molecular weight and functionality, as well as the overall polymer content.(14-18)

In our previous work, we have described a class of synthetic biodegradable polymers, exhibiting Lower Critical Solution Temperature (LCST) behavior in an aqueous solution that potentially can be used to design injectable *in situ* forming hydrogels.(19-20) The aforementioned polymer has an A-B-A architecture consisting of thermosensitive poly(*N*-(2-

hydroxypropyl)methacrylamide lactate) (p(HPMAm-lac) A-blocks that are partly modified with methacrylate moieties, to allow chemical cross-linking using photopolymerization, and a B-block of poly(ethylene glycol) (PEG).(21-22) The p(HPMAm-lac) A-blocks exhibit thermosensitive behavior, having a cloud point (CP) that can be tuned by the average length of the lactate side chains.(21) This property allows the design of a polymer that self-assembles in aqueous solution upon injection *in vivo*, because its CP is lower than 37°C. (23) This body temperature induced formation of a macroscopic gel at the site of injection is particularly beneficial for the patient, implying minimally invasive administration, enhanced shape adaptation and cost reduction compared to surgical implantation.(24-25) Moreover, the use of thermosensitive polymer-gels permits the encapsulation of active compounds during the network formation, overcoming complexities and limitations associated with post-loading techniques.

Despite the numerous advantages of physically cross-linked hydrogels, their rapid swelling and subsequent dissolution in physiological environment limits their applicability as controlled delivery systems. Therefore, chemical cross-linking methods are additionally used to stabilize the hydrogel structure.(26-29) To this end, in our approach UV photopolymerization is applied upon association of the thermosensitive blocks above their CP and, as a result, the structural stability of the hydrogel is remarkably enhanced.(30-34) Photopolymerization is a widely utilized technique to realize spatially and temporally controlled chemical cross-linking of hydrogels suitable for drug delivery and tissue engineering. Potentially, it can be implemented by means of laparoscopy or trans-dermal illumination in case of subcutaneously injected depot systems.(35-36)

Besides thermosensitivity, degradability is another advantageous characteristic of our hydrogel system, which is ensured by the presence of hydrolytically sensitive ester bonds in the lactate side chains as well as in the ester bonds connecting PEG and the thermo-blocks.(37) Under physiological conditions, hydrolytical degradation of the hydrogel eventually results in low-toxic degradation products, i.e. PEG, p(HPMAm), polymethacrylic and lactic acid, which can be either metabolized or eliminated through renal filtration.

We have shown that the described thermosensitive polymer based hydrogel is a suitable controlled delivery system for proteins, being the release mechanism mediated by Fickian diffusion of the biomolecule through the gel network.(30) It was further shown that the diffusivity of entrapped proteins could be tailored by the polymer concentration and depended on the protein molecular weight. Additionally, the preservation of the structural and functional integrity of the protein was demonstrated.(30)

The present study aimed to explore the tailorability of the described hydrogel by the molecular structure of the polymer, varying PEG's molecular weight (MW) and degree of methacrylation (DM), and investigates how these properties affect the cross-link density. The flexibility of the polymer chemistry indeed offers the opportunity to create a variety of

hydrogels with well-defined physicochemical properties and reproducible and modular release profiles.(16, 18, 38)

4.2.   Materials and Methods

4.2.1   Materials

Unless indicated otherwise, the chemicals were obtained from Sigma-Aldrich and were used as received. L-lactide was obtained from Purac Biochem BV (Gorinchem, The Netherlands) and Irgacure 2959 was obtained from Ciba Specialty Chemicals Inc. 4,4´-Azobis(4-cyanopentanoic acid) was obtained from Fluka Chemie AG (Buchs, Switzerland). HPMAm-monolactate and HPMAm-dilactate were synthesized according to a previously reported method.(21) The synthesis of triblock copolymers with PEGs as middle block and polyHPMAm-lactate as outer blocks was described previously (22, 30-31) and applied in this study for the preparation of triblock copolymers having fixed p(HPMAm-lac) A-blocks of 22 kDa, derivatized with 20% of methacrylate groups and PEGs of varying molecular weight (4, 10, 20, 40 kDa) B-blocks, and polymers having a PEG 10 kDa B-block, p(HPMAm-lac) 22 kDa A-blocks, modified with 10, 20 and 30% of methacrylate moieties. Bovine serum albumin (BSA), fluorescein isothiocyanate bovine serum albumin (FITC-BSA) and Nile Red (NR) were purchased from Sigma Aldrich.

4.2.2. ^{1}H NMR Spectroscopy

^{1}H NMR (300 MHz) spectra were recorded on a Gemini 300 MHz spectrometer (Varian Associates Inc., NMR Instruments, Palo Alto, CA) using DMSO-d_6 as a solvent. Chemical shifts were referred to the solvent peak (δ = 2.49 ppm for DMSO-d_6).

4.2.3.   Gel Permeation Chromatography

The molecular weights of the polymers were determined by GPC using a Plgel 5 µm MIXED-D column (Polymer Laboratories) with a column temperature of 40 ºC. DMF containing 10 mM LiCl was used as eluent with an elution rate of 0.7 ml/min, and the sample concentration was 5 mg/ml in the same eluent. Poly(ethylene glycols) with defined molecular weights were used as calibration standards.(21)

4.2.4.   Determination of the Cloud Point

The cloud point (CP) of the polymers was measured with static light scattering using a Horiba Fluorolog fluorometer (650 nm, 90º angle). The polymers were dissolved at a

concentration of 3 mg/ml in ammonium acetate buffer (pH 5.0, 120 mM). The heating rate was approximately 1 ºC/ min and every 0.2 ºC the scattering intensity was measured at 90º angle. The CP is defined as the onset of increasing scattering intensity.(37)

4.2.5. *Synthesis of Methacrylated Triblock Copolymers*

Thermosensitive triblock copolymers consisting of PEG 4, 10, 20 and 40 kDa as hydrophilic block and pHPMAm$_{lac}$ as thermosensitive outer blocks with a HPMAm-monolactate/HPMAm-dilactate ratio of 50/50 were synthesized by free radical polymerization using (PEG-ABCPA)$_n$ macroinitiators according to a method described earlier.(22) The OH side groups of p(HPMAm-lac) were partially methacrylated using the following procedure. The triblock copolymers (28.5 mmol) were dissolved in dry THF under a N$_2$ atmosphere. Dimethylaminopyridine (DMAP) (0.15, 0.30 and 0.45 mmol, for 10, 20 and 30% methacrylation, respectively) and triethylamine (TEA) (3.8, 7.6 and 11.4 mmol for 10, 20 and 30% methacrylation, respectively) were added at 0ºC. Methacrylic anhydride (MA) (3.8, 7.6 and 11.4 mmol for 10, 20 and 30% methacrylation, respectively) at 1:1 molar ratio with TEA was added as last component. The reaction mixture was subsequently stirred for 24 hours at room temperature. Afterwards, the polymers were diluted with water, dialyzed (membrane with a cut-off of 12-14 kDa) against water for two days and isolated by freeze-drying. The synthesized polymers were characterized by ^{1}H NMR (DMSO-d_6): δ 7.35 (1H, b, N*H*), 6.15 & 5.80 (2H, d, C=C*H$_2$*), 5.4 (1H, d, CH-O*H*), 4.95 (d, CO-C*H*(CH$_3$)-O), 4.1 (1H, d, CO-C*H*(CH$_3$)-OH), 3.60 (904H, s, OC*H$_2$*C*H$_2$* (PEG-protons)), 3.4 (2H, s, NHC*H$_2$*), 2.2-0.6 (main chain protons and CH$_3$ of lactate groups). The degree of methacrylation (DM), defined as the percentage of OH groups derivatized with methacrylate moieties was calculated from the ratio of the average intensity of the peaks at 6.15 and 5.80 and intensity of the peak at 5.4 ppm as follows: $((I_{6.15}+I_{5.8})/2) / ((I_{6.15}+I_{5.8})/2 +I_{5.4}) \times 100\%$.(31)

4.2.6. *Preparation of Placebo and Protein Loaded Hydrogels*

Hydrogels of 100 mg were prepared in cylindrically shaped glass vials (diameter of 5 mm) as follows. Triblock copolymers (20 and 35 mg) were dissolved in 60 and 65 µl PBS buffer pH 7.4 (8.2 g/l NaCl; 3.1 g/l NaH$_2$PO$_4$12H$_2$O; 0.3 g/l NaH$_2$PO$_4$, supplemented with 0.02% NaN$_3$), respectively. Next, 20 µl of an Irgacure 2959 solution (2.5 mg/ml) was added. The final polymer concentrations were 20 and 35 wt%, while the Irgacure concentration was 0.05 wt%. The samples were then incubated at 4 ºC for 2 hours to fully dissolve the polymers and subsequently heated to 40 ºC before photopolymerization. A BluePoint lamp 4 (350-450 nm, Honle UV technology, light intensity of 450 mW/cm^2) was used during 5 minutes for the photopolymerization of the hydrogels. A glass filter between the sample and the light source

was used to cut off light wavelenght below 300 nm and prevent protein degradation. BSA or FITC-BSA loaded hydrogels were prepared according to a slightly different procedure. The triblock copolymers, 20 and 35 mg, were dissolved in 40 and 25 µl of PBS solution (composition see above), for 20 and 35 wt% polymer hydrogels, respectively. Upon dissolution of the polymer at 4 °C, 20 µl of an Irgacure solution in PBS (2.5 mg/ml) and 20 µl of a BSA (100 mg/ml) or FITC-BSA (10 mg/ml) solution in the same buffer was added to yield a hydrogel containing 2 wt% protein or 0.2 wt% fluorescently labeled-protein, 0.05 wt% Irgacure and 20 or 35 wt% polymer. The hydrogels were first physically (thermogelling) and subsequently chemically photo cross-linked as described above.

4.2.7. Swelling and Degradation Studies

Hydrogels were prepared in 1 ml glass vials and the exact weight of the gel was measured (W_0). The vials were incubated at 37 ºC and 0.9 ml PBS buffer pH 7.4, containing 0.02% NaN_3 was added. At regular intervals, the incubation buffer was removed and the weight of the gel was measured (W_t) to calculate the swelling ratio (SR = W_t/W_0). Next, 0.9 ml buffer was added and the samples were further incubated at 37 ºC.(30)

4.2.8. Rheological Characterization

The rheological analysis of the photopolymerized hydrogels was performed on an AR-G2 rheometer (TA-Instruments) equipped with UHP device connected to a BluePoint 4 mercury lamp (Honle UV technology, range 230-500 nm, intensity of 50 mW/cm^2). Gels were studied at 37 °C using a plate-plate geometry. A 0.1% strain was applied. The physically cross-linked gels were photopolymerized *in situ* while measured.(30)

4.2.9. Release Studies

In vitro release of BSA from the photopolymerized gels was studied in 1 ml cylindrical glass vials. The hydrogels (100 mg), placed on the bottom of the vial, were exposed to 0.9 ml of PBS buffer pH 7.4 (8.2 g/l NaCl; 3.1 g/l $NaH_2PO_412H_2O$; 0.3 g/l NaH_2PO_4, supplemented with 0.02% to prevent bacterial growth). Only the top surface of the hydrogels was exposed to the incubation medium. The vials were incubated in a shaking waterbath of 37°C. Samples of 150 l of the acceptor medium were taken in time and replaced by an equal volume of fresh buffer. The concentration of BSA was determined using an Acquity UPLC^{TM} with a BEH C18 1.7 µm, 2.1 x 50 mm column. A mobile phase gradient, from 100% of eluent A (95/5/0.1% H_2O/acetonitrile/trifluoroacetic acid) to 100% of B (100/0.1% acetinitrile/trifluoroacetic acid) in 10 minutes runtime was used. The injection volumes of the samples were 5 µl, the flow rate was 0.250 ml/min and detection was done at 280 nm. For

calibration, three solutions of BSA freshly dissolved at concentrations of 0.1, 0.5 and 1 mg/ml were prepared and the injected volumes varied from 0.5 to 7.5 µl.

4.2.10. *Confocal Laser Scanning Microscopy (CLSM)*

FITC-BSA loaded hydrogels were prepared as described in the previous section. Prior to photopolymerization, the hydrogels were heated at 37°C and a trace amount of NR was added to the hydrogel. The hydrogels were incubated at 37°C for 2 hours to allow partioning of NR into the hydrophobic domains of the gels. Subsequently, the hydrogels were placed on a microscope slide and covered with a sealed cover-slip. The hydrogel was photopolymerized and confocal images were obtained using a Zeiss/Biorad Radiance 2100MP multiphoton microscope (Jena, Germany) equipped with Argon (488 nm) and HeNe (543 nm and 633 nm) lasers and a 100× water immersion objective lens. Fluorescence detection was performed with standard filter cubes settings for the detection of the FITC and NR labels. The hydrogels were maintained at a temperature of 37 °C using a Solent Scientific climate chamber (Segensworth, UK).

4.3.   **Results and Discussion**

4.3.1. *Polymer characteristics*

A series of A-B-A triblock copolymers consisting of pHPMAm-lac A-blocks of approximately 22 kDa, PEG molecular weight (MW) of 10 kDa (B block) and with a varying methacrylation extent (DM) of 10, 20 and 30 % were synthesized. Also triblock copolymers with different PEG B-block molecular weight of 4, 10 and 20 kDa were prepared, while keeping the methacrylation extent and the A-blocks molecular weight constant (20% and 22 kDa, respectively). The polymers are abbreviated as M_xP_y, where M_x indicates the degree of methacrylation (i.e. M_{10} for a DM of 10%) and P_y the PEG molecular weight (i.e. P_{10} for PEG 10 kDa).

Scheme 1 shows the chemical structure and **Table 1** the characteristics of the synthesized polymers.

For all the synthesized polymers, the copolymer composition (DP1:DP2 ratio), as determined by ^{1}H-NMR, corresponded to the feed ratio of 50:50. The polymer M_0P_{10} (Table 1) had a CP of 29°C, which dropped to 21, 14 and 8°C upon 10 ($M_{10}P_{10}$), 20 ($M_{20}P_{10}$) and 30% ($M_{30}P_{10}$) methacrylation, respectively. As reported previously, this decrease in CP is due to an increased polymer hydrophobicity as a result of the introduction of methacrylate groups on the lactate side chains.(30-31) The variation of PEG molecular weight had no influence on the cloud point of the triblock copolymers $M_{20}P_4,$ $M_{20}P_{10},$ $M_{20}P_{20}$ and $M_{20}P_{40}$ (Table 1).
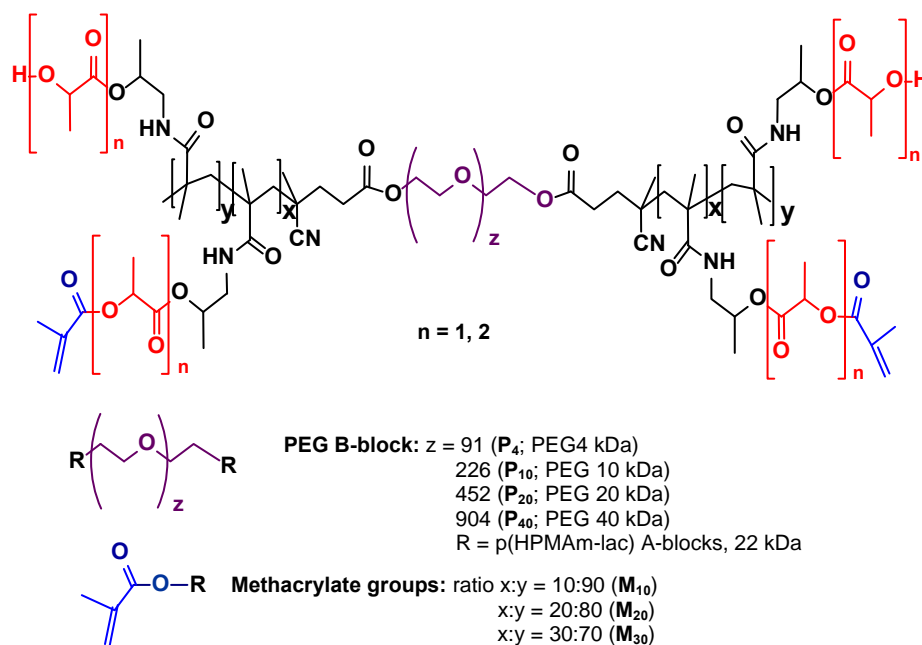
PEG B-block: z = 91 (**P₄**; PEG4 kDa)
226 (**P₁₀**; PEG 10 kDa)
452 (**P₂₀**; PEG 20 kDa)
904 (**P₄₀**; PEG 40 kDa)
R = p(HPMAm-lac) A-blocks, 22 kDa

Methacrylate groups: ratio x:y = 10:90 (**M₁₀**)
x:y = 20:80 (**M₂₀**)
x:y = 30:70 (**M₃₀**)

Scheme 1. Chemical structure of A-B-A triblock copolymers composed of methacrylated p(HPMAm-lac) A-blocks and PEG B-block.

The molecular weights of the polymers, calculated according to ^{1}H-NMR and measured by GPC are listed in Table 1. It appears that the values based on GPC analysis exceed those based on ^{1}H-NMR analysis. It was shown earlier that this discrepancy can be ascribed on the use of PEG homopolymers as GPC standards that display larger hydrodynamic volumes than the triblock copolymers.(22, 39) All the synthesized polymers had a yield of polymerization of 72 ± 3 % and the conversion of the methacrylic anhydride during the methacrylation reaction was 45 ± 5%, in agreement with previous results.(30-31)

Hydrogels, with initial solid contents of 20 and 35% were prepared from the different triblock copolymers listed in Table 1.

Table 1. Characteristics of A-B-A triblock copolymers composed of (methacrylated) p(HPMAm-lac) A-blocks and PEG B-block.

Name	PEG M_W (kDa)	DM (%)[a]	M_n A-blocks (kDa)[a]	M_n triblock (kDa)/PDI[b]	CP[c] (°C)
M_0P_{10}	10	0	23.5	38.1/1.9	29
$M_{10}P_{10}$	10	10	22	39.2/2.0	21
$M_{20}P_{10}$	10	20	23	39.7/1.8	14
$M_{30}P_{10}$	10	30	21.5	40.1/1.8	8
$M_{20}P_4$	4	20	23.5	27.1/2.1	15
$M_{20}P_{20}$	20	20	22.5	47.5/2.0	14
$M_{20}P_{40}$	40	20	23	53.2/1.9	16

[a] Determined by ^{1}H-NMR; [b] Determined by GPC; [c] Determined by SLS

4.3.2. *Mechanical Characterization of Hydrogels*

The chemical cross-linking efficiency after UV-photopolymerization was studied by determination of the unreacted methacrylic groups, upon degradation of the gels (**Table 2**), as described earlier.(30) It was found that, regardless of the PEG molecular weight and the extent of methacrylation, the methacrylate conversion was approximately 75% and 95% for hydrogels of 35 and 20% polymer concentrations, respectively.

These data are in line with previous observations, where it was reasoned that the decreased methacrylate conversion at increased polymer concentration can be attributed to the higher cloudiness of polymer richer hydrogels, leading to diminished capability of the light to penetrate into the sample.(30)

The mechanical characterization of the hydrogels was performed by rheological measurements. In previous papers, we demonstrated that physical hydrogels are formed at temperatures below 37°C (22) and that the UV photopolymerization induced a remarkable and immediate stabilization of the hydrophobic domains by chemical cross-linking of the methacrylate groups on the lactate side chains. (30)

In **Figure 1**, the influence of methacrylation extent on the rheological properties of 20 and 35 wt% polymer hydrogels is shown. As expected, the storage moduli clearly indicate that for both polymer concentrations the cross-linking density increases with increasing methacrylation extent, indicating the formation of a tighter and more rigid network when the polymer is derivatized with more methacrylate moieties. For all the hydrogel formulations

studied, tan δ (G''/G') was found between 0.1 and 0.3 demonstrating that almost fully elastic gels were formed.

Table 2. Methacrylate conversion of hydrogels consisting of A-B-A triblock copolymers (Table 1).

Name	Polymer content (wt%)	Methacrylate conversion (%)
$M_{10}P_{10}$	20	94±3
	35	79±5
$M_{20}P_{10}$	20	93±7
	35	71±6
$M_{30}P_{10}$	20	94±1
	35	76±3
$M_{20}P_4$	20	98±2
	35	75±5
$M_{20}P_{20}$	20	94±4
	35	78±6

Figure 2 shows the effect of PEG middle block molecular weight on the mechanical properties of hydrogels. In line with expectations, the hydrogel with the highest polymer concentration exhibited the highest G' (9.4 ± 0.3 kPa and 37.6 ± 0.6 kPa, for 20 $M_{20}P_4$ and 35 $M_{20}P_4$ wt%, respectively). However, $M_{20}P_{20}$ hydrogels showed higher storage moduli as compared to $M_{20}P_{10}$ analogues. This evidence did not confirm the trend observed in non-photopolymerized hydrogels, where polymers of shorter PEG length yielded a stronger hydrogel.(40) Hydrogels having shorter PEG length are expected to have higher G' for two reasons. Firstly, because at equal weight percentage of the polymer, the molar concentration of $M_{20}P_4$, having the smallest molecular weight, is higher as compared to the molar concentration of $M_{20}P_{10}$ and $M_{20}P_{20}$. Secondly, because $M_{20}P_4$ hydrogels, characterized by a remarkable hydrophobicity above the CP, expelled some water upon gel formation, resulting in a higher polymer concentration. This was not observed for $M_{20}P_{10}$ and $M_{20}P_{20}$ hydrogels, where the hydrophobicity of the p(HPMAm-lac) chains above the CP is well balanced by the hydrophilicity of the PEG middle block. The higher molar concentration of $M_{20}P_4$ gels along with its marked hydrophobicity might also lead to a different number of self-assembling thermosensitive chains associated in each hydrophobic domain.
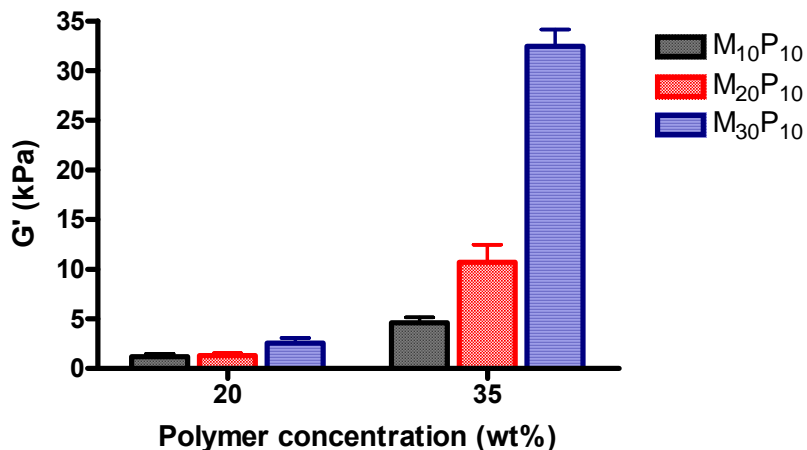
Figure 1. Effect of methacrylation extent of $M_{10}P_{10}$, $M_{20}P_{10}$ and $M_{30}P_{10}$ (Table 1) on storage moduli (G') of photopolymerized hydrogels for 20 and 35 wt% of polymer concentration. Data are shown as mean ± standard deviation; n = 3.
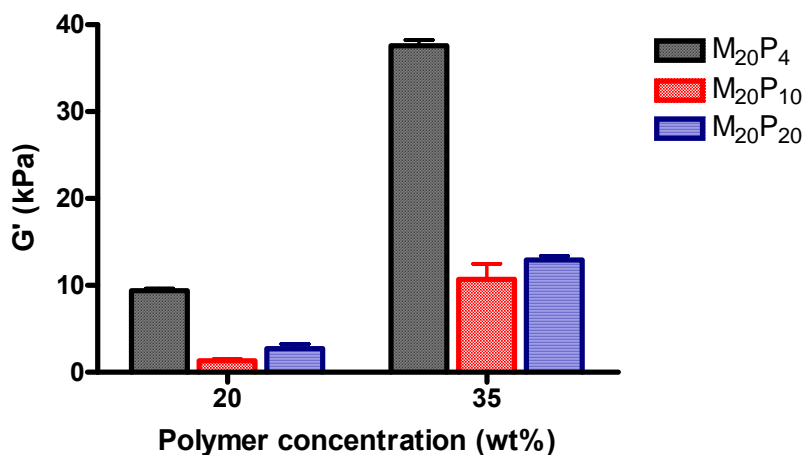

Figure 2. Effect of PEG middle block molecular weight of $M_{20}P_4$, $M_{20}P_{10}$ and $M_{20}P_{20}$ (Table 1) on storage moduli (G') of photopolymerized hydrogels for 20 and 35 wt% of polymer concentration. Data are shown as mean ± standard deviation; n = 3.

The observation that the $M_{20}P_{20}$ hydrogels had higher G' as compared to $M_{20}P_{10}$ for both hydrogel concentration (Figure 2) is most likely due to the larger contribution of the entanglements of the PEG 20 kDa chains to the network strength. The evidence that PEG 20 kDa chain entanglements play a crucial role in the $M_{20}P_{20}$ network properties is reflected by the substantial higher viscosity of the $M_{20}P_{20}$ solution compared to $M_{20}P_{10}$ and $M_{20}P_4$ below the CP (data not shown).

4.3.3. *Degradation Behavior of Hydrogels*

The degradation of the different photocrosslinked hydrogels was studied by incubating them at pH 7.4 and 37 °C. **Figure 3**A shows that hydrogels of 20 wt% degraded in 22, 70 and 110 days, for $M_{10}P_{10}$, $M_{20}P_{10}$ and $M_{30}P_{10}$, respectively, whereas hydrogels of 35 wt%, in Figure 3B, exhibited longer degradation time of 37, 225 and 310 days for $M_{10}P_{10}$, $M_{20}P_{10}$ and $M_{30}P_{10}$, respectively. Similarly, 20 wt% hydrogels composed of PEGs of different molecular weight degraded in 27 and 70 days for $M_{20}P_{20}$ and $M_{20}P_{10}$ gel, respectively (**Figure 4**A), while 35 wt% hydrogels degraded in 101 and 225 days for $M_{20}P_{20}$ and $M_{20}P_{10}$, respectively (Figure 4B). The degradation time of both 20 and 35 wt% $M_{20}P_4$ hydrogels exceeded 250 days. In agreement with the gel mechanical properties, these results show that the degradation behavior can be fine tuned by the molecular design of the polymer, in particular, by the extent of methacrylation and by molecular weight of the PEG block. Generally speaking the higher the G' values (and thus the higher the crosslink density), the longer the degradation time (compare data of Figures 1 and 2 with Figures 3 and 4). Only the degradation behavior of $M_{20}P_{20}$ is not in line with rheological data, since this gels showed the poorest stability despite its high G' value compared to their $M_{20}P_{10}$ analogues. This observation reinforces the hypothesis that the entanglements of the longer PEG 20 kDa polymer chains are partially responsible for the high G' values of the $M_{20}P_{20}$ hydrogels, but do not contribute to the long-term stability of the hydrogel.

The degradation mechanism of p(HPMAm-lac)-PEG based hydrogels is due to hydrolysis of the numerous ester bonds present in the polymer networks as described earlier.(37, 41) It was shown that the lactate side chains of p(HPMAm-lac) with a free terminal OH group are hydrolyzed in approximately one week. The terminal lactate moiety in the HPMAm-dilactate is degraded faster than the one in the HPMAm-monolactate, because by a nucleophilic attack of the hydroxy terminus, the ester bond that is located two lactate units further on in the side chain is hydrolyzed in a so-called backbiting mechanism. When these lactate side chains are hydrolyzed, the network becomes more hydrophilic and consequently can absorb more water, resulting in an increasing swelling ratio during the first week, which was indeed observed for almost all degrading hydrogels (Figures 3 and 4). The lactate groups attached to the polymerized methacrylate groups are expected to hydrolyze by random chain scission at a much slower rate, due to the lack of a hydroxy terminus. Therefore, a high cross-linking density leads to slow degradation kinetics because of the high number of derivatized hydroxyl groups.
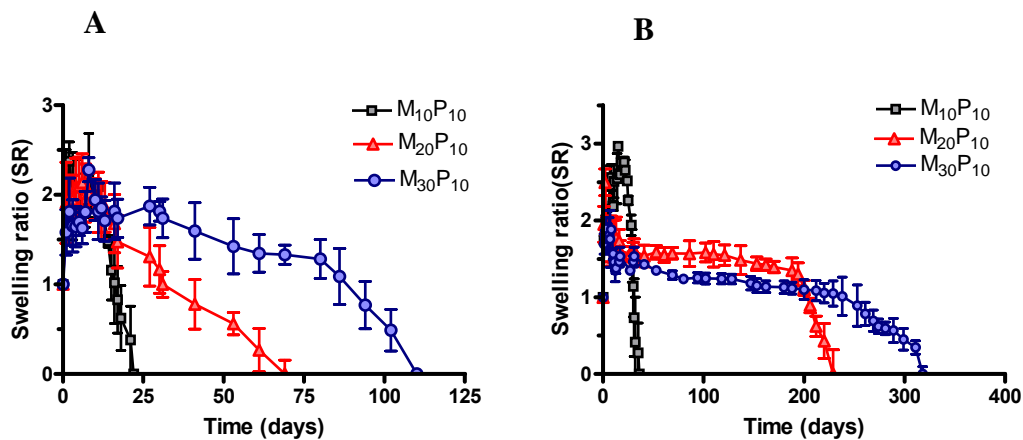
Figure 3. Effect of methacrylation extent on degradation profiles of $M_{10}P_{10}$, $M_{20}P_{10}$ and $M_{30}P_{10}$ hydrogels (Table 1) during incubation at 37°C in PBS buffer pH 7.4, for **A)** 20 and **B)** 35 wt% polymer concentration. Data are shown as mean ± standard deviation; n = 3.
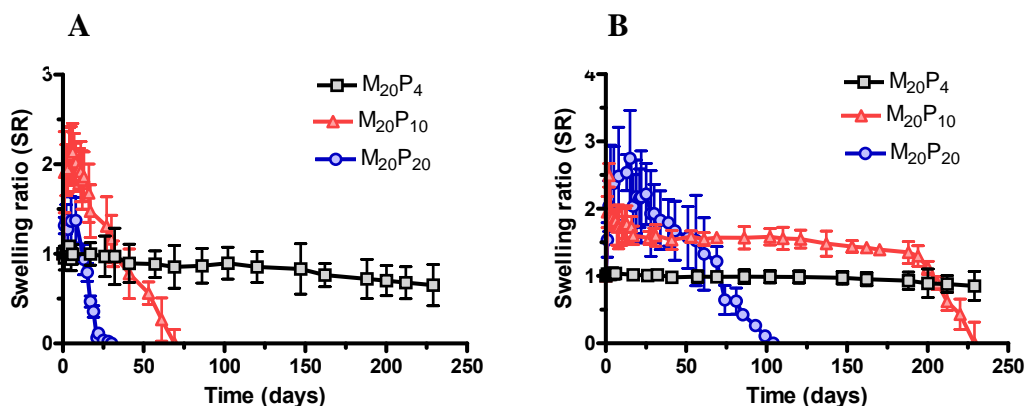

Figure 4. Effect of PEG middle block molecular weight on degradation profiles of $M_{20}P_4$, $M_{20}P_{10}$ and $M_{20}P_{20}$ hydrogels (Table 1) during incubation at 37°C in PBS buffer pH 7.4, for **A)** 20 and **B)** 35 wt% polymer concentration. Data are shown as mean ± standard deviation; n = 3.

4.3.4. *Release Behavior of Hydrogels*

The influence of polymer concentration, extent of methacrylation and molecular weight on BSA release was investigated. In **Figure 5** the release profiles of BSA from photopolymerized hydrogels are shown for different methacrylation degrees. Unexpectedly, $M_{10}P_{10}$, $M_{20}P_{10}$ and $M_{30}P_{10}$ hydrogels of 20 wt% polymer concentration had the same protein release behavior, being the protein released with the same kinetics in approximately 10 days (Figure 5A). The

release mechanism was investigated by fitting the release curves to the Rigter-Peppas equation: (42-43)

$$M_t / M_\infty = k\, t^n$$

where M_t / M_∞ represents the fractional release of the loaded protein, k is a kinetic constant, t is the release time and n is the diffusional exponent that can be related to the release mechanism of the entrapped molecules. If n = 0.5, the release is governed by Fickian diffusion. If n = 1, molecules are released by surface erosion, while both mechanisms play a role in the release if n has a value between 0.5 and 1.

The experimental release curves fitted to n-values of 0.5 as the data points scaled linearly with the square root of time up to a cumulative release of 80–100% (Figure 5B), suggesting first order release kinetics.(44) This fit implies a typical diffusion-controlled release of the loaded protein with a hydrogel mesh size bigger than the hydrodynamic diameter of the investigated protein. Similar behavior was observed in our previous study, where a diffusion governed release of model proteins of molecular weights ranging between 14 and 150 kDa was found.(30)
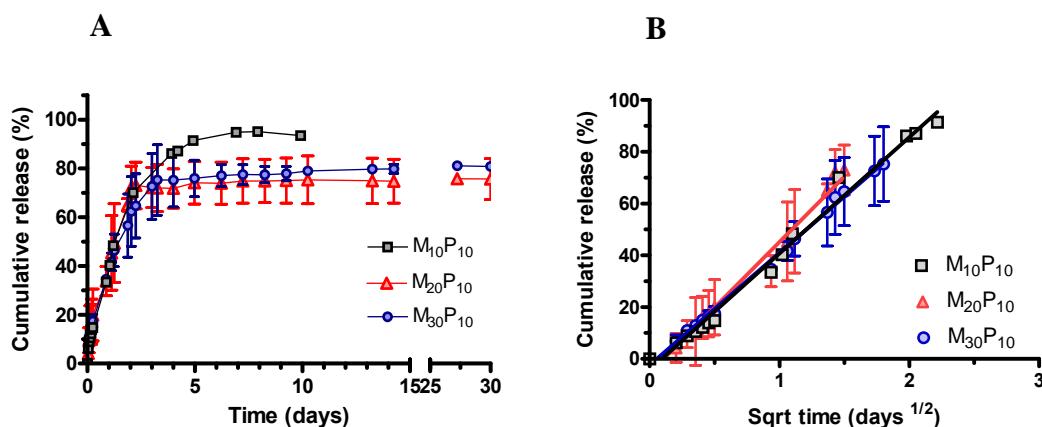

Figure 5. A) BSA release from $M_{10,20,30}P_{10}$ hydrogels (Table 1) of 20 wt% polymer concentration. **B)** Cumulative release of BSA as a function of the square root of time for $M_{10,20,30}P_{10}$ hydrogels of 20 wt% polymer concentration. Data are shown as mean ± standard deviation; n = 3.

From these results it can be concluded that although the rheological properties and degradation kinetics are dependent on the extent of methacrylation, the release kinetics are hardly affected by this parameter. At low polymer concentration, the density of hydrophobic domains is low and the protein likely resides preferentially in the hydrophilic areas of the hydrogels. The increase of extent of methacrylation affects the cross-link density within the hydrophobic domains but does not influence the hydrophilic compartments.

The release of BSA from $M_{10,20,30}P_{10}$ hydrogels of 35 wt% polymer concentration is shown in **Figure 6**. A biphasic release kinetics comprising an initial fast release during approximately 5 days, followed by a slower release phase highly influenced by the cross-link density, was observed. When the polymer concentration of $M_{10,20,30}P_{10}$ hydrogels increases from 20 to 35 wt%, the volume fraction of the hydrophobic domains also increases and the protein partitions both in the hydrophilic and in the hydrophobic areas of the hydrogels. The rapid release during the initial stage is most likely caused by protein that is released from the hydrophilic domains in the gels. As pointed out above, this release is not affected by the extent of methacrylation. The second phase of release can then be attributed to protein encapsulated in the hydrophobic domains of the gels. However, since the chemical cross-links are present in the hydrophobic domains, the release of BSA encapsulated in these compartments is dependent on the DM. In particular, the mobility of the protein is more restricted in hydrogels of higher methacrylation degree.

A

B
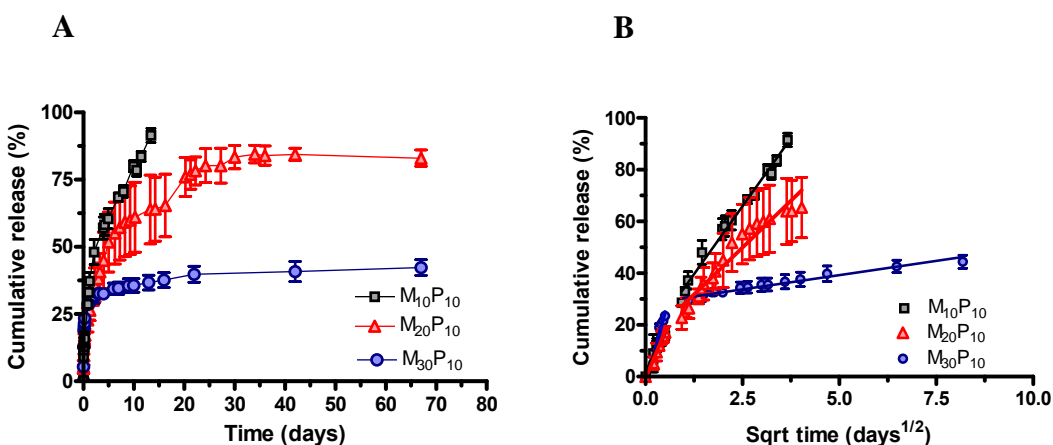
Figure 6. A) BSA release from $M_{10,20,30}P_{10}$ hydrogels (Table 1) of 35 wt% polymer concentration. **B)** Cumulative release of BSA as a function of the square root of time for $M_{10,20,30}P_{10}$ hydrogels of 35 wt% polymer concentration. Data are shown as mean ± standard deviation; n = 3.

Hydrogels of different PEG's molecular weight showed similar BSA release behavior for 20 and 35 wt% polymer concentration (**Figures 7** and 8). However, in contrast to the results of rheological and degradation studies, the hydrogels of longer PEG chains, $M_{20}P_{20}$, displayed relatively slow BSA release kinetics in 5 and 67 days, for 20 and 35 wt% polymer concentration, respectively. Surprisingly, the $M_{20}P_4$ hydrogels, instead, exhibited very fast release in 2.5 and 4 days for 20 and 35 wt% polymer concentrations, respectively (discussed further in the next section). A small burst release (approximately 4 and 2 % for 20 and 35 wt% polymer hydrogels) was also observed in the release kinetics of $M_{20}P_4$ hydrogels, likely

attributable to the slight shrinkage of hydrogel and the expulsion of protein upon gel formation.

A

B
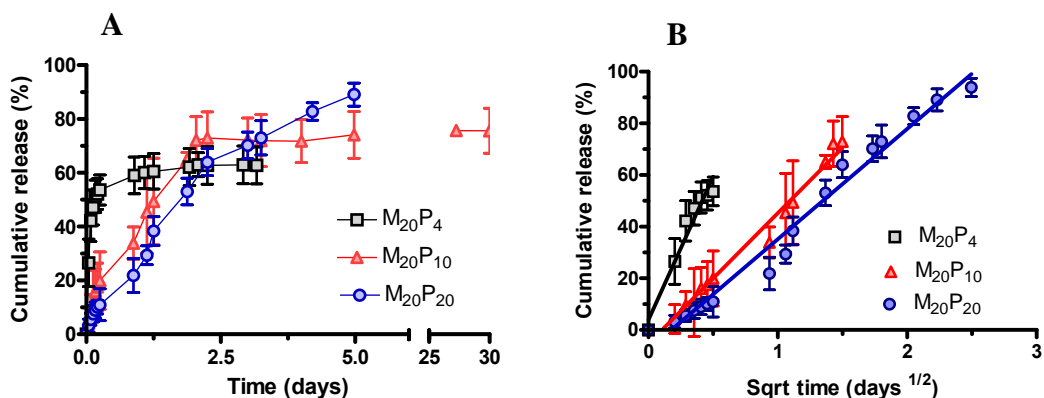
Figure 7. A) BSA release from $M_{20}P_{4,10,20}$ hydrogels (Table 1) of 20 wt% polymer concentration. **B)** Cumulative release of BSA as a function of the square root of time for $M_{20}P_{4,10,20}$ polymer hydrogels of 20 wt% polymer concentration. Data are shown as mean ± standard deviation; n = 3.

A

B
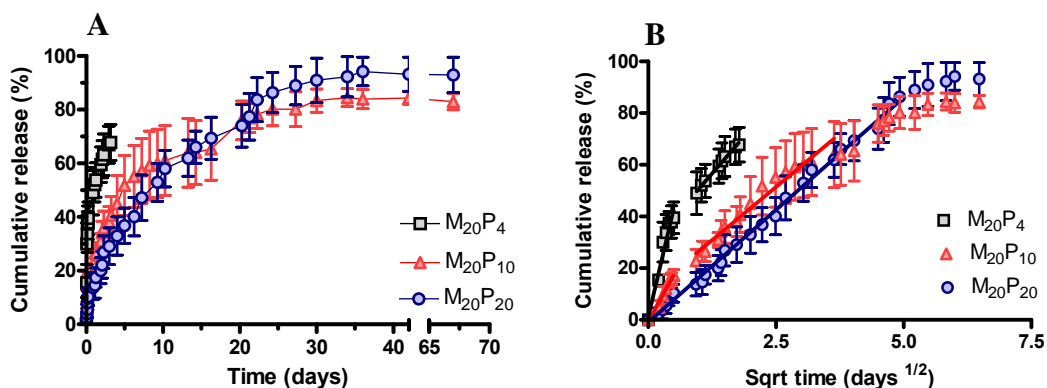
Figure 8. A) BSA release from $M_{20}P_{4,10,20}$ hydrogels (Table 1) of 35 wt% polymer concentration. **B)** Cumulative release of BSA as a function of the square root of time for $M_{20}P_{4,10,20}$ polymer hydrogels of 35 wt% polymer concentration. Data are shown as mean ± standard deviation; n = 3

Diffusion controlled (n=0.5) monophasic release was shown for 20 wt% $M_{20}P_4$, $M_{20}P_{10}$ and $M_{20}P_{20}$ hydrogels as well as for 35 wt% $M_{20}P_{20}$ hydrogels, where the hydrophilicity is most predominant. $M_{20}P_4$ and $M_{20}P_{10}$ hydrogels at 35 wt% polymer concentration, with higher hydrophobicity, displayed biphasic release (**Figure 8**A and B). Most of the studied hydrogels (20 wt% $M_{10,20,30}P_{10}$, 35 wt% $M_{10,20}P_{10}$, 20 and 35 wt% $M_{20}P_{20}$) showed quantitative release within the experimental error (cumulative release higher than 80%), however some formulations (35 wt% $M_{30}P_{10}$, 20 and 35 wt% $M_{20}P_{4,20}$), having relatively high hydrophobic

domains volume fractions, exhibited incomplete BSA release during the studied time-scale. This observation leads to the conclusion that when the protein is located mainly in the hydrophilic PEG domains or in hydrophobic domains of relatively low cross-link density, the protein is totally released by diffusion and the degradation of the matrix is not an important factor, whereas when the protein resides in highly cross-linked hydrophobic domains, its mobility is remarkably restricted and degradation of the hydrogel is needed for the complete release thereof. These findings were supported by Fluorescence Recovery After Photobleaching (FRAP) experiments(45) (Appendix B), where decreasing mobile fractions were found with increasing cross-link densities. Also the protein diffusional behavior in polymer networks of both different methacrylate extent and PEG length was studied by FRAP analysis and compared to the release kinetics. Good agreement between FRAP and release data was found as the diffusion coefficients of (fluorescently labeled)-BSA followed the same trends both in FRAP and release experiments (Appendix B).

The tailorability of protein release from chemically cross-linked thermosensitive hydrogels was studied also by Wang *et al.* (46) Similarly to $M_{20}P_{10}$ and $M_{20}P_{20}$ hydrogels of 35 wt % solid content, a quantitative BSA release of 35 days from Pluronic F127-poly(caprolactone) copolymer based hydrogels was found and the *in vitro* release rate was negatively correlated to the molecular weight of proteins, as we also reported previously for photocrosslinked p(HPMAm-lac)-PEG-p(HPMAm-lac) hydrogels.(30) However, in contrast to our studies, where the release mechanism was diffusional, Wang *et al.* demonstrated that both diffusion and degradation of the matrix contributed to the protein release. Other UV-cured (thermosensitive) hydrogels showed faster release kinetics. Photo-polymerized Hyaluronic acid/Pluronic hydrogels were used by Kim and Park to investigate the release of human growth hormone.(47) A release time span of 13 days was found at 37°C and the mechanism was governed by erosion. BSA was released in 5 days from photo-polymerized degradable PEG hydrogels based on di-acrylated oligo-lactide derivatized PEG hydrogels(32) and the release depended on both permeability of the matrix prior to degradation and its degradation rate.

Leach *et al.* (48) developed highly diffusive photocrosslinkable hyaluronic acid-polyethylene glycol hydrogels that showed a decrease of BSA diffusion coefficient (D) with increasing concentration of hydrogel precursors, as also found in the present (Appendix B) as well as in other studies.(49) Moreover, in line with our release kinetics from the hydrophilic gel compartments, where diffusion coefficients of BSA varying from 1.11 to 52.9 μm^2/sec were found (Appendix B), a range of Ds from 8.5 to 45.4 μm^2/sec was obtained from Hyaluronic acid/Pluronic hydrogels.(48) The diffusion coefficients based on release experiments from the hydrophobic domains, ranging between 0.01 and 3.5 μm^2/sec were comparable to the ones published for photo-crosslinked low molecular weight PEG hydrogels. (50-51) However, the use of these hydrogels is limited because of lack of biodegradability, therefore the system we

describe in the present paper, showing slowly diffusive release phases, represents an advantage over the existing hydrogel systems.

4.3.5. *Confocal Laser Scanning Microscopy*

To gain more insight into the hydrogel microstructure, confocal laser scanning microscopy (CLSM) was performed on $M_{20}P_{4,10,20,40}$ hydrogels, in which the hydrophobic domains were stained with the hydrophobic dye NR and the hydrophilic pores with FITC-BSA. $M_{20}P_{40}$ was used only in CLSM studies because its high viscosity even below the CP, due to entanglement of the PEG chains, makes the injectability of the hydrogel difficult and thus practical application of this gel system is limited. However, this polymer is a valuable tool to investigate the hydrogel structural organization at different molecular designs. From **Figure 9**, an evident hydrogel micro-porosity dependency on PEG molecular weight can be seen, as previously also observed in our studies on p(HPMAm-lac)-PEG-p(HPMAm-lac) physical hydrogels.(40) A similar behavior was observed for hydrogels of 20 wt% polymer concentration (data not shown). This remarkable porosity of hydrogels of small PEG molecular weight is likely due to a phase separation with hydrophilic domains surrounded by a polymer-rich phase. The extent of phase separation within the hydrogel is strongly related to the hydrophilicity-hydrophobicity balance between PEG and p(HPMAm-lac).

The observed phase separation explains the BSA release behavior of the studied hydrogels. BSA, localized in the water-rich phase separated domains, is expected to be minimally restricted in mobility and thereby rapidly released. Likely, the micropores are interconnected by smaller hydrophilic nanopores, which are hardly visible on CLSM pictures, but their presence is proven by the co-localization of FITC-BSA (Figure 9E) and NR (Figure 9F) in the polymer-rich phase, shown for $M_{20}P_{40}$ hydrogels. In the superimposed picture (Figure 9D) where the double staining is shown, the presence of FITC-BSA in the nano-pores of the polymer-rich phase is poorly visible, due to the higher signal given by NR as compared to FITC-BSA. On the other hand, the mobility of the BSA encapsulated in the hydrophilic domains of the hydrogel networks where the micro-phase separation is minimal or indiscernible, like in case of $M_{20}P_{20}$ and even more markedly of $M_{20}P_{40}$ hydrogels, is much more limited. In fact, prior to release, the protein has to diffuse through smaller hydrophilic domains, as compared to more phase-separated hydrogels. Finally, the protein possibly entrapped in the hydrophobic domains is immobile or slowly diffusing, due to the presence of chemical cross-links, that represent barriers to the macromolecular diffusion.
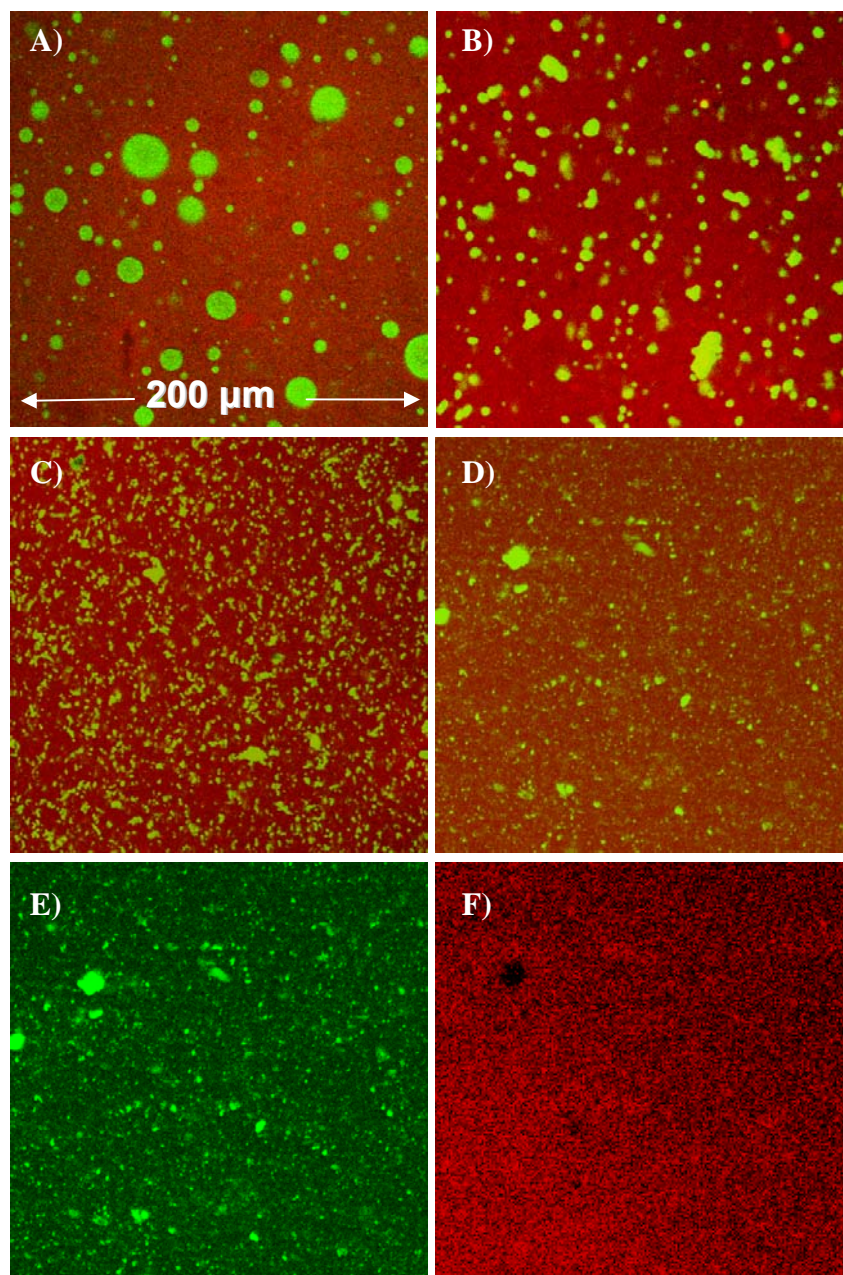
Figure 9. CLSM pictures of $M_{20}P_{4,10,20}$ hydrogels (Table 1) double stained with hydrophobic NR (in red) and hydrophilic FITC-BSA (in green). **A)** 35 wt% $M_{20}P_4$ hydrogels. **B)** 35 wt% $M_{20}P_{10}$ hydrogels. **C)** 35 wt% $M_{20}P_{20}$ hydrogels. **D), E) and F)** 35 wt% $M_{20}P_{40}$ hydrogels; pictures show the FITC-BSA/NR double staining (D) as well as the FITC-BSA staining (E) and NR staining (F).

The demonstrated polymer phase separation lends itself to explain also the mechanical properties of the hydrogels. Likely, the phase separation induces the formation of domains with high polymer concentration that highly contribute to the gel strength. The hydrophilic-hydrophobic balance plays a key-role in the structural organization of the hydrogel, leading to phase separation and to the tendency to expel water if the hydrophobic character of the hydrogels is dominant.

4.4.   Conclusions

In this paper, we described how the molecular design of a thermosensitive methacrylate bearing A-B-A triblock copolymer tailored the mechanical properties, degradation and protein release behavior of hydrogels prepared using these polymers. Increasing degree of methacrylation and decreasing PEG molecular weight led to higher cross-link density and to the formation of hydrogels of increased storage modulus and enhanced stability to the hydrolytic degradation at physiological pH. BSA was released from hydrogels by a mechanism mainly governed by diffusion. Nevertheless, the cross-link density not always correlated to the BSA release rate, which was independent of the extent of methacrylation for 20 wt% hydrogels and for the initial phase of the biphasic release of 35 wt% polymer gels. The extent of methacrylation affected indeed the cross-link density within the hydrophobic domains and only the release rate of BSA that resides partly in those self-assembled domains can be tailored by the cross-link density. On the other hand, hydrogels of longer PEG polymer chain exhibited an unexpected slower release rate. CLSM analysis clarified that the gels were phase-separated into water-rich hydrophilic and polymer-rich hydrophobic domains and that the extent of phase separation could be controlled by the PEG block length of the polymer. Hydrogels of small PEG blocks showed large hydrophilic domains from which the protein was rapidly released. Hydrogels of longer PEG blocks showed a more homogeneous structure resulting in slower protein diffusion.

In conclusion, the studied hydrogels are excellent candidates as injectable biomaterials for the controlled delivery of biotherapeutics because their versatility and flexibility allow precise tailoring of mechanical properties, degradation profiles and release behavior to the desired pharmacokinetics of each specific drug.

Acknowledgements

References

1. Blanchard J (1998) Controlled Drug Delivery: Challenges and Strategies Edited by Kinam Park (Purdue University). American Chemical Society: Washington, DC. *Journal of American Chemical Society* 120(18):4554-4555.

2. Deo SK, Moschou EA, Peteu SF, Bachas LG, Daunert S, Eisenhardt PE, & Madou MJ (2003) Peer Reviewed: Responsive Drug Delivery Systems. *Analytical Chemistry* 75(9):206 A-213 A.

3. D'Emanuele A (1996) Responsive polymeric drug delivery systems : Meeting the patient's needs. *Clinical Pharmacokinetics* 31(4):241-245.

4. Bruguerolle B (1998) Chronopharmacokinetics: Current Status. *Clinical Pharmacokinetics* 35(2):83-94.

5. Gupta P, Vermani K, & Garg S (2002) Hydrogels: from controlled release to pH-responsive drug delivery. *Drug Discovery Today* 7(10):569-579.

6. Peppas NA, Bures P, Leobandung W, & Ichikawa H (2000) Hydrogels in pharmaceutical formulations. *European Journal of Pharmaceutics and Biopharmaceutics* 50(1):27-46.

7. Nguyen MK & Lee DS Injectable (2010) Biodegradable Hydrogels. *Macromolar Bioscience*. In Press doi: 0.1002/mabi.200900402.

8. Frokjaer S & Otzen DE (2005) Protein drug stability: a formulation challenge. *Nature Reviews Drug Discovery* 4(4):298-306.

9. van de Weert M, Hennink WE, & Jiskoot W (2000) Protein Instability in Poly(Lactic-co-Glycolic Acid) Microparticles. *Pharmaceutical Research* 17(10):1159-1167.

10. Jiskoot W, van Schie R, Carstens M, & Schellekens H (2009) Immunological Risk of Injectable Drug Delivery Systems. *Pharmaceutical Research* 26(6):1303-1314.

11. Iza M, Stoianovici G, Viora L, Grossiord JL, & Couarraze G (1998) Hydrogels of poly(ethylene glycol): mechanical characterization and release of a model drug. *Journal of Controlled Release* 52(1-2):41-51.

12. van de Wetering P, Metters AT, Schoenmakers RG, & Hubbell JA (2005) Poly(ethylene glycol) hydrogels formed by conjugate addition with controllable swelling, degradation, and release of pharmaceutically active proteins. *Journal of Controlled Release* 102(3):619-627.

13. Bourke S, Al-Khalili M, Briggs T, Michniak B, Kohn J, & Poole-Warren L (2003) A photo-crosslinked poly(vinyl alcohol) hydrogel growth factor release vehicle for wound healing applications. *AAPS Journal* 5(4):101-111.

14. Mason MN, Metters AT, Bowman CN, & Anseth KS (2001) Predicting Controlled-Release Behavior of Degradable PLA-b-PEG-b-PLA Hydrogels. *Macromolecules* 34(13):4630-4635.

15. Siepmann J & Peppas NA (2000) Hydrophilic Matrices for Controlled Drug Delivery: An Improved Mathematical Model to Predict the Resulting Drug Release Kinetics (the "sequential Layer" Model). *Pharmaceutical Research* 17(10):1290-1298.

16. Anderson DG, Tweedie CA, Hossain N, Navarro SM, Brey DM, Van Vliet KJ, Langer R, & Burdick JA (2006) A Combinatorial Library of Photocrosslinkable and Degradable Materials. *Advanced Materials* 18(19):2614-2618.

17. Nathanael RL, Kimberly AS, & Mark WG (2003) The Convergent Synthesis of Poly(glycerol-succinic acid) Dendritic Macromolecules. *Chemistry - A European Journal* 9(22):5618-5626.

18. Hennink WE, Cadée JA, Jong SJ, Franssen O, Stenekes RJH, Talsma H, & Dijk-Wolthuis WNE (2002) Molecular Design of Biodegradable Dextran Hydrogels for the Controlled Release of Proteins. *Biomedical Polymers and Polymer Therapeutics*, Part 1: 3-18.

19. Jeong B & Gutowska A (2002) Lessons from nature: stimuli-responsive polymers and their biomedical applications. *Trends in Biotechnology* 20(7):305-311.

20. Klouda L & Mikos AG (2008) Thermoresponsive hydrogels in biomedical applications. *European Journal of Pharmaceutics and Biopharmaceutics* 68(1):34-45.

21. Soga O, van Nostrum CF, & Hennink WE (2004) Poly(N-(2-hydroxypropyl) Methacrylamide Mono/Di Lactate): A New Class of Biodegradable Polymers with Tuneable Thermosensitivity. *Biomacromolecules* 5(3):818-821.

22. Vermonden T, Besseling NAM, van Steenbergen MJ, & Hennink WE (2006) Rheological Studies of Thermosensitive Triblock Copolymer Hydrogels. *Langmuir* 22(24):10180-10184.

23. Zhang H-f, Zhong H, Zhang L-l, Chen S-b, Zhao Y-j, Zhu Y-L, & Wang J-t (Modulate the phase transition temperature of hydrogels with both thermosensitivity and biodegradability. *Carbohydrate Polymers* 79(1):131-136.

24. Kretlow JD, Klouda L, & Mikos AG (2007) Injectable matrices and scaffolds for drug delivery in tissue engineering. *Advanced Drug Delivery Reviews* 59(4-5):263-273.

25. Van Tomme SR, Storm G, & Hennink WE (2008) In situ gelling hydrogels for pharmaceutical and biomedical applications. *International Journal of Pharmaceutics* 355(1-2):1-18.

26. Hennink WE & van Nostrum CF (2002) Novel crosslinking methods to design hydrogels. *Advanced Drug Delivery Reviews* 54(1):13-36.

27. Paradossi G, Finelli I, Cerroni B, & Chiessi E (2009) Adding Chemical Cross-Links to a Physical Hydrogel. *Molecules* 14(9):3662-3675.

28. Machado L, Bavaresco V, Pino E, Zavaglia C, & Reis M (2004) TA of pval hydrogel cross-linked by chemical and eb irradiation process used as artificial articular cartilage. *Journal of Thermal Analysis and Calorimetry* 75(2):445-451.

29. Vanderhooft JL, Alcoutlabi M, Magda JJ, & Prestwich GD (2009) Rheological Properties of Cross-Linked Hyaluronan-Gelatin Hydrogels for Tissue Engineering. *Macromolar Bioscience* 9(1):20-28.

30. Censi R, Vermonden T, van Steenbergen MJ, Deschout H, Braeckmans K, De Smedt SC, van Nostrum CF, di Martino P, & Hennink WE (2009) Photopolymerized thermosensitive hydrogels for tailorable diffusion-controlled protein delivery. *Journal of Controlled Release* 140(3):230-236.

31. Vermonden T, Fedorovich NE, van Geemen D, Alblas J, van Nostrum CF, Dhert WJA, & Hennink WE (2008) Photopolymerized Thermosensitive Hydrogels: Synthesis, Degradation, and Cytocompatibility. *Biomacromolecules* 9(3):919-926.

32. West JL & Hubbell JA (1995) Photopolymerized hydrogel materials for drug delivery applications. *Reactive Polymers* 25(2-3):139-147.

33. Nguyen KT & West JL (2002) Photopolymerizable hydrogels for tissue engineering applications. *Biomaterials* 23(22):4307-4314.

34. Lu S & Anseth KS (1999) Photopolymerization of multilaminated poly(HEMA) hydrogels for controlled release. *Journal of Controlled Release* 57(3):291-300.

35. Elisseeff J, Anseth K, Sims D, McIntosh W, Randolph M, & Langer R (1999) Transdermal photopolymerization for minimally invasive implantation. *Proceeding of the National Academy of Sciences U. S. A.* 96(6):3104-3107.

36. Bryant SJ, Nuttelman CR, & Anseth KS (2000) Cytocompatibility of UV and visible light photoinitiating systems on cultured NIH/3T3 fibroblasts in vitro. *Journal of Biomaterial Science Polymer Edition* 11:439-457.

37. Neradovic D, van Steenbergen MJ, Vansteelant L, Meijer YJ, van Nostrum CF, & Hennink WE (2003) Degradation Mechanism and Kinetics of Thermosensitive Polyacrylamides Containing Lactic Acid Side Chains. *Macromolecules* 36(20):7491-7498.

38. Alakhov VY & Kabanov AV (2005) Block copolymeric biotransport carriers as versatile vehicles for drug delivery. *Expert Opinion on Investigational Drugs* 7(9):1453-1473.

39. Soga O, van Nostrum CF, Ramzi A, Visser T, Soulimani F, Frederik PM, Bomans PHH, & Hennink WE (2004) Physicochemical Characterization of Degradable Thermosensitive Polymeric Micelles. *Langmuir* 20(21):9388-9395.

40. Vermonden T, Jena SS, Barriet D, Censi R, van der Gucht J, Hennink WE, & Siegel RA (2009) Macromolecular Diffusion in Self-Assembling Biodegradable Thermosensitive Hydrogels. *Macromolecules* 43(2):782-789.

41. Rijcken CJ, Snel CJ, Schiffelers RM, van Nostrum CF, & Hennink WE (2007) Hydrolysable core-crosslinked thermosensitive polymeric micelles: Synthesis, characterisation and in vivo studies. *Biomaterials* 28(36):5581-5593.

42. Ritger PL & Peppas NA (1987) A simple equation for description of solute release II. Fickian and anomalous release from swellable devices. *Journal of Controlled Release* 5(1):37-42.

43. Serra L, Doménech J, & Peppas NA (2006) Drug transport mechanisms and release kinetics from molecularly designed poly(acrylic acid-g-ethylene glycol) hydrogels. *Biomaterials* 27(31):5440-5451.

44. Schwartz JB, Simonelli AP, & Higuchi WI (1968) Drug release from wax matrices I. Analysis of data with first-order kinetics and with the diffusion-controlled model. *Journal of Pharmaceutical Science* 57(2):274-277.

45. Brandl F, Kastner F, Gschwind RM, Blunk T, Teßmar J, & Göpferich A (2010) Hydrogel-based drug delivery systems: Comparison of drug diffusivity and release kinetics. *Journal of Controlled Release* 142(2):221-228.

46. Wang B, Zhu W, Zhang Y, Yang Z, & Ding J (2006) Synthesis of a chemically-crosslinked thermo-sensitive hydrogel film and in situ encapsulation of model protein drugs. *Reactive and Functional Polymers* 66(5):509-518.

47. Kim MR & Park TG (2002) Temperature-responsive and degradable hyaluronic acid/Pluronic composite hydrogels for controlled release of human growth hormone. *Journal of Controlled Release* 80(1-3):69-77.

48. Leach JB & Schmidt CE (2005) Characterization of protein release from photocrosslinkable hyaluronic acid-polyethylene glycol hydrogel tissue engineering scaffolds. *Biomaterials* 26(2):125-135.

49. Amsden B (1998) Solute Diffusion within Hydrogels. Mechanisms and Models. *Macromolecules* 31(23):8382-8395.

50. Mellott MB, Searcy K, & Pishko MV (2001) Release of protein from highly cross-linked hydrogels of poly(ethylene glycol) diacrylate fabricated by UV polymerization. *Biomaterials* 22(9):929-941.

51. Cruise GM, Scharp DS, & Hubbell JA (1998) Characterization of permeability and network structure of interfacially photopolymerized poly(ethylene glycol) diacrylate hydrogels. *Bomaterials*

Chapter 5

In-Situ Forming Hydrogels by Tandem Thermal Gelling and Michael Addition Reaction between Thermosensitive Triblock Copolymers and Thiolated Hyaluronan

Roberta Censi,[a,b] Peter J. Fieten,[a] Piera di Martino,[b] Wim E. Hennink,[a] Tina Vermonden[a]

[a] Department of Pharmaceutics Utrecht Institute for Pharmaceutical Sciences (UIPS); Utrecht University; P.O. Box 80082, 3508 TB Utrecht, The Netherlands.

[b] Department of Chemical Sciences; Camerino University; via S. Agostino 1, 62032, Camerino (MC), Italy.

Abstract

This study reports on the synthesis, characterization and peptide release behavior of an *in situ* physically and chemically cross-linking hydrogel. (Meth)acrylate bearing ABA-triblock copolymers consisting of a poly(ethylene glycol) (PEG) middle block, flanked by thermosensitive blocks of random *N*-isopropylacrylamide (pNIPAm)/*N*-(2-hydroxypropyl) methacrylamide dilactate (pHPMAm$_{lac2}$) and exhibiting lower critical solution temperature behavior in aqueous solution were synthesized. Upon body temperature induced physical gelation, these polymers were cured by Michael type addition reaction with thiolated hyaluronic acid (HA-SH) to yield injectable *in situ* gelling, biodegradable but structurally stable and biocompatible hydrogels. These stable and elastic networks were prepared by mixing (meth)acrylated ABA-triblock copolymers and thiolated hyaluronic acid at a ratio thiol/(meth)acrylate groups of 1/1. The simultaneous physical and chemical gelation kinetics, investigated by rheological measurements, demonstrated that the physical networks were progressively stabilized as the Michael addition reaction between (meth)acrylate and thiol groups proceeded and that acrylated thermosensitive polymers had a higher reactivity with thiol groups, as compared to methacrylate analogues, resulting in a faster gel formation. The networks, characterized by a remarkable initial structural stability, degraded in time at physiological conditions. The degradability is ensured by the presence of hydrolytically sensitive ester bonds in the cross-links, as well as in the lactate side chains and between PEG and thermosensitive blocks. Methacrylated polymer gels loaded with a model peptide (bradykinin), showed a diffusion controlled release of this peptide, tailorable by the polymer concentration. This tandem system, displaying *in situ* physical and chemical gelation has a high potential for biomedical applications, such as delivery of peptide and protein biopharmaceuticals.

126

5.1. Introduction

Most systemically administered pharmaceutical peptides and proteins undergo rapid elimination and cause high plasma peak concentrations, which often results in undesired side effects. In this study a non-invasive and patient-friendly delivery system, capable to protect and release polypeptides in a sustained manner is investigated. We designed an injectable hydrogel, that exhibits a body temperature induced gelation at the site of injection and of which the structure is stabilized through a Michael addition reaction.

Injectable, self-assembling hydrogels are receiving increasing attention because of their desirable properties for drug delivery and tissue engineering applications. Their advantages over preformed chemically crosslinked polymer hydrogels are the use of minimally invasive methods for administration, *in vivo* shape adaptation and ease of drug encapsulation.(1-2) Different physical interactions can be exploited for the design of *in situ* gelling systems, among which the use of thermosensitive polymers is of particular importance. Polymers exhibiting LCST behavior (Lower Critical Solution Temperature) are soluble in aqueous solutions at low temperature and self-assemble above their cloud point (CP), being suitable as injectable materials if their CP is between room and body temperature.(3-4) A general drawback of self-assembling hydrogels however is their limited mechanical strength and low stability due to swelling and subsequent dissolution of the polymers. To improve the gel strength and stability, the use of covalent cross-linking strategies,(5-6) among which photo-cross-linking, is well known.(7-9) Recently, also click chemistry between azides and acetylenes is used to obtain well-defined network structures.(10-12) A drawback of these chemical cross-linking techniques is their need for catalysts, which can be toxic. Therefore, *in situ* gelation is usually not applicable for these kinds of hydrogels.

Michael addition reaction between thiol and acrylate or methacrylate groups (13-14) is a particularly suitable mechanism for *in-situ* chemical cross-linking because it occurs at physiological conditions without the need for (toxic) catalysts. (15-18) Because of its advantageous properties, Michael addition reaction has been successfully applied for the preparation of a number of hydrogels for biomedical applications, (17, 19-25) reviewed by Mather *et al*. (26)

Besides injectability and stability issues, also biocompatibility is an important property that should be taken into consideration for the design of hydrogels for biomedical purposes. A well known strategy to ensure biocompatibility and cell adhesion and proliferation in the gels is the use of natural polymers such as polypeptides and polysaccharides. Hyaluronic acid (HA) is a natural polysaccharide, which can be found in synovial fluids, extracellular matrix, connective tissues and organs. HA is a linear polymer consisting of alternating D-glucuronic acid and *N*-acetyl-D-glucosamine moieties and is known for its favorable physical (e.g. viscosity, hydration) and biological (protein and cell

interactions) properties.(27) In our approach, hyaluronic acid was derivatized with thiol moieties, (28-30) as shown in **Scheme 1**, and used as a curing agent for thermal gelling (meth)acrylate bearing polymer hydrogels.(30-33)

Cellesi *et al.* have described the simultaneous thermal gelling and Michael addition cross-linking of telechelic pluronic for the design of a synthetic substitute of alginate.(17) Tandem physically and chemically gelling systems based on poly(NIPAAm-*co*-cysteamine) (14) and on poly(NIPAAm-*co*-HEMA-acrylate) (34) and poly(NIPAAm-*co*-PEG-acrylate) (35) copolymers have been described by Vernon *et al.* More recently, Park *et al.* reported on injectable HA/Pluronic F127 composite tissue-adhesive hydrogels (31) and Wang *et al.* described the preparation of Michael addition cross-linked injectable thiol- and vinyl-modified poly(*N*-isopropylacrylamide) (PNIPAAm)-based copolymer hydrogels for controlled drug delivery. (36)
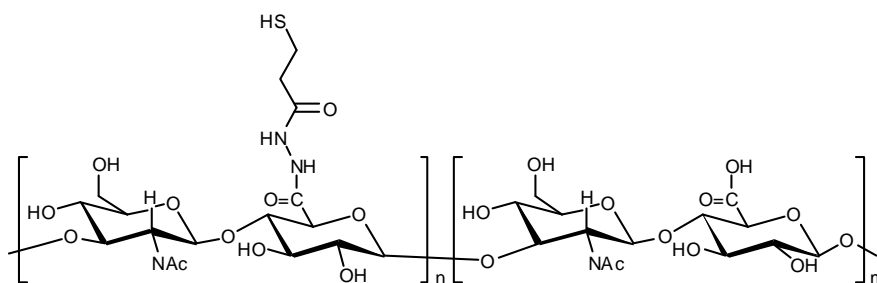

Scheme 1 Chemical structure of partially thiolated hyaluronic acid (HA-SH).

Recently, we applied a similar cross-linking approach to design a novel hydrogel composed of thermosensitive biodegradable polymers capable to cross link via Michael addition reaction with thiolated hyaluronic acid. This hydrogel possesses an innovative combination of advantageous aspects, such as stability at the site of injection, due to the rapid thermal gelling upon injection, structural stability, due to Michael addition cross-linking, biocompatibility and cell adhesion properties, due to the presence of hyaluronic acid, biodegradability and flexibility.

The thermosensitive polymers were designed with an ABA-triblock architecture consisting of a hydrophilic poly(ethylene glycol) (PEG) middle block and flanking thermosensitive blocks of random copolymer of *N*-isopropylacrylamide (NIPAm) and *N*-(2-hydroxypropyl) methacrylamide dilactate (HPMAm$_{lac2}$) in a NIPAm/HPMAm$_{lac2}$ ratio of 76/24, as shown in **Scheme 2**. pNIPAm is a non-degradable thermosensitive polymer with a cloud point of 32ºC. (37-38) When the hydrophobic HPMAm$_{lac2}$ (24 mol %) is copolymerized with NIPAm, the cloud point of the obtained copolymer decreases to 23ºC.

Furthermore, the introduction of HPMAm$_{lac2}$ makes the polymer biodegradable, because under physiological conditions, the lactate side chains will be hydrolyzed in time, yielding a more hydrophilic polymer (random pNIPAm and poly(*N*-(2-hydroxypropyl) methacrylamide monolactate) with a cloud point above 37°C. (39-40) Therefore at body temperature the hydrolyzed polymers are expected to dissolve and can be excreted by renal filtration when the molecular weight is below the renal excretion treshold of 50 kDa. (41) To enable a Michael addition reaction between the triblock copolymers and the thiolated HA, acrylate and methacrylate groups were introduced in the side chains of the HPMAm$_{lac2}$ units.

In the present work, we describe the synthesis, characterization and potential biomedical applications of this injectable *in situ* gelling, initially structurally stable but biodegradable hydrogel, prepared by tandem physical gelation and chemical stabilization of the themal gelling network by Michael addition cross-linking with thiolated hyaluronic acid.
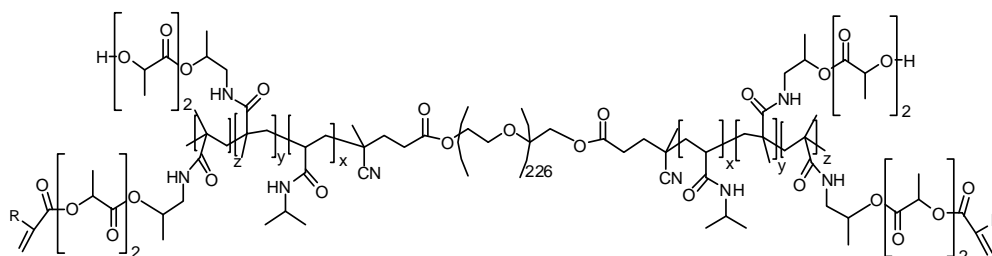
Scheme 2 Chemical structure of ABA-triblock copolymers consisting of a PEG$_{10000}$ B-block and random pNIPAm-HPMAm$_{lac2}$ A-blocks (R=H or CH$_3$ for pNHPta and pNHPtma respectively).

5.2.4. Materials and Methods

5.2.1. Materials

All commercial chemicals were obtained from Aldrich unless indicated otherwise and were used as received. L-Lactide was obtained from Purac Biochem BV (Gorinchem, The Netherlands). Low molecular weight hyaluronic acid (sodium hyaluronate) with a molecular weight of 35000 Da was supplied by Lifecore (Minnesota, U.S.A.) Hydroxypropylmethacrylamide-dilactate (HPMAm-dilactate) was synthesized according to a previously reported method. [42] 3,3'-Dithiobis(propanoic dihydrazide) (DTP) was synthesized by the method described by Vercruysse *et al*. [43]

5.2.2. ^{1}H NMR Spectroscopy

Polymers dissolved in CDCl$_3$, DMSO-*d6* or D$_2$O were characterized on a Varian

Mercury Plus 300 spectrometer. Chemical shifts were referred to the solvent peak (δ = 7.24 ppm for $CHCl_3$, 2.54 ppm for DMSO and 4.79 ppm for H_2O).

5.2.3. Gel Permeation Chromatography (GPC)

The molecular weights of the polymers were determined by GPC using a Plgel 5 µm MIXED-D column (Polymer Laboratories) with a column temperature of 40 ºC. DMF containing 10 mM LiCl was used as eluent with an elution rate of 0.7 ml/min, and the sample concentration was 5 mg/ml in the same eluent. Poly(ethylene glycols) with defined molecular weights were used as calibration standards.

5.2.4. Synthesis of thermosensitive triblock copolymers

Thermosensitive ABA triblock polymers were prepared according to a previously described procedure (**Scheme 3**). [42] 4,4'-azobis(4-cyanopentanoic acid) (ABCPA, Fluka) was used to prepare a PEG_{10000}-ABCPA macroinitiator with PEG molecular weight of 10000. This initiator was used to copolymerize $HPMAm_{lac2}$ (25%) and NIPAm (75%) to obtain triblock copolymers with $pHPMAmlac_2$/NIPAm as outer blocks and PEG as midblock.

The OH side groups of $HPMAm_{lac2}$ were partially methacrylated or acrylated by the following procedure. (39) Triblock copolymer (1 g) was dissolved in 100 mL of dry THF under N_2 atmosphere. Dimethylaminopyridine (3 mg) and triethylamine (90 µL) were added at 0ºC. Methacrylic anhydride or acrylic anhydride was added in an anhydride/OH molar ratio of 0.5. The reaction mixture was subsequently stirred for 24 hours at room temperature. Afterwards, the polymers were diluted with water, dialysed (membrane with a cut-off of 12-14 kDa) against water for two days and isolated by freeze-drying. The final thermosensitive triblock copolymers are abbreviated as pNHPtma (polyNIPAm/$HPMAm_{lac2}$-PEG triblock methacrylated) and pNHPta (polyNIPAm/$HPMAm_{lac2}$-PEG triblock acrylated), respectively.

5.2.4a. Before (meth)acrylation:
^{1}H NMR ($CDCl_3$) δ 6.5 (H3, H9), 5.2-4.8 (H13), 4.45-4.25 (H12), 4.05-3.8 (H4), 3.7-3.5 (H16), 2.6-0.8 (other protons). The monomer ratio (mol/mol) in the block polymer was determined from the ratio of the integral of H4 of NIPAm/ H12 of $HPMAm_{lac2}$. The M_n of the thermosensitive blocks was calculated by comparison of the NIPAm and $HPMAm_{lac2}$ integrals with the integral of PEG protons. The obtained ratio of NIPAm/$HPMAm_{lac2}$ was 74/26. The total mass of the thermosensitive blocks was 27 kDa (M_n of A-B-A triblock polymer = 13.5-10-13.5 kDa).

Cloud point: 23.1 ºC for polymer dissolved in 120 mM ammonium acetate buffer pH 5 at a polymer concentration of 2 mg/mL by static light scattering at a wavelength of 650

nm. The cloud point was defined as the onset of increased scattering intensity.
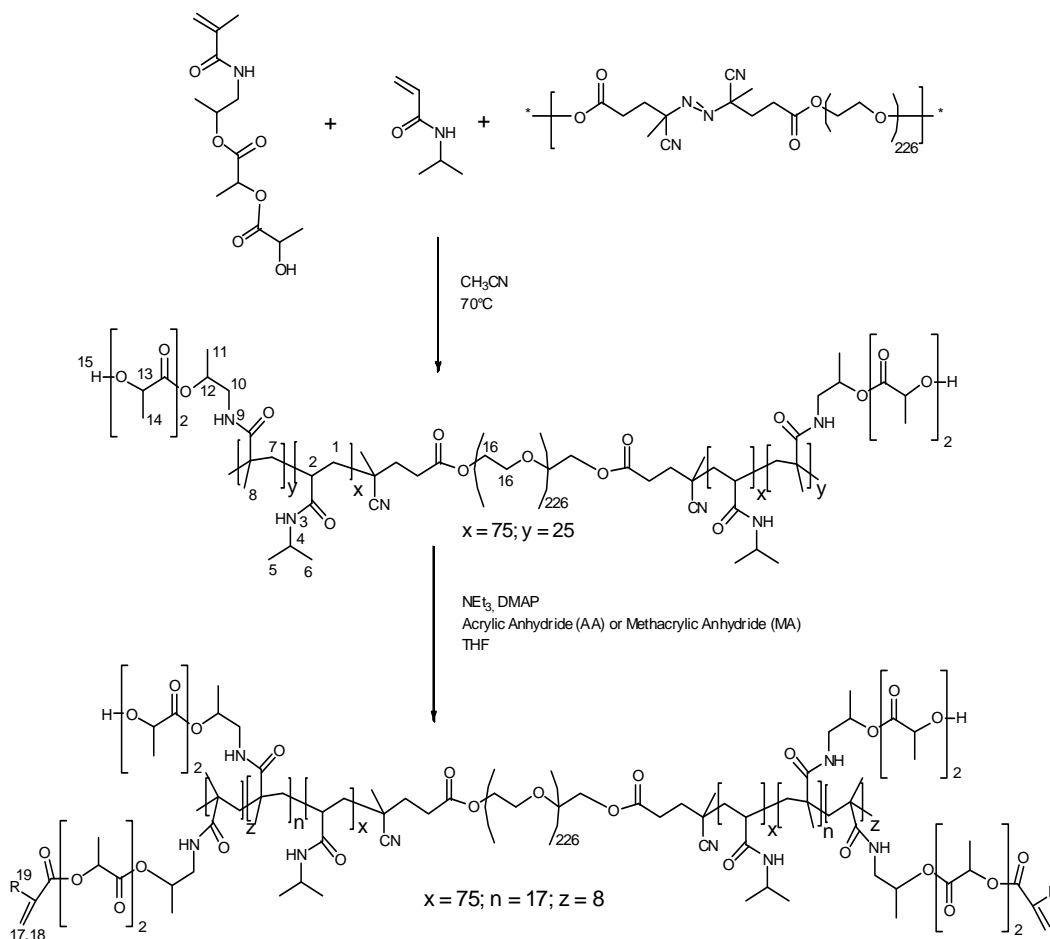
Scheme 3 Synthesis route of (meth)acrylate bearing ABA-triblock copolymers consisting of a PEG$_{10000}$ B-block and random pNIPAm-HPMAm$_{lac2}$ A-blocks (R=H or CH$_3$ for pNHPta and pNHPtma respectively).

5.2.4b. After methacrylation:

^{1}H NMR (DMSO-d$_6$): δ 7.35 (H3, H9), 6.15 & 5.80 (H17, H18), 5.4 (H15), 4.95 (H13), 4.2 (H13 next to OH), 3.8 (H4), 3.60 (H16), 3.3-0.6 (other protons). The degree of methacrylation (DM) was calculated from the ratio of the average intensity of the peaks at 6.15 and 5.80 and intensity of the peak at 5.4 ppm as follows: $((I_{6.15}+I_{5.8})/2)$ / $((I_{6.15}+I_{5.8})/2 +I_{5.4})$ × 100%. The degree of methacrylation, defined as the percentage of

OH groups derivatized by methacrylate moieties, was 28%.

GPC: Mw = 46 kDa; Mn = 22 kDa; PDI = 2.14

Cloud point: 18.8ºC

5.2.4c After acrylation:

^{1}H NMR (DMSO-d_6) δ 7.35 (H3, H9), 6.2, 6.1, 6.0 (H17, H18, H19), 5.4 (H15), 4.95 (H13), 4.2 (H13 next to OH), 3.8 (H4), 3.60 (H16), 3.3-0.6 (other protons). The degree of acrylation (DA) was calculated from the ratio of the average intensity of the peaks at 6.2, 6.1 and 6.0 and intensity of the peak at 5.4 ppm as follows: $((I_{6.2}+I_{6.1}+I_{6.0})/3)$ $/((I_{6.2}+I_{6.1}+I_{6.0})/3) +I_{5.4}) \times 100\%$. The degree of acrylation, defined as the percentage of OH groups derivatized by acrylate moieties, was 32%.

GPC: M_w = 57 kDa; M_n = 23 kDa; PDI = 2.5

Cloud point: 16.0 ºC.

5.2.5. Synthesis of thiolated hyaluronic acid (HA-SH)

Thiolated hyaluronic acid was synthesized according to the procedure described by Shu *et al.* [28] Briefly, 0.5 g of sodium hyaluronate (M_n = 37.9 kDa, PDI = 1.27, measured by GPC) was dissolved in water and 482 mg (1.70 mmol) of DTP was added while stirring. The pH was adjusted to 4.75 with 1 M HCl and subsequently 388 mg of 1-ethyl-3[3-(dimethylamino)propyl]carbodiimide (EDC, 2.02 mmol) was added while keeping the pH at 4.75. The solution was stirred at room temperature for 48 hours and the reaction was stopped by increasing the pH to pH 7 with 1 M NaOH. Then, 2.0 g of dithiothreitol (DTT) was added and the pH was raised to 8.5. The reaction mixture was stirred for another 24h. and subsequently acidified to pH 3.5 with 1 M HCl. The mixture was purified by dialysis (Mw cutoff = 3500 Da) against dilute HCl (pH 3.5) containing 100 mM NaCl and finally against water at 4°C. The final product was obtained as a white powder after lyophilization. The degree of substitution (DS), defined as the number of DTP residues per 100 disaccharide units, was determined by ^{1}H NMR and detection of free thiols by Ellman's method.

^{1}H NMR (D$_2$O): δ = 4.6-3.3 protons of hyaluronic acid), 2.85 (CH$_2$-SH), 2.70 (CH$_2$CH$_2$SH), 2.00 (NHCOCH$_3$), DS: 54%.

Thiol content, defined as percentage of disaccharide units of HA derivatized with free thiol groups determined by Ellman's method: 50%,

These two different methods showed good agreement between the DS values, within the experimental error. The DS is indicated as a mean value of 52%.

GPC: M_n = 39.8 kDa, PDI = 1.26

5.2.6.   Viscotek

A viscotek GPC was used for characterization of hyaluronic acid and thiolated hyaluronic acid. A TDA 302 with triple detector array, column: Grade GMPWxL no.H3371 and detector: GPC max VE 2001 GPC solvent sample module were used. As a standard, PEO with a concentration of 5 mg/ml was used and also the samples had a concentration of 5 mg/ml. The eluens was ammonium acetate buffer pH 5 (concentration 120 mM).

5.2.7.   *Preparation of the placebo and bradykinin loaded hydrogels*

Gels of a volume of 200 μl were prepared in cylindrical shaped glass vials (diameter of 5 mm) as follows. pNHPtma or pNHPta was dissolved in 100 μl of PBS buffer pH 7.4 (8.2 g/l NaCl; 3.1 g/l NaH_2PO_4 12 H_2O; 0.3 g/l NaH_2PO_4, supplemented with 0.02% NaN_3). The samples were gently mixed using a needle and stored at 4 °C for 1 hour to allow the complete dissolution of the polymer. Separately, HA-SH was dissolved in 100 μl of the same buffer at room temperature for 1 hour, mixed using a needle. Upon complete dissolution, the HA-SH solution was mixed with the pNHPtma or pNHPta solutions at room temperature. The final concentration of the polymers was 20 and 5.4 wt% for pNHPt(m)a and HA-SH, respectively. The aforementioned concentrations corresponded to a ratio between thiol and (meth)acrylate groups of 1/1. Upon homogeneous mixing of the two polymer solutions, the samples were incubated at 37 °C for 1 hour, unless indicated otherwise.

BK loaded hydrogels were prepared according to a slightly different procedure. PNHPtma was dissolved in 60 μl of PBS buffer at 4°C, next 40 μl of a peptide solution (100 mg/ml) was added to the pNHPtma or pNHPta solution prior addition of the HA-SH solution. The peptide concentration was 2 wt%. The final polymer concentration was 20 and 5.4 wt% or 9 and 2.4 wt%, for pNHPtma and HA-SH, respectively, equal to a thiol/(meth)acrylate groups ratio of 1/1. Upon mixing the (meth)acrylated and thiolated polymer solutions, the gels were incubated at 37°C for 1 hour to allow the Michael addition reaction.

5.2.8.   Rheology

An AR-G2 rheometer equipped with a Peltier plate. A 20 mm 1° steel cone-plate geometry was used for both the temperature- and the time-sweep rheological experiments. A frequency of 1Hz and a strain of 1% was used in all experiments. The temperature-sweep ranged from 5°C till 45°C with a heating or cooling rate of 1 ºC/min and the time-sweeps were performed during 4 hours. The time-sweep measurements were performed at 37°C during 4 hours. For both time- and temperature-sweep

experiments a solvent trap was used to prevent evaporation.

5.2.9.   *Swelling and degration studies*

0.9 ml of PBS buffer at pH 7.4 containing 0.02% NaN_3 was added on top of empty gels (W_0), prepared according to the described procedure and incubated at 37 °C for 1 h before starting the swelling experiments At regular intervals the weight of the gel upon removal of excess of buffer was measured (W_t) upon removal of the excess of buffer to calculate the swelling ratio ($SR=W_t/W_0$) as the ratio between the weight of the gel at different time points and the initial gel weight (W_0). After each measurement 0.9 ml of fresh buffer was added and the vials stored again in the water bath at 37 °C.

5.2.10.   *(Meth)acrylate conversion measurements*

The gels, prepared as described above, were incubated at 37ºC for 0.5, 1, 4, 24 and 50h and subsequently degraded in 4 ml of NaOH 0.02 M at 37 °C for 30 min. Upon complete degradation of the gel, the solution was neutralized by adding 0.5 ml of acetic acid 2 M. Degraded pNHPt(m)a was used as control. For quantification and detection of methacrylic acid a Waters Acquity UPLC trade system was used with a BEH C18 1.7 µm, 2.1×50 mm column, equipped with a UV detector operating at 210 nm. The eluent used was 95/5/0.1% H_2O/acetonitrile/trifluoro acetic acid (TFAA).(5, 9) Acrylic acid was quantified using the above mentioned UPLC system equipped with a HSS T3 1.8 µm, 2.1×50 mm column. The UV detection was done at 210 nm and H_2O acidified with 0.1% TFAA was used as eluent. For both acrylic and methacrylic acid a flow rate of 0.5 ml/min and a column temperature of 50 °C were used.

5.2.11.   *Bradykinin release studies*

In vitro peptide release from Michael type cross-linked gels was studied using Bradykinin (M_w = 1.1 kDa) as a model peptide. Gels were prepared according to the described procedure and incubated at 37 °C for 1 h before starting the release experiments. Next, 0.9 ml of PBS buffer pH 7.4 was applied on top of the gels and the vials were incubated in a shaking water bath at 37 °C. Samples of 0.15 ml were taken in time and replaced by an equal volume of fresh buffer. The concentration of Bradykinin in the different samples was determined by using an Acquity UPLC trade; with a BEH C18 1.7 µm, 2.1×50 mm column. An eluent gradient, from 30 to 70% of eluent A was used, where eluent A was 95/5/0.1% H_2O/acetonitrile/TFAA and eluent B was 100/0.1% acetonitrile/TFAA. The injection volumes of the samples were 5 µl, the flow rate 0.25 ml/min and detection was performed at 280 nm.

The release mechanism was studied by fitting the experimental release data to the Ritger–Peppas equation: (44-45)

$$M^t/M^\infty = kt^n$$

Where M^t/M^∞ represents the fractional release of the loaded peptide, k is a kinetic constant, t is the release time and n is the diffusional exponent that can be related to the release mechanism of the entrapped molecules. If n=0.5, the release is governed by Fickian diffusion. If n=1, the molecules are released by surface erosion, while both mechanisms play a role in the release if n has a value between 0.5 and 1.

The peptide diffusion coefficients were calculated by the early-time approximation equation of Fick's second law: [44]

$$M^t/M^\infty = 4 \ (Dt \ /\pi\delta^2)^{1/2}$$

where M^t/M^∞ represents the fractional release of the entrapped peptide, D is the diffusion coefficient, t is the release time and δ is the diffusional distance, equal to the thickness of the gel.

5.3.   Results and Discussion

5.3.1.   Gelation kinetics and rheological properties

pNHPt(m)a triblock copolymers showed a degree of (meth)acrylation (DM or DA), defined as the percentage of OH-groups that were derivatized in the polymer, of 28% and 32%, respectively, as determined by ^{1}H-NMR. The (meth)acrylation rendered the polymers more hydrophobic and the cloud point dropped from 23ºC before (meth)acrylation to 19 and 16ºC for methacrylated and acrylated polymers, respectively.

HA-SH had a degree of thiolation of 52%, defined as percentage of disaccharide units of HA derivatized with free thiol groups, as determined by ^{1}H-NMR.

The hydrogels were prepared by mixing a pNHPTma or pNHPTa solution in PBS buffer pH 7.4 with a HA-SH solution in the same buffer at 37°C. The concentration was 20 wt% and 5.4 wt% for pNHPt(m)a and HA-SH, respectively corresponding to a molar ratio thiol/(meth)acrylate groups of 1/1.

Figure 1 shows photographs of pNHPtma (1) and pNHPta (2) mixed with HA-SH incubated at 37ºC at different time points. The progressive conversion of (meth)acrylate and thiol groups into chemical cross-links by Michael addition reaction resulted in a notable increase in viscosity. After 0.5 h (1a, 2a) white opalescent viscous solutions were obtained; after 1 h (1b, 2b) a further increase in viscosity was observed and within 4 h

(1c, 2c) stable hydrogels were formed. As expected, acrylated gels (2a-c) showed slightly faster gelation kinetics than the methacrylated systems (1a-c).
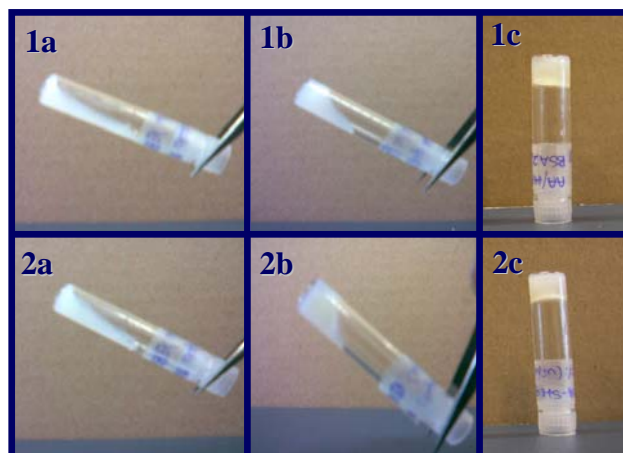

Figure 1. Pictures of polymer solutions/gels (polymer concentration: 20 wt% pNHPt(m)a, 5.4 wt% HA-SH; ratio thiol/(meth)acrylate groups = 1/1) during Michael addition reaction at 37°C for 0.5 h (a), 1 h (b) and 4 h (c) for HA-SH and pNHPtma (1) and pNHPta (2), respectively.

Rheological characterization of the mixed system was performed at 37 ºC as shown in **Figure 2**. Already at time = 0 the formation of a physical network was observed in both the acrylate and methacrylate modified polymer formulations. This behavior is ascribed to the thermosensitive properties of pNHPt(m)a polymers, that self-assemble at body temperature by hydrophobic interaction of the pNIPAm/pHPMAm$_{lac2}$ chains.
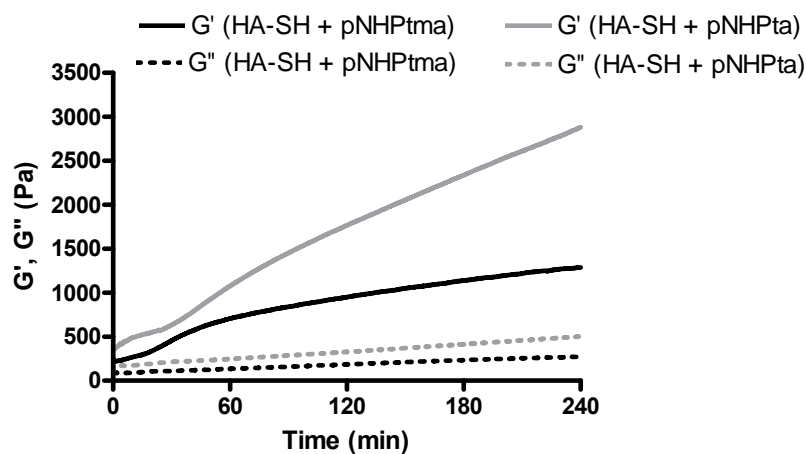

Figure 2: Storage (*G'*) and loss (*G''*) moduli at 37 ºC as a function of time directly after mixing of HA-SH with pNHPtma and pNHPta, respectively. Polymer concentration: 20 wt% pNHPtma or pNHPta + 5.4 wt% HA-SH.

The formation of self-essembled hydrogel upon injection is particularly beneficial for its intended biomedical application, as it would allow *in situ* stability of the network upon administration, before the chemical cross-linking occurs. In time, a gradual increase of storage and loss moduli (*G′* and *G″*, respectively) was observed, confirming that the structure of the gels was progressively stabilized by the formation of chemical cross-links.

The acrylated system displayed higher values of *G′* and *G″* as compared to the methacrylated one, indicating the formation of a gel of higher cross-link density after 4 hours. This observation is likely due to the faster reaction kinetics of acrylate groups with thiol groups, as compared to the methacrylate modified polymers.

Temperature sweep analysis of HA-SH + pNHPtma gels during the Michael addition curing were performed. **Figure 3**a shows that upon mixing of HA-SH with pNHPtma and increase of the temperature from 4 to 45ºC, a slight and reversible increase of G′ was observed. When the temperature is higher than the cloud point of the polymer, the thermosensitive chains self-assemble, leading to the formation of hydrophobic domains.(46)At increasing incubation time at 37ºC, higher values of G′ were reached, as the Michael addition reaction occurred between methacrylate and thiol groups within the hydrophobic domains, resulting in a more stable and irreversible network.

The G′ values during the cooling cycles at different time points demonstrated the formation of the covalent cross-links, as at temperatures below the cloud point viscoelastic networks were still present and increasing values of G′ at 5°C were observed at increasing curing time. It was further shown that thermal and chemical gelation mechanisms act synergistically to enhance the mechanical properties of the gels. After 50 hours the hydrogels displayed remarkable values of G′ (3.6 kPa) and tan(δ) values below 0.2 at 37°C, as shown in figure 3b, and no further increase of the storage modulus in time was observed, indicating that full conversion of methacrylate and thiol groups was achieved.

The hydrogel methacrylate conversion was further investigated by the indirect method of the quantification of the unreacted methacrylate groups and compared to the acrylate conversion in order to gain insight into the gelation kinetics. **Figure 4** shows that the (meth)acrylate groups were converted in time, until reaching quantitative conversion after 50 hours incubation. This observation implies that the Michael addition reaction was the only cross-linking pathway involved in the gelation process, as the ratio between thiols and (meth)acrylates is 1:1, and the formation of disulfide bonds due to auto-oxidation of thiols was negligible. The Michael addition was confirmed to be the only cross-linking pathway by rheological time-sweep experiments of HA-SH solutions 5.4 wt% at 37 °C, that showed no increase in G′ values in time, indicating negligible disulfide bond formation (Appendix C, Figure 1SI). The acrylate groups showed higher conversion into chemical cross-links by Michael addition as compared to the methacrylates at corresponding time-points. For instance, a conversion of approximately 60 and 20% after

0.5h was shown by acrylated and methacrylated polymers, respectively.
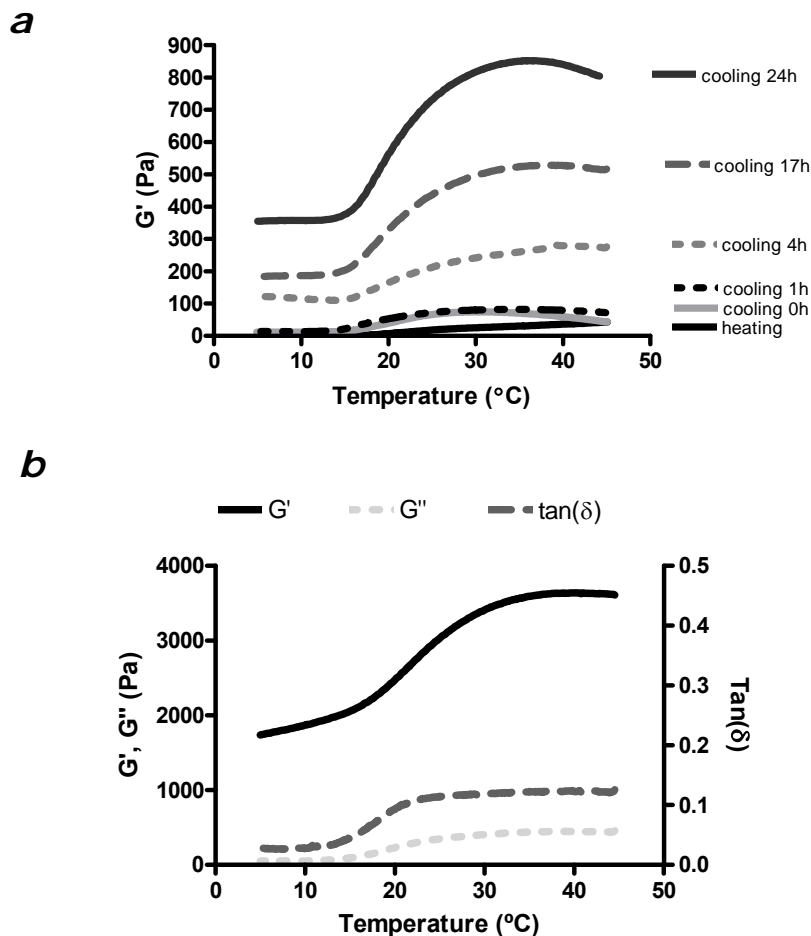
Figure 3: (a) Storage modulus(*G′*) of HA-SH + pNHPtma gels during heating cycles (heating rate 1 ºC/min) directly after mixing of HA-SH with pNHPtma and during cooling cycles after Michael addition reaction for 0, 1, 4, 17 and 24h. (b) Tan δ, storage (*G′*) and loss (*G″*) moduli of HA-SH + pNHPtma gels during a cooling cycle upon quantitative conversion of methacrylate groups. (Polymer concentration: 20 wt% pNHPtma + 5.4 wt% HA-SH).

   (Meth)acrylate conversion experiments further showed that the Michael addition followed relatively slow kinetics, in particular in case of methacrylate derivatized hydrogels. The slow kinetics are most likely caused by the limited accessibility of the (meth)acrylate moieties for Michael addition reaction with thiol derivatized hydrophilic hyaluronic acid, as the methacrylate groups are situated in phase-separated hydrophobic domains of thermosensitive blocks at 37ºC.(47) At 37 °C, indeed, the thermosensitive pNIPAAm/pHPMAmlac2 chains are in a dynamic equilibrium between the relaxed and the

self-assembled state. The difference in cross-linking rate between acrylates and methacrylates can be attributed to the higher reactivity of acrylate groups toward Michael addition reaction with thiols due to less steric hindrance as compared to methacrylates as well as to the less hydrophobic character of acrylate groups that makes the accessibility of HA-SH easier.
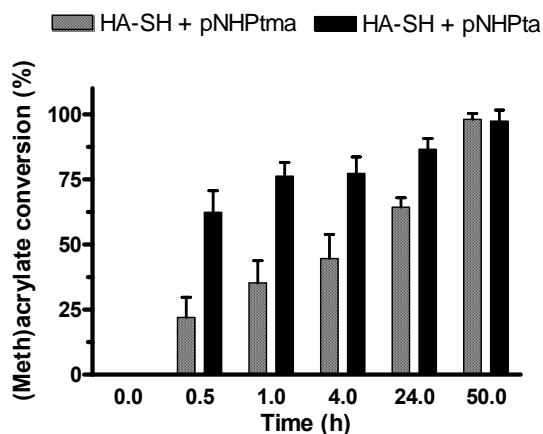

Figure 4: (Meth)acrylate conversion in time (polymer concentration: 20 wt% pNHPt(m)a + 5.4 wt% HA-SH; ratio thiol/(meth)acrylate groups = 1/1). Data are shown as mean ± standard deviation (n=3).

5.3.2. Swelling and degradation of hydrogels

The swelling and degradation kinetics of hydrogels at 37ºC (**Figure 5**) show that during incubation with PBS buffer pH 7.4 the pNHPtma/HA-SH and pNHPta/HA-SH gels absorbed water, resulting in swelling ratio (*SR*) values up to 2.5 in approximately 6 and 15 days and subsequently the gels degraded completely in 84 and 118 days, respectively. When the lactate groups are cleaved, the polymer becomes more hydrophilic and consequently will absorb more water, resulting in an increased swelling ratio during the first days.

The degradation of the hydrogels is caused by the hydrolysis of the esters between PEG and thermo blocks as well as between lactate and methacrylate groups. (39, 42, 46)Rheological data (Figure 2), showing that the acrylate gels had higher cross-link density than the methacrylate gels, explain the slower degradation of the former gels. The high reactivity of the acrylate groups towards thiol groups might represent a drawback with respect to the biomedical applications these hydrogels are designed for. In the presence of cells or proteins, acrylate moieties might be more reactive towards thiols or amines present in cysteine or lysine residues of proteins, peptides encapsulated in the hydrogels network or present on the cell membranes, leading to cytotoxicity and/or

chemical immobilization of the active in the gel. Further, acrylic monomers have been reported to be more toxic than their methacrylic analogues. (48),(49) It has also been shown that binding of proteins, such as BSA, to hydrogel precursors through Michael addition reaction might occur.(50) Therefore, further characterization studies were focused on methacrylated gels, which are envisioned to show a better cytocompatibility and to be more protein and peptide friendly.
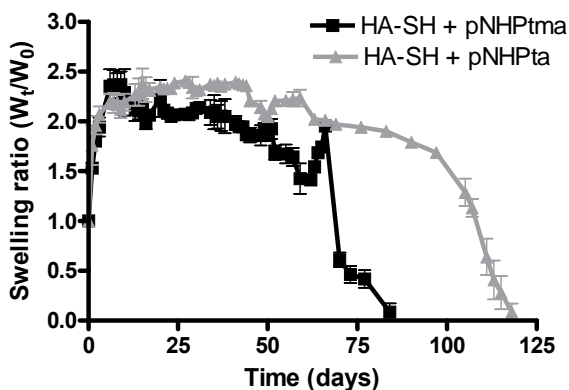

Figure 5: Swelling ratio (=gel weight at time t (W_t)/ initial gel weight (W_0)) of polymer gels (polymer concentration: 20 wt% pNHPt(m)a + 5.4 wt% HA-SH; ratio thiol/(meth)acrylate groups = 1/1) for HA-SH and pNHPt(m)a, respectively. Data are shown as as mean ± standard deviation (n=2).

5.3.3. Peptide release behavior of hydrogels

The suitability of the HA-SH/pNHPtma gels for the delivery of peptides was studied. To this end, Bradykinin (BK) was selected as a model peptide since its molecular weight (1.1 kDa) is representative for a wide range of therapeutic peptides. A continuous release of the peptide from gels of 9 and 20 wt% pNHPtma was observed (**Figure 6**a). BK was quantitatively released from hydrogels of 9 wt% polymer concentration in 120 hours, while the hydrogel of higher polymer content showed slower release kinetics with a cumulative release of approximately 77% in 220 hours. The incomplete recovery of bradykinin from the hydrogel of higher polymer concentration can be explained by the higher density of hydrophobic domains formed by self-assembled pNIPAm/pHPMAm$_{lac2}$ at 20 wt% initial solid content. When the density of the hydrophobic domains is high, the peptide will partition both into hydrophobic and hydrophilic domains.[47] The release of the peptide from the hydrophobic compartments probably requires significant degradation of the network, that occurs on a longer time-scale (see swelling/degradation studies) than the one considered in the release experiments. Due to the progressive dilution of the release medium during the experiment, quantification of the peptide was impossible after

500 hours because its concentration reached the detection limit of the analytical technique used.

From the release profiles, it can be concluded that the polymer concentration tailors not only the cross-linking density and pore size of the network but consequently also the release kinetics of the peptide.

Figure 6b shows that the cumulative release scaled linearly with the square root of time, up to a cumulative release of 83 and 75%, for pNHPtma and pNHPta, respectively. This first order kinetics means that the release is diffusion governed and implies that the pores in the hydrogel network are bigger than the hydrodynamic diameter of the peptide. (9, 44-45)
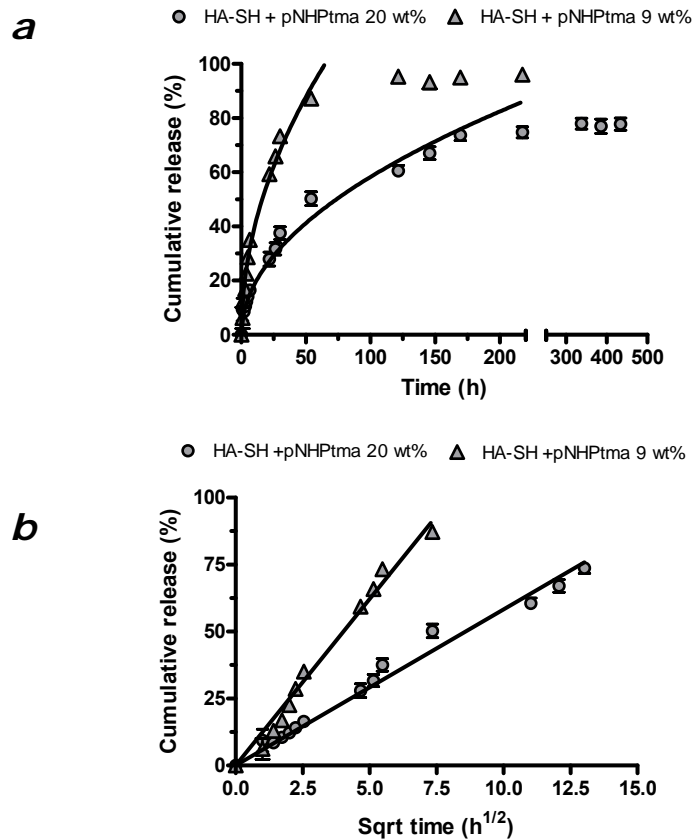
Figure 6: Bradykinin cumulative release from pNHPtma/HA-SH gels of 20 and 9 wt% pNHPtma after Michael addition reaction for 1h. Release kinetics are shown as a function of time (a) and as a function of the square root of time (b). Data are shown as mean ± standard deviation (n=3).

BK diffusion coefficients, calculated by the early-time approximation equation of Fick's second law, were 22.7±1.5 and 11.2±1.9 μm^2/s for gels of 9 and 20 wt% pNHPtma

content, respectively. These values correspond to a 8 to 16 fold decrease in peptide mobility when compared to the diffusion coefficient of BK in water at 37°C, as extrapolated from diffusion coefficients in water of other proteins(51-52) and demonstrated the suitability of the studied hydrogel as diffusion controlled delivery system.

5.4.   Conclusions

  In conclusion, we have shown that the combination of thermosensitive gelling and Michael addition cross-linking is an attractive approach for the preparation of injectable, mechanically stable and biodegradable hydrogels with favorable properties for the delivery of peptides.

Acrylated thermosensitive polymers showed higher reactivity towards thiol groups, yielding gels with faster gel formation kinetics and higher mechanical strength. The degradability of the system is ensured by the presence of hydrolitically sensitive ester bonds within the thermosensitive polymer and enzymatically degradable bonds of the hyaluronic acid. The suitability of the methacrylated gels as diffusion controlled delivery system for peptides was demonstrated and the tailorability of the release kinetics by the gel characteristics was assessed.

Acknowledgements

References

1. Hoffman AS (2002) Hydrogels for biomedical applications. *Advanced Drug Delivery Reviews* 54(1):3-12.

2. Van Tomme SR, Storm G, & Hennink WE (2008) In situ gelling hydrogels for pharmaceutical and biomedical applications. *International Journal of Pharmaceutics* 355(1-2):1-18.

3. Klouda L & Mikos AG (2008) Thermoresponsive hydrogels in biomedical applications. *European Journal of Pharmaceutics and Biopharmaceutics* 68(1):34-45.

4. Jeong B, Kim SW, & Bae YH (2002) Thermosensitive sol-gel reversible hydrogels. *Advanced Drug Delivery Reviews* 54(1):37-51.

5. Vermonden T, Fedorovich NE, van Geemen D, Alblas J, van Nostrum CF, Dhert WJA, & Hennink WE (2008) Photopolymerized Thermosensitive Hydrogels: Synthesis, Degradation, and Cytocompatibility. *Biomacromolecules* 9(3):919-926.

6. Jeong KJ & Panitch A (2009) Interplay between Covalent and Physical Interactions within Environment Sensitive Hydrogels. *Biomacromolecules* 10(5):1090-1099.

7. Burdick JA, Chung C, Jia X, Randolph MA, & Langer R (2004) Controlled Degradation and Mechanical Behavior of Photopolymerized Hyaluronic Acid Networks. *Biomacromolecules* 6(1):386-391.

8. Tai H, Wang W, Vermonden T, Heath F, Hennink WE, Alexander C, Shakesheff KM, & Howdle SM (2009) Thermoresponsive and Photocrosslinkable PEGMEMA-PPGMA-EGDMA Copolymers from a One-Step ATRP Synthesis. *Biomacromolecules* 10(4):822-828.

9. Censi R, Vermonden T, van Steenbergen MJ, Deschout H, Braeckmans K, De Smedt SC, van Nostrum CF, di Martino P, & Hennink WE (2009) Photopolymerized thermosensitive hydrogels for tailorable diffusion-controlled protein delivery. *Journal of Controlled Release* 140(3):230-236.

10. Malkoch M, Vestberg R, Gupta N, Mespouille L, Dubois P, Mason AF, Hedrick JL, Liao Q, Frank CW, Kingsbury K, & Hawker CJ (2006) Synthesis of well-defined hydrogel networks using Click chemistry. *Chemical Communications* (26):2774-2776.

11. Crescenzi V, Cornelio L, Di Meo C, Nardecchia S, & Lamanna R (2007) Novel Hydrogels via Click Chemistry: Synthesis and Potential Biomedical Applications. *Biomacromolecules* 8(6):1844-1850.

12. DeForest CA, Polizzotti BD, & Anseth KS (2009) Sequential click reactions for synthesizing and patterning three-dimensional cell microenvironments. *Nature Materials* 8(8):659-664.

13. van Dijk M, Rijkers DTS, Liskamp RMJ, van Nostrum CF, & Hennink WE (2009) Synthesis and Applications of Biomedical and Pharmaceutical Polymers via Click Chemistry Methodologies. *Bioconjugate Chemistry* 20(11):2001-2016.

14. Robb SA, Lee BH, McLemore R, & Vernon BL (2007) Simultaneously Physically and Chemically Gelling Polymer System Utilizing a Poly(NIPAAm-co-cysteamine)-Based Copolymer. *Biomacromolecules* 8(7):2294-2300.

15. Niu G, Zhang H, Song L, Cui X, Cao H, Zheng Y, Zhu S, Yang Z, & Yang H (2008) Thiol/Acrylate-Modified PEO-PPO-PEO Triblocks Used as Reactive and Thermosensitive Copolymers. *Biomacromolecules* 9(10):2621-2628.

16. Peattie RA, Rieke ER, Hewett EM, Fisher RJ, Shu XZ, & Prestwich GD (2006) Dual growth factor-induced angiogenesis in vivo using hyaluronan hydrogel implants. *Biomaterials* 27(9):1868-1875.

17. Cellesi F, Weber W, Fussenegger M, Hubbell JA, & Tirelli N (2004) Towards a fully synthetic substitute of alginate: Optimization of a thermal gelation/chemical cross-linking scheme (ldquotandemrdquo gelation) for the production of beads and liquid-core capsules. *Biotechnology and Bioengineering* 88(6):740-749.

18. Hiemstra C, van der Aa LJ, Zhong Z, Dijkstra PJ, & Feijen J (2007) Rapidly in Situ-Forming Degradable Hydrogels from Dextran Thiols through Michael Addition. *Biomacromolecules* 8(5):1548-1556.

19. Elbert DL, Pratt AB, Lutolf MP, Halstenberg S, & Hubbell JA (2001) Protein delivery from materials formed by self-selective conjugate addition reactions. *Journal of Controlled Release* 76(1-2):11-25.

20. Ferruti P, Bianchi S, Ranucci E, Chiellini F, & Caruso V (2005) Novel poly(amido-amine)-based hydrogels as scaffolds for tissue engineering. *Macromolecular Biosciences* 5(7):613-622.

21.   Ferruti P, Bianchi S, Ranucci E, Chiellini F, & Piras AM (2005) Novel Agmatine-Containing Poly(amidoamine) Hydrogels as Scaffolds for Tissue Engineering. *Biomacromolecules* 6(4):2229-2235.

22.   Lutolf MP & Hubbell JA (2003) Synthesis and Physicochemical Characterization of End-Linked Poly(ethylene glycol)-co-peptide Hydrogels Formed by Michael-Type Addition. *Biomacromolecules* 4(3):713-722.

23.   Lutolf MP, Tirelli N, Cerritelli S, Cavalli L, & Hubbell JA (2001) Systematic Modulation of Michael-Type Reactivity of Thiols through the Use of Charged Amino Acids. *Bioconjugate Chemistry* 12(6):1051-1056.

24.   Rizzi SC & Hubbell JA (2005) Recombinant Protein-co-PEG Networks as Cell-Adhesive and Proteolytically Degradable Hydrogel Matrixes. Part I: Development and Physicochemical Characteristics. *Biomacromolecules* 6(3):1226-1238.

25.   Vernon B, Tirelli N, Bächi T, Haldimann D, & Hubbell JA (2003) Water-borne, *in situ* crosslinked biomaterials from phase-segregated precursors. *Journal of Biomedical Materials Research* 64A(3):447-456.

26.   Mather BD, Viswanathan K, Miller KM, & Long TE (2006) Michael addition reactions in macromolecular design for emerging technologies. *Progress in Polymer Science* 31(5):487-531.

27.   Morra M, Cassinelli C, Cascardo G, Nagel M-D, Della Volpe C, Siboni S, Maniglio D, Brugnara M, Ceccone G, Schols HA, & Ulvskov P (2004) Effects on Interfacial Properties and Cell Adhesion of Surface Modification by Pectic Hairy Regions. *Biomacromolecules* 5(6):2094-2104.

28.   Shu XZ, Liu Y, Luo Y, Roberts MC, & Prestwich GD (2002) Disulfide Cross-Linked Hyaluronan Hydrogels. *Biomacromolecules* 3(6):1304-1311.

29.   Butterworth PHW, Baum H, & Porter JW (1967) A modification of the Ellman procedure for the estimation of protein sulfhydryl groups. *Archives of Biochemistry and Biophysics* 118(3):716-723.

30.   Jin R, Moreira Teixeira LS, Krouwels A, Dijkstra PJ, van Blitterswijk CA, Karperien M, & Feijen J (2010) Synthesis and characterization of hyaluronic acid-poly(ethylene glycol) hydrogels via Michael addition: An injectable biomaterial for cartilage repair. *Acta Biomaterialia* 6(6):1968-77.

31.   Lee Y, Chung HJ, Yeo S, Ahn C-H, Lee H, Messersmith PB, & Park TG (2010) Thermo-sensitive, injectable, and tissue adhesive sol-gel transition hyaluronic acid/pluronic composite hydrogels prepared from bio-inspired catechol-thiol reaction. *Soft Matter* 6(5):977-983.

32.   Hahn SK, Oh EJ, Miyamoto H, & Shimobouji T (2006) Sustained release formulation of erythropoietin using hyaluronic acid hydrogels crosslinked by Michael addition. *International Journal of Pharmaceutics* 322(1-2):44-51.

33.   Hahn SK, Park JK, Tomimatsu T, & Shimoboji T (2007) Synthesis and degradation test of hyaluronic acid hydrogels. *International Journal of Biological Macromolecules* 40(4):374-380.

34.   Lee BH, West B, McLemore R, Pauken C, & Vernon BL (2006) In-Situ Injectable Physically and Chemically Gelling NIPAAm-Based Copolymer System for Embolization. *Biomacromolecules* 7(6):2059-2064.

35.   Cheng V, Lee BH, Pauken C, & Vernon BL (2007) Poly(*N*-isopropylacrylamide-*co*-poly(ethylene glycol))-acrylate simultaneously physically and chemically gelling polymer systems. *Journal of Applied Polymer Science* 106(2):1201-1207.

36.   Wang Z-C, Xu X-D, Chen C-S, Yun L, Song J-C, Zhang X-Z, & Zhuo R-X (2010) In Situ Formation of Thermosensitive PNIPAAm-Based Hydrogels by Michael-Type Addition Reaction. *ACS Applied Material Interfaces*.

37.   Heskins M & Guillet JE (1968) Solution Properties of Poly(N-isopropylacrylamide). *Journal of Macromolecular Sciences, Part A: Pure Applied Chemistry* 2(8):1441 - 1455.

38.   Schild HG (1992) Poly(N-isopropylacrylamide): experiment, theory and application. *Progress in Polymer Science* 17(2):163-249.

39.   Rijcken CJ, Snel CJ, Schiffelers RM, van Nostrum CF, & Hennink WE (2007) Hydrolysable core-crosslinked thermosensitive polymeric micelles: Synthesis, characterisation and in vivo studies. *Biomaterials* 28(36):5581-5593.

40.   Soga O, van Nostrum CF, Ramzi A, Visser T, Soulimani F, Frederik PM, Bomans PHH, & Hennink WE (2004) Physicochemical Characterization of Degradable Thermosensitive Polymeric Micelles. *Langmuir* 20(21):9388-9395.

41.   Fang J, Sawa T, Akaike T, & Maeda H (2002) Tumor-targeted Delivery of Polyethylene Glycol-conjugated D-Amino Acid Oxidase for Antitumor Therapy via Enzymatic Generation of Hydrogen Peroxide. *Cancer Research* 62(11):3138-3143.

42.   Neradovic D, van Steenbergen MJ, Vansteelant L, Meijer YJ, van Nostrum CF, & Hennink WE (2003) Degradation Mechanism and Kinetics of Thermosensitive Polyacrylamides Containing Lactic Acid Side Chains. *Macromolecules* 36(20):7491-7498.

43.   Vercruysse KP, Marecak DM, Marecek JF, & Prestwich GD (1997) Synthesis and in Vitro Degradation of New Polyvalent Hydrazide Cross-Linked Hydrogels of Hyaluronic Acid. *Bioconjugate Chemistry* 8(5):686-694.

44.   Ritger PL & Peppas NA (1987) A simple equation for description of solute release II. Fickian and anomalous release from swellable devices. *Journal of Controled Release* 5(1):37-42.

45.   Serra L, Doménech J, & Peppas NA (2006) Drug transport mechanisms and release kinetics from molecularly designed poly(acrylic acid-g-ethylene glycol) hydrogels. *Biomaterials* 27(31):5440-5451.

46.   Vermonden T, Besseling NAM, van Steenbergen MJ, & Hennink WE (2006) Rheological Studies of Thermosensitive Triblock Copolymer Hydrogels. *Langmuir* 22(24):10180-10184.

47.   Vermonden T, Jena SS, Barriet D, Censi R, van der Gucht J, Hennink WE, & Siegel RA (2009) Macromolecular Diffusion in Self-Assembling Biodegradable Thermosensitive Hydrogels. *Macromolecules* 43(2):782-789.

48.   Yoshii E (1997) Cytotoxic effects of acrylates and methacrylates: Relationships of monomer structures and cytotoxicity. *Journal of Biomedical Materials Research* 37(4):517-524.

49.   Chan K & O'Brien PJ (2008) Structure-activity relationships for hepatocyte toxicity and electrophilic reactivity of α,β-unsaturated esters, acrylates and methacrylates. *Journal of Applied Toxicology* 28(8):1004-1015.

50.   Hiemstra C, Zhong Z, van Steenbergen MJ, Hennink WE, & Feijen J (2007) Release of model proteins and basic fibroblast growth factor from in situ forming degradable dextran hydrogels. *Journal of Controlled Release* 122(1):71-78.

51.   Merrill EW, Dennison KA, & Sung C (1993) Partitioning and diffusion of solutes in hydrogels of poly(ethylene oxide). *Biomaterials* 14(15):1117-1126.

52.   Burczak K, Fujisato T, Hatada M, & Ikada Y (1994) Protein permeation through poly(vinyl alcohol) hydrogel membranes. *Biomaterials* 15(3):231-238.

Chapter 6

Printable Photopolymerizable Thermosensitive p(HPMA-lactate)-PEG Hydrogel as Scaffold for Tissue Engineering

Roberta Censi,[a,b] Wouter Schuurman,[c,d] Jos Malda,[c] Giorgio di Dato,[a]
Petra E. Burgisser,[c] Wouter J. A. Dhert,[c,d] Cornelus F. van Nostrum,[a]
Piera di Martino,[b] Tina Vermonden[a] *and* Wim E. Hennink[a]

[a] Department of Pharmaceutics, Utrecht Institute for Pharmaceutical Sciences (UIPS), Utrecht University, P.O. Box 80082, 3508 TB Utrecht, The Netherlands

[b] Department of Chemical Sciences, Camerino University, via S, Agostino 1, 62032, Camerino (MC), Italy

[c] Department of Orthopaedics, University Medical Center Utrecht P.O. Box 85500, 3508 GA Utrecht, The Netherlands

[d] Department of Equine Sciences, Faculty of Veterinary Medicine, Utrecht University, P.O. Box 80163, 3508 TD Utrecht, The Netherlands

Submitted for publication

Abstract

Bioprinting is a new technology that holds potential to have significant impact in regenerative medicine as it allows engineering tissues with biomimetic organization and decreased diffusion distances for nutrients and metabolites. This technique requires hydrogels with adequate mechanical properties for the preparation of structurally stable and well-defined three-dimensional (3D) constructs and that ensure viability and differentiation of encapsulated cells. The aim of this study is to evaluate the suitability of a biodegradable, photopolymerizable and thermosensitive A-B-A triblock copolymer hydrogel as a synthetic extracellular matrix for engineering tissues by means of 3D fiber deposition (3DF). The polymer is composed of poly(*N*-(2-hydroxypropyl)methacrylamide lactate) A-blocks, partly derivatized with methacrylate groups and hydrophilic poly(ethylene glycol) B-blocks of a molecular weight of 10 kDa. The temperature triggered formation of a dimensionally stable gel in buffer is assessed. It is shown that the presence of additional chemical cross-links by photopolymerization enhances the gel stability, leading to constructs with an elastic modulus of 119 kPa (25 wt% polymer content) and a degradation time of approximately 190 days. A power law dependence of the storage plateau modulus of photopolymerized hydrogels on polymer concentration is observed for both physically and chemically cross-linked hydrogels, demonstrating similar mechanical characteristics to natural semi-flexible polymers, including collagen. Moreover, the hydrogel shows suitable mechanical properties for bioprinting, allowing subsequent layer-by-layer deposition of gel fibers to form stable constructs up to at least 0.6 cm (37 layers) with different patterns and strand spacing. The resulting scaffolds have reproducible vertical porosity and the ability to maintain separate localization of encapsulated fluorescent microspheres. Furthermore, high viability is observed for encapsulated chondrocytes after 1 and 3 days of culture. In summary, based on the gel characteristics and behavior of the embedded cells we conclude that the evaluated hydrogel is an interesting candidate for bioprinting of constructs that recapitulate the intricate 3D structure of cells and matrix in natural tissues.

6.1. Introduction

Bioprinting is a novel approach in tissue engineering for scaffold preparation based on computer aided layer-by-layer or dropwise deposition of cell-laden hydrogels.(1-4) This rapid prototyping-derived technique allows the preparation of complex three dimensional (3D) cell laden scaffolds, conferring reproducible control over cell placement, with respect to anatomical geometry, and providing a highly porous microenvironment, amenable to nutrients and oxygen diffusion.(5-9)

The development of novel tissue engineering strategies, using a manifold of 3D patterning techniques, such as fiber templating(10), litography(11) or 3D fiber deposition(1, 12-13) whereby cells are combined with a matrix and printed to yield a 3D construct that subsequently can be transplanted *in vivo*, offers a novel and potential route towards tissue regeneration.(14-16)

The possibility to incorporate different types of living cells and to deposit different materials within a scaffold by using 3DF, allows the creation of grafts that closely resemble the hierarchy of cells and matrix in natural tissues.(17) The success of this approach highly depends upon the biomaterial, promoting tissue formation by the incorporated cells, being biocompatible, processable into a suitable 3D structure and eventually biodegradable without harmful effects.(18-22) Furthermore, the biomaterial should have sufficient porosity to facilitate nutrients and oxygen supply and tissue ingrowth and it should be able to support cell proliferation, differentiation and function.

Hydrogels are 3D networks of cross-linked hydrophilic polymers that fulfill some of these requirements, and are therefore extensively used as supportive matrices for tissue engineering. So far, both natural (alginate, chitosan, hyaluronic acid, collagen, fibrin, etc.)(23-26) and synthetic (poly(ethylene glycol) (PEG), poly(N-isopropylacrylamide), Pluronic, etc.)(27-30) hydrogels have been used *in vitro* as scaffolding material for tissue engineering, but each suffers from different drawbacks. Natural polymers possess an inherent biocompatibility and often positive cell interaction and modulation,(31) but also large lot-to-lot variation, poor mechanical properties and lack of tailorability. On the other hand, synthetic polymers have well-defined structures with possibilities to fine-tune their properties, but biodegradability and biocompatibility often represent an issue.

Therefore, in the present study, a biodegradable, synthetic, photopolymerizable and thermosensitive hydrogel, that exhibits an advantageous combination of properties, is used for the development of 3D printed scaffolds. The polymer has an A-B-A architecture consisting of thermosensitive poly(*N*-(2-hydroxypropyl)methacrylamide lactate)(32) (p(HPMAm-lac) A-blocks that are partly modified with methacrylate moieties, to allow chemical cross-linking using photopolymerization, and a B-block of poly(ethylene glycol) (PEG).(33-35) The p(HPMAm-lac) A-blocks exhibit thermosensitive behavior,(21, 36-37) having a cloud point (CP) that can be tuned by the average length of the lactate side chains.(32)

Bioprinted hydrogel based scaffolds can be used for the regeneration of a number of tissues such as bone, skin, liver, cartilage, replicating the hierarchical structures of natural tissues at an unprecedented level. In this paper, the potential of the studied hydrogel for engineering zonal cartilage is addressed. The use of hydrogels for cartilage repair is particularly attractive as they reflect several characteristics of native cartilage, being able to homogeneously encapsulate chondrocytes in a highly hydrated, structurally stable and highly diffusive 3D network. Articular cartilage is an avascular supporting connective tissue, exhibiting a low metabolic rate and a low regenerative potential. It has a hydrogel-like structure consisting of 70% water, 20% collagen, responsible for the tensile properties, and 10% proteoglycans, providing compression resistance.(38) The ability of articular cartilage to function as a low-friction and wear-resistant load bearing tissue depends upon its zonal structural organization and biochemical composition. The superficial zone (10–20% thickness) is composed of a collagen network aligned parallel to the surface and low content of proteoglycans. In the middle zone (30–50% thickness), the collagen network is randomly oriented and in the deep zone (30–50% thickness) the collagen network is oriented perpendicularly to the bone and the proteoglycan content is high.(38-40) Because of lack of healing capacity of the tissue, due to poor blood supply, local cartilage damage eventually leads to generalized cartilage degeneration and permanent loss of organization and functionality.

The treatment of choice for generalized cartilage damage is prosthetic joint replacement,(41) whereas for focal lesions, either microfracture or cell-based therapy can be used.(42-43) However, although clinical outcomes are satisfactory for these methods, they have drawbacks: prostheses have a limited life span, whereas microfracture and chondrocyte implantation do not fully restore the organization and consequently the functionality of native cartilage. By using 3D printing techniques, ideally, patient-derived cells can be mixed with the hydrogel matrix and printed at defined locations within a single scaffold, mimicking the natural cell distribution and potentially enhancing clinical outcomes.(2, 44-45)

The goal of this study was to evaluate the suitability of methacrylate bearing HPMAm-lac-PEG based hydrogels for organ printing. Upon printing, the scaffold is photopolymerized to provide the cells with long-term mechanical support and, in time, is expected to gradually degrade into biocompatible products. The printability, mechanical properties, degradation behavior and chondrocyte compatibility was evaluated for this hydrogel.

6.2.   Experimental Section

6.2.1. *Materials*

All chemicals were obtained from Sigma-Aldrich and used as received, unless stated otherwise. All solvents were purchased from Biosolve. Tetrahydrofuran (THF) was distilled

from sodium/benzophenone and stored over 3 Å molecular sieves. Phosphate buffered saline (PBS) (8.2 g l^{-1} NaCl; 3.1 g l^{-1} $NaH_2PO_412H_2O$; 0.3 g l^{-1} NaH_2PO_4) used to prepare the hydrogels for mechanical characterization and degradation studies was obtained from Braun (The Netherlands). HPMAm (hydroxypropylmethacryliamide) was obtained from Zentiva a.s. (Praha, Czech Republic), L-lactide from Purac Biochem BV (Gorinchem, The Netherlands) and 2-hydroxy-1-[4-(2-hydroxyethoxy)phenyl]-2-methyl-1-propanone (Irgacure 2959) from Ciba Specialty Chemicals Inc (Basel, Switzerland). DMAP (dimethylaminopyridine) and 4,4´-Azobis(4-cyanopentanoic acid) (ABCPA) were purchased from Fluka Chemie AG (Buchs, Switzerland). HPMAm-monolactate and HPMAm-dilactate were synthesized according to a previously reported method.(32) The synthesis of triblock copolymers with PEG as middle block and polyHPMAm-lactate as outer blocks was described previously (33-35) and applied in this study for the preparation of a triblock copolymer having p(HPMAm-lac) A-blocks of 23.5 kDa, derivatized with 30% of methacrylate groups and PEG B-blocks of 10 kDa molecular weight. Dye-Trak "F" fluorescent microspheres (fluorescent lemon and fluorescent orange) were purchased from Triton technology (San Diego, CA). Type II collagenase was obtained from Worthington Biochemical Corp (Lakewood, NJ). DMEM [Dulbecco's Modified Eagle Medium] insulin-transferrin-selenium mixture (ITS-X), penicillin and streptomycin were obtained from Invitrogen (Carlsbad, CA). Fetal bovine serum was obtained from Biowhittaker (Walkersville, MD) and FGF-2 and TGF-b2 from R&D Systems (Minneapolis, MN). Human serum albumin from Cealb (Sanquin, Utrecht, The Netherlands) was used.

6.2.2. Synthesis of (PEG-ABCPA)$_n$ Macroinitiator

(PEG-ABCPA)$_n$ was synthesized slightly modifying the procedure described by Neradovic *et al*(46) and Vermonden et al.(33) In detail, 10 g (1 mmol) of PEG (number-average molar mass M_n = 10000 g mol^{-1}), 280 mg (1 mmol) of ABCPA, 91.6 mg (0.3 mmol) of 4-(dimethylamino)pyridinium-4-toluenesulfonate (DPTS) and 618 mg (3 mmol) of *N,N'*-dicyclohexylcarbodiimide (DCC) were dissolved in 60 ml of a 1:1 mixture of dichloromethane and dry THF. The mixture was stirred at room temperature at 0°C for 1 hour and subsequently at room temperature for 24 h under nitrogen atmosphere. The formed dicyclourea (DCU) was filtered off, and the organic solvents were removed by rotary evaporation. The product was suspended in water, filtrated over hyflo and dialyzed for 48 hours at 4°C against water using a dialysis membrane with a cut-off of 12-14 kDa. The macroinitiator was obtained in a high yield (- 80%) after freeze-drying and characterized by ^{1}H NMR in CDCl$_3$ and gel permeation chromatography (GPC).

6.2.3. Synthesis of Methacrylated Triblock Copolymers

A thermosensitive triblock copolymer consisting of PEG 10 kDa as hydrophilic block and pHPMAm$_{lac}$ as thermosensitive outer blocks with a HPMAm-monolactate/HPMAm-dilactate

ratio of 50/50 was synthesized by free radical polymerization using (PEG-ABCPA)$_n$ macroinitiator according to a method described earlier.(33) The OH side groups of p(HPMAm-lac) were partially methacrylated using the following procedure. The triblock copolymer (7 g, 21 mmol) was dissolved in dry THF under a N$_2$ atmosphere, DMAP (21 mg, 174 mmol) and triethylamine (TEA) (601 µl, 4.35 mmol) were added at 0ºC. Finally, methacrylic anhydride (MA) (648 µl, 4.35 mmol) at 1:1 molar ratio with TEA was added. The reaction mixture was subsequently stirred for 24 hours at room temperature, followed by the addition of approximately 20 ml water. Next the reaction mixture was dialyzed (membrane with a cut-off of 12-14 kDa) against water for two days at 4˚C and isolated by freeze-drying. The synthesized polymers were characterized by ^{1}H NMR (300 MHz, DMSO-d_6, δ): 7.35 (b,1H, NH), 6.15 & 5.80 (d, 2H, C=CH_2), 5.4 (d, 1H, CH-OH), 4.95 (d, CO-CH(CH$_3$)-O), 4.1 (d, 1H, CO-CH(CH$_3$)-OH), 3.60 (s, 904H, OCH_2CH_2 (PEG-protons)), 3.4 (s, 2H, NHCH_2), 2.2-0.6 (main chain protons and CH$_3$ of lactate groups). The degree of methacrylation (DM), defined as the percentage of OH groups derivatized with methacrylate moieties was calculated from the ratio of the average intensity of the peaks at 6.15 and 5.80 and intensity of the peak at 5.4 ppm as follow:(34)

$$((I_{6.15}+I_{5.8})/2) / ((I_{6.15}+I_{5.8})/2 +I_{5.4}) \times 100\% \tag{2}$$

6.2.4. ^{1}H NMR Spectroscopy

^{1}H NMR (300 MHz) spectra were recorded on a Gemini 300 MHz spectrometer (Varian Associates Inc., NMR Instruments, Palo Alto, CA) using DMSO-d_6 and CDCl$_3$ as solvents. Chemical shifts were referred to the solvent peak (δ = 2.49 ppm and δ = 7.24 ppm, for DMSO-d_6 and CDCl$_3$, respectively).

6.2.5. Gel Permeation Chromatograph

The molecular weights of the polymers were determined by GPC using a Plgel 5 µm MIXED-D column (Polymer Laboratories) with a column temperature of 40 ºC. DMF containing 10 mM LiCl was used as eluent with an elution rate of 0.7 ml min^{-1}, and the sample concentration was 5 mg ml^{-1} in the same eluent. Poly(ethylene glycols) with defined molecular weights were used as calibration standards.(32)

Determination of the Cloud Point: The cloud point (CP) of the polymers was measured with static light scattering using a Horiba Fluorolog fluorometer (650 nm, 90º angle). The polymers were dissolved at a concentration of 3 mg ml^{-1} in ammonium acetate buffer (pH 5.0, 120 mM). The heating rate was approximately 1 ºC min^{-1} and every 0.2 ºC the scattering intensity was measured at 90º angle. The CP is defined as the onset of increasing scattering intensity.(47)

6.2.6. *Rheological Characterization*

The rheological analysis of the (non)-photopolymerized hydrogels was performed on an AR-G2 rheometer (TA-Instruments). Triblock copolymer solutions at a concentration of 20, 25, 30 and 35 wt % were prepared in PBS pH 7.4 supplemented with 0.2 wt% NaN_3 at 4°C and Irgacure 2959 (0.05 wt %) was added. The physical gels were prepared heating the polymer solutions from 5 to 45 °C at a rate of 1 °C min^{-1}. Non-photopolymerized gels were studied using a cone-plate geometry (steel, 20 mm diameter with an angle of 1°). A solvent trap was used to prevent evaporation of the solvent and 1% strain was applied.[33]

To analyze the photopolymerized hydrogels the AR G-2 rheometer was equipped with a UV lightguide connected to a BluePoint lamp 4 (350-450 nm, Honle UV technology, light intensity of 50 mW/cm^2). Gels were studied at 37 °C using a plate–plate geometry at 0.1% strain and 1 Hz frequency. The diameter of the geometry was 20 mm and the gap between the plates 300 µm.[35] Strain sweep experiments were performed at 37°C using a plate–plate geometry at 0.2 Hz frequency and a strain range between 0.001 and 10. The polymer solutions were measured as such or upon 5 min UV irradiation.

6.2.7. *3D printing of methacrylated HPMAm-lac-PEG triblock copolymer scaffolds*

A BioScaffolder dispensing system (Sys Eng, Salzgitter-Bad, Germany) was used for 3D printing of hydrogel scaffolds. The pneumatic syringe dispenser was loaded with the triblock copolymer solution (25 wt%), containing 0.05 wt% Irgacure 2959. The dispenser at room temperature extruded the hydrogel on a stationary platform preheated at 40°C according to a CAD/CAM aided pattern in a layer-by-layer deposition mode. Rectangular 3D scaffolds of 37 (0.6 cm) and 12 layers (0.19 cm), for DMA and degradation studies, respectively, were printed with 0/90° configuration, strand spacing of 1.5 mm and 25 µm of fiber thickness. A Nikon D40 camera equipped with AF-S NIKKOR 18-55mm 1:3.5-5.6 GII ED objective was used to take pictures of the scaffolds. After deposition, the scaffolds were photopolymerized using a Superlite S-UV 2001AV lamp (Lumatec, Munchen, Germany), which emits UVA and blue light (320–500 nm, intensity of 6 mW cm^{-2} at 365 nm).

In a separate experiment, two polymer solutions were loaded with two different Dye-Trak "F" fluorescent microspheres (fluorescent lemon and fluorescent orange) of 15 µm diameter at a concentration of $1*10^6$ spheres per ml. The two microsphere containing polymer/Irgacure 2959 solutions were loaded into two separate extruding syringes and 2 or 3 layer scaffolds were printed using the settings described above resulting in alternating layers of different hydrogels and several patterns and strand spacing. Subsequently, the scaffolds were photopolymerized for 10 minutes using a Superlite S-UV 2001AV lamp (Lumatec, Munchen, Germany, blue light 320–500 nm, intensity of 6 mW cm^{-2} at 365 nm) and imaged using an

Olympus BX51 microscope (Olympus DP70 camera (Hamburg, Germany) equipped with an epifluorescence set-up.

6.2.8. Conversion of methacrylate groups after photopolymerization

To evaluate the conversion of methacrylate groups after photopolymerization, the resulting porous scaffolds were incubated in 5 ml of 0.2 M NaOH for 3 hours at 37 ºC. The gels completely degraded during this incubation. Next, the solution was neutralized by addition of 2 ml of 2M acetic acid, prior to analysis of methacrylic acid. The methacrylate conversion was calculated by comparing the unreacted methacrylic acid of the degraded gels to the initial amount of methacrylic acid prior to photo-cross-linking. Methacrylic acid was detected by Acquity UPLC^{TM}, equipped with a BEH C18 1.7   m, 2.1 x 50 mm column. The eluent used was 95/5/0.1% H_2O/acetonitrile/trifluoroacetic acid. A calibration curve was obtained by injecting different volumes (from 0.1 to 7.5 µl) of a 0.1 mM methacrylic acid solution.(34-35)

6.2.9. DMA Measurements

The elastic moduli (E) of the 3D printed and solid cylindrical scaffolds (both composed of 25 wt% polymer) were determined by dynamic mechanical analysis (DMA), performed with a DMA 2980 Dynamic Mechanical Analyzer (TA Instruments, New Castle, England) in the controlled force mode. Photopolymerized 3D printed constructs were cut in cylinders of approximately 5 × 6 mm (diameter × height) while the solid scaffolds were molded and photo-cross-linked in cylinders of 4.5 × 4 mm (diameter × height). These constructs were placed between the parallel plates (upper plate 6 mm, lower plate 45 mm) and a force ramp from 0.001 to 1.0 N at a rate of 0.1 N min^{-1} was applied at 25 ºC. The elastic modulus (E) was the slope of the linear range of the curve stress vs α, where α was calculated as follows:

$$α = (h / Δh) + 1 \qquad\qquad\qquad (3)$$

h represents the initial height and Δh is the dimensional change of the measured scaffold during compression.

6.2.10. Swelling and Degradation Studies

The degradation behavior of 3D scaffolds was studied in PBS pH 7.4, supplemented with 0.2 wt% NaN_3, at 37°C. Scaffolds consisting of 12 layers were prepared according to the above described procedure and placed in a 15 ml glass vial with screw cap. The initial weight of the scaffolds was measured (W_0) and upon addition of 5 ml PBS the vials were incubated at 37°C.

At regular intervals, the incubation buffer was removed and the weight of the scaffolds was measured (W_t) to calculate the swelling ratio:

$$SR = W_t/W_0 \tag{4}$$

Next, 5 ml PBS was added and the samples were further incubated at 37 °C.(35)

6.2.11. Cell Encapsulation and Viability analysis

Full-thickness healthy articular cartilage was obtained from the femoral condyles and femoropatellar groove of fresh equine cadavers (n = 2; age, 2-10 years) under aseptic conditions. After overnight digestion using 0.15% type II collagenase at 37°C, the cell suspension was filtered (100-μm cell strainer) and washed 3 times with phosphate-buffered saline. Cells were then resuspended in expansion medium (DMEM supplemented with 10% fetal bovine serum, 100 units ml^{-1} penicillin and 100 μg ml^{-1} streptomycin and 10 ng ml^{-1} FGF-2) and counted using a hemacytometer. Chondrocytes were expanded in monolayer cultures (5000 cells cm^{-2}) in expansion medium until 90% confluency. After expansion, cells were mixed in 25 wt% pHPMAm-lac-PEG triblock copolymer solution at 4°C containing 0.05 wt% Irgacure 2959. Cells were encapsulated at a density of $5.0*10^6$ cells ml^{-1} for LIVE/DEAD assays. Constructs of 100 μl were fabricated using two sterilized glass slides and two PVC spacers of 2 mm height. The hydrogel-cell solution at room temperature was put on a glass, the spacers were placed, and the second glass was put on top of the gel, yielding a cylindrical shaped construct. The previously mentioned Superlite S-UV 2001AV lamp (Lumatec, Munchen, Germany) was used to cross-link the cell-laden hydrogel constructs.

Constructs were cultured in differentiation medium (DMEM supplemented with 0.2 mM ascorbic acid 2-phosphate, 0.5% human serum albumin, 1x ITS-X, 100 units/mL penicillin and 100 unit/mL streptomycin, and 5 ng/mL TGF-b2). Samples for LIVE/DEAD assays were taken after 1 and 3 days.

To visualize cell viability, LIVE/DEAD Viability Assay (Molecular Probes MP03224, Eugene, USA) was performed according to the manufacturer's recommendations. The samples were examined using a light microscope (Olympus, BX51, United States) and photomicrographs taken with an Olympus DP70 camera (United States). The excitation/emission filters were set at 488/530 nm to observe living (green) cells and at 530/580 nm to detect dead (red) cells. Live and dead cells were counted for 4 samples per time point, at four locations within each construct.

6.3.   Results and Discussion

6.3.1. *Polymer Synthesis and Characterization*

(PEG-ABCPA)$_n$ macroinitiator was synthesized by DCC coupling reaction of PEG (molecular weight (M_W) of 10 kDa) and ABCPA with a yield of 79% and characterized by GPC and ^{1}H-NMR. GPC analysis showed that ~6 molecules of PEG 10 kDa were coupled, (number average molecular weight was 58 kDa with a polydispersity index (PDI) of 2.3). A small peak of unreacted free PEG was visible in the GPC chromatogram (Appendix D, **Figure 1SI**), an observation also confirmed by ^{1}H-NMR (a ratio PEG/ABCPA of 1.2 was calculated by comparing PEG protons to those of ABCPA) (Apendix D, **Figure 2SI**).(46) Removal of unreacted ABCPA, achieved by the purification method used, prevented the formation of polymers of HPMAm-lactate without PEG chain during the subsequent radical copolymerization (Appendix D, **Figure 3SI**).

A thermosensitive A-B-A triblock copolymer consisting of pHPMAm-lac A-blocks of approximately 23.5 kDa, as determined by ^{1}H-NMR and PEG B-block of a M_W of 10 kDa was synthesized by free radical copolymerization using a (PEG-ABCPA)$_n$ macroinitiator and HPMAm mono and dilactate in a molar ratio of 1/1 with a yield of 73 %. The pendant OH groups on the lactate side chains of the polymer were then partly methacrylated in order to allow the formation of chemical cross-links by photopolymerization. The structure of the final polymer is depicted in **Scheme 1**.
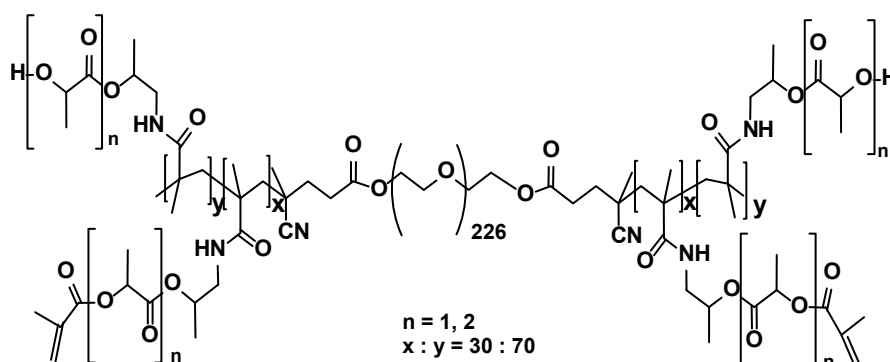
Scheme 1. Chemical structure of A-B-A triblock copolymer composed of methacrylated p(HPMAm-lac) A-blocks and PEG B-block.

The synthesized products are abbreviated as MI, M_0P_{10} and $M_{30}P_{10}$, for macro-initiator, non-methacrylated and methacrylated triblock copolymers, respectively, and their characteristics are listed in **Table 1**.

Table 1. Characteristics of PEG-ABCPA macroinitiator and A-B-A triblock copolymers composed of (methacrylated) p(HPMAm-lac) A-blocks and PEG B-block.

Name	M_W (kDa)	M_n (kDa)	PDI	DM (%)	CP (°C)
MI	136[b]	58[b]	2.3[b]	N.A.	N.A.
M_0P_{10}	48[b]	57[a] 32[b]	1.5[b]	N.A.	29[c]
$M_{30}P_{10}$	48[b]	57[a] 32[b]	1.5[b]	30[a]	11[c]

[a] Determined by ^{1}H-NMR [b] Determined by GPC [c] Determined by SLS

The triblock copolymer M_0P_{10} was obtained with a yield of approximately 74% and a HPMAm-monodilactate/HPMAm-dilactate ratio of 1, corresponding to the feed ratio and resulting in a CP of the polymer of 29 °C. Based on ^{1}H NMR, a M_n of 57 kDa was calculated. It appears that the M_n based on ^{1}H-NMR analysis exceeds that measured by GPC analysis (M_n 32 kDa). It was shown earlier that this discrepancy can be ascribed to the use of PEG homopolymers as GPC standards that display larger hydrodynamic volumes than the triblock copolymers in the used eluent.(33, 35)

As expected, upon methacrylation, the $M_{30}P_{10}$ polymer displayed the same molecular weight as the non-methacrylated M_0P_{10} polymer. The yield was 88% and the polymer had a methacrylation degree of 30%, (calculated based on ^{1}H-NMR). Similarly to previously reported data, the introduction of methacrylate groups on the lactate side chains of the polymer led to an increase of hydrophobicity and consequently to a decrease in CP to 11 °C.(34-35)

6.3.2. *Hydrogel Mechanical Properties*

In order to be used in organ printing, the hydrogels must possess adequate mechanical properties, allow easy extrusion through the pneumatic dispensing system described earlier and maintain dimensional stability upon computer aided layer-by-layer fiber deposition. Besides processability requirements, the hydrogel must provide for encapsulated cells with long-term mechanical support and eventually degrade into biocompatible products when new tissue is formed.(20) All the abovementioned requirements for organ printing were addressed in this study, starting with the characterization of the gelation kinetics of $M_{30}P_{10}$ triblock copolymer hydrogel.

A hydrogel composed of 25 wt% $M_{30}P_{10}$ triblock copolymer was prepared and characterized by rheological analysis. **Figure 1** shows the effect of temperature on the visco-

elastic properties of the hydrogel and demonstrates that at low temperatures (5 °C), $M_{30}P_{10}$ has a liquid-like behavior in aqueous solution with a storage modulus (G') close to zero and dominated by the loss modulus (G").(33) This behavior is particularly beneficial for the encapsulation of cells that can be easily and homogeneously mixed at high concentration with the cold polymer solution. The temperature controlled dispensing system can be then loaded with the polymer solution, in which the cells are mixed, and the adequate viscosity can be tuned by adjusting the dispenser temperature. As can be seen in Figure 1, indeed, a range of G' between 0 and 350 Pa was obtained when increasing the temperature between 5 and 45 °C, with 21 °C often referred to as the gelation temperature (T_{gel}) where G' starts to dominate G".

Upon extrusion, the cell-laden hydrogel fibers are deposited layer-by-layer on a fixed collector, pre-heated at 40 °C, according to a computer-aided pattern. As a visco-elastic material, displaying a G' of 350 Pa and a tan (δ) of 0.3, is formed at 40 °C (Figure 1), it can be concluded that the thermosensitive character of the studied hydrogel is particularly beneficial for organ printing application as it ensures that the hydrogel keeps its dimensional stability upon extrusion.
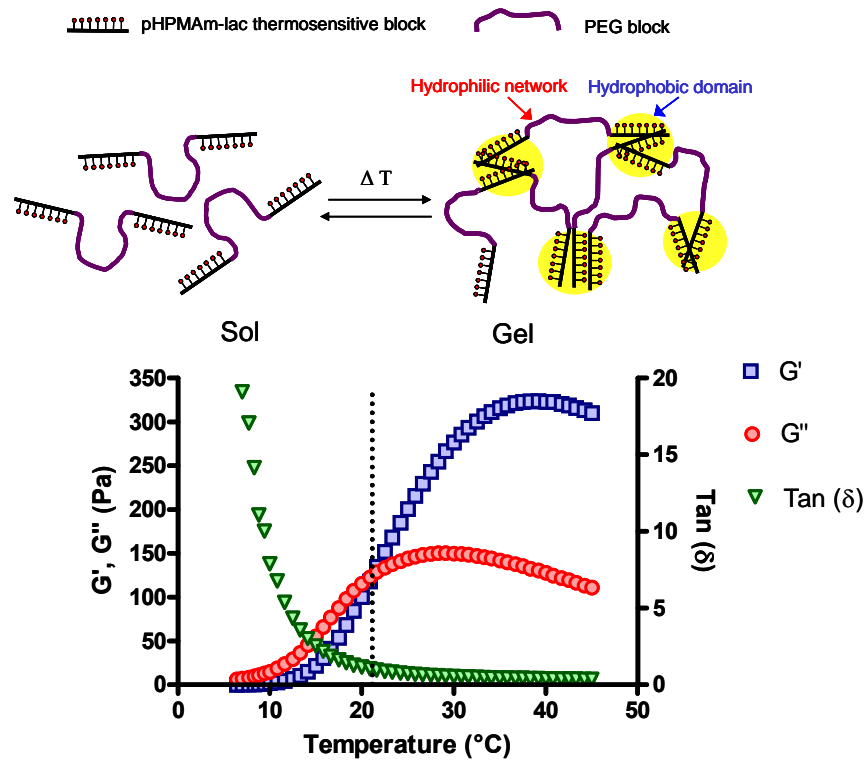

Figure 1. Effect of temperature on storage modulus (G'), loss modulus (G") and tan (δ) of a hydrogel of 25 wt% polymer concentration in PBS.

However, the mechanical properties of the physically cross-linked hydrogel does not provide long-term stability, as the thermo-gel undergoes relatively rapid dissolution in culture, releasing the cells prematurely.(34) Therefore, a chemical cross-linking strategy was employed to stabilize the hydrogel structure.(34) Upon printing, the 3D scaffold was exposed to UV light for 300 seconds and the formation of chemical cross-links within the hydrophobic domains is induced, when the biocompatible photoinitiator (Irgacure 2959, 0.05 wt%)(48) was dissolved in the polymer solution.

Figure 2 shows the effect of the photopolymerization on the rheological properties of the hydrogels. As can be seen in Figure 2 and as demonstrated earlier,(35) the storage modulus of the hydrogel remarkably increased upon UV exposure, due to the stabilization of the hydrophobic domains via chemical cross-links. For example, G' increased approximately by a factor 100 for the 25 wt% $M_{30}P_{10}$ hydrogel during photopolymerization (from 0.35 to 36 kPa).Figure 2 further shows that G' increased with increasing polymer concentration, demonstrating the possibility to tailor the stiffness of the hydrogel by changing the solid content. For all the tested polymer concentrations, the photopolymerized hydrogels exhibited tan (δ) values of 0.1, meaning that almost fully elastic matrices were formed.
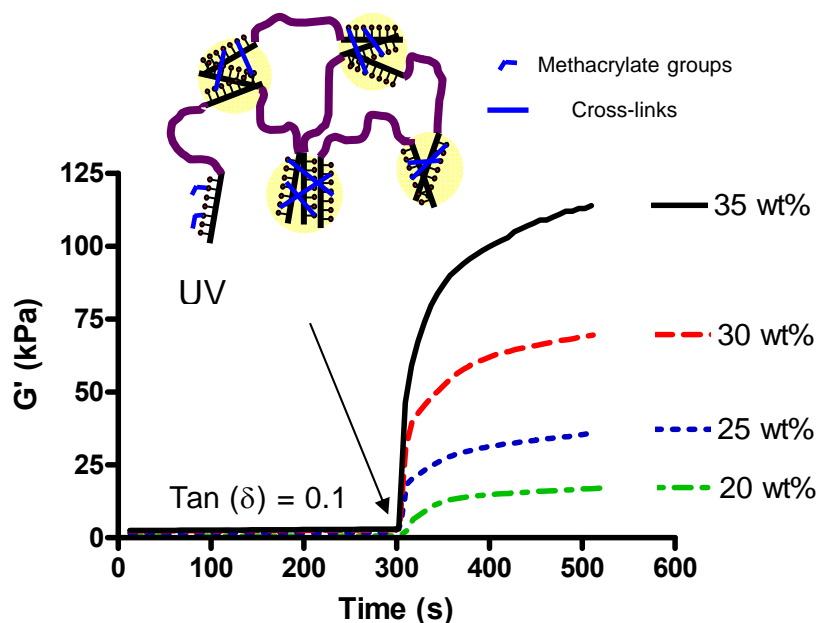

Figure 2. Effect of photopolymerization on mechanical properties of 20, 25, 30 and 35 wt% polymer hydrogels at 37°C. The storage modulus (G') is shown as a function of time. UV irradiation was applied after 300 sec.

In **Figure 3**, it can be observed that for physical hydrogels (triangles), the storage modulus (G') at 37 °C scaled with polymer concentration (C) according to a power law

equation (1). Similarly, chemically cross-linked hydrogels (squares in Figure 3), prepared by photopolymerization for 5 minutes at 37 °C, displayed the same power law scaling between storage modulus at plateau level (G'$_\infty$) and C:

$$G'_{(\infty)} \text{ (Pa)} = A * C \text{ (wt \%)}^K \tag{1}$$

where A is equal to 0.71 ± 0.19 and 5.3 ± 0.60 * 10^{-3} and very similar K values of 3.37 ± 0.08 and 3.40 ± 0.32 were found for photo-polymerized and physical hydrogels, respectively.

This non-linear rheological behavior is typically found for semi-flexible polymers and can be ascribed to differences in hydrogel inner structure, at increasing polymer concentration, due to different self-assembly of the thermosensitive chains. At temperatures higher than the polymer cloud point, the thermosensitive chains arrange into hydrophobic domains, that increase in size as well as density at increasing polymer concentration, resulting in power law dependence between G'$_\infty$ and C. The formation of larger polymer-rich clusters at increasing concentration, indeed, greatly contributes to the hydrogel strength even at low polymer volume increase. The non-linear mechanical properties in thermally assembled p(HPMAm-lac-PEG-p(HPMAm-lac) based hydrogels was also observed earlier by Vermonden *et al.*(33)
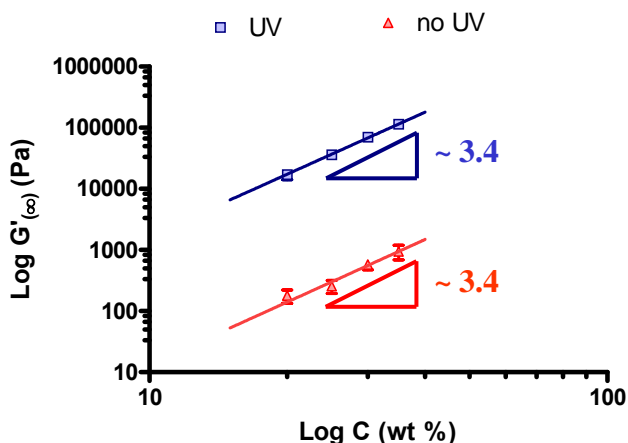

Figure 3. Power law dependence of the storage plateau modulus (G'$_\infty$) of photopolymerized (blue squares) and physical hydrogels (red triangles) at 37 °C on polymer concentration (C). The solid lines represent the fit, calculated by power law. Data are shown as mean ± standard deviation, n = 3.

Many biopolymers, such as DNA, collagen, actin dislay semi-flexible behavior,(49-52) unlike ordinary flexible polymers, such as polystyrene, poly(methyl methacrylate) or polylactide-PEG-polylactide block copolymers, that show a linear dependence of G'$_\infty$ on

concentration.(53) Semi-flexible polymers based networks are of great technological interest because they exhibit a high modulus at relatively low polymer volume fraction(52) and, despite their abundance among natural biomaterials, only a few semi-flexible synthetic polymers are described in literature.(54-55)
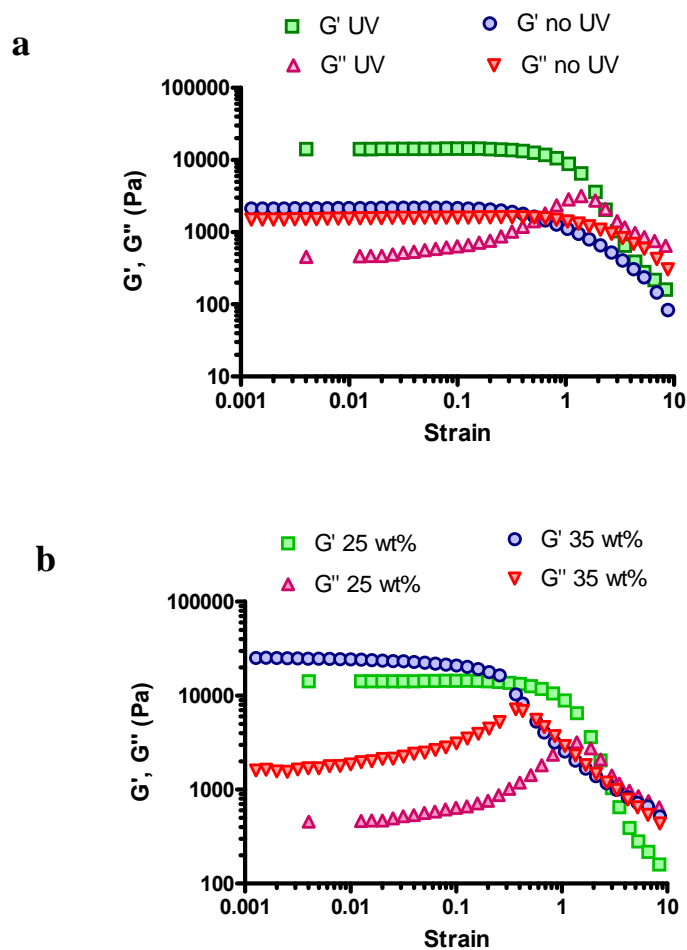

Figure 4. Strain-softening behavior of thermally and chemically assembled 25 wt% polymer hydrogels (A) and of UV polymerized hydrogels of 25 and 35 wt% (B). Hydrogels were measured at 37 °C and at a frequency of 0.2 Hz.

As compared to networks of natural biopolymers described in literature, a higher value of K was found for photopolymerized and physical hydrogels. Rammensee *et al* reported a $G'_\infty \sim C^2$ dependence of both cross-linked and non-cross-linked spider silk hydrogels. Similarly, MacKintosh *et al* showed that for entangled solutions of actin, the plateau modulus scaled

with concentration as $G'_\infty \sim C^{11/5}$ and predicted a stronger ($G'_\infty \sim C^{5/2}$) dependence for densely cross-linked hydrogels.(52) In $M_{10}P_{30}$ based hydrogel, a higher value of K (3.4) was found, demonstrating the possibility to increase the elastic modulus of the photo-crosslinked hydrogel to an even higher extent at low polymer volume fractions. The value of 3.4 is similar to the one reported by Vader *et al.* for collagen type I networks, showing $G'_\infty \sim C^3$ dependence.(56) As collagen is one of the most abundant components of natural tissues, the described hydrogels appear to be a promising candidate for tissue regeneration purposes.

It is believed that the rheological behavior and the dependence of storage modulus on polymer concentration can be tuned by the preparation procedure of the hydrogel. As we demonstrated previously, the heating rate remarkably affects the hydrogel self-assembly.(57) When the hydrogel self-assembles by heat shock (immediate temperature change from 4 to 37 °C), its inner structure shows a homogeneous distribution of nano/micro phase separated polymer assemblies. In contrast, at slower heating rate, a larger extent of phase-separation and the formation of larger polymer-rich domains were demonstrated. Initial investigations showed indeed that the concentration dependent mechanical properties can be fine-tuned by changes in the heating rate.

Non-linear mechanical behavior was also observed in (non)photo-polymerized hydrogels at 37 °C with increasing shear strain from 0.001 to 10 (**Figure 4**). In contrast to many biopolymers, exhibiting strain-stiffening, $M_{10}P_{30}$ hydrogels, both when thermally and chemically cross-linked (Figure 4A) and for different polymer concentrations (Figure 4B), showed strain-softening behavior, with substantial decrease of G' and predominance of loss modulus for strain values higher than 0.1. This behavior is often found in (permanently) cross-linked elastic networks and is attributed to the redistribution of internal stresses upon progressive slip of the cross-links with increasing shear strain and to the eventual breakage of the reversible cross-links or of the photopolymerized network at high strains.(54, 58) As expected, the physical hydrogels are disrupted at lower strain values as compared to chemical networks (Figure 4A), as their cross-links can be more easily destabilized by internal stresses. Interestingly, comparing photopolymerized hydrogels of different polymer concentration (Figure 4B), it can be noted that the networks of higher polymer concentration start to soften and break at lower strain as compared to their analogues of lower solid content. Matrices of higher polymer concentration, indeed, have a higher cross-link density that make then more rigid and brittle, therefore they tend to break at lower shear strains as compared to more flexible networks of lower polymer content.

6.3.3. 3D Printed Scaffolds

Figure 5 shows that computer controlled deposition of 25 wt% $M_{30}P_{10}$ hydrogels resulted in the formation of 3D porous hydrogels with a thickness up to a total height of approximately 0.6 cm (37 layers) and regular squared vertical pores of 1.2 × 1.2 × 6 mm (length × width ×

height) throughout the printed matrix. Clearly, that the combination of thermosensitivity and photopolymerization has beneficial effects on 3D printing, as it allows the preparation of matrices with remarkable thickness, precise and reproducible internal design and porosity and good dimensional stability. The weight of subsequent hydrogel layers caused the fusion of transversal pores during stacking of layers, as pointed by the white arrow in Figure 5c. The fusion of transversal pores, commonly found in 3DF of soft materials like hydrogels,(3) could represent a potential limitation of the current printing technology, however, despite the presence of pores only vertically, the high diffusivity of the studied hydrogel matrix,(57, 59) can be sufficient to provide rapid diffusion of hydrophilic nutrients and metabolites of incorporated cells.(3) Furthermore, the possibility to overcome this limitation is envisioned by photo-polymerizing the extruded hydrogel fibers during deposition, in order to increase the gel structural stability and prevent its fusion with the underlying fiber.
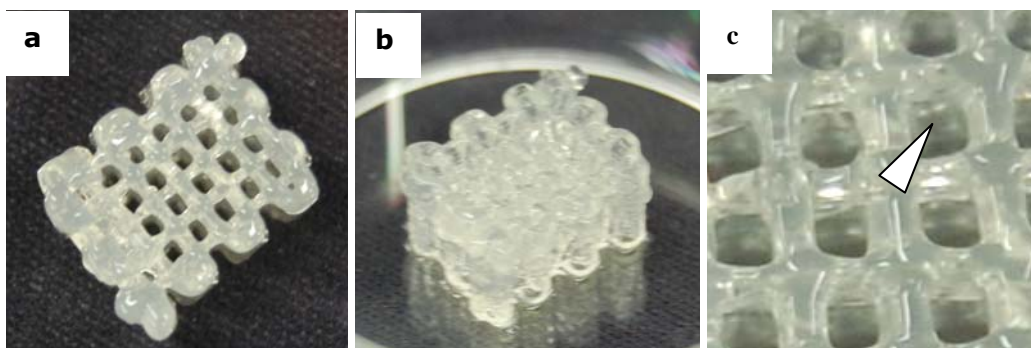

Figure 5. Photographs of 3D printed 25 wt% $M_{30}P_{10}$ hydrogels (dimensions: 1 × 1.5 × 0.59 cm, strand spacing: 1.5 mm, 37 layers). a) Top vision, b) Lateral vision, c) Detail of vertical pores with fused transversal pores (white arrow).

Figure 6 shows microscopy pictures of layered and adjacent 25 wt% $M_{30}P_{10}$ hydrogel fibers loaded with Dye-Trak "F" fluorescent microspheres (fluorescent lemon and fluorescent orange). The microspheres are easy to handle and to detect by microscopy, they are of similar size as cells and are used here as a model for different cells types. Several patterns were generated (straight layered fibers in Figure 6a, 6b and 6e and adjacent circular/squared fibers in Figure 6c and 6d).

These pictures illustrate the printability of the studied hydrogel with highly defined patterning and limited flattening or fiber fusion was observed. By comparing Figures 6a and 6e, it can be observed that the same layered design can be realized at different strand spacing (1.5 mm and 0.8 mm, for Figure 6a and 6e, respectively) and pore shape is maintained, demonstrating that a good resolution can be achieved during 3D printing of the studied thermosensitive material.

Both the layered and the adjacent fluorescent microsphere loaded hydrogels (Figure 6) displayed excellent maintenance of distinct localization of the cell mimicking microspheres, leading to the conclusion that the hydrogel can potentially be used for the engineering organized tissue structures, such as cartilage constructs with biomimetic zones, as long as the hydrogel maintains integrity, supports survival of cells during the printing process and allows subsequent cell differentiation and tissue formation.
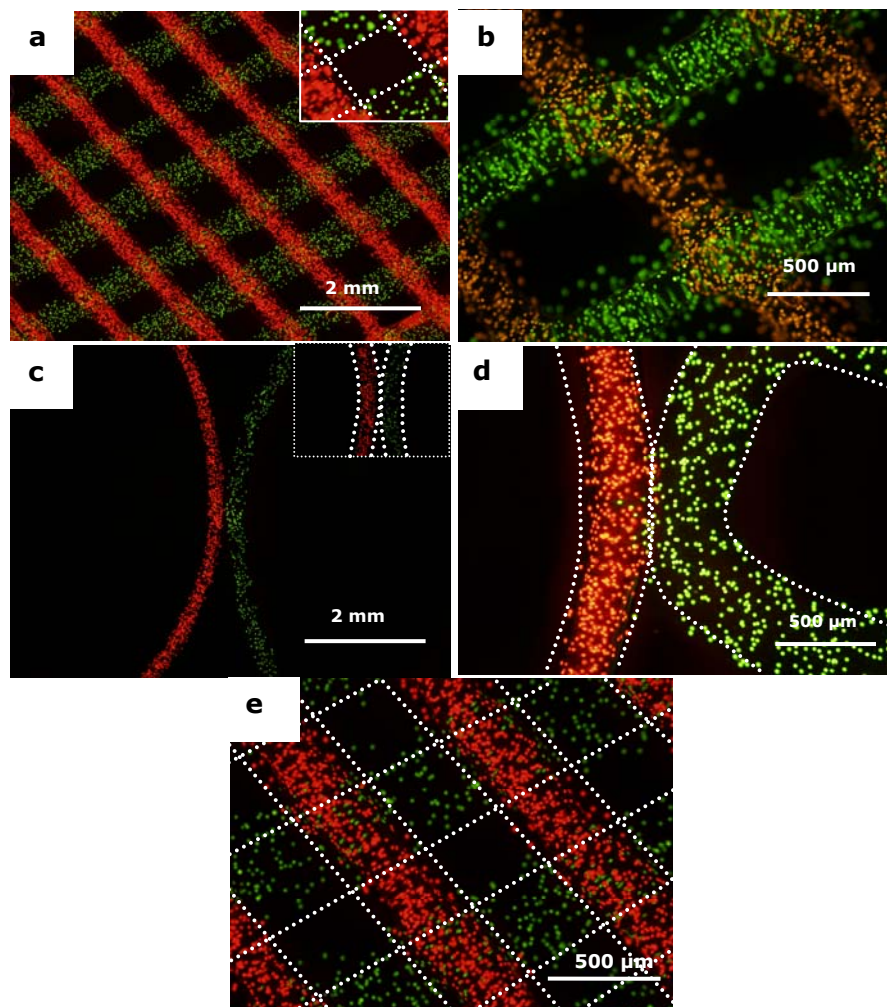
Figure 6. Microscopy pictures of subsequently printed layers of 25 wt% $M_{30}P_{10}$ hydrogels loaded with Dye-Trak "F" fluorescent microspheres, fluorescent lemon and fluorescent orange at the concentration of $1*10^6$ spheres per ml. a) 2 and b) 3 layers angled scaffold (1.5 mm strand spacing) with distinct localization of fluorescent microspheres. c) and d) printing of adjacent fibers with circular patterns with maintenance of distinct dye localization. e) 2 layers scaffold with 0.8 mm strand spacing.

6.3.4. Mechanical characterization and degradation behavior of 3D scaffolds

Porous scaffolds consisting of 37 layers (0.25 μm thickness each layer) of 25 wt% $M_{30}P_{10}$ hydrogel and having dimensions of $1 \times 1.5 \times 0.6$ cm and strands spacing of 1.5 mm were printed and subsequently photopolymerized during 10 minutes in the presence of Irgacure 2959 as photoinitiator. The efficiency of the photopolymerization was assessed and 88 ± 7 of the available methacrylate groups had reacted (UPLC analysis), which is in line with previous data on the photopolymerization of solid scaffolds, where a methacrylate conversion of 90 ± 2 was found.(34-35) It is clear that regardless of the shape, porosity and hydrogel volume, the photopolymerization process is very efficient for hydrogels of 25 wt% $M_{30}P_{10}$ polymer concentration.The stabilization of the hydrophobic domains by chemical cross-links influenced the mechanical and degradation behavior of the (porous 3D printed) hydrogels. An elastic modulus (E) of 119 ± 4 kPa was obtained for 3D printed scaffolds of 37 layers. This value is comparable with that of a solid scaffold of equal polymer composition, which had elastic modulus of 108 ± 7 kPa. This observation can be explained by the lack of transversal pores in the 3D constructs that made the compression resistance of the printed scaffolds similar to that of solid cylinders. Also, the scaffolds might suffer from a larger extent of water evaporation during the printing process, resulting in slightly higher polymer concentrations and stronger gels as compared to the solid scaffolds. We reported earlier E values of 40 to 70 kPa for solid scaffolds of 25 wt % p(HPMAm-lac)-PEG triblock copolymer with methacrylation degrees ranging from 4 to 9%,(34) demonstrating the possibility to tailor the elastic modulus of the matrices by the methacrylation extent.
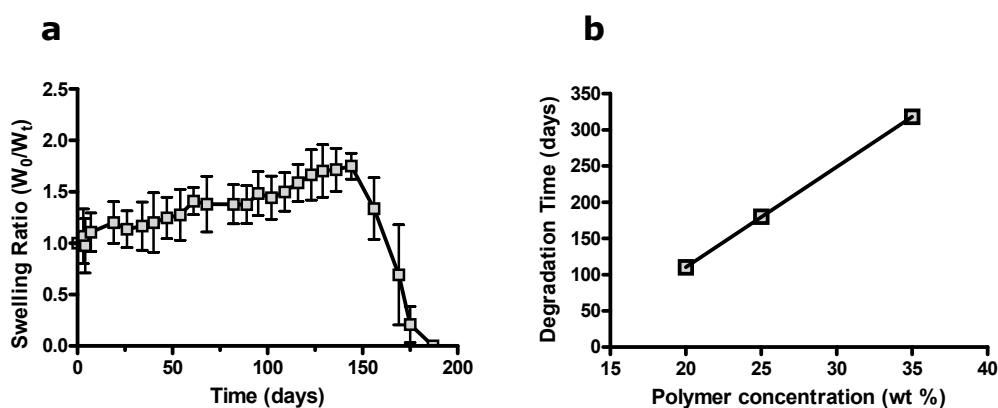
Figure 7. a) Degradation profile of 12 layered 3D scaffolds of 25 wt% $M_{30}P_{10}$ hydrogel (dimensions: $1 \times 1.5 \times 0.6$ cm, strand spacing: 1.5 mm) at 37 °C and pH 7.4. Data are shown as mean $\pm$ SD, n = 3. b) Degradation times of 20 and 35 wt% $M_{30}P_{10}$ solid cylindrically shaped photopolymerized hydrogels (100 mg) and 12 layered 3D scaffolds of 25 wt% $M_{30}P_{10}$ hydrogel (dimensions: $1 \times 1.5 \times 0.6$ cm; strand spacing: 1.5 mm; 250 mg) at 37 °C and pH 7.4.

Other photopolymerized PEG based solid hydrogels studied for cartilage engineering showed values of E from 60 to 500 kPa, a range that includes the elastic modulus found in the present study for 3D printed scaffolds.(60) The degradation rate of porous scaffolds composed of 12 layers of 25 wt% $M_{30}P_{10}$ hydrogels was studied by incubating them at pH 7.4 and 37 °C. **Figure 7a** shows that the scaffolds degraded completely in approximately 190 days upon a swelling phase of about 130 days, where the scaffolds doubled their weight (swelling ratio of 2), due to uptake of water. The degradation time of the scaffolds relates very well to the degradation time of cylindrical gels of 100 mg weight based on 20 and 35 wt % $M_{30}P_{10}$ (Figure 7a).(59) Regardless of the weight of the (porous) matrix (100 and 750 mg for cylindrical gels and porous scaffolds, respectively), indeed, the degradation time scales linearly with polymer concentration (Figure 7b). With increasing polymer concentration the concentration of hydrolytically sensitive ester bonds increases. The gels dissolve when most of the ester bonds are hydrolyzed and consequently the degradation time increases with polymer concentration in the gel, in line with previous studies.(47, 61)

The observed degradation time-scale of the scaffolds is suitable for cartilage regeneration purposes, as long-term mechanical support is provided and complete degradation of the material is ensured when the extracellular matrix of the chondrocytes is expected to be formed.

6.3.5. *Viability of Equine Articular Chondrocytes in Photopolymerized Hydrogels*

To assess to which extent photopolymerized hydrogels affect the viability of encapsulated chondrocytes, their survival was studied in cylindrical solid scaffolds of 100 µl volume after 1 and 3 days culture. Upon encapsulation of the chondrocytes in the 25 wt% hydrogel and subsequent photo-polymerization, a homogeneous distribution of cells throughout the hydrogel was observed (data not shown). Excellent viability (94 ± 3 %) was observed after 1 day of culture and no significant decrease in cell survival was found after 3 days (viability of 85 ± 7 %). As shown earlier for human Mesenchymal Stromal Cells (hMSCs),(34) the investigated material also supports viability of chondrocytes, which establishes the basis for further implementation of these materials in the field of cartilage engineering.

6.4. Conclusions

In this paper, we reported on the use of a photopolymerizable thermosensitive and biodegradable hydrogel based on PEG and HPMA-lactate for 3D printing aimed at application for cartilage engineering. We demonstrated that the hydrogel mechanical properties well adapt to the process of 3D printing, as structurally stable 3D scaffolds with well defined vertical porosity and enhanced stability by photopolymerization were successfully printed by subsequent deposition of gel fibers up to at least 37 layers. Scaffold pattern and strand

spacing could easily be tuned and the potential ability of the constructs to provide precise tissue mimicking cell organization was shown. The semi-flexible character of the studied polymer, demonstrated by the power law scaling of the hydrogel storage moduli with the polymer concentration, establishes similarities with many natural polymers, including collagen. This analogy is promising for biomedical applications, in particular, the correlation with collagen makes this biomaterial potentially suitable as synthetic extra-cellular matrix for engineering cartilage. The good mechanical resistance and tunable degradation rate of the hydrogels offer potential long-term support to the encapsulated cells until the new tissue is formed. Importantly, the high chondrocyte viability was observed after 1 and 3 days, further emphasized the suitability of the studied hydrogel as a promising candidate for bioprinting applications.

Future studies will be addressed towards the design of complex 3D constructs with appropriate properties for engineering articular cartilage with biomimetic zones and long-term tissue formation both *in vitro* and *in vivo* will be investigated. The high tailorability of the hydrogels, in terms of mechanical properties, degradation behavior and diffusivity(35, 59, 62-63), as well as the possibility to regulate cell behavior by incorporating and releasing growth factors in a diffusion controlled and tailorable fashion(35, 62) and the functionalization of polymer hydroxyl groups with adhesive peptides(64) hold great potential for a successful further development.

Acknowledgements

References

1. Klein TJ, Rizzi SC, Reichert JC, Georgi N, Malda J, Schuurman W, Crawford RW, & Hutmacher DW (2009) Strategies for Zonal Cartilage Repair using Hydrogels. *Macromolecular Bioscience* 9(11):1049-1058.

2. Fedorovich NE, De Wijn JR, Verbout AJ, Alblas J, & Dhert WJA (2008) Three-Dimensional Fiber Deposition of Cell-Laden, Viable, Patterned Constructs for Bone Tissue Printing. *Tissue Engineering - Part A* 14(1):127-133.

3. Fedorovich NE, Swennen I, Girones J, Moroni L, van Blitterswijk CA, Schacht E, Alblas J, & Dhert WJA (2009) Evaluation of Photocrosslinked Lutrol Hydrogel for Tissue Printing Applications. *Biomacromolecules* 10(7):1689-1696.

4. Mironov V, Visconti RP, Kasyanov V, Forgacs G, Drake CJ, & Markwald RR (2009) Organ printing: Tissue spheroids as building blocks. *Biomaterials* 30(12):2164-2174.

5. El-Ayoubi R, DeGrandpre C, DiRaddo R, Yousefi A-M, & Lavigne P (2009) Design and Dynamic Culture of 3D-Scaffolds for Cartilage Tissue Engineering. *Journal of Biomaterials Applications* doi: 10.1177/0885328209355332.

6. Hollister SJ (2005) Porous scaffold design for tissue engineering. *Nature Materials* 4(7):518-524.

7. Masood SH, Singh JP, & Morsi Y (2005) The design and manufacturing of porous scaffolds for tissue engineering using rapid prototyping. *The International Journal of Advanced Manufacturing Technology* 27(3):415-420.

8. Moutos FT, Freed LE, & Guilak F (2007) A biomimetic three-dimensional woven composite scaffold for functional tissue engineering of cartilage. *Naure. Materials* 6(2):162-167.

9. Woodfield TBF, Malda J, de Wijn J, Péters F, Riesle J, & van Blitterswijk CA (2004) Design of porous scaffolds for cartilage tissue engineering using a three-dimensional fiber-deposition technique. *Biomaterials* 25(18):4149-4161.

10. Yoshida H, Matsusaki M, & Akashi M (2009) Scaffold-Mediated 2D Cellular Orientations for Construction of Three Dimensionally Engineered Tissues Composed of Oriented Cells and Extracellular Matrices. *Advanced Functional Materials* 19(7):1001-1007.

11. Suh KY & Lee HH (2002) Capillary Force Lithography: Large-Area Patterning, Self-Organization, and Anisotropic Dewetting. *Advvanced Functional Materials* 12(6-7):405-413.

12. Hutmacher DW, Sittinger M, & Risbud MV (2004) Scaffold-based tissue engineering: rationale for computer-aided design and solid free-form fabrication systems. *Trendsin Biotechnology* 22(7):354-362.

13. Fedorovich NE, Alblas J, de Wijn JR, Hennink WE, Verbout AJ, & Dhert WJA (2007) Hydrogels as Extracellular Matrices for Skeletal Tissue Engineering: State-of-the-Art and Novel Application in Organ Printing. *Tissue Engineering - Part A* 13(8):1905-1925.

14. Klein TJ, Malda J, Sah RL, & Hutmacher DW (2009) Tissue Engineering of Articular Cartilage with Biomimetic Zones. *Tissue Engineering - Part B Reviews* 15(2):143-157.

15. Klein TJ, Schumacher BL, Schmidt TA, Li KW, Voegtline MS, Masuda K, Thonar EJMA, & Sah RL (2003) Tissue engineering of stratified articular cartilage from chondrocyte subpopulations. *Osteoarthritis Cartilage* 11(8):595-602.

16. Waldman SD, Grynpas MD, Pilliar RM, & Kandel RA (2003) The use of specific chondrocyte populations to modulate the properties of tissue-engineered cartilage. *Journal of Orthopaedic Research* 21(1):132-138.

17. Fedorovich NE, De Wijn JR, Verbout AJ, Alblas J, & Dhert WJ (2008) Three-dimensional fiber deposition of cell-laden, viable, patterned constructs for bone tissue printing. (Translated from eng) *Tissue Engineering - Part A* 14(1):127-133

18. Reinout S (2008) Smart biomaterials for tissue engineering of cartilage. *Injury* 39(1):77-87.

19. Vinatier C, Guicheux J, Daculsi G, Layrolle P, & Weiss P (2006) Cartilage and bone tissue engineering using hydrogels. *Bio-Medical Material Engineering* 16(0):S107-S113.

20. Vinatier C, Mrugala D, Jorgensen C, Guicheux J, & Noël D (2009) Cartilage engineering: a crucial combination of cells, biomaterials and biofactors. *Trends in Biotechnology* 27(5):307-314.

21. Van Tomme SR, Storm G, & Hennink WE (2008) In situ gelling hydrogels for pharmaceutical and biomedical applications. *International Journal of Pharmaceutics* 355(1-2):1-18.

22. Jeong B & Gutowska A (2002) Lessons from nature: stimuli-responsive polymers and their biomedical applications. *Trends in Biotechnology* 20(7):305-311.

23. Grandolfo M, D'Andrea P, Paoletti S, Martina M, Silvestrini G, Bonucci E, & Vittur F (1993) Culture and differentiation of chondrocytes entrapped in alginate gels. *Calcified Tissue International* 52(1):42-48.

24. Hauselmann H, Fernandes R, Mok S, Schmid T, Block J, Aydelotte M, Kuettner K, & Thonar E (1994) Phenotypic stability of bovine articular chondrocytes after long-term culture in alginate beads. *Journal of Cell Science* 107(1):17-27.

25. Francis Suh JK & Matthew HWT (2000) Application of chitosan-based polysaccharide biomaterials in cartilage tissue engineering: a review. *Biomaterials* 21(24):2589-2598.

26. Tomoats U, Natsu O, Sugur U, & Kier O (1984) Chondrocytes Embedded in Collagen Gels Maintain Cartilage Phenotype During Long-term Cultures. *Clinical Orthopaedics and Related Research* 186:231-239.

27. Sims CD, Butler PEM, Casanova R, Lee BT, Randolph MA, Lee WPA, Vacanti CA, & Yaremchuk MJ (1996) Injectable Cartilage Using Polyethylene Oxide Polymer Substrates. *Plastic and Reconstructive Surgery* 98(5):843-850.

28. Ibusuki S, Iwamoto Y, & Matsuda T (2003) System-Engineered Cartilage Using Poly(N-isopropylacrylamide)-Grafted Gelatin as in Situ-Formable Scaffold: In Vivo Performance. *Tissue Engineering* 9(6):1133-1142.

29. Nagahama K, Ouchi T, & Ohya Y (2008) Temperature-Induced Hydrogels Through Self-Assembly of Cholesterol-Substituted Star PEG-<I>b</I>-PLLA Copolymers: An Injectable Scaffold for Tissue Engineering. *Advanced Functional Materials* 18(8):1220-1231.

30. Chaouat M, Visage CL, Baille WE, Escoubet B, Chaubet F, Mateescu MA, & Letourneur D (2008) A Novel Cross-linked Poly(vinyl alcohol) (PVA) for Vascular Grafts. *Advanced Functional Materials* 18(19):2855-2861.

31. Morra M, Cassinelli C, Cascardo G, Nagel M-D, Della Volpe C, Siboni S, Maniglio D, Brugnara M, Ceccone G, Schols HA, & Ulvskov P (2004) Effects on Interfacial Properties and Cell Adhesion of Surface Modification by Pectic Hairy Regions. *Biomacromolecules* 5(6):2094-2104.

32. Soga O, van Nostrum CF, & Hennink WE (2004) Poly(N-(2-hydroxypropyl) Methacrylamide Mono/Di Lactate):â€‰ A New Class of Biodegradable Polymers with Tuneable Thermosensitivity. *Biomacromolecules* 5(3):818-821.

33. Vermonden T, Besseling NAM, van Steenbergen MJ, & Hennink WE (2006) Rheological Studies of Thermosensitive Triblock Copolymer Hydrogels. *Langmuir* 22(24):10180-10184.

34. Vermonden T, Fedorovich NE, van Geemen D, Alblas J, van Nostrum CF, Dhert WJA, & Hennink WE (2008) Photopolymerized Thermosensitive Hydrogels: Synthesis, Degradation, and Cytocompatibility. *Biomacromolecules* 9(3):919-926.

35. Censi R, Vermonden T, van Steenbergen MJ, Deschout H, Braeckmans K, De Smedt SC, van Nostrum CF, di Martino P, & Hennink WE (2009) Photopolymerized thermosensitive hydrogels for tailorable diffusion-controlled protein delivery. *Journal of Controlled Release* 140(3):230-236.

36. Jeong B, Kim SW, & Bae YH (2002) Thermosensitive sol-gel reversible hydrogels. *Advanced Drug Delivery Reviews* 54(1):37-51.

37. Klouda L & Mikos AG (2008) Thermoresponsive hydrogels in biomedical applications. *European Journal of Pharmaceutics and Biopharmaceutics* 68(1):34-45.

38. Topp MDC, Leunen IH, Dijkstra PJ, Tauer K, Schellenberg C, & Feijen J (2000) Quasi-living polymerization of N-isopropylacrylamide onto poly(ethylene glycol). *Macromolecules* 33(14):4986-4988.

39. Marcelino J, Carpten JD, Suwairi WM, Gutierrez OM, Schwartz S, Robbins C, Sood R, Makalowska I, Baxevanis A, Johnstone B, Laxer RM, Zemel L, Kim CA, Herd JK, Ihle J, Williams C, Johnson M, Raman V, Alonso LG, Brunoni D, Gerstein A, Papadopoulos N, Bahabri SA, Trent JM, & Warman ML (1999) CACP, encoding a secreted proteoglycan, is mutated in camptodactyly-arthropathy-coxa vara-pericarditis syndrome. *Nature Genetics* 23(3):319-322.

40. Schumacher BL, Block JA, Schmid TM, Aydelotte MB, & Kuettner KE (1994) A Novel Proteoglycan Synthesized and Secreted by Chondrocytes of the Superficial Zone of Articular Cartilage. *Archives of Biochemistry and Biophysics* 311(1):144-152.

41.	Kim S (2008) Changes in surgical loads and economic burden of hip and knee replacements in the US: 1997-2004. *Arthritis Care Research* 59(4):481-488.

42.	Ochi M, Adachi N, Nobuto H, Yanada S, Ito Y, & Agung M (2004) Articular Cartilage Repair Using Tissue Engineering Technique;Novel Approach with Minimally Invasive Procedure. *Artificial Organs* 28(1):28-32.

43.	Saris DBF, Vanlauwe J, Victor J, Almqvist KF, Verdonk R, Bellemans J, & Luyten FP (2009) Treatment of Symptomatic Cartilage Defects of the Knee. *American Journal of Sports Medicine* 37(1 suppl):10S-19S.

44.	Boland T, Xu T, Damon B, & Cui X (2006) Application of inkjet printing to tissue engineering. *Biotechnology Journal* 1(9):910-917.

45.	David V, Malay D, Tao X, Priya K, Sunil O, & Thomas B (2005) Advances in tissue engineering: Cell printing. *Journal of Thoracic and Cardiovascular Surgery* 129(2):470-472.

46.	Neradovic D, van Nostrum CF, & Hennink WE (2001) Thermoresponsive Polymeric Micelles with Controlled Instability Based on Hydrolytically Sensitive N-Isopropylacrylamide Copolymers. *Macromolecules* 34(22):7589-7591.

47.	Neradovic D, van Steenbergen MJ, Vansteelant L, Meijer YJ, van Nostrum CF, & Hennink WE (2003) Degradation Mechanism and Kinetics of Thermosensitive Polyacrylamides Containing Lactic Acid Side Chains. *Macromolecules* 36(20):7491-7498.

48.	Bryant SJ, Nuttelman CR, & Anseth KS (2000) Cytocompatibility of UV and visible light photoinitiating systems on cultured NIH/3T3 fibroblasts in vitro. *Journal of Biomaterial Science. Polymer Edition* 11:439-457.

49.	Narine SS & Marangoni AG (1999) Fractal nature of fat crystal networks. *Physical Review E* 59(2):1908.

50.	Yan H, Nykanen A, Ruokolainen J, Farrar D, Gough JE, Saiani A, & Miller AF (2008) Thermo-reversible protein fibrillar hydrogels as cell scaffolds. *Faraday Discussions* 139:71-84.

51.	Rammensee S, Huemmerich D, Hermanson KD, Scheibel T, & Bausch AR (2006) Rheological characterization of hydrogels formed by recombinantly produced spider silk. *Applied Physics A: Material Scienceand Processing* 82(2):261-264.

52.	MacKintosh FC, Käs J, & Janmey PA (1995) Elasticity of Semiflexible Biopolymer Networks. *Physical Review Letters* 75(24):4425.

53.	Sanabria-DeLong N, Crosby AJ, & Tew GN (2008) Photo-Cross-Linked PLA-PEO-PLA Hydrogels from Self-Assembled Physical Networks: Mechanical Properties and Influence of Assumed Constitutive Relationships. *Biomacromolecules* 9(10):2784-2791.

54.	Erk KA, Henderson KJ, & Shull KR (2010) Strain Stiffening in Synthetic and Biopolymer Networks. *Biomacromolecules* 11(5):1358-1363.

55.	Pellens L, Corrales RG, & Mewis J (2004) General nonlinear rheological behavior of associative polymers. *Journal of Rheology* 48(2):379-393.

56.	Vader D, Kabla A, Weitz D, & Mahadevan L (2009) Strain-Induced Alignment in Collagen Gels. *PLoS ONE* 4(6):e5902.

57.	Vermonden T, Jena SS, Barriet D, Censi R, van der Gucht J, Hennink WE, & Siegel RA (2009) Macromolecular Diffusion in Self-Assembling Biodegradable Thermosensitive Hydrogels. *Macromolecules* 43(2):782-789.

58.	Rubinstein M & Panyukov S (2002) Elasticity of Polymer Networks. *Macromolecules* 35(17):6670-6686.

59.	Censi R, Vermonden T, Deschout H, Braeckmans K, Di Martino P, De Smedt S, Van Nostrum C, & Hennink WE (2010) Photopolymerized Thermosensitive Poly(HPMAlactate)-PEG Based Hydrogels: Effect of Network Design on Mechanical Properties, Degradation and Release Behavior. *Biomacromolecules* In Press.

60.	Bryant SJ, Bender RJ, Durand KL, & Anseth KS (2004) Encapsulating chondrocytes in degrading PEG hydrogels with high modulus: Engineering gel structural changes to facilitate cartilaginous tissue production. *Biotechnology and Bioengineering* 86(7):747-755.

61.	Rijcken CJ, Snel CJ, Schiffelers RM, van Nostrum CF, & Hennink WE (2007) Hydrolysable core-crosslinked thermosensitive polymeric micelles: Synthesis, characterisation and in vivo studies. *Biomaterials* 28(36):5581-5593.

62.   Censi R, Fieten PJ, di Martino P, Hennink WE, & Vermonden T (2010) In Situ Forming Hydrogels by Tandem Thermal Gelling and Michael Addition Reaction between Thermosensitive Triblock Copolymers and Thiolated Hyaluronan. *Macromoleculse* 43(13): 5771–5778.

63.   Tai H, Wang W, Vermonden T, Heath F, Hennink WE, Alexander C, Shakesheff KM, & Howdle SM (2009) Thermoresponsive and Photocrosslinkable PEGMEMA-PPGMA-EGDMA Copolymers from a One-Step ATRP Synthesis. *Biomacromolecules* 10(4):822-828.

64.   Salinas CN & Anseth KS (2009) Decorin moieties tethered into PEG networks induce chondrogenesis of human mesenchymal stem cells. *Journal of Biomedical Material Research, Part A* 90A(2):456-464.

Chapter 7

In Vivo Biocompatibility and Biodegradability of Photopolymerized PEG-p(HPMAm-lactate)-based Hydrogels

Roberta Censi,[a,b] Sander van Putten,[c] Tina Vermonden,[a] Piera di Martino,[b] Cornelus F. van Nostrum,[a] Marco C. Harmsen,[c] Ruud A. Bank[c] *and* Wim E. Hennink[a]

[c] Department of Pathology and Medical Biology, University Medical Centre Groningen, University of Groningen, Hanzeplein 1, 9713 GZ Groningen, The Netherlands

[a] Department of Pharmaceutics Utrecht Institute for Pharmaceutical Sciences (UIPS), Utrecht University, P.O. Box 80082, 3508 TB Utrecht, The Netherlands

[b] Department of Chemical Sciences, Camerino University, via S, Agostino 1, 62032, Camerino (MC), Italy

In preparation

Abstract

Hydrogels are three-dimensional networks of cross-linked hydrophilic polymers widely used for protein delivery and tissue engineering. In order to be eligible for *in vivo* applications, the hydrogels must be biocompatible. In this study the host angiogenic and inflammatory responses *in vivo* after implantation of photopolymerized thermosensitive poly(hydroxypropyl methacrylamide)-poly(ethylene glycol)-poly(hydroxypropyl methacrylamide) triblock copolymer hydrogels are investigated. Hydrogels consisting of polymers with different cross-link densities were subcutaneously implanted in Balb/c mice and the histological evaluation of the tissue response was performed. The different implants showed an acute and localized inflammatory reaction upon implantation mainly characterized by infiltration of neutrophils, whose levels remarkably decreased in time. The acute inflammatory reaction was followed by a milder chronic inflammation mediated by macrophages infiltration. The number of macrophages was associated with the biodegradation and resorption of the biomaterial and increased in time as their degradation progressed. This mild inflammatory reaction stimulated tissue ingrowth and angiogenesis, leading to good engraftment of the hydrogels to the host tissue, which was stronger for hydrogels of lower cross-link density. Apoptotic cells, muscle damage or adverse systemic response were not observed, confirming that the investigated hydrogels possess good biocompatibility. Finally, good agreements between in vitro and in vivo degradation was found, meaning that hydrolysis is the main mechanism governing the degradation.

7.1. Introduction

Hydrogels are cross-linked networks of hydrophilic polymers, capable to retain large amounts of water yet remaining insoluble and maintaining their three-dimensional structure. In order to be eligible for biomedical applications, hydrogels must fulfill requirements of biocompatibility and non-toxicity. Biocompatibility has been defined previously as "the ability of a material to perform, with an appropriate host response in a specific application".(1) Generally speaking, hydrogels have a good biocompatibilty,(2) therefore they are used and under investigation for a variety of biomedical and pharmaceutical applications, such as contact lenses,(3) drug delivery systems,(4-5) scaffolds for tissue engineering,(6) soft tissue replacement,(7) vascular prostheses,(8) and coatings for stents and catheters.(9) Their inherent biocompatibility originates from their soft and rubbery nature that minimizes irritation of surrounding tissues and their low free energy at the interface with body tissues, which results in low adherence of cells and proteins to gel surfaces.(2)

Among the developed hydrogel systems, *in situ* gel-forming thermosensitive polymers have emerged as promising candidates for biomedical applications, as they allow minimally invasive administration by simple injection.(10-11) In an effort to develop suitable materials for *in situ* gelling systems, a number of biodegradable synthetic polymers has been reported. A class of biomaterials of particular interest in the field of injectable hydrogels are thermosensitive poly(ethylenglycol) (PEG) based block copolymers. Examples of these compounds are copolymers of PEG with biodegradable aliphatic polyesters, such as polylactide (PLA),(12) poly(D,L-lactide-*co*-glycolide) (PLGA), poly(ε-caprolactone) (PCL)(13), and polyphosphazenes(14). PEG has been often used because it is a functional hydrophilic and non-toxic polymer that renders surfaces of materials protein-resistant.(15-18) This polymer was also used for conjugation to pharmaceutical proteins in order increase their circulation times.(19) Further, it has been shown that PEG promotes long-term stabilization and bioactivity of immobilized enzymes.(20) It is well known that polymers resistant to protein adsorption are attractive materials for *in vivo* application as they prevent tissue adherence and inflammation.(21-22) However, despite the attractive properties of PEG-based hydrogel and soft materials in general, implantation of hydrogels is often associated with transient inflammatory phenomena,(23-24) whose duration and intensity is dependent on the surface area/volume and type of biomaterial. It is has been shown in many studies that injected polymeric implants induce an acute inflammation response, mainly characterized by the presence of neutrophils, followed by a more chronic inflammation. This chronic inflammation is generally caused by infiltration of polymorphonuclear leucocytes (PMNs), macrophages, fibroblasts, and lymphocytes, and generally evolves in the so called foreign body reaction, where monocytes, macrophages, foreign body giant cells, neovascularization and the formation of a fibrous capsule are observed.(25)

To date, only a few of the aforementioned thermosensitive PEG-based polymers have been characterized for their in vivo biocompatibility. For example, PEG-PLGA-PEG has demonstrated hemocompatible by Duan *et al*,(26) while Kim *et al* showed biocompatibility of subcutaneously injected thermosensitive PEG-PCL diblock copolymer gels.(27) A pH- and thermo-sensitive block copolymer hydrogel, based on poly(ε-caprolactone-*co*-lactide)– poly(ethylene glycol)–poly(ε-caprolactone-*co*-lactide) (PCLA–PEG–PCLA) block copolymer end capped with sulfamethazine oligomers (SMOs) also demonstrated biocompatible after an initial acute inflammatory response during two weeks.(28) Further, polyethylene glycol (PEG)-based hydrogels were implanted by Mahoney *et al*. into the striatum and cerebral cortex of non-human primates and good biocompatibility was observed, demonstrating the potential of these gels for local drug delivery or neural tissue regeneration.(29)

The aim of this study was to evaluate the *in vivo* biocompatibility of photopolymerized thermosensitive PEG-p(HPMAm-lac) triblock copolymer hydrogels. The effect of the network characteristics, with respect to cross-link density, varied by extent of methacrylation, on tissue response was studied after subcutaneous (dorsolateral) implantation of the photopolymerized gels in Balb/c mice. Moreover, an evaluation of the degradation *in vivo* of the implanted hydrogels was provided and correlated to *in vitro* behavior.

7.2.   Materials and Methods

7.2.1.   Materials

All chemicals were obtained from Sigma-Aldrich and used as received, unless stated otherwise. All solvents were purchased from Biosolve. Tetrahydrofuran (THF) was distilled from sodium/benzophenone and stored over 3 Å molecular sieves. HPMAm (hydroxypropyl-methacrylamide) was obtained from Zentiva a.s. (Praha, Czech Republic), L-lactide from Purac Biochem BV (Gorinchem, The Netherlands), 2-hydroxy-1-[4-(2-hydroxyethoxy)phenyl]-2-methyl-1-propanone (Irgacure 2959) from Ciba Specialty Chemicals Inc (Basel, Switzerland). DMAP (dimethylaminopyridine) and 4,4′-Azobis(4-cyanopentanoic acid) (ABCPA) were purchased from Fluka Chemie AG (Buchs, Switzerland). Methacrylated rhodamine (RhodMA) was obtained from PolySciences Europe (Eppelheim, Germany). HPMAm-monolactate and HPMAm-dilactate were synthesized according to a previously reported method.(30)

7.2.2   Synthesis of Methacrylated Triblock Copolymers

Thermosensitive triblock copolymers consisting of PEG 10 kDa as hydrophilic block and pHPMAm$_{lac}$ as thermosensitive outer blocks with a HPMAm-monolactate/HPMAm-dilactate ratio of 50/50 were synthesized by free radical polymerization using (PEG-

ABCPA)$_n$ macroinitiator according to a method described earlier.(31) Derivatization with methacrylate groups of 8, 20 and 25% of the OH side groups of p(HPMAm-lac) was carried out using the following procedure. The triblock copolymer (1.7 g (5.5 mmol)) was dissolved in dry THF under a N$_2$ atmosphere, DMAP (3.3 mg (27.2 μmol), 6.6 mg (54.3 μmol) and 9.9 mg (80.9 μmol), for 8, 20 and 25% derivatization, respectively) and triethylamine (TEA) (95 μl (684 μmol), 189 μl (1.37 mmol) and 282 μl (2.0 mmol), for 8, 20 and 25% derivatization, respectively) were added at 0 ºC. Finally, methacrylic anhydride (MA) (102 μl (684 μmol), 204 μl (1.37 mmol) and 303 μl (2.0 mmol), for 10, 20 and 30% derivatization, respectively) at 1:1 molar ratio with TEA was added. The reaction mixture was subsequently stirred for 24 hours at room temperature, followed by the addition of approximately 20 ml water. Next, the reaction mixture was dialyzed (membrane with a cut-off of 12-14 kDa) against sterile water for two days at 4˚C and isolated by freeze-drying. The synthesized polymers were characterized by ^{1}H NMR (300 MHz, DMSO-d_6, δ): 7.35 (b,1H, N*H*), 6.15 & 5.80 (d, 2H, C=C*H$_2$*), 5.4 (d, 1H, CH-O*H*), 4.95 (d, CO-C*H*(CH$_3$)-O), 4.1 (d, 1H, CO-C*H*(CH$_3$)-OH), 3.60 (s, 904H, OC*H$_2$*C*H$_2$* (PEG-protons)), 3.4 (s, 2H, NHC*H$_2$*), 2.2-0.6 (main chain protons and CH$_3$ of lactate groups). The polymers had a degree of methacrylation of 8, 20 and 25%, as determined by 1H-NMR. The degree of methacrylation (DM), defined as the percentage of OH groups derivatized with methacrylate moieties was calculated from the ratio of the average intensity of the peaks at 6.15 and 5.80 and intensity of the peak at 5.4 ppm as follow:(32)

$$((I_{6.15}+I_{5.8})/2) / ((I_{6.15}+I_{5.8})/2 +I_{5.4}) \times 100\% \qquad (1)$$

The polymers were synthesized using sterile glassware washed with ehanol and stored overnight at 180 °C and sterile water for dialysis. The polymers were tested for endotoxin contamination using the LAL-assay. The endotoxin levels of all of the polymers were below the treshold recommended by the FDA (i.e. below 0.5 EU/ml).

7.2.3. ^{1}*H NMR Spectroscopy*

^{1}H NMR (300 MHz) spectra were recorded on a Gemini 300 MHz spectrometer (Varian Associates Inc., NMR Instruments, Palo Alto, CA) using DMSO-d_6 and CDCl$_3$ as solvents. Chemical shifts were referred to the solvent peak (δ = 2.49 ppm and δ = 7.24 ppm, for DMSO-d_6 and CDCl$_3$, respectively).

7.2.4.   Gel Permeation Chromatography

The molecular weights of the polymers were determined by GPC using a Plgel 5 μm MIXED-D column (Polymer Laboratories) with a column temperature of 40 ºC. DMF containing 10 mM LiCl was used as eluent with an elution rate of 0.7 ml min^{-1}, and the sample concentration was 5 mg ml^{-1} in the same eluent. Poly(ethylene glycols) with defined molecular weights were used as calibration standards.[30]

7.2.5.   Determination of the Cloud Point

The cloud point (CP) of the polymers was measured with static light scattering using a Horiba Fluorolog fluorometer (650 nm, 90º angle). The polymers were dissolved at a concentration of 3 mg/ml in ammonium acetate buffer (pH 5.0, 120 mM). The heating rate was approximately 1 ºC min^{-1} and every 0.2 ºC the scattering intensity was measured at 90º angle. The CP is defined as the onset of increasing scattering intensity.[33]

7.2.6.   Preparation of Hydrogels

Cylindrically shaped hydrogels of 125 mg (diameter of 4.5 mm and height of 8 mm) and 25 wt% polymer concentration were prepared in 1 ml sterile syringes as follows. Methacrylate bearing triblock copolymers were dissolved in sterile NaCl 0.9 % aqueous solution and dissolved for 2 hours at 4 °C. Next, an Irgacure 2959 solution (2.5 mg/ml) in NaCl 0.9% was added. Typically, for 100 mg hydrogel, 25 mg of polymer was dissolved in 55 μl NaCl 0.9% solution and subsequently 20 μl of Irgacure solution 2.5 mg/ml was added. The final polymer concentrations was 25 wt%, while the Irgacure concentration was 0.05 wt%. The samples were then incubated at 37 ºC for 10 minutes before photopolymerization. A BluePoint lamp 4 (350-450 nm, Honle UV technology, light intensity of 450 mW/cm^2) was used during 5 minutes for photopolymerization of the hydrogels. A glass filter between the sample and the light source was used to decrease intensity and heat production, thereby to prevent sample evaporation.

7.2.7.   Animals and Surgical Procedure

All animal experiments were approved by the local Animal Care and Use Committee of the University of Groningen and performed according to governmental and international guidelines on animal experiments. The gels were implanted in 12 week old male Balb/c mice (Harlan, Horst, The Netherlands) in dorsolateral subcutaneous pockets. The animals were anaesthetized with 4% isoflurane (induction) followed by 2% isoflurane (maintenance) inhalation in combination with a 2:1 mixture of O_2/N_2O. The back was shaved and disinfected

and subcutaneous pockets were made to the left and right through incisions. The gels (n=3 per gel per time point) were implanted subcutaneously at 1 cm from the site of incision. After 5, 10, 21 or 42 days, the gels plus surrounding tissue were dissected from the subcutaneous pocket. Next, the discs were divided in two groups: the first group was snap frozen for immunohistochemical analysis, and the second group was fixed with 2% (v/v) glutaraldehyde in 0.1 M phosphate buffer (pH 7.4) for histological analysis. Thereafter, the animals were sacrificed by cervical dislocation.

7.2.8. Histological Techniques

7.2.8a Light microscopy

For plastic embedding, the glutaraldehyde fixed materials were dehydrated in graded alcohol dilution series and embedded in Technovit 7100 (Heraeus Kulzer, Wehrheim, Germany) according to the manufacturer's protocol. Sections of 2 μm were cut and stained with Toluidine Blue (Fluka Chemie, Buchs, Switzerland) and analyzed by light microscopy.

7.2.8b Immunohistochemistry

All immunohistochemical stainings were performed on longitudinal sections (5 μm) cut from snap frozen explants, which were fixed with acetone. Sections were pre-incubated with 10% serum from the species that produced the secondary antibody. Subsequently, sections were incubated with rat-anti-F4/80 antibody (Dako) to detect macrophages, rat-anti-Ly6G antibody (BD Pharmingen) to detect neutrophils[34] and rat-anti-CD31 (BD Pharmingen) to detect endothelial cells, as a marker for blood vessels. This was followed by H_2O_2 treatment to inhibit endogenous peroxidase activity. Endogenous avidins and biotins were blocked using a Biotin Blocking System (Dako). Bound antibodies were detected with biotin-conjugated rabbit-anti-rat IgG, followed by a streptavidin-HRP complex (both from Dako). Staining was performed with 3-amino-9-ethylcarbazole (AEC, Sigma) and Mayer's hematoxylin (Fluka Chemie).

7.3. Results and Discussion

7.3.1. Polymer Synthesis and Characterization

Thermosensitive A-B-A triblock copolymers consisting of pHPMAm-lac A-blocks with a M_n of 22 kDa, as determined by ^{1}H-NMR and PEG B-block of a M_n of 10 kDa were synthesized by free radical copolymerization using a (PEG-ABCPA)$_n$ macroinitiator and HPMAm mono and dilactate in a molar ratio of 1/1. The pendant OH groups of the lactate side chains of the polymer were subsequently methacrylated to an extent of 8, 20 and 25% in order to allow the formation of chemical cross-links by photopolymerization.

The synthesized products are abbreviated as M_0, M_8, M_{20} and M_{25} for non-methacrylated and 8, 20 and 25% methacrylate derivatized triblock copolymers, respectively, and their characteristics are listed in **Table 1**.

Table 1. Characteristics of A-B-A triblock copolymers composed of (methacrylated) p(HPMAm-lac) A-blocks and PEG B-block.

Name	M_W (kDa)	M_n (kDa)	PDI	DM (%)	CP (°C)
M_0	44[b]	54[a] 26[b]	1.7[b]	N.A.	29[c]
M_8	44[b]	57[a] 25[b]	1.8[b]	8[a]	22[c]
M_{20}	45[b]	57[a] 25[b]	1.8[b]	20[a]	16[c]
M_{25}	46[b]	57[a] 25.5[b]	1.8[b]	25[a]	13[c]

[a] Determined by ^{1}H-NMR; **[b]** Determined by GPC; **[c]** Determined by SLS

The M_0 triblock copolymer was obtained with a yield of approximately 75% and a HPMAm-monodilactate/HPMAm-dilactate ratio of 1/1, corresponding to the feed ratio; CP of the polymer was 29 °C. Based on ^{1}H NMR, a M_n of 54 kDa was calculated and this value exceeded the one estimated by GPC analysis ($M_{n\ =}$ 26 kDa) most likely due to the use of PEG homopolymers as GPC standards that display larger hydrodynamic volumes than the triblock copolymers in the used eluent.(31) The methacylated triblock copolymers (M_8, M_{20} and M_{25}) had similar molecular weights as the non-methacrylated M_0 polymer (Table 1). The weight percent yield after the methacrylation reactions was 90 ± 10%. Similarly to previously reported data (31, 35), the introduction of methacrylate groups on the lactate side chains of the polymer led to an increase of hydrophobicity and consequently to a decrease in CP from 29 °C for M_0 to 22, 16 and 13 °C for M_8, M_{20} and M_{25}, respectively.

The conversion of methacrylate groups into chemical cross-links upon photopolymerization is between 80 and 90% for hydrogels of 25 wt% polymer concentration, according to previously performed studies (35-36) (see chapters 3 and 4).

7.3.2. Hydrogel Degradation

In this study, the tissue response to implanted photopolymerized thermosensitive hydrogels based on p(HPMAm-lac)-PEG-p(HPMAm-lac) triblock copolymers was studied. All implanted hydrogels had the same polymer content (25 wt %), but different extent of methacrylation, which is directly correlated to the cross-link density and the degradation rate of the hydrogels *in vitro*. Generally speaking, the degradation rate of hydrogels decreases with increasing cross-link density. From previous studies it is estimated that the M_8, M_{20} and M_{25},.hydrogels degrade *in vitro* (buffer pH 7.4 and at 37 °C) in 32, 110 and 140 days, respectively.(35-36) **Figure 1** shows the histological overview of the tissue response upon implantation of the photopolymerized hydrogels. In line with expectations, hydrogels of lower methacrylation extent (M_8) showed signs of biodegradation already a few days after implantation, and at day 10 (Figure 2D), fragmentation of the gel, likely due to the mechanical stresses of the tissues on the soft degrading material, was observed. At day 42, no hydrogel (fragments) were present at the site of implantation, demonstrating that the M_8 was degraded in line with *in vitro* data. This observation establishes a good correlation between the *in vitro* and *in vivo* degradation, indicating that the *in vivo* degradation is due to the chemical hydrolysis of the cross-links and that enzymes do not play a significant role in the degradation process. M_{20} hydrogels showed higher resistance to degradation *in vivo* (Figure 2B, 2E, 2H, 2K). Despite some initial fragmentation, most likely due to the surgical implantation procedure, M_{20} gel showed slower degradation as compared to M_8 hydrogels. This trend was confirmed with the most stable M_{25} hydrogels, showing some fragmentation visible only 42 days after implantation.

7.3.3. The Foreign Body Reaction to Hydrogels with Different Degrees of Methacrylation

The tissue response to the M_8, M_{20} and M_{25} gels was studied after subcutaneous dorsolateral implantation in Balb/c mice. Specifically, the cellular fluxes of neutrophils and macrophages as well as the development of vasculature were studied.

The presence of neutrophils at the site of implantation was examined histologically (Figure 1), and confirmed using immunohistochemistry investigations using antibodies detecting Ly6G (**Figure 2**).

The implantation of M_8, M_{20} and M_{25} photopolymerized hydrogels activated the infiltration of neutrophils, typically observed in acute inflammatory reactions. The number of infiltrating neutrophils appeared to be dependent on the degree of methacrylation, as at day 5 higher numbers of these cells were observed in hydrogels of lower methacrylation extent, as compared to highly cross-linked hydrogels ($M_8>M_{20}>M_{25}$). Moreover, the extent of infiltration within the hydrogel was also influenced by the methacrylation extent. At early time-points,

indeed, the neutrophils were located mainly in the vicinity of the interface between the implants and the surrounding tissues for M_{20} and M_{25} gels, whereas these cells also invaded the bulk of M_8 hydrogel. A decrease in number of infiltrating neutrophils in M_8 and M_{20} implants in time was observed. Particularly, M_8 hydrogels, despite showing massive infiltration at day 5 (Figure 2A), exhibited limited positive staining for neutrophils at day 21 (Figure 2J).


Histological overview
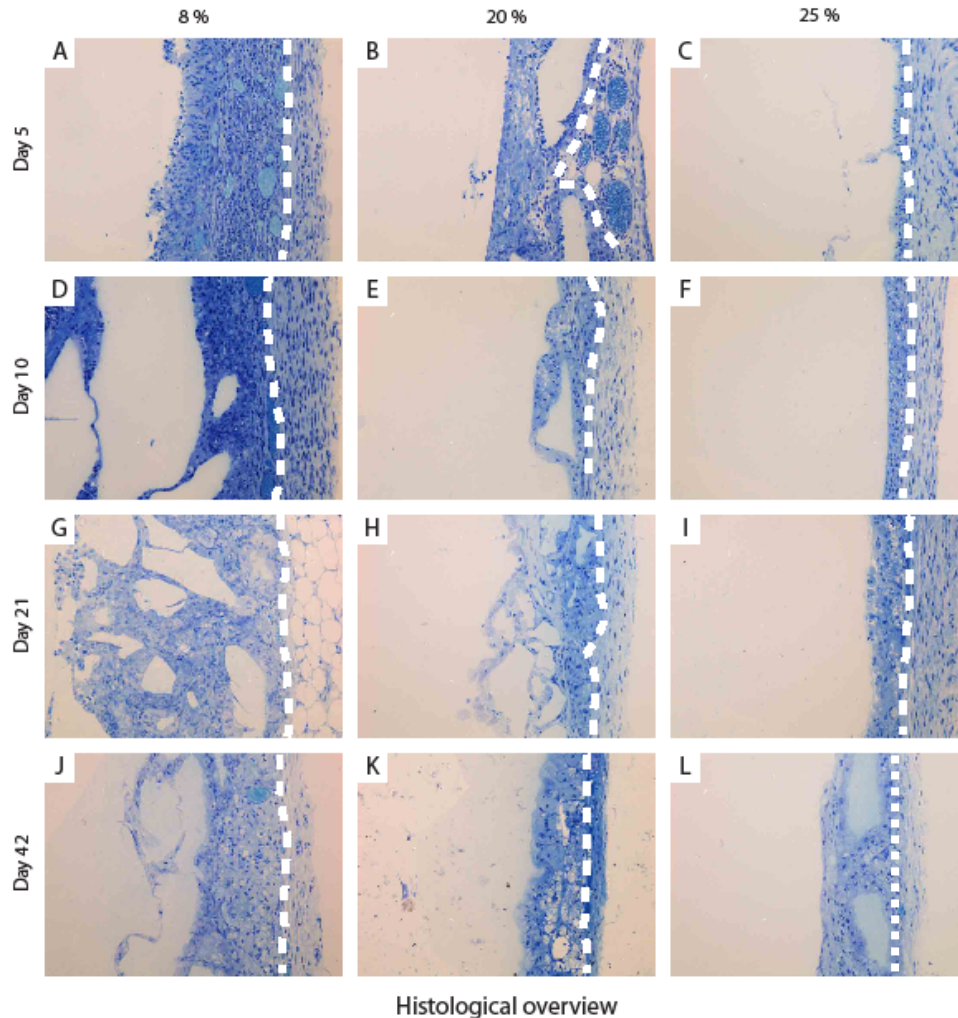
Figure 1. Histological overview of the tissue response to M_8 (A,D,G,J), M_{20} (B,E,H,K) and M_{25} (C,F,I,L) at day 5 (A-C), 10 (D-F), 21 (G-I) and 42 (J-L). The dotted line indicates the border between ingrowth (left side of the line) and surrounding tissue (right side of the line). Original magnifications 200x. Pictures are representative of 3 samples.

Interestingly, immunochemistry evaluation of the implants of M_{20} revealed no presence of neutrophils at day 21, with a slight increase again at day 42. In contrast, M_{25} gels, maintained

 the same low levels of inflammatory cells at day 5 and 10 post implantation and showed a slight increase at day 21. However, at day 42 in all the formulations only a few neutrophils were present. Similarly to neutrophils concentrations, the number of infiltrating macrophages, analyzed by immunohistochemistry with antibodies detecting F4/80, depended on the methacrylation degree, as the highest number of macrophages was observed for M_8 hydrogels (**Figure 3**).However, in contrast to neutrophils, the infiltrated macrophages showed rather low levels at early time-points and a slight increase in time until day 10 for M_{20} and until day 21 for M_8 and M_{25} hydrogels. Interestingly, it was shown that large areas of the matrix of the relatively fast degrading M_8 hydrogel were invaded by macrophages already at early time-points, whereas for the slowly degrading implants, the macrophages were mainly localized at the border between the gel and the surrounding tissue at day 5 and 10 and infiltration towards inner areas of the gel from day 21. It appears that, the macrophages infiltration is correlated to biodegradation and bioresorption of the implant.

This observation is in line with other studies carried out on biodegradable hydrogels; for example Cadée *et al*. performed a comparative biocompatibility study, where hydrogels based on biodegradable dextran-lactate-hydroxyethyl methacrylate (dex-lac-HEMA) or non biodegradable dextran-mathacrylate (dex-MA) were implanted subcutaneously in rats.(37) It turned out that dex-MA implants were surrounded by tissue in which low numbers of macrophages were present and in time the formation of a fibrous capsule around the gel was observed. In contrast, degradable dex-lac-HEMA matrices showed increasing infiltration of macrophages with progressing hydrogel degradation and the formation of a fibrous capsule was not observed. Importantly, they demonstrated that some of these macrophages contained vacuoles with hydrogel particles, confirming the role of these cells in phagocytoting the degrading hydrogel. In another study, it was shown that the extent of the observed inflammatory response after implantation of degradable dextran hydrogels highly depended on the animal model used. De Jong *et al.* demonstrated that mice are a particularly sensitive to develop an inflammatory response towards implanted biomaterials, as compared to rats.(38)Macrophages are antigen presenting cells and therefore their potential activation of lymphocytes must be investigated in order to assess whether the studied hydrogels elicit an immune response. This aspect will be the topic of further studies.

Angiogenesis in the tissue where the gels were implanted was examined histologically (Figure 1), and confirmed using immunohistochemistry with antibodies detecting CD31 (**Figure 4**). In M_{25} implants at day 5, angiogenesis was not observed within the biomaterial likely as a consequence of its slow degradation and lack of macrophages infiltration (Figure 4C). Only within the border zones of the material, first signs of angiogenesis were observed in these samples (Figure 4C). As the degradation of M_{25} hydrogels progressed, some angiogenesis in the bulk of the gel was observed (Figures 4C, 4F, 4I, 4L). In contrast, the initial macrophages infiltration, observed in faster degrading hydrogels (M_{20} and M_8), was related to blood vessel formation within the implant already at early time-points (Figures 4A,

4B). In line with M_{25} gels, the angiogenesis of M_8 and M_{20} matrices progressed until day 42, with M_8 implants showing the highest extent of vascularization.
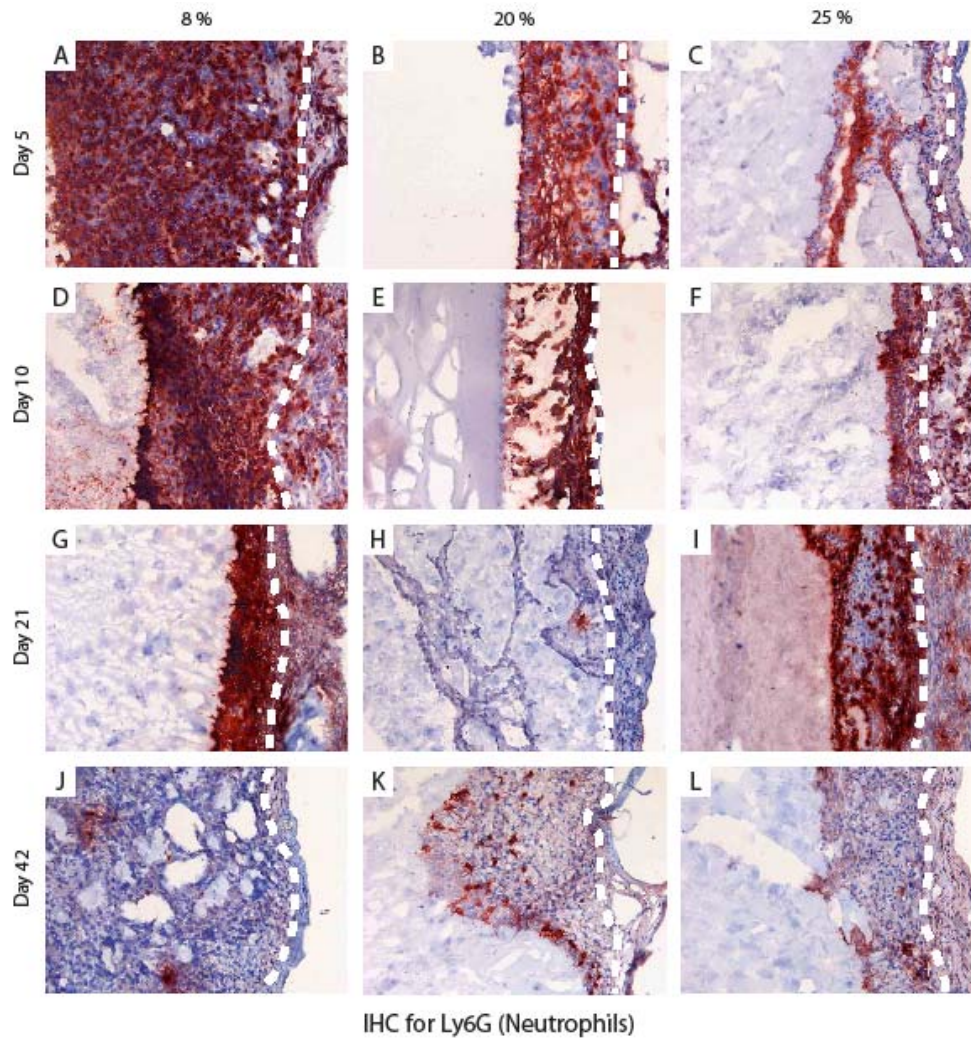
gure 2. Immunohistochemical detection of neutrophils (Ly-6G) within the gels M_8 (A,D,G,J), M_{20} (B,E,H,K) and M_{25} (C,F,I,L) and in the tissue surrounding the gels at day 5 (A-C), 10 (D-F), 21 (G-I) and 42 (J-L). The dotted line indicates the border between ingrowth (left side of the line) and surrounding tissue (right side of the line). Original magnifications 200x. Pictures are representative of 3 samples.

IHC for F4/80 (Macrophages)
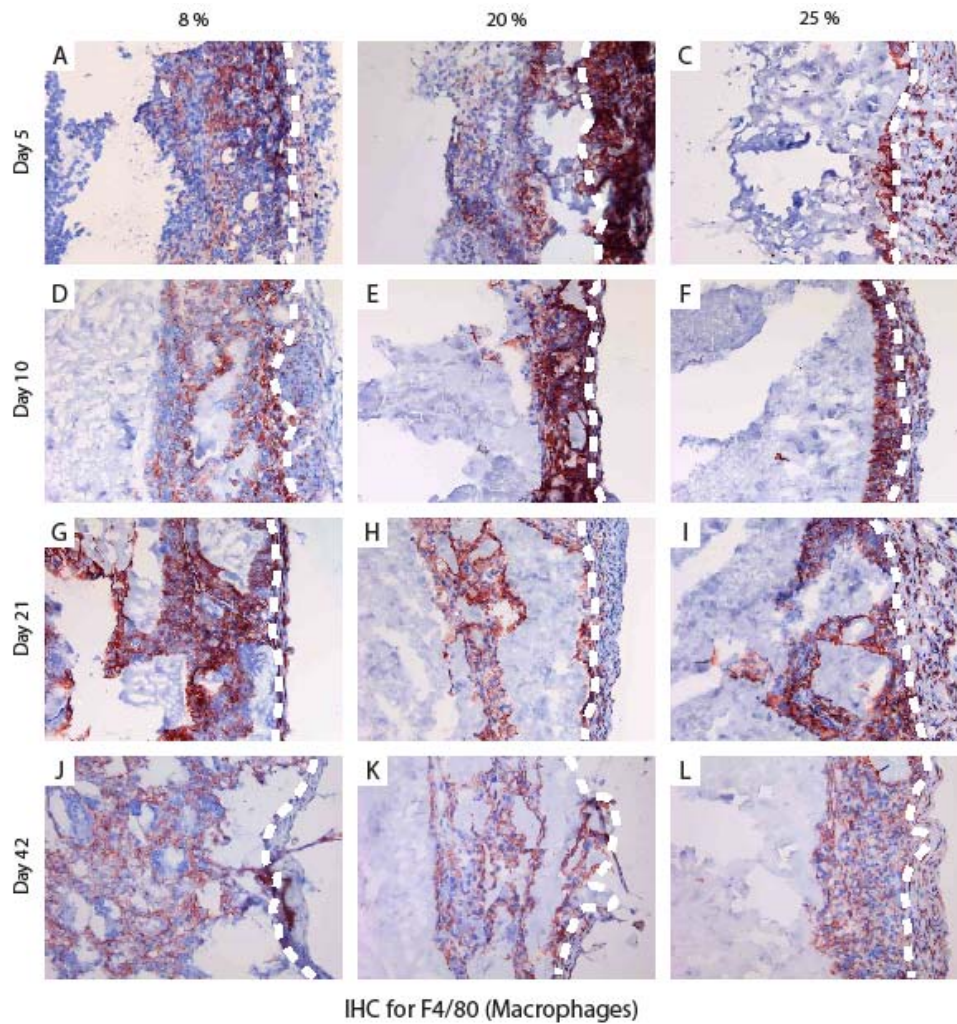
Figure 3. Immunohistochemical detection of macrophages (F4/80) within the gels M_8 (A,D,G,J), M_{20} (B,E,H,K) and M_{25} (C,F,I,L) and in the tissue surrounding the gels at day 5 (A-C), 10 (D-F), 21 (G-I) and 42 (J-L). The dotted line indicates the border between ingrowth (left side of the line) and surrounding tissue (right side of the line). Original magnifications 200x. Pictures are representative of 3 samples.

Table 2 summarizes the major results on tissue response to the implantation of M_8, M_{20} and M_{25} photopolymerized hydrogels. Taken together, the histological data lead to the following considerations. The implantation of the hydrogels was associated with an acute inflammatory response, as expected from previous observations (4, 37, 39), which was more intense for fast degrading implants. This acute phase was associated with initial high

numbers of infiltrating neutrophils and resolved in time, as demonstrated by the progressive attenuation of neutrophils infiltration in all the implants. This initial phase was followed by a chronic inflammation, characterized by slightly increasing levels of macrophages, due to the bioresorption of the degrading polymer.(40-43) This foreign-body reaction, schematically represented in **Figure 5**, is a common tissue response that has been described in literature for a number of degradable biomaterials, like scaffolds consisting of poly(lactic-*co*-glycolic acid) (PLGA),(44) hydrogels based on crosslinked dermal sheep collagen,(45) and tyrosine-derived polymers.(46) In these studies, the extent and duration of this reaction depended upon the degradation rate.

A prominent vascular host tissue response with formation of a densely vascularized granulation tissue was observed towards implanted hydrogels exhibiting remarkable macrophages infiltration (i.e. M_8). This observation may indicate that the start of degradation and resorption of the biomaterial results in infiltration of macrophages, which are responsible for phagocytosis of hydrogel fragments, tissue ingrowth and formation of new blood vessels. Macrophages are indeed well known to be capable of inducing angiogenesis.(47) On the other hand, it has been shown that an overwhelming inflammatory response may act inhibitorily on the process of angiogenesis.(48) This phenomenon was not observed in our hydrogel implants, thus the observed inflammation can be considered of minor extent. Angiogenesis can also be induced by activated leukocytes, which produce several angiogenic factors, in particular, vascular endothelial growth factor (VEGF).(49-50)

It appears that the observed host tissue response, resulting in continuous infiltration of inflammatory cells until the hydrogel is completely degraded, resulted in a good engraftment of the implants, meaning that the implanted synthetic matrix has the ability to positively interact with the host tissue, leading to fusion of the matrix with the natural surrounding tissue. This effect is mediated by a mild chronic inflammatory response and is marked in our studies for hydrogels of lower extent of methacrylation. Most likely, the engraftment of hydrogels of higher methacrylation degree (M_{20} and M_{25}), which need longer time to show significant degradation, would be more extensive on a longer timescale, which was not considered in this study.

IHC for CD31 (Blood Vesssels)
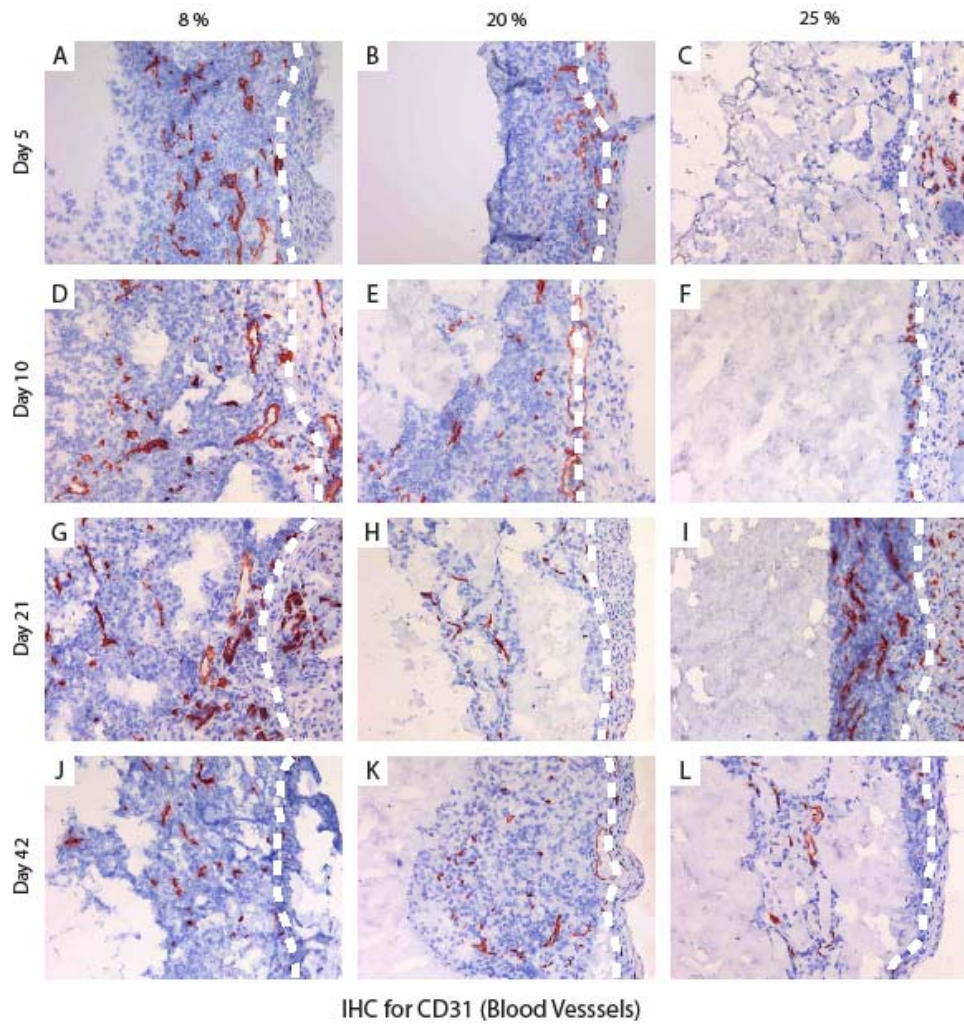
Figure 4. Immunohistochemical detection of blood vessels (CD-31) within the gels M_8 (A,D,G,J), M_{20} (B,E,H,K) and M_{25} (C,F,I,L) and in the tissue surrounding the gels at day 5 (A-C), 10 (D-F), 21 (G-I) and 42 (J-L). The dotted line indicates the border between ingrowth (left side of the line) and surrounding tissue (right side of the line). Original magnifications 200x. Pictures are representative of 3 samples.
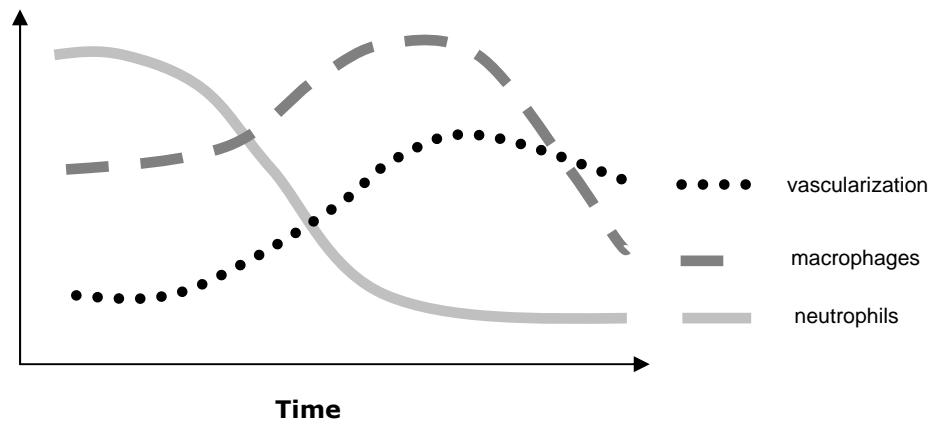
Time

Figure 5. Schematic representation of the relative variation of the number of inflammatory cells and extent of vascularization as a function of time after implantation

7.4.   Conclusions

In the present study the effect of the network characteristics of p(HPMAm-lac)-PEG-p(HPMAm-lac) hydrogels, with respect to extent of methacrylation, on the tissue response upon subcutaneous implantation in mice was investigated. Initial acute foreign-body reaction, elicited by all implants investigated was followed by a milder chronic inflammation, where decreasing neutrophils levels and continuous infiltration of macrophages, associated with hydrogel degradation, were observed. The number of infiltrated macrophages was directly correlated to the degradation kinetics of the material. The relatively fast degrading M8 hydrogel, (having a methacrylation degree of 8%) showed higher numbers of infiltrating inflammatory cells. The observed mild chronic inflammation stimulated tissue ingrowth and angiogenesis, leading to good engraftment of the implanted hydrogels in the host tissue. This engraftment ability of the studied photopolymerized hydrogels is an extremely appealing property for tissue engineering applications, where fusion of the synthetic matrix into the natural extracellular matrix of surrounding host cells is highly desirable. In conclusion, this study shows that photopolymerized p(HPMAm-lac)-PEG-p(HPMAm-lac) based hydrogels demonstated good biocompatibility and are therefore attractive materials for pharmaceutical and biomedical applications.

Table 2. Tissue reaction to photopolymerized p(HPMAm-lac)-PEG-p(HPMAm-lac) triblock copolymer hydrogels of 25 wt% polymer concentration and methacrylation extents of 8 (M_8), 20 (M_{20}) and 25% (M_{25}).

Hydrogel implant	Days after implantation	Neutrophils S	Neutrophils I	Macrophages S	Macrophages I	Vascularization S	Vascularization I
M_8	5	+++	++++	±	++	-	++
	10	++	+++	++	++	+	+++
	21	+	++	++	+++	++	+++
	42	-	±	-	+	±	++
M_{20}	5	++	+++	+++	++	+	+
	10	-	+	±	+++	±	++
	21	-	-	±	++	±	++
	42	±	±	-	+	±	++
M_{25}	5	±	+	+	±	+	-
	10	+	+	+	+	±	-
	21	+	++	+	+++	+	++
	42	±	±	±	+	±	+

S = in the tissues surrounding the implant; I = infiltrating
+ to ++++ = sporadic to severe; - = not present

References

1.   Williams DF ed (1999) *The Williams dictionary of Biomaterials* Liverpool.

2.   Park H & Park K (1996) Biocompatibility Issues of Implantable Drug Delivery Systems. *Pharmaceutical Research* 13(12):1770-1776.

3.   Ritu A, Shailley J, Sumit M, Raja N, Usha Kaul R, & Dinesh Kumar M (2004) Efficacy of continuous wear PureVision contact lenses for therapeutic use. *Contact lens & anterior eye : the journal of the British Contact Lens Association* 27(1):39-43.

4.   Bos GW, Jacobs JJL, Koten JW, Van Tomme S, Veldhuis T, van Nostrum CF, Den Otter W, & Hennink WE (2004) In situ crosslinked biodegradable hydrogels loaded with IL-2 are effective tools for local IL-2 therapy. *European Journal of Pharmaceutical Sciences* 21(4):561-567.

5.   Nam K, Watanabe J, & Ishihara K (2004) Modeling of swelling and drug release behavior of spontaneously forming hydrogels composed of phospholipid polymers. *International Journal of Pharmaceutics* 275(1-2):259-269.

6.   Nguyen KT & West JL (2002) Photopolymerizable hydrogels for tissue engineering applications. *Biomaterials* 23(22):4307-4314.

7.   Woerly S, Plant GW, & Harvey AR (1996) Cultured rat neuronal and glial cells entrapped within hydrogel polymer matrices: a potential tool for neural tissue replacement. *Neuroscience Letters* 205(3):197-201.

8.   West JL & Hubbell JA (1996) Separation of the arterial wall from blood contact using hydrogel barriers reduces intimal thickening after balloon injury in the rat: The roles of medial and luminal factors in arterial healing. *Proceedings of the National Academy of Sciences of the United States of America* 93(23):13188-13193.

9.   Denstedt JD, Reid G, & Sofer M (2000) Advances in ureteral stent technology. *World Journal of Urology* 18(4):237-242.

10.   Van Tomme SR, Storm G, & Hennink WE (2008) In situ gelling hydrogels for pharmaceutical and biomedical applications. *International Journal of Pharmaceutics* 355(1-2):1-18.

11.   Kretlow JD, Klouda L, & Mikos AG (2007) Injectable matrices and scaffolds for drug delivery in tissue engineering. *Advanced Drug Delivery Reviews* 59(4-5):263-273.

12.   Jeong B, Bae YH, Lee DS, & Kim SW (1997) Biodegradable block copolymers as injectable drug-delivery systems. *Nature* 388(6645):860-862.

13.   Hyun H, Kim YH, Song IB, Lee JW, Kim MS, Khang G, Park K, & Lee HB (2007) In Vitro and in Vivo Release of Albumin Using a Biodegradable MPEG-PCL Diblock Copolymer as an in Situ Gel-Forming Carrier. *Biomacromolecules* 8(4):1093-1100.

14.   Lee BH & Song S-C (2004) Synthesis and Characterization of Biodegradable Thermosensitive Poly(organophosphazene) Gels. *Macromolecules* 37(12):4533-4537.

15.   Du H, Chandaroy P, & Hui SW (1997) Grafted poly-(ethylene glycol) on lipid surfaces inhibits protein adsorption and cell adhesion. *Biochimica et Biophysica Acta (BBA) - Biomembranes* 1326(2):236-248.

16.   Lee JH, Jeong BJ, & Lee HB (1997) Plasma protein adsorption and platelet adhesion onto comb-like PEO gradient surfaces. *Journal of Biomedical Materials Research* 34(1):105-114.

17.   Lee JH, Kopecek J, & Andrade JD (1989) Protein-resistant surfaces prepared by PEO-containing block copolymer surfactants. *Journal of Biomedical Materials Research* 23(3):351-368.

18.   Drumheller PD & Hubbell JA (1995) Densely crosslinked polymer networks of poly(ethylene glycol) in trimethylolpropane triacrylate for cell-adhesion-resistant surfaces. *Journal of Biomedical Materials Research* 29(2):207-215.

19.   Veronese FM & Harris JM (2002) Introduction and overview of peptide and protein pegylation. *Advanced Drug Delivery Reviews* 54(4):453-456.

20.   Peppas NA, Keys KB, Torres-Lugo M, & Lowman AM (1999) Poly(ethylene glycol)-containing hydrogels in drug delivery. *Journal of Controlled Release* 62(1-2):81-87.

21.   Press P ed (1985) *Surface and Interfacial Aspects of Biomedical Polymers, Vol. 2: Potein Adsorption*New York).

22.   Society AC ed (1982) *Interfacial Phenomena and Applications, ACS Symposium Series 199*Washington DC)

23. Marchant R, Hiltner A, Hamlin C, Rabinovitch A, Slobodkin R, & Anderson JM (1983) *In vivo* biocompatibility studies. I. The cage implant system and a biodegradable hydrogel. *Journal of Biomedical Materials Research* 17(2):301-325.

24. Gilding D (1981) *"Biodegradable polymers,"* in Biocompatibility of implant materials (CRC Press, Boca Raton, FL).

25. Anderson JM (1988) Inflammatory response to implants. *ASAIO Transactions* 34(2):101-107.

26. Duan Y, Nie Y, Gong T, Wang Q, & Zhang Z (2006) Evaluation of blood compatibility of MeO-PEG-poly (DL-lactic-*co*-glycolic acid)-PEG-OMe triblock copolymer. *Journal of Applied Polymer Science* 100(2):1019-1023.

27. Kim MS, Kim SK, Kim SH, Hyun H, Khang G, & Lee HB (2006) In Vivo Osteogenic Differentiation of Rat Bone Marrow Stromal Cells in Thermosensitive MPEG–PCL Diblock Copolymer Gels. *Tissue Engineering* 12(10):2863-2873.

28. Shim WS, Kim J-H, Park H, Kim K, Chan Kwon I, & Lee DS (2006) Biodegradability and biocompatibility of a pH- and thermo-sensitive hydrogel formed from a sulfonamide-modified poly(ε-caprolactone-co-lactide)-poly(ethylene glycol)-poly(ε-caprolactone-co-lactide) block copolymer. *Biomaterials* 27(30):5178-5185.

29. Bjugstad KB, Redmond Jr DE, Lampe KJ, Kern DS, Sladek Jr JR, & Mahoney MJ (2008) Biocompatibility of PEG-based hydrogels in primate brain. *Cell Transplantation* 17(4):409-415.

30. Soga O, van Nostrum CF, & Hennink WE (2004) Poly(N-(2-hydroxypropyl) Methacrylamide Mono/Di Lactate): A New Class of Biodegradable Polymers with Tuneable Thermosensitivity. *Biomacromolecules* 5(3):818-821.

31. Vermonden T, Besseling NAM, van Steenbergen MJ, & Hennink WE (2006) Rheological Studies of Thermosensitive Triblock Copolymer Hydrogels. *Langmuir* 22(24):10180-10184.

32. Vermonden T, Fedorovich NE, van Geemen D, Alblas J, van Nostrum CF, Dhert WJA, & Hennink WE (2008) Photopolymerized Thermosensitive Hydrogels: Synthesis, Degradation, and Cytocompatibility. *Biomacromolecules* 9(3):919-926.

33. Neradovic D, van Steenbergen MJ, Vansteelant L, Meijer YJ, van Nostrum CF, & Hennink WE (2003) Degradation Mechanism and Kinetics of Thermosensitive Polyacrylamides Containing Lactic Acid Side Chains. *Macromolecules* 36(20):7491-7498.

34. Daley JM, Thomay AA, Connolly MD, Reichner JS, & Albina JE (2008) Use of Ly6G-specific monoclonal antibody to deplete neutrophils in mice. *Journal of Leukocyte Biology* 83(1):64-70.

35. Censi R, Vermonden T, van Steenbergen MJ, Deschout H, Braeckmans K, De Smedt SC, van Nostrum CF, di Martino P, & Hennink WE (2009) Photopolymerized thermosensitive hydrogels for tailorable diffusion-controlled protein delivery. *Journal of Controlled Release* 140(3):230-236.

36. Censi R, Vermonden T, Deschout H, Braeckmans K, Di Martino P, De Smedt S, Van Nostrum C, & Hennink WE (2010) Photopolymerized Thermosensitive Poly(HPMAlactate)-PEG Based Hydrogels: Effect of Network Design on Mechanical Properties, Degradation and Release Behavior. *Biomacromolecules* In Press.

37. Cadée JA, Van Luyn MJA, Brouwer LA, Plantinga JA, Van Wachem PB, De Groot CJ, Den Otter W, & Hennink WE (2000) In vivo biocompatibility of dextran-based hydrogels. *Journal of Biomedical Materials Research* 50(3):397-404.

38. De Jong WH, Dormans JAMA, Van Steenbergen MJ, Verharen HW, & Hennink WE (2007) Tissue response in the rat and the mouse to degradable dextran hydrogels. *Journal of Biomedical Materials Research - Part A* 83(2):538-545.

39. Cadée JA, Brouwer LA, Den Otter W, Hennink WE, & Van Luyn MJA (2001) A comparative biocompatibility study of microspheres based on crosslinked dextran or poly(lactic-co-glycolic)acid after subcutaneous injection in rats. *Journal of Biomedical Materials Research* 56(4):600-609.

40. Anderson JM, Rodriguez A, & Chang DT (2008) Foreign body reaction to biomaterials. *Seminars in Immunology* 20(2):86-100.

41. Anderson JM (2001) Biological responses to materials. *Annual Review of Materials Science* 31:81-110.

42. Anderson JM (1994) In vivo biocompatibility of implantable delivery systems and biomaterials. *European Journal of Pharmaceutics and Biopharmaceutics* 40(1):1-8.

43. Anderson JM & Miller KM (1984) Biomaterial biocompatibility and the macrophage. *Biomaterials* 5(1):5-10.

44. Rücker M, Laschke MW, Junker D, Carvalho C, Schramm A, Mülhaupt R, Gellrich N-C, & Menger MD (2006) Angiogenic and inflammatory response to biodegradable scaffolds in dorsal skinfold chambers of mice. *Biomaterials* 27(29):5027-5038.

45. Van Wachem PB, Van Luyn MJA, Olde Damink LHH, Dijkstra PJ, Feijen J, & Nieuwenhuis P (1994) Biocompatibility and tissue regenerating capacity of crosslinked dermal sheep collagen. *Journal of Biomedical Materials Research* 28(3):353-363.

46. Hooper KA, Macon ND, & Kohn J (1998) Comparative histological evaluation of new tyrosine-derived polymers and poly (L-lactic acid) as a function of polymer degradation. *Journal of Biomedical Materials Research* 41(3):443-454.

47. Bingle L, Lewis CE, Corke KP, Reed M, & Brown NJ (2006) Macrophages promote angiogenesis in human breast tumour spheroids in vivo. *British Journal of Cancer* 94(1):101-107.

48. Sung H-J, Meredith C, Johnson C, & Galis ZS (2004) The effect of scaffold degradation rate on three-dimensional cell growth and angiogenesis. *Biomaterials* 25(26):5735-5742.

49. Shaw JP, Chuang N, Yee H, & Shamamian P (2003) Polymorphonuclear neutrophils promote rFGF-2-induced angiogenesis in Vivo. *Journal of Surgical Research* 109(1):37-42.

50. Möhle R, Green D, Moore MAS, Nachman RL, & Rafii S (1997) Constitutive production and thrombin-induced release of vascular endothelial growth factor by human megakaryocytes and platelets. *Proceedings of the National Academy of Sciences of the United States of America* 94(2):663-668.

Chapter 8

Summary

&

Perspectives

8.1.   Summary

Hydrogels have a long history – ophthalmic devices are the earliest examples, with Wichterle *et al.* creating soft contact lenses from cross-linked 2-hydroxyethyl methacrylate (HEMA) networks. Since then, the applications of hydrogels have expanded into new directions, including drug delivery and tissue engineering. Hydrogels have shown to be suitable materials to interface biological systems, minimize cell and protein adherence and foreign body reaction. Considerable efforts are being addressed to specifically engineer polymeric materials capable to cross-link in physiological medium, in which proteins can be encapsulated and protected against degradation and cells can be accommodated and retain their viability and functionality. Hydrogels are aimed to release active protein therapeutics in a tailorable and controlled fashion over a prolonged period of time or support cell proliferation and tissue/organ formation. Ultimately, upon exerting their function, ideally they degrade into excretable and non-harmful products.

These precise topics – controlled delivery of proteins and regeneration of artificial organs - defines the goal of this thesis that is centered on the feasibility, mechanistic insights and applications of injectable *in situ* gelling hydrogels based on newly developed thermosensitive triblock copolymers, as described in **chapter 1**. In this chapter, the general features of hydrogels are outlined, with respect to their cross-linking methods and polymer characteristics. Particular emphasis is given to cross-linking methods for *in situ* gelling, like photopolymerization, Michael addition reaction and hydrophobic interaction by thermo-gelling. The characteristics of natural and synthetic polymers, with special focus on poly(ethylene glycol) (PEG) and poly(hydroxypropyl methacrylamide) p(HPMAm) are also briefly overviewed. PEG and p(HPMAm) are the main components of the hydrogel studied in this thesis that consists of a thermosensitive ABA triblock copolymer, composed of a hydrophilic PEG B-block, flanked with thermosensitive poly(*N*-(2-hydroxypropyl) methacrylamide lactate (p(HPMAm-lac) A-blocks. These polymers are able to self-assemble in aqueous solution in response to increasing temperature, forming visco-elastic networks. When the lactate side chains of the p(HPMAm-lac) A-blocks are partly derivatized with (meth)acrylate moieties, the networks can be chemically cross-linked. In chapter 1, the use of hydrogels for protein delivery and tissue engineering is also shortly discussed.

Chapter 2 elaborates in more detail on the application of hydrogels as protein delivery systems. Hydrogels are excellent candidates to enable clinical and commercial development of protein therapeutics with otherwise very unfavorable pharmacokinetics (i.e. very short half-life), excessive systemic toxicity, and poor chemical, physical and enzymatic stability. These delivery systems are potentially able to maintain the protein serum/tissue concentration within the therapeutic window for a prolonged period of time, while preserving its stability. Recent developments in hydrogel systems designed to serve these functions are reviewed. Both chemically as well as physically cross-linked networks for *in situ* gelling are discussed, with particular emphasis on networks assembled by thermo-gelling, photopolymerization and

Michael addition, since these are methods investigated in this thesis. Their *in vitro* and *in vivo* protein release behavior is described, highlighting specific aspects like release mechanisms and methods to study them, stability of the therapeutics during formulation and release. Also shortcomings of the present generation of hydrogels for protein delivery (burst and incomplete release, high diffusivity) are discussed as well as strategies to tailor and improve release performance.

In **chapter 3,** the release of proteins from thermosensitive p(HPMAm-lac)-PEG-p(HPMAm-lac) hydrogels was investigated. To this end, a polymer having a middle PEG block of 10 kDa and thermosensitive outer blocks of approximately 25 kDa was synthesized and in a subsequent reaction 10% of the available hydroxyl groups were derivatized with methacrylate groups. When this polymer and a protein were dissolved at room temperature in aqueous medium of physiological pH, a clear solution was obtained, which underwent a sol-gel phase transition in response to an increase in temperature above 31 °C.   In our approach, a tandem cross-linking method by additional photopolymerization, in the presence of a biocompatible photoinitiator, Irgacure 2959, was used to provide sufficient mechanical strength and gel stability. By varying the polymer concentration, hydrogels with different mechanical properties were formed, of which the cross-link density, swelling and degradation behavior could be tuned. It was demonstrated that three model proteins (lysozyme, bovine serum albumin (BSA) and immunoglobulin G (IgG), ranging in molecular weight (MW) between 14 and 150 kDa) were quantitatively released in 2 to 17 days, depending on the protein size and polymer concentration. The release mechanism was governed by Fickian diffusion, a finding that was confirmed by Fluorescence Recovery After Photobleaching (FRAP) experiments. Protein diffusion coefficients (from 9 to 16 fold lower in gels than in water) measured by FRAP perfectly correlated those calculated from release profiles. Importantly, the secondary structure and the enzymatic activity of lysozyme were fully preserved, demonstrating the protein friendly nature of the studied delivery system.

In a subsequent study, reported in **chapter 4,** we explored how the molecular design of the thermosensitive p(HPMAm-lac)-PEG-p(HPMAm-lac) tailored the mechanical properties, degradation and protein release behavior of hydrogels based on this polymer. This work was directed to the development of a hydrogel based delivery platform, wherein the flexibility of the polymer chemistry offered the opportunity to create a variety of hydrogels with well-defined physicochemical properties and reproducible and modular release profiles. Achieving tailorable hydrogel properties allows ideally fulfilling the therapeutical requirements, making the protein drug available at the desired time and the right dose. Polymers of varying PEG's MW and degree of methacrylation (DM) were investigated. It was found that an increasing DM and a decreasing PEG MW resulted in increasing gel strength and cross-link density, which tailored the degradation profiles from 25 to over 300 days. BSA was released from hydrogels from 10 days to more than 2 months and its mechanism was mainly governed by diffusion. Some of the studied hydrogel formulations, especially the ones containing higher polymer

concentration, showed a biphasic diffusional release: an initial and relatively fast release of the protein present in the hydrophilic PEG-rich pores followed by a slower diffusional release of the protein residing in the hydrophobic domains composed of the thermosensitive chains. While a clear effect of PEG's MW on BSA release was observed, the DM not always influenced the release rate. The DM influenced the cross-link density only within the hydrophobic domains of self-assembled thermosensitive chains and the release of the protein fraction residing in this compartment could be tailored by the DM. On the other hand, changes in PEG's MW led to changes in protein release from the hydrophilic pores. Surprisingly, lower PEG MW's resulted in faster release rate. This phenomenon was clarified by confocal microscopy studies, which revealed a remarkable phase separation in hydrogels of shorter PEG and the formation of larger hydrophilic pores, from which the protein was rapidly released.

Chapter 5 reports on the design of a novel hydrogel system where thermosensitive (meth)acrylate bearing ABA-triblock copolymers consisting of a PEG middle block, flanked by thermosensitive blocks of random *N*-isopropylacrylamide (pNIPAm)/(pHPMAm-lac) were combined with thiolated hyaluronic acid (HA-SH) in a (meth)acrylate/thiol groups ratio of 1/1. The two polymers formed an injectable *in situ* gelling system by tandem cross-linking, comprising temperature induced physical gelation followed by Michael type addition reaction between thiol groups on HA-SH and methacrylate moieties on the triblock copolymer. Michael addition cross-linking is an advantageous cross-linking method as it occurs at physiological conditions without the need for catalysts or external stimuli (i.e. UV light). Moreover, using a modified natural polymer (HA-SH) as a Michael addition species affords other benefits. Hyaluronic acid (HA) is a polysaccharide known for its favorable physical (e.g. viscosity, hydration) and biological (protein and cell interactions) properties. The combination of natural and synthetic polymers within a hydrogel matrix is generally acknowledged as an effective strategy to enhance biocompatibility and positive interaction of the gel with encapsulated proteins and cells.

The simultaneous physical and chemical gelation was investigated by rheological analysis, demonstrating that the physical networks were progressively stabilized as the Michael addition reaction between (meth)acrylate and thiol groups proceeded. The acrylated thermosensitive polymers had a higher reactivity towards thiol groups, as compared to methacrylate analogues, resulting in a faster increase in gel strength. The networks degraded at physiological conditions by hydrolysis of the ester bonds in the cross-links, as well as in the lactate side chains and between PEG and thermosensitive blocks; more specifically the acrylated systems degraded in 120 days while the methacrylated gel degraded in 80 days. Methacrylated polymer gels released a model peptide (bradykinin) by diffusion and its release was tailored by polymer concentration from 60 to 175 hours.

Another interesting application of the photopolymerized thermosensitive p(HPMAm-lac)-

PEG-p(HPMAm-lac) hydrogels in the field of tissue engineering was explored in **chapter 6,** where a bioprinting technology was used to design three-dimensional (3D) scaffolds aimed at the regeneration of cartilage. Bioprinting is a scaffold preparation technique based on computer aided layer-by-layer 3D fiber deposition of cell-laden hydrogels that holds potential in the regeneration of tissues with a precise hierarchical organization. This technique requires hydrogels with adequate requisites, in terms of mechanical strength and ability to be extruded in form of fibers. With this respect, thermogelling systems are ideal candidates, as they can be extruded as flowable/low viscosity solutions by simply adjusting the temperature of the extruder and generate a free-standing 3D scaffold when these fibers are deposited in a layer-by-layer mode on a collector preheated above the gel temperature of the polymer. It was demonstrated that the hydrogel mechanical properties well adapted to the process of 3D printing, as structurally stable 3D scaffolds with well defined vertical porosity and enhanced stability by photopolymerization were successfully printed by subsequent deposition of gel fibers up to at least 37 layers. The scaffolds displayed an elastic modulus of 119 kPa (25 wt% polymer content) and a degradation time of approximately 190 days. Scaffold pattern and strand spacing could easily be tuned and the potential ability of the constructs to provide precise tissue mimicking cell organization was shown.

Rheological characterization of the thermally assembled and photopolymerized hydrogels showed a semi-flexible character of the studied polymer-gel, demonstrated by power law scaling of the hydrogel storage moduli with the polymer concentration. This finding established similarities of the studied synthetic polymer with natural extracellular matrix-forming polymers, including collagen. Furthermore, high viability was observed for encapsulated equine chondrocytes after 1 and 3 days of culture.

Chapter 7 reports on an *in vivo* biocompatibility study of photopolymerized p(HPMAm-lac)-PEG-p(HPMAm-lac). As observed for other hydrogel systems, upon implantation, a localized inflammatory reaction in the surrounding tissues of the implant was noted, which slightly intensified in time, during the entire duration of the studied period (42 days), as shown by a persistent number of infiltrating macrophages. This response is associated with bioresorption of the implanted material as macrophages are attracted to the implantation site to phagocytate the degrading material. However, this inflammatory cell infiltration can be considered as a mild reaction, as confirmed by the absence of a systemic effect, and by the constantly decreasing number of infiltrating neutrophils observed for all implanted hydrogels. The inflammatory reaction is inversely correlated to the degradation time, therefore to the methacrylation degree of the hydrogels. Moreover, necrotic tissue was not observed at the site of implantation and a remarkable tissue ingrowth and vascularization, activated by macrophages, in the implants were observed, indicating adequate engraftment of the studied hydrogels within the host tissue. Finally, complete resorption of hydrogels of lower methacrylation extent was observed after 42 days, as expected based on *in vitro* degradation

experiments, whereas some non-degraded biomaterial was assessed in case of hydrogels of higher cross-link density. Although some strategies can be implemented to reduce excessive macrophages infiltration, the considered photopolymerized thermosensitive hydrogels hold excellent potential for *in vivo* applications.

In conclusion, this thesis describes novel injectable thermosensitive hydrogels, exhibiting biodegradability, good protein, cell and tissue compatibility and high degree of tailorability, with respect to mechanical properties, degradation and release behavior. This tailorability was implemented by modulating the polymer design and by using two different *in situ* chemical cross-linking methods. The ability of these hydrogels to serve several biomedical functions, from controlled protein release to tissue engineering was demonstrated. The results reported in this thesis bring this hydrogel technology one step forward towards clinical application.

8.2.   Discussion and Perspectives

8.2.1.   Injectability

The thermosensitive p(HPMAm-lac)-PEG-p(HPMAm-lac) triblock copolymer, which is the central theme of this thesis, was designed for the preparation of injectable *in situ* gelling systems for protein delivery and tissue engineering. *In situ* gelling materials have gained increasing interest in the last 10 years as they allow minimally invasive administration by simple injection, avoiding implantation by surgical intervention. As a result, patient's comfort and compliance are greatly enhanced. Additionally, self-administration of the dosage form might be applied without the need for specialized medical personnel, decreasing the burden of costly medical treatments on health care systems. In this thesis, the body temperature triggered formation of the gel at the injection site is combined with two chemical cross-linking methods: photopolymerization (chapters 3, 4, 6 and 7) and Michael addition reaction (chapter 5). These two chemical cross-linking methods were applied to increase the stability of the hydrogel network preventing premature dissolution of gel and release of encapsulated drug. Photopolymerization and Michael addition can be potentially applied *in situ*. However, several aspects need to be evaluated for their successful use *in vivo*.(1)

UV and visible light can be applied *in vivo* by transdermal illumination or minimally invasive devices like catheters or laparoscopic equipments. Transdermal illumination was demonstrated to be feasible for this purpose by Elisseeff *et al.*, who studied the penetration of UV and visible light through the skin and showed the possibility to form fully cross-linked networks within 2 minutes at a specific wavelength and intensity.(2) However the depth of injection highly influenced the cross-link efficiency, therefore, good training of the medical personnel to achieve effective and reproducible gel formation and avoid dosage form failure is of crucial importance. On the other hand, laparoscopic devices or catheters are safer in this respect, as they expose the hydrogel directly to UV or visible light.

One important issue to be evaluated *in vivo* is the effect of photopolymerization on biological tissues. It was indeed reported for some hydrogels that UV cross-linking *in situ* led to remarkable adherence of the depot system to surrounding tissues, most likely due to coupling reactions of hydrogel precursors to membrane proteins.(3) This effect is material-dependent and has to be studied for p(HPMAm-lac)-PEG-p(HPMAm-lac) hydrogels before proceeding towards clinical application.

Michael addition occurs *in situ* without the use of an external stimulus, therefore, the triblock copolymer and the cross-linker (thiolated hyaluronic acid) can be injected easily by a dual syringe and the cross-linking takes place spontaneously between the complementary thiol and (meth)acrylate groups. However, the kinetics of this reaction might be of concern. As it was observed in chapter 5, complete conversion of acrylate and methacrylate groups occurred in 24 and 50 hours, respectively. Although the progressive formation of cross-links

led to free-standing hydrogels after less than 1 hour, it is necessary to establish *in vivo* whether this is sufficient time to prevent burst release of the encapsulated therapeutic. In order to accelerate Michael addition kinetics, the triblock copolymer can be derivatized with maleimide or vinyl sulfone groups,(4-5) compounds well known for their higher reactivity towards thiol groups, as compared to acrylate or methacrylate moieties.

8.2.2.   *Protein release*

The extensive protein delivery studies performed on p(HPMAm-lac)-PEG-p(HPMAm-lac) hydrogels allowed a better understanding of the mechanisms governing the release and clarified the effect of cross-link density on release behavior. The release rate of proteins could be tailored from 2 days up to 2 months and the mechanism was in all cases mediated by Fickian diffusion, meaning that the hydrodynamic radius of the protein is smaller than the pores in the hydrogel network. To tailor the release profiles to even longer timescales and possibly achieve zero order release kinetics, in turn dependent on swelling/degradation kinetics, where the protein is initially immobilized in the network, different polymer architectures can be designed.

To this aim, pHPMAm-lac can be grafted onto multi arm star PEG, as depicted in **Figure 1**. As compared to networks formed of linear polymers, the hydrogels obtained from the self-assembly of star-shaped copolymers are expected to have smaller and denser PEG hydrophilic pores (Figure 1), where the mobility of the encapsulated protein is highly restricted. The synthesis of the thermosensitive star shaped copolymer was tackled in a pilot study described in Appendix E. Currently, the synthesized polymer is being evaluated for its ability to form hydrogels in response to a temperature change and the need for chemical cross-linking to confer higher mechanical strength and stability needs to be investigated. Optimization of the hydrogel network properties will be the topic of future studies and eventually its ability to release proteins in a controlled manner will be investigated.

Besides *in vitro* characterization of the studied thermosensitive systems, the assessment of protein stability is an important issue to be taken into account towards clinical application. The formulation and release of therapeutically relevant proteins must be studied and characterized by using a number of complementary analytical techniques (i.e. fluorescence, CD, *etc.*) to evaluate the preservation of structural stability. Furthermore, the *in vivo* efficacy of the delivery system to release active proteins must be ensured. According to the amount of protein to be delivered and the release time to be achieved, a number of parameters needs to be considered, such as surface area of the depot system upon injection, hydrogel volume and amount of loaded protein.

Protein therapeutics with short half-lives that need to be released in a sustained fashion are normally administered to patients suffering from chronic diseases. Examples of such

proteins are cytokines (i.e. interleukin, interferons), growth factors or hormones (i.e human growth hormone) and they are ideal candidates to be tested in new hydrogel formulations.
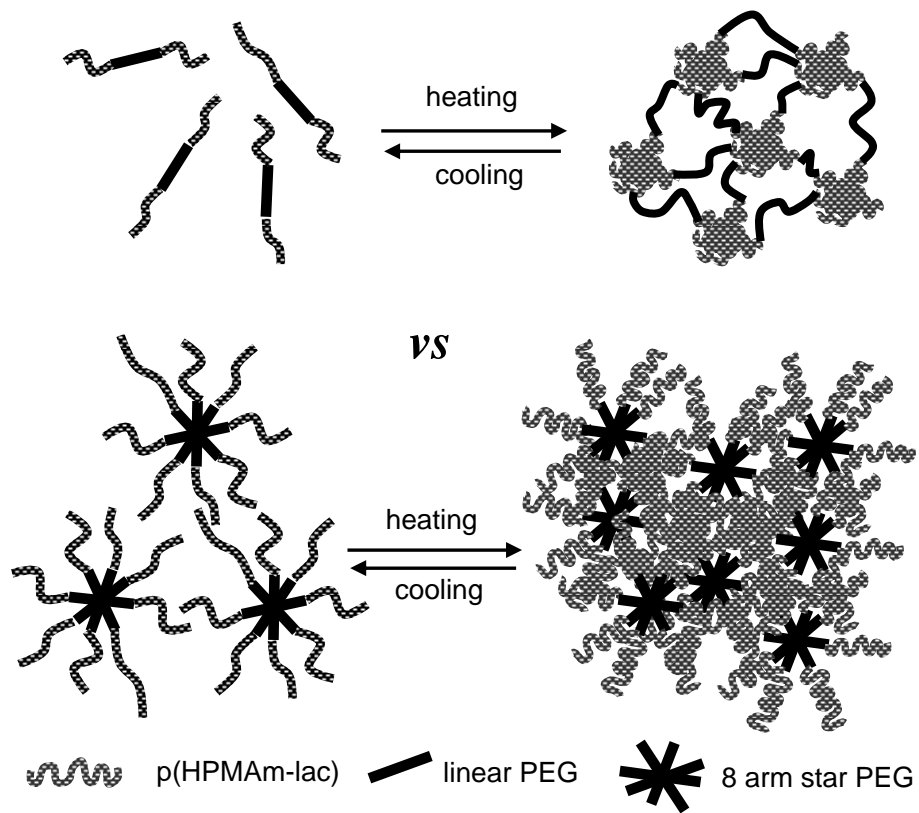

Figure 1. Schematic representation of thermally assembled hydrogels based on linear and star shaped polymers.

8.2.3. Tissue engineering

Because of their soft and rubbery nature, resembling natural tissues, hydrogels have been demonstrated excellent materials for tissue engineering. As described in chapter 6, photopolymerized thermosensitive p(HPMAm-lac)-PEG-p(HPMAm-lac) hydrogels are suitable for bioprinting of three-dimensional (3D) scaffolds aimed at the regeneration of tissues with biomimetic organization. In the specific application of cartilage engineering, the ability of the hydrogel material to support chondrocyte viability was demonstrated. However, further in vitro and in vivo studies have to be carried out to investigate cell differentiation and tissue formation. The studied polymer lends itself to several chemical modifications, such as changes in molecular weight of the PEG as well as of the thermosensitive blocks, extent of

methacrylation and HPMAm mono/dilactate ratio, allowing fine-tuning of polymer cloud point and mechanical properties, degradation behavior and diffusivity of the hydrogels.(6-8) This tailorability opens the possibility to find ideal conditions for the design of complex 3D constructs with appropriate properties for engineering a large number of tissues with biomimetic zones. Besides its potential as structural support, the studied hydrogel holds the potential to regulate cell behavior by incorporating and releasing growth factors in a controlled and tailorable fashion, as demonstrated in chapters 3, 4 and 5 using model proteins and peptides. Moreover, the hydroxyl groups of the polymer can be functionalized with peptides containing adhesive domains (such as KLER or RGD) (9) to enhance cell adhesion and proliferation.

Finally, the thermosensitive hydrogel prepared by Michael addition with thiolated hyaluronic acid is expected to be a promising candidate for tissue engineering due to the well known advantageous biological properties of the hyaluronic acid (10) that as shown in literature exhibits positive interaction with encapsulated cells.

8.2.4. Biodegradation

Hydrogels based on thermosensitive p(HPMAm-lac)-PEG-p(HPMAm-lac) have been extensively characterized *in vitro* for their biodegradability. Their degradation mechanism is based on physiological pH triggered hydrolysis of the many ester bonds present in the polymer. (8, 11) It was shown that the lactate groups attached to the polymerized methacrylate groups hydrolyze at a much slower rate than the lactate chains containing a free hydroxyl terminus. Therefore, highly cross-linked networks, where a higher amount of methacrylate modified lactates are present degrade at a slower rate as compared to networks containing more free hydroxyl terminated lactate chains, as shown in chapter 3, 4 and 5. A good *in vitro-in vivo* correlation in hydrogel biodegradability was found, meaning that hydrolysis is the main mechanism involved in the hydrogel degradation also *in vivo*. The molecular weight and the fate of the degradation products are important aspects to be clarified. In order to be excretable via renal filtration, a polymer needs to be soluble and have a molecular weight below the renal excretion cut-off. For example, it was shown that linear PEG can be excreted up to a molecular weight of 50 kDa, however the excretion threshold for (p(HPMAm-lac)-PEG-p(HPMAm-lac) and its degradation products is not known. Therefore the molecular weight of the degrading compounds has to be determined and their ability to be excreted needs to be assessed.

Recently, Paulusse *et al.* reported on the synthesis of novel cyclic monomers, containing degradable functionalities that can be used for the preparation of linear copolymers *via* RAFT polymerization in combination with other classes of monomers containing methacrylate groups (i.e. 2-hydroxyethyl methacrylate (HEMA)).(12) Potentially, HPMAm-lac could be likewise copolymerized with the monomers described by Paulusse in order to incorporate one or more

orthogonally reactive units into the vinyl backbone, leading to tunable and stepwise degradation of the thermosensitive polymer into products with controllable molecular weight. Of all the monomers synthesized by Paulusse, those containing ester groups are of particular interest for our purpose as they can be hydrolyzed at physiological pH. **Figure 2** shows the chemical structure of copolymers of HPMAm-lac and degradable monomers containing ester groups. An additional benefit of this strategy is the introduction of a site suitable for chemical cross-linking or functionalization in the backbone of the thermosensitive chains (Figure 2).

When the hydrogel is cross-linked via photopolymerization, also another polymeric degradation product is formed (polymethacrylic acid), whose molecular weight needs to be investigated and possibly tuned to the excretable molecular weight by changing the ratio between photoinitiator and methacrylate groups. Moreover, another interesting aspect to be studied is the degradation of the hydrogels cross-linked by hyaluronic acid *in vivo*, where the presence of hyaluronidases, might accelerate the degradation rate of this hydrogels.
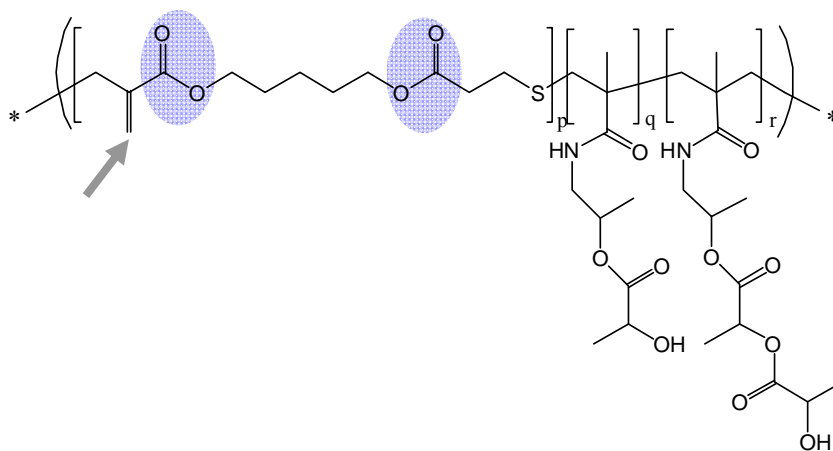

Figure 2. Chemical structure of copolymer of HPMAm-lac and degradable cyclic monomers containing ester groups (blue circles) (potentially hydrolyzable at physiological pH) and groups for chemical cross-linking or additional backbone functionalization (arrow).

8.2.5. *Biocompatibility*

Biocompatibility is an essential requirement to accomplish successful clinical application of novel biomaterials. Photopolymerized thermosensitive p(HPMAm-lac)-PEG-p(HPMAm-lac) hydrogels showed in mice no systemic toxicity, tissue damage or cell apoptosis. The studied implant showed only local inflammatory reaction in the tissues surrounding the depot systems, which is always associated with the bioresorption of synthetic materials. The hydrogel described in chapter 5, where HA is combined with (HPMAm-lac)-PEG-p(HPMAm-lac) is expected to exhibit good biocompatibility, enhanced also by the presence of HA, a

 naturally occurring polymer with appealing biological properties. Experimental proof of this expectation has to be provided.

8.2.6.   *Scale-up stability and sterility*

Other general issues to be tackled for further development of the described thermosensitive hydrogel technology into the clinic are upscaling, stability and sterility. Large scale preparation of clinical grade polymers (e.g. PLGA, poly- -caprolactone etc) has been shown feasible. The main limiting factor in the scale-up process of the synthesis of the polymers described in this thesis resides in the preparation and purification of the monomers HPMAm-lac$_{1,2}$. These compounds are synthesized at low yield (8-10%) and their purification from the reaction mixture is generally costly and time-consuming. In chapter 5, the need of these (expensive) monomers was reduced by randomly copolymerizing *N*-isopropylacrylamide (NIPAm) and HPMAm-lac$_2$ in a NIPAm/HPMAm-lac$_2$ ratio of 76/24. NIPAm is a commercially available monomer and its homopolymer is non-degradable and thermosensitive, with a cloud point of 32ºC. (13-14) When the hydrophobic HPMAm-lac$_2$ (24 mol %) is copolymerized with NIPAm, the cloud point of the obtained copolymer decreases to 23ºC, being still suitable for injection as a liquid when dissolved in aqueous medium. Furthermore, the introduction of HPMAm-lac$_2$ makes the polymer biodegradable, because under physiological conditions, the lactate side chains will be hydrolyzed in time, yielding a more hydrophilic polymer (random pNIPAm and poly(*N*-(2-hydroxypropyl) methacrylamide monolactate) with a cloud point above 37°C. (8, 11, 15) However, it is obvious that this approach is still not an ideal solution to overcome the limitations associated with HPMAm-lac$_{1,2}$ production and alternative routes for the synthesis of these monomers need to be established.

The thermosensitive polymer can be easily lyophilized and in this form it shows long-term stability. The polymer has to be then mixed with protein therapeutic and reconstituted in saline solution before administration.

Finally, the sterility of the polymer can be ensured in two ways: synthesis in aseptic conditions or sterilization after production; both strategies are effective in circumventing possible bacterial contamination. The stability of the polymer to the different sterilization methods available (autoclave, filtration, *etc.*) needs to be assessed.

In conclusion,   this thesis describes novel biodegradable, injectable and thermosensitive hydrogels, as an excellent candidate for controlled protein/peptide delivery and tissue engineering. Its potential to enter the clinic and make an impact on patients' health is envisioned. Before achieving this goal, some important issues need to be tackled in preclinical and clinical studies.

References

1.   Baroli B (2006) Photopolymerization of biomaterials: issues and potentialities in drug delivery, tissue engineering, and cell encapsulation applications. *Journal of Chemical Technology & Biotechnology* 81(4):491-499.

2.   Elisseeff J, Anseth K, Sims D, McIntosh W, Randolph M, & Langer R (1999) Transdermal photopolymerization for minimally invasive implantation. *Proceedings of the National Academy of Sciences of the United States of America* 96(6):3104-3107.

3.   Sawhney AS, Pathak CP, van Rensburg JJ, Dunn RC, & Hubbell JA (1994) Optimization of photopolymerized bioerodible hydrogel properties for adhesion prevention. *Journal of Biomedical Materials Research* 28(7):831-838.

4.   Hiemstra C, van der Aa LJ, Zhong Z, Dijkstra PJ, & Feijen J (2007) Rapidly in situ-forming degradable hydrogels from dextram triols through Michael addition. *Biomacromolecules* 8(5):1548-1556.

5.   Hiemstra C, Van Der Aa LJ, Zhong Z, Dijkstra PJ, & Feijen J (2007) Novel in situ forming, degradable dextran hydrogels by michael addition chemistry: Synthesis, rheology, and degradation. *Macromolecules* 40(4):1165-1173.

6.   Soga O, van Nostrum CF, & Hennink WE (2004) Poly(N-(2-hydroxypropyl) Methacrylamide Mono/Di Lactate): A New Class of Biodegradable Polymers with Tuneable Thermosensitivity. *Biomacromolecules* 5(3):818-821.

7.   Tai H, Wang W, Vermonden T, Heath F, Hennink WE, Alexander C, Shakesheff KM, & Howdle SM (2009) Thermoresponsive and Photocrosslinkable PEGMEMA-PPGMA-EGDMA Copolymers from a One-Step ATRP Synthesis. *Biomacromolecules* 10(4):822-828.

8.   Neradovic D, van Steenbergen MJ, Vansteelant L, Meijer YJ, van Nostrum CF, & Hennink WE (2003) Degradation Mechanism and Kinetics of Thermosensitive Polyacrylamides Containing Lactic Acid Side Chains. *Macromolecules* 36(20):7491-7498.

9.   Salinas CN & Anseth KS (2009) Decorin moieties tethered into PEG networks induce chondrogenesis of human mesenchymal stem cells. *Journal of Biomedical Materials Research, Part A* 90A(2):456-464.

10.   Morra M, Cassinelli C, Cascardo G, Nagel M-D, Della Volpe C, Siboni S, Maniglio D, Brugnara M, Ceccone G, Schols HA, & Ulvskov P (2004) Effects on Interfacial Properties and Cell Adhesion of Surface Modification by Pectic Hairy Regions. *Biomacromolecules* 5(6):2094-2104.

11.   Rijcken CJ, Snel CJ, Schiffelers RM, van Nostrum CF, & Hennink WE (2007) Hydrolysable core-crosslinked thermosensitive polymeric micelles: Synthesis, characterisation and in vivo studies. *Biomaterials* 28(36):5581-5593.

12.   Paulusse JMJ, Amir RJ, Evans RA, & Hawker CJ (2009) Free Radical Polymers with Tunable and Selective Bio- and Chemical Degradability. *Journal of the American Chemical Society* 131(28):9805-9812.

13.   Heskins M & Guillet JE (1968) Solution Properties of Poly(N-isopropylacrylamide). *Journal of Macromolecular Sciences, Part A: Pure Applied Chemistry* 2(8):1441 - 1455.

14.   Schild HG (1992) Poly(N-isopropylacrylamide): experiment, theory and application. *Progress in Polymer Science* 17(2):163-249.

15.   Soga O, van Nostrum CF, Ramzi A, Visser T, Soulimani F, Frederik PM, Bomans PHH, & Hennink WE (2004) Physicochemical Characterization of Degradable Thermosensitive Polymeric Micelles. *Langmuir* 20(21):9388-9395.

Appendices

Appendix A: Supporting Information Chapter 2

A1. Rheology of non-photopolymerized gels

A1.1.   Methods

Rheological characteristics of non-photopolymerized gels were studied on an AR G-2 (TA-Instruments), using a cone-plate geometry (steel, 20 mm diameter with an angle of 1º) and using a solvent trap to prevent evaporation of the solvent. A strain of 0.1% and a single frequency of 1 Hz were applied.

A1.2.   Results

Figure 1SI shows the G' and G'' of a 35% aqueous solution of triblock copolymer in the temperature range from 5 to 45 °C.
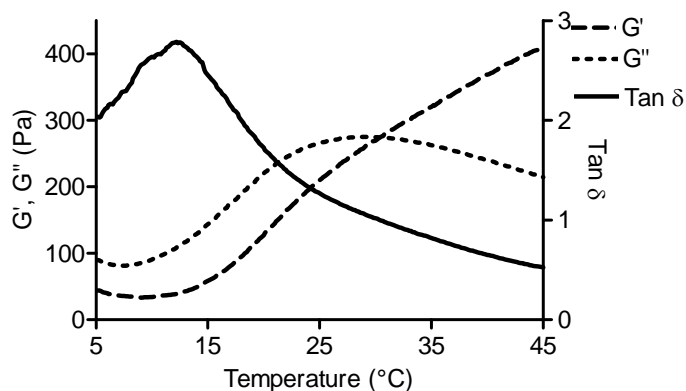

Figure 1SI. Storage modulus (G'), loss modulus (G'') and tan δ (G''/G') of an aqueous system of p(HPMAm-lac)-PEG-p(HPMAm-lac) triblock copolymer (35% w/w) as a function of temperature.

In agreement with previous observations (1), the storage modulus increases with increasing temperature. At 31 °C, when the loss modulus equals the storage modulus, the gel point was reached (2-3). Above 31°C the non-polymerized gels showed typical viscoelastic behavior with *tan δ (=G''/G')* varying between 0.5 and 1. The polymer solutions at lower concentrations (20 and 25%) did not show gelation up to 45 ºC. This confirms that the gelation point is dependent on the polymer concentration (1) and the critical gel concentration is between 25 and 35% w/w for temperatures below 45 °C.

A2.   Lysozyme structure and activity

A2.1.   Methods

The enzymatic activity of lysozyme was determined using the decrease in optical dispersion at 450 nm of a *M. luteus* suspension, essentially as described previously (4-5). The enzymatic activity of lysozyme in the release samples was related to that of native lysozyme

The secondary structure of released lysozyme (in PBS solution pH 7.4, at the concentration of 0.1 mg/ml) was studied by circular dichroism (CD) measurements, from 200 nm to 260 nm and using a cuvette with a path length of 0.5 cm. The spectra of the released lysozyme were compared to that of native lysozyme dissolved in PBS at pH 7.4 at the same concentration as the released lysozyme.

A2.2.   Results

CD measurements revealed that there were no changes in the spectra of the lysozyme released after 168 hours when compared to native lysozyme (**Figure 2SI**), indicating that the secondary structure of the protein was preserved.
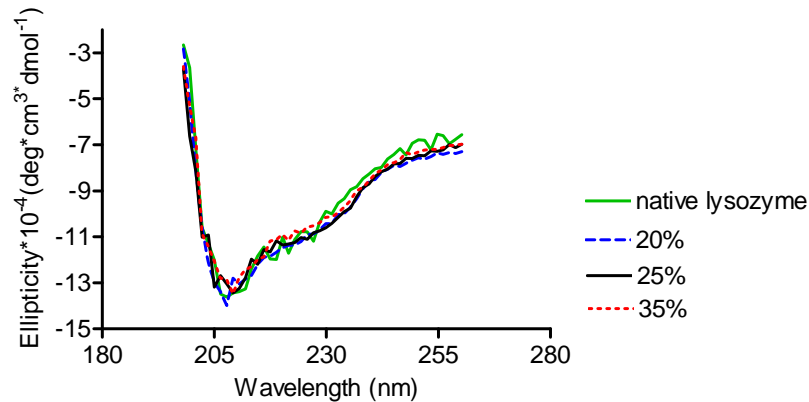
Figure 2SI. Far UV circular dichroism spectra of lysozyme released from photopolymerized hydrogels (20, 25, 35% w/w polymer concentration) compared to the spectrum of reference native lysozyme.
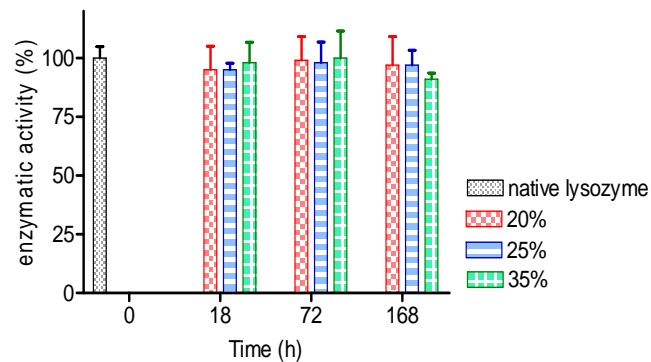

Figure 3SI. Residual enzymatic activity of lysozyme released from photopolymerized hydrogels compared to activity of reference native lysozyme.

The bioactivity assay showed that the specific activity of released lysozyme after 18, 72 and 168 hours was unaltered (**Figure 3SI**), when compared with that of the native protein.

References

1. Vermonden T, Besseling NAM, van Steenbergen MJ, & Hennink WE (2006) Rheological Studies of Thermosensitive Triblock Copolymer Hydrogels. *Langmuir* 22(24):10180-10184.

2. Larson RG (1998) *The Structure and Rheology of Complex Fluids* (Oxford Univ Pr, New York).

3. Chambon F & Winter HH (1987) Linear Viscoelasticity at the Gel Point of a Crosslinking PDMS with Imbalanced Stoichiometry. *Journal of Rheology* 31(8):683-697.

4. Ghaderi R & Carlfors J (1997) Biological Activity of Lysozyme After Entrapment in Poly (d,l-lactide-co-glycolide)-Microspheres. *Pharmaceutical Research* 14(11):1556-1562.

5. van de Weert M, Hoechstetter J, Hennink WE, & Crommelin DJA (2000) The effect of a water/organic solvent interface on the structural stability of lysozyme. *Journal of Controlled Release* 68(3):351-35

Appendix B: Supporting Information Chapter 4

B1.   Materials and methods

The mobility of FITC-labeled BSA (obtained from Sigma Aldrich) in 20 and 35 wt% hydrogels having different methacrylation extent or PEG B-block length was studied by FRAP analysis. FITC-BSA loaded gels were prepared as described in the Material and Methods section of the main text. Prior to photopolymerization, a spatula tip of the mentioned hydrogels was placed between two objective glasses, separated by a 0.5 mm thick adhesive spacer (Secure-Seal Spacer, Molecular Probes, Leiden, The Netherlands). Next, the gel was photopolymerized during 5 minutes. Measurements were performed using a previously published FRAP method.[1] FRAP experiments were carried out at a temperature of 37°C on a confocal scanner laser microscope (MRC1024 UV, Bio-Rad, Hemel Hempstead, UK) modified for bleaching arbitrary regions. A 488-nm line of a 4W Ar-ion laser (Stabilite 2017; Spectra Physics, Darmstadt, Germany) was used for photobleaching and imaging. Uniform disks of 40 μm diameter were bleached at high laser intensity (between 2 and 5 mW at the sample) of the scanning laser beam and the recovery of fluorescence in that area was monitored during 1 min by using a strongly attenuated laser beam (between 10 and 50 μW). The microscope was equipped with a 10× objective lens (CFI Plan Apochromat; Nikon, Badhoevedorp, The Netherlands). The local diffusion coefficient and immobile fraction were calculated from the experimental recovery curve by fitting the appropriate FRAP model.(1)

B2.   Results and Discussion

Figure 1SIA shows that 20 wt% polymer hydrogels of varying methacrylation degree do not show statistically significant differences in diffusion coefficients of FITC-BSA because at this concentration the protein, mainly located in the hydrophilic pores of the network, is not hindered in its mobility by the chemical cross-links that stabilize the hydrophobic domains. On the contrary, at higher polymer concentration (35 wt%), the protein is also partly located in the hydrophobic domains, where a higher cross-link density leads to a decrease in mobility, as shown in Figure 1SI A. In **Figure 2SI**, diffusion coefficients and mobile fractions of polymer hydrogels of different PEG blocks is reported. Both diffusion coefficients (Figure 2SIA) and mobile fractions (Figure 2SI B) decrease with increasing PEG molecular weight. As clear from confocal laser scanning microscopy (Chapter 4), the hydrogels undergo a phase-separation into hydrophilic and hydrophobic domains with bigger hydrophilic pores at lower PEG molecular weight. In bigger hydrophilic pores the protein mobility is less restricted.

A

B
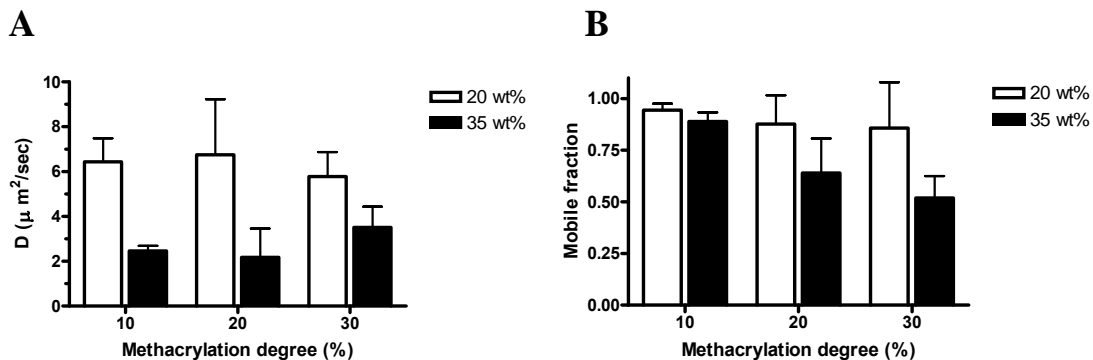
Figure 1SI. A) Diffusion coefficients and **B)** mobile fractions of polymer hydrogels having different methacrylation extent (10, 20 and 30%) calculated for a fluorescence recovery time of 1 min. Data are shown for 20 (white bars) and 35 wt% (black bars) polymer concentration as mean ± standard deviation; n = 3.

A

B
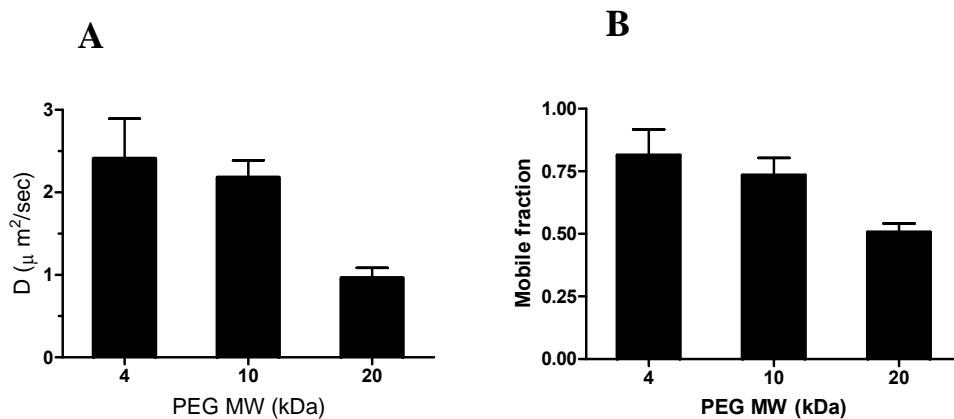
Figure 2SI. A) Diffusion coefficients and **B)** mobile fractions of polymer hydrogels (35 wt% polymer concentration) having different PEG length (4, 10 and 20 kDa) calculated for a fluorescence recovery time of 1 min. Data are shown as mean ± standard deviation; n = 3.

In order to study the correlation between FRAP and release data, the diffusion coefficients of BSA in release experiments (**Figures 3SI** and **4SI**) were calculated by the early-time approximation equation of Fick's second law:(2)

$$M_t / M_\infty = 4 (Dt / \pi\delta^2)^{1/2}$$

Where M_t / M_∞ is the BSA fractional release, D the diffusion coefficient, t the release time and δ the diffusional distance, equal to the thickness of the gels (4.5 and 4.0 mm for 20 and 35 wt% polymer concentration, respectively).

The BSA diffusion coefficients were calculated both for the hydrophilic (Figures 3SI A and 4SI A) and the hydrophobic domains (Figures 3SI B and 4SI B) and compared to those experimentally determined by FRAP measurements. For $M_{10,20,30}P_{10}$ hydrogels, 20 wt% polymer concentration, D values ranging from 5.8 to 6.8 and from 7.8 to 10.9 μm^2/sec were observed in FRAP and release measurements, respectively. These data demonstrated within the experimental error good correlation between release and FRAP data.(3) The good agreement between release and FRAP experiments, showing no influence of the methacrylation extent on BSA diffusion coefficients in 20 wt% $M_{10,20,30}P_{10}$ hydrogels, leads to conclude that the protein release was governed exclusively by diffusion and swelling/degradation of the matrix does not contribute to the release mechanism.

At the polymer concentration of 35 wt%, where a biphasic release was observed, FRAP showed D values falling between diffusion coefficients calculated according to BSA release from the hydrophilic and the hydrophobic domains (black bars in Figure 3SI A-B). Since large bleach areas were used for the FRAP experiments, covering both hydrophilic and hydrophobic domains, the resulting D values take into consideration both the fast and slow-diffusing BSA in the hydrogel network. Mobile fractions determined by FRAP exhibited excellent correlation with release data, as the mobile fraction corresponded to the cumulative fractional release for both 20 and 35 wt% hydrogels. This observation implies that the protein, residing in the hydrophobic domains of increasing methacrylation extent, has highly restricted mobility and needs further degradation of the hydrogel matrix to be fully released.

A

B
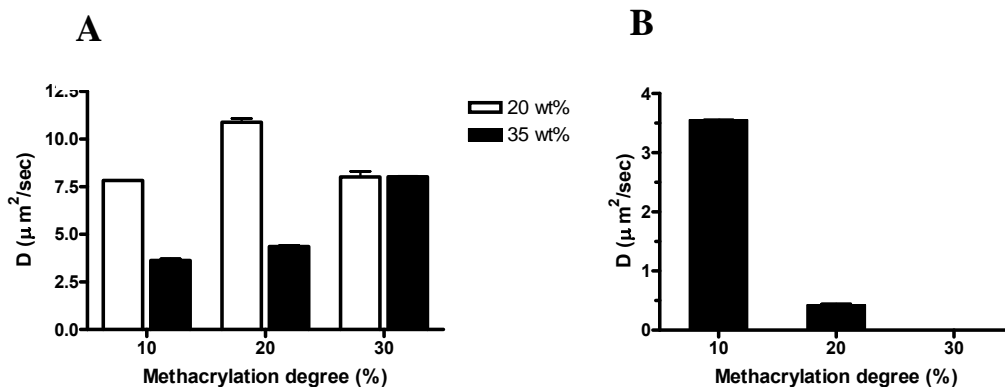
Figure 3SI. Diffusion coefficients of BSA in polymer hydrogels having different methacrylation extent (10, 20 and 30%) calculated by fitting the release profile from the hydrophilic (A) and the hydrophobic domains (B) to Fick's second law. Data are shown for 20 (white bars) and 35 wt% (black bars) polymer concentration as mean ± standard deviation; n = 3.

Figure 4SI represents the diffusion coefficients of BSA encapsulated in hydrogels of different PEG molecular weight, calculated from release profiles. A single diffusion coefficient was calculated based upon the monophasic release of 20 wt% $M_{20}P_{4,10,20}$ and 35 wt% $M_{20}P_{20}$,

whereas two D's were calculated for 35 wt% $M_{20}P_{4,10}$, as a biphasic release was observed. FRAP data, shown in Figure 2SI only for 35 wt% $M_{20}P_{4,10,20}$ hydrogels, indicated intermediate diffusion coefficients between those calculated according to release kinetics in hydrophilic and hydrophobic domains (Figure 4SI), similarly to 35 wt% $M_{10,20,30}P_{10}$ hydrogels.

A

B
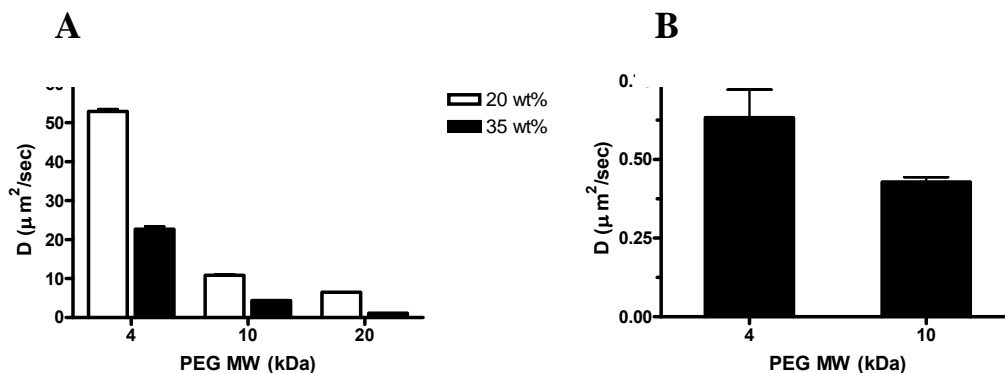
Figure 4SI. Diffusion coefficients of BSA in polymer hydrogels having different PEG molecular weight (4, 10 and 20 kDa) calculated by fitting the release profile from the hydrophilic (A) and the hydrophobic domains (B) to Fick's second law. Data are shown for 20 (white bars) and 35 wt% (black bars) polymer concentration as mean ± standard deviation; n = 3.

References

1. Braeckmans K, Peeters L, Sanders NN, De Smedt SC, & Demeester J (2003) Three-Dimensional Fluorescence Recovery after Photobleaching with the Confocal Scanning Laser Microscope. *Biophysical Journal* 85(4):2240-2252.

2. Ritger PL & Peppas NA (1987) A simple equation for description of solute release II. Fickian and anomalous release from swellable devices. *Journal of Controlled Release* 5(1):37-42.

3. Brandl F, Kastner F, Gschwind RM, Blunk T, Teßmar J, & Göpferich A (2010) Hydrogel-based drug delivery systems: Comparison of drug diffusivity and release kinetics. *Journal of Controlled Release* 142(2):221-228.

Appendix C: Supporting Information Chapter 5

C1. Time-sweep experiments of HA-SH and pNHPt(m)a solutions

The same experimental settings as described in Chapter 5 for time-sweep experiments were used.

In principle, the chemical cross-linking process of the hydrogels can follow two different pathways, the Michael addition cross-linking between thiols on HA and (meth)acrylates on pNHPt(m)a and the disulfide bonding between thiols. In order to investigate the contribution of these two pathways to the hydrogel formation, control rheological experiments on HA-SH solution 5.4 wt% in PBS pH 7.4 (**Figure 1SI**) and pNHPtma solution 20 wt% in the same buffer (**Figure 2SI**) at 37 °C were performed during 200 and 150 minutes, respectively.

Figure 1SI shows that HA-SH solutions 5.4 wt% displayed very low values of G' (< 2 Pa), which did not increase significantly in time, meaning that no or negligible disulfide bonding occurred at the used experimental conditions. Therefore, it can be concluded that Michael addition cross-linking is responsible for the covalent network formation.
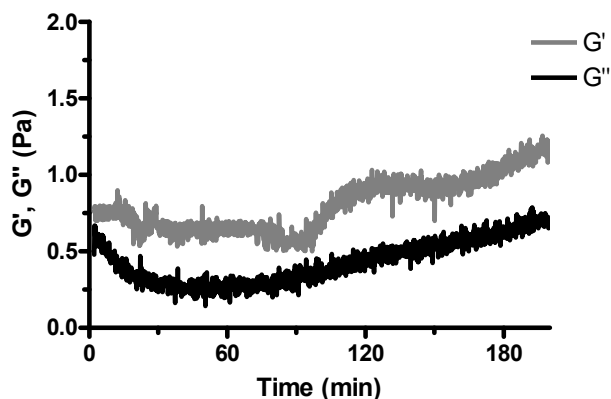
Figure 1SI. Storage (*G'*) and loss (*G"*) moduli of HA-SH solution 5.4 wt% in PBS pH7.4 as a function of time at 37 °C.

Figure 2SI shows that at 37 °C pNHPtma solutions 20 wt% behaved as a weak viscoelastic material, as the storage modulus dominates the loss modulus. This behavior is due to the thermosensitive properties of the polymer. However, at the used concentration, the physical networks are very weak, as they have very low values of G'. When combined with 5.4 wt% of HA-SH, pNHPtma hydrogels increased their strength remarkably in time. After 150 minutes, G' of the HA-SH/pNHPtma gel is approximately 25 times higher than G' of pNHPtma gel. It can be concluded that, although the thermal self-assembly of pNHPtma polymer contributes to an initial stability of the network, making in situ stability of the gel upon

injection possible, Michael addition cross-linking with HA-SH is needed to enhance the hydrogel strength and prevent the hydrogel dissolution.
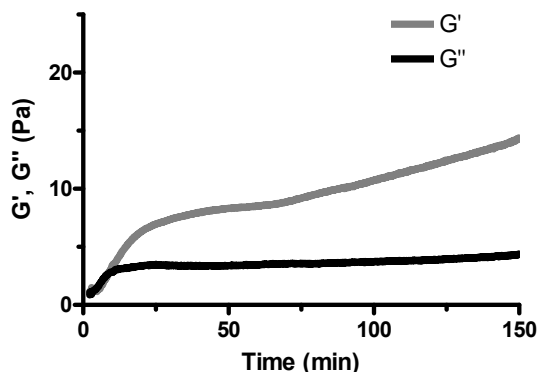
Figure 2SI. Storage (*G′*) and loss (*G″*) moduli of pNHPtma hydrogel 20 wt% in PBS pH7.4 as a function of time at 37 °C.

C2. Dynamic Mechanical Analysis (DMA)

A DMA 2980 Dynamic Mechanical Analyzer (TA-Instruments) in the controlled force mode was used for elastic modulus measurements. Hydrogels of approximately 5 × 6 mm (diameter × height) were placed between the parallel plates and a force ramp from 0.001 to 1.0 N at a rate of 0.1 N/min was applied at 25 ºC.
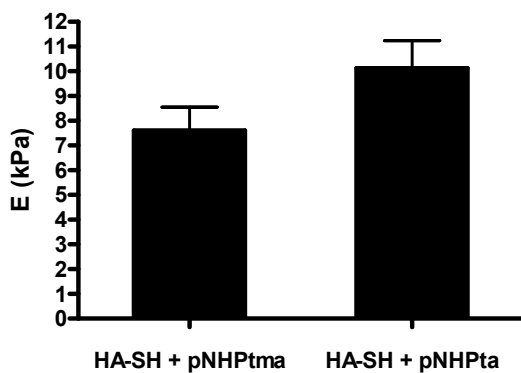
Figure 3SI. Elastic moduli of polymer gels (polymer concentration: 20 wt% pNHPt(m)a + 5.4 wt% HA-SH; molar ratio thiol:(meth)acrylate groups = 1:1) after Michael addition reaction for 24h. Data are shown as mean ± standard deviation; n=3.

Elastic modulus (E) values of approximately 8 and 10 kPA, for methacrylate and

acrylate modified polymer hydrogels were observed (**Figure 3SI**). The slightly higher E value displayed by acrylated gels as compared to the corrspondent methacrylated networks finds explanation in the higher acrylate conversion into chemical cross-links exhibited by pNHPta gels after 24 hours, as shown in figure 4 of the main text. DMA measurements are in agreement with the mechanical characterization performed on pNHPt(m)a hydrogels (Figure 2, chapter 5), where faster gelation kinetics of pNHPta hydrogels due to higher reactivity of acrylates toward Michael addition was demonstrated.

C3.   Temperature-sweep of pNHPtma and pNHPta + HA-SH polymer gels

The same experimental settings as described in the main article for temperature sweep experiments were used.

At increasing temperature from 5 to 45ºC, gelation starts at 14 and 21 °C for pNHPta and pNHPtma hydrogels, respectively (**Figure 4SI**). This difference in gel point, defined as temperature at which G' equals G'', can be attributed to the slightly lower CP of pNHPta as compared to pNHPtma polymers (16 and 18.8 °C, respectively), as well as to the faster formation of Michael addition cross-links in pNHPta hydrogels.
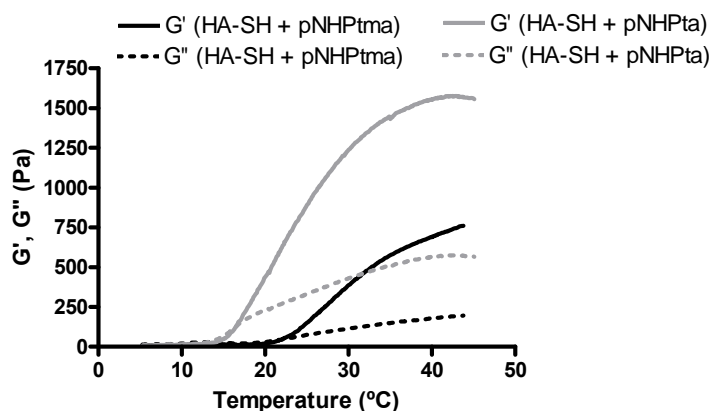
Figure 4 SI: Storage (*G'*) and loss (*G''*) moduli as a function of temperature (heating rate 1 ºC/min) directly after mixing of HA-SH with pNHPtma and pNHPta, respectively. Polymer concentration: 20 wt% pNHPtma or pNHPta + 5.4 wt% HA-SH.

Appendix D: Supporting Information Chapter 6
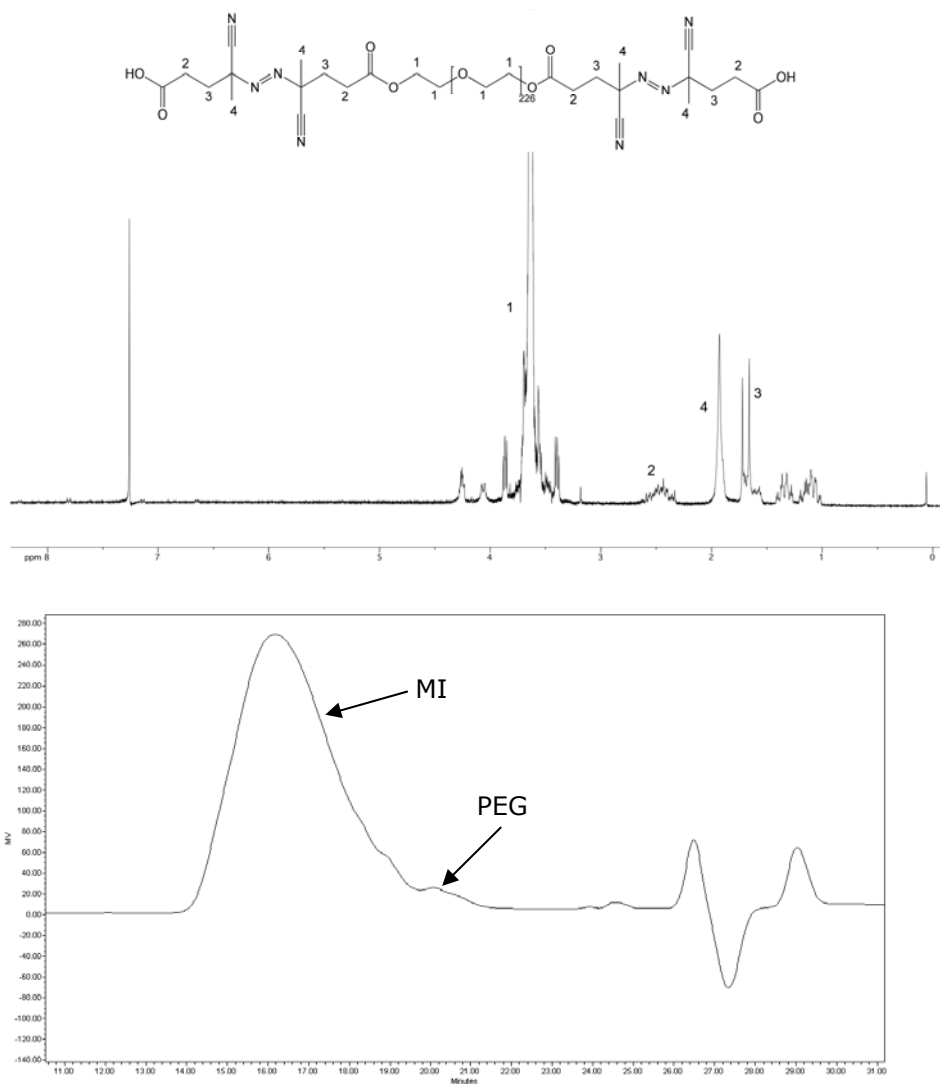
Figure 1SI. GPC chromatogram of (PEG-ABCPA)$_n$ macroinitiator (MI); a trace amount of unreacted PEG (< 1 % based on AUC)

Figure 2SI. ^{1}H-NMR spectrum of (PEG-ABCPA)$_n$ macroinitiator (MI) in CDCl$_3$. By comparing the integration of PEG protons to those of ABCPA, a ratio PEG/ABCPA of 1.2 was calculated, demonstrating the presence of a small amount of unreacted PEG in the MI.
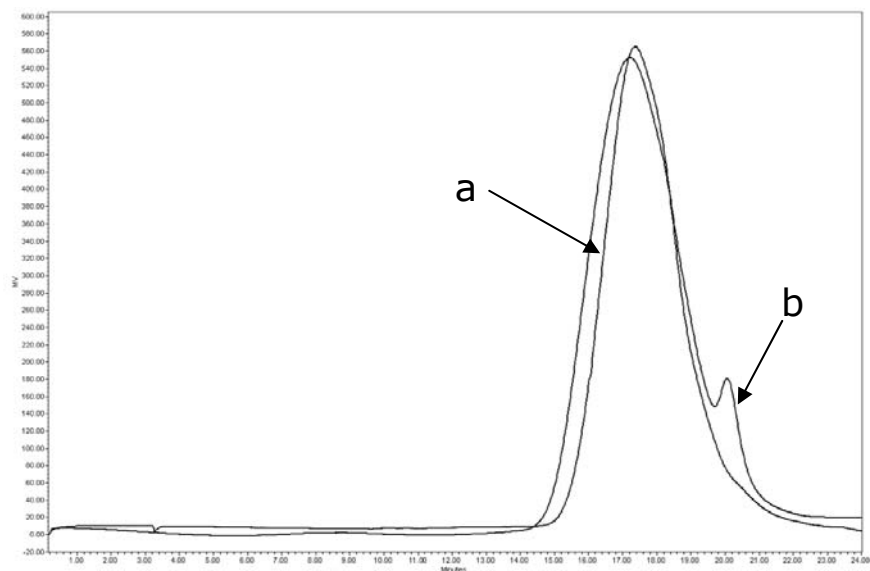
Figure 3SI. Comparison of GPC chromatograms of PEG-pHPMAm-lactate triblock copolymers ($M_{30}P_{10}$) synthesized using dialyzed (a) and non-dialyzed (b) (PEG-ABCPA)$_n$ macroinitiator. The presence of unreacted ABCPA in the non-dialyzed macroinitiator leads to the formation of polymers of HPMAm-lactate without PEG chain during the radical copolymerization of PEG and HPMAm-lactate, visible as side peak in chromatogram (b). It appears that dialysis is an effective method to purify the unreacted ABCPA from the macroinitiator and prevent the formation of polymers of HPMAm-lactate without PEG chain, as shown in chromatogram (a).

Appendix E

Synthesis of thermosensitive star shape copolymer based on poly(hydroxypropyl methacrylamide lactate) and star poly(ethylene glycol)

Thermosensitive star shape copolymer based on poly(hydroxypropyl methacrylamide lactate) and star poly(ethylene glycol) (PEG-(p(HPMAm-lac)$_8$)) was synthesized by applying the route described in **Figure 1**. Briefly, mercaptoacetic acid was reacted with triphenyl methanol (in a molar ratio of 1) in anhydrous trifluoroacetic acid, while stirring for 2 hours at room temperature to protect the thiol group (step 1). The product, precipitated in diethyl ether, had a yield of 70%. Subsequently, the trityl-protected mercaptoacetic acid was esterified with 8 arm star PEG 10 kDa by DCC coupling reaction, using 4-(dimethylamino)pyridinium 4-toluene-sulfonate (DPTS) as a catalyst and a ratio between thiol and hydroxyl group of 1 (step 2). The reaction was carried out for 16 hours in a 50/50 mixture of tetrahydrofuran/dichloromethane.

Step 1. Protection mercaptoacetic acid by triphenyl methanol
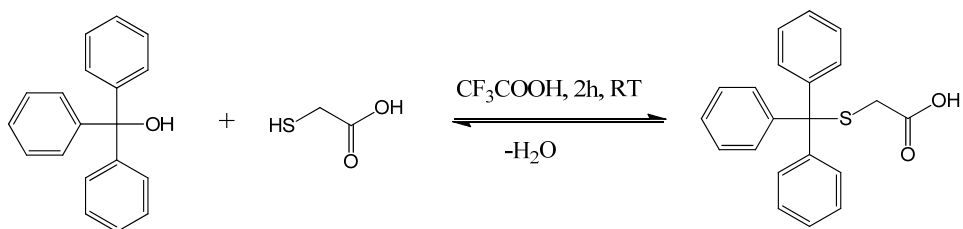
Step 2. DCC coupling reaction between PEG 8 arms and protected mercapto acetic acid.
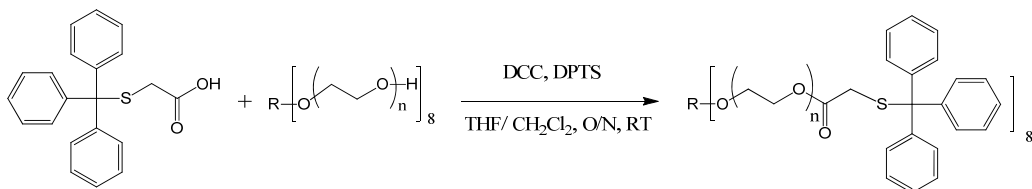
R = hexaglycerine core:
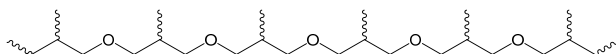
Step 3. Deprotection thiol groups
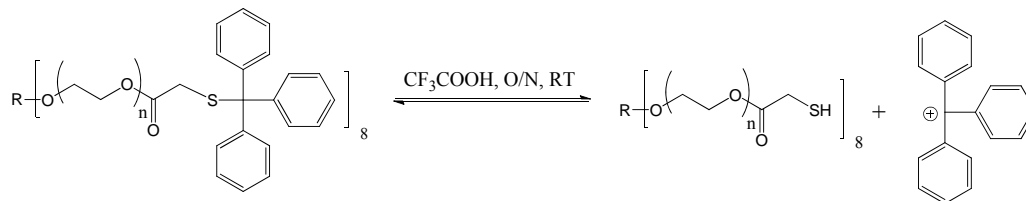
Step 4. Copolymerization thiolated star PEG and HPMAm-lac$_{1-2}$
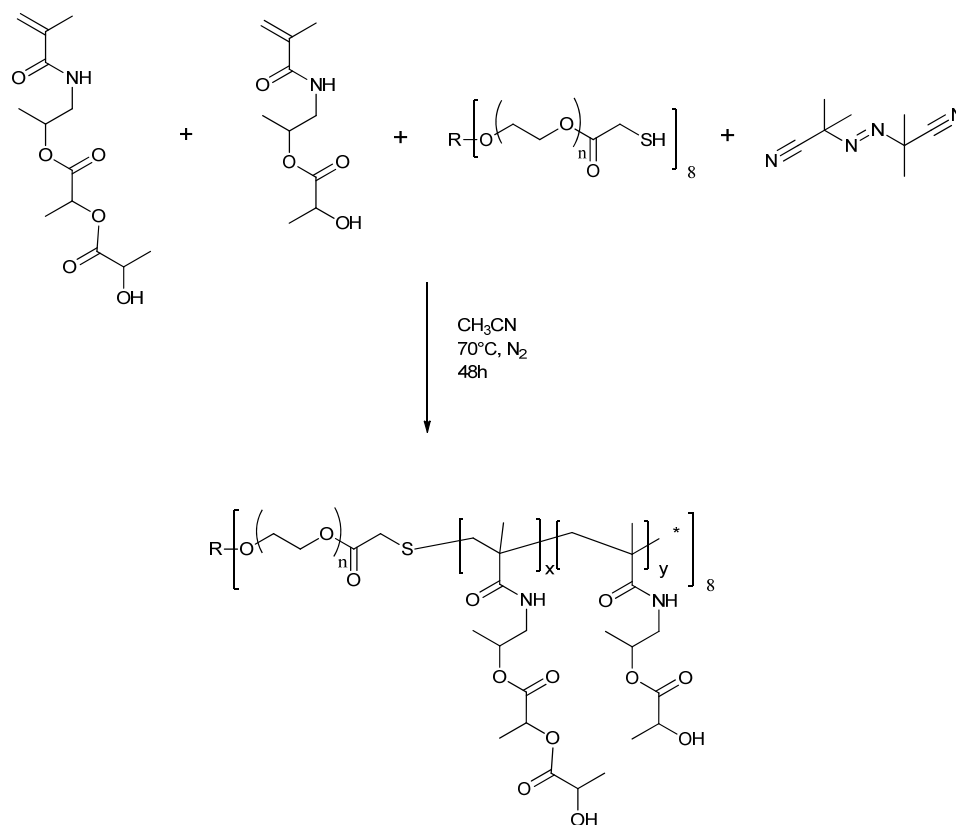
Figure 2. Synthetic route of star shaped PEG-(p(HPMAm-lac)$_8$ copolymer consisting of PEG 8 arms 10 kDa flanked with thermosensitive p(HPMAm-lac) side chains.

The product was isolated after precipitation with diethylether and a yield of approximately 65% was obtained. ^{1}H-NMR analysis in dimethyl sulfoxide (DMSO) showed that 5.5 arms of PEG were derivatized with protected mercaptoacetic acid. Next, thiolated PEG was deprotected in anhydrous trifluoroacetic acid and purified by precipitation in diethylether (step 4). With a

yield of approximately 60%, the product was characterized by ^{1}H-NMR in DMSO to assess the absence of protecting group, additionally, the free thiol groups were quantified by Ellmann's reaction, which showed that 85% of the protected groups were deprotected. Finally, a chain transfer agent (CTA) polymerization was performed from the thiolated PEG using *N*-2-hydroxypropyl methacrylamide mono and dilactate (HPMAm-lac$_{1,2}$) (ratio HPMAm-lac$_1$/HPMAm-lac$_2$ = 1) as monomers, and 2,2 '-Azodiisobutyronitrile (AIBN) as initiator. The reaction was carried out in acetonitrile at 70 °C, under nitrogen atmosphere for 48 hours. The CTA reaction had a yield of 65% and resulted in a copolymer exhibiting thermosensitive behavior (LCST 29 °C) and having a M$_n$ of 27.1 kDa and M$_w$ of 48.6, as determined by GPC. **Figure 2** shows the shift of the GPC peak of PEG towards shorter retention time upon copolymerization with the thermosensitive chains.

(a)

(b)
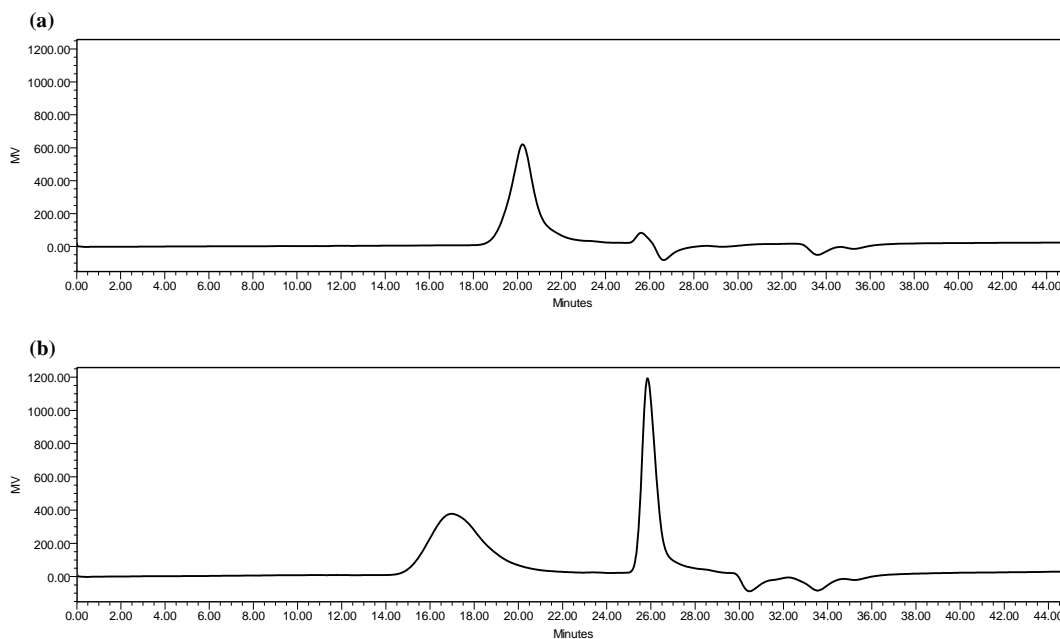
Figure 2. GPC chromatograms of (a) 8 arms star PEG 10 kDa and (b) (p(HPMAm-lac)$_8$-PEG copolymer based on 8 arms star PEG 10 kDa.

222

Nederlandse samenvatting

Hydrogelen hebben een lange geschiedenis. De ontwikkeling van hydrogelen voor zachte contactlenzen startte al in 1960 en sindsdien is de toepassing van hydrogelen een nieuwe richting ingeslagen naar geneesmiddelafgifte en 'tissue engineering'. Aangezien hydrogelen bestaan uit polymeernetwerken die grote hoeveelheden water kunnen bevatten, hebben ze veel overeenkomst met natuurlijke weefsels waardoor het aantrekkelijke materialen zijn voor biomedische toepassingen.

Tegenwoordig wordt veel aandacht geschonken aan het ontwikkelen van polymeren die geschikt zijn om onder fysiologische omstandigheden netwerken te vormen, waarin eiwitten kunnen worden ingesloten en tegelijkertijd worden beschermd tegen degradatie. Het ultieme doel is therapeutisch actieve eiwitten over een lange periode op een gereguleerde manier te kunnen afgeven aan de patiënt.

Ook hebben hydrogelen grote potentie binnen het relatief nieuwe veld van 'tissue engineering'. Cellen kunnen worden ingesloten in de polymeermatrix en in deze beschermde omgeving kunnen de cellen groeien en differentiëren en uiteindelijk het beschadigd weefsel herstellen. Een belangrijke eis aan materialen voor deze toepassingen is dat ze bioafbreekbaar zijn in uitscheidbare en onschadelijke producten.

Deze onderwerpen – gereguleerde afgifte van eiwitten en regeneratie van weefsels – vormen het centrale thema van dit proefschrift, waarin de toepasbaarheid van injecteerbare, *in situ* gelerende hydrogelen gebaseerd op temperatuurgevoelige triblokcopolymeren wordt beschreven.

In **hoofdstuk 1** worden de algemene eigenschappen van hydrogelen geschetst met speciale aandacht voor vernettingsmethoden voor polymeren die geschikt zijn voor *in situ* gelering, zoals fotopolymerisatie, Michael-additiereacties en temperatuurgedreven zelf-assemblage

In **hoofdstuk 2** wordt een uitgebreid overzicht gegeven van hydrogelen als eiwitafgiftesystemen. Het gebruik van hydrogelen als afgiftesysteem kan een oplossing zijn voor de snelle eliminatie van therapeutische eiwitten uit de bloedbaan. Een constant gereguleerde afgifte zorgt ervoor dat de dosis binnen de therapeutische grenzen blijft en voorkomt dat herhaaldelijke injecties nodig zijn. Daarom zijn hydrogelen met name interessant voor afgifte van farmaca bij chronische aandoeningen. Dit hoofdstuk beschrijft verschillende afgiftemechanismen, zowel *in vitro* als *in vivo* en methoden om de afgiftesnelheid van eiwitten uit hydrogelen te meten en te moduleren.

Hoofdstuk 3 rapporteert de afgifte van drie verschillende eiwitten (lysozym, BSA en IgG) uit temperatuurgevoelige hydrogelen die opgebouwd zijn uit triblokcopolymeren bestaande uit een hydrofiel polyethyleenglycol (PEG) middenblok geflankeerd door twee temperatuurgevoelige poly(hydroxypropyl methacrylamide lactaat) (pHPMAlac) blokken. Deze polymeren zijn oplosbaar in water bij lage temperatuur en zelfassembleren bij temperaturen

hoger dan 31 ºC. Bovendien is 10% van de lactaatgroepen gefunctionaliseerd met methacrylaatgroepen die gebruikt worden om na temperatuur-geïnduceerde gelering, de gelen te stabiliseren door middel van fotopolymerisatie. De afgifte van bovengenoemde eiwitten verliep diffusie-gereguleerd en resulteerde in een snelle afgifte van kleine eiwitten (lysozym) en een langzamere afgifte van grotere eiwitten (IgG). Verder kan de afgiftesnelheid gevarieerd worden door veranderingen in polymeerconcentratie.

Hoofdstuk 4 beschrijft het vervolg op deze studie, waarin de precieze moleculaire structuur van de polymeren is gevarieerd om hydrogelen te verkrijgen met gewenste mechanische eigenschappen, afgifte- en degradatiesnelheid. Opvallend is dat hydrogelen gebaseerd op polymeren met een korte hydrofiele PEG-keten een snelle eiwitafgifte vertoonden. Dit fenomeen werd verklaard met behulp van confocale microscopie experimenten, die een sterke fasescheiding in hydrofiele en hydrofobe gebieden aantoonden voor deze gelen.

Hoofdstuk 5 beschrijft een nieuw hydrogelsysteem dat bestaat uit twee componenten. De eerste component is het temperatuurgevoelige polymeer zoals beschreven in hoofdstuk 3 en 4. De tweede component is hyaluronzuur (HA) gefunctionaliseerd met thiolgroepen (HA-SH). Deze thiolgroepen kunnen een Michael-additiereactie ondergaan met de methacrylaat- of acrylaatgroepen aan het temperatuurgevoelige polymeer onder fysiologische omstandigheden. De reactie tussen deze twee polymeren levert dan een chemisch verknoopt netwerk op dat gedeeltelijk bestaat uit het natuurlijke HA. Het gebruik van een combinatie van synthetische en natuurlijke polymeren in een hydrogelmatrix wordt gezien als een effectieve strategie om de biocompatibiliteit te vergroten en tegelijkertijd een betere interactie te verkrijgen tussen cellen en gel. De simultane thermische gelering en Michael-additiereactie is bestudeerd met reologiemetingen. Een fysisch verknoopt netwerk werd in enkele uren gestabiliseerd door de vorming van chemische knooppunten tussen de verschillende polymeerketens. De sterkte en degradatiesnelheid van deze gelen bleek afhankelijk van het gebruik van acrylaat- of methacrylaatgroepen aan de temperatuurgevoelige polymeren. Deze gelen zijn ook gebruikt om de *in vitro* afgifte van een modelpeptide (bradykinine) te bestuderen. De afgifte van dit peptide was diffusie-gereguleerd en de afgiftesnelheid kon gevarieerd worden door veranderingen in polymeerconcentratie.

Een andere interessante toepassing van de gefotopolymeriseerde temperatuurgevoelige hydrogelen voor tissue engineering is onderzocht in **hoofdstuk 6**. De polymeren zijn gebruikt voor een 3D-printtechniek waarbij driedimensionale hydrogelscaffolds zijn ontworpen voor kraakbeenregeneratie. De polymeeroplossingen zijn bij lage temperatuur geprint op een verwarmde ondergrond. Door de thermische gelering ontstaat direct een stabiele gel. Verschillende lagen van gelvezels zijn op deze manier geprint en daarna gestabiliseerd door UV-belichting. De gelen konden geprint worden tot ten minste 37 lagen en deze scaffolds hadden een elastische modulus van 119 kPa. De mogelijkheid om deze materialen te gebruiken voor het ontwerp van scaffolds met eigenschappen van georganiseerd weefsel werd

aangetoond. Bovendien is in deze hydrogelen een goede overleving van chondrocyten aangetoond na 1 en 3 dagen.

Hoofdstuk 7 rapporteert een biocompatibiliteitsstudie betreffende de gefotopolymeriseerde temperatuurgevoelige hydrogelen na implantatie in muizen. Er treedt een lokale ontstekingsreactie op in het aangrenzende weefsel met een groot aantal geïnfiltreerde macrofagen gedurende de hele tijdsduur van het experiment (42 dagen). Deze ontstekingsreactie is geassocieerd met de bioresorptie van het materiaal en kan gezien worden als een milde reactie omdat er geen systemische reactie optrad en een constante afname van geïnfiltreerde neutrofielen in de tijd werd waargenomen. De *in vitro* degradatietijd van de gelen komt goed overeen met die gevonden *in vivo*.

Concluderend kan vastgesteld worden dat het werk beschreven in dit proefschrift heeft laten zien dat de nieuwe injecteerbare temperatuurgevoelige hydrogelen een goede biodegradeerbaarheid, goede eiwit-, cel- en weefselcompatibiliteit en veel aanpassingsmogelijkheden met betrekking tot mechanische eigenschappen, degradatie en afgiftesnelheid bezitten. Daarmee is aangetoond dat het veelbelovende materialen zijn voor zowel gereguleerde eiwitafgifte als voor tissue engineering.

Riassunto

Un idrogel è un sistema colloidale costituito da reticoli tridimensionali di polimeri naturali e/o artificiali, in grado di attrarre considerevoli quantità di acqua ed, allo stesso tempo, di rimanere insolubili in questo mezzo grazie alla presenza di legami crociati, fisici e/o chimici, che legano le catene polimeriche. Gli idrogeli hanno una lunga storia, che inizia nel 1960, quando Wichterle ed i sui colleghi crearono le prime lenti a contatto morbide. Da allora, l'uso degli idrogeli si è espanso considerevolmente verso nuove direzioni, che comprendono il rilascio controllato dei farmaci e l'ingegneria tissutale. Questo crescente interesse per gli idrogeli depende dalla loro dimostrata capacità di interagire positivamente con i sistemi biologici, minimizzando l'aderenza di cellule e proteine e la reazione da corpo estraneo, quando impiantati nell'organismo. Innumerevoli sforzi sono attualmente diretti alla progettazione di idrogeli capaci di formarsi spontaneamente a condizioni fisiologiche, nei quali proteine farmaceutiche possono essere incapsulate e protette dalla degradazione e cellule possono essere accomodate, mantenendo la loro vitalità e funzionalità. Lo scopo ultimo degli idrogeli è quello di rilasciare le proteine incapsulate in maniera controllata per un periodo di tempo prolungato e/o di sostenere la proliferazione delle cellule di cui esso è caricato per la rigenerazione di tessuti/organi artificiali. Infine, dopo aver esercitato la funzione per cui sono preposti, gli idrogeli devono spontaneamente degradare, trasformandosi in prodotti sicuri per la salute umana ed eliminabili dall'organismo tramite vie metaboliche o filtrazione renale.

E' proprio intorno ai temi del rilascio controllato dei farmaci biotecnologici e della rigenerazione di tessuti ed organi artificiali che questa tesi si sviluppa ed ha come scopo quello di dimostrare la potenzialità in questi campi di un idrogelo iniettabile che gelifica spontaneamente a condizioni fisiologiche ed è basato su un copolimero termosensibile a triblocchi di nuova concezione. Il **capitolo 1** descrive le caratteristiche generali degli idrogeli, con particolare attenzione ai metodi di formazione dei legami crociati per idrogeli iniettabili, quali l'addizione di Michael e la fotopolimerizzazione, ed alle caratteristiche dei polimeri di cui essi sono costituiti, come ad esempio glicole polietilenico (PEG) e polidrossipropil metacrilammide (p(HPMAm)).

Il **capitolo 2** approfondisce l'applicazione degli idrogeli come sistemi per il rilascio controllato delle proteine. Il capitolo spiega come gli idrogeli siano utili nel superare le limitazioni associate alla somministrazione di proteine farmaceutiche, quali l'emivita molto breve, la tossicità sistemica, l'instabilità fisica, chimica ed enzimatica. I recenti sviluppi in questo campo vengono poi presentati, passando in rassegna i più significativi idrogeli che gelificano in seguito alla somministrazione e descrivendo vari aspetti del rilascio delle proteine *in vitro* ed *in vivo*, come il meccanismo, i metodi innovativi usati per lo studio, la stabilità del farmaco, le limitazioni ancora esistenti nel comportamento di rilascio degli idrogeli e le strategie per superarle.

Nel **capitolo 3** si descrive l'uso di un polimero costituito da un blocco centrale di PEG, legato a due catene laterali termosensibili di poli(lattato di idrossi propil metacrilammide) (p(HPMAm-lac)-PEG-p(HPMAm-lac)) per la preparazione di un idrogel per il rilascio di proteine. Tale polimero a triblochi è solubile (dunque iniettabile) in medium acquoso a temperatura ambiente e assembla spontaneamente a formare un idrogel a temperatura corporea. Per rendere questo idrogel più stabile in condizioni fisiologiche, il polimero è stato modificato con gruppi methacrilati al fine di introdurre legami crociati covalenti, tramite breve esposizione alla luce UV. Questo capitolo mstra come sia possibile variare le caratteristiche meccaniche e la stabilità alla degradazione dell'idrogel al variare della concentrazione del polimero, la quale influenza anche le cinetiche di rilascio. Lisozima, albumina da siero bovino ed immunoglobulina G monoclonale sono state utilizzate come proteine modello e completamente rilasciate dall'idrogel con un meccanismo di diffusione fickiana e con preservazione della struttura ed attività biologica.

In uno studio successivo, riportato nel **capitolo 4**, abbiamo esplorato come la struttura molecolare del polimero influenzi le caratteristiche finali dell'idrogel. Questo lavoro è volto allo sviluppo di una piattaforma, in cui la flessibilità della chimica polimerica offre l'opportunità di creare una varietà di idrogeli con caratteristiche chimico-fisiche ben definite e profili di rilascio riproducibili e modulabili. L'ottenimento di profili di rilascio modulabili permette di rispondere ai bisogni terapeutici di ciascun farmaco, che è idealmente reso disponibile al tempo ed alla dose desiderata. I profili di degradazione del farmaco sono variati da 25 a 300 giorni, mentre quelli di rilascio da 10 giorni a più di mesi, in base al peso molecolare ed al grado di metacrilazione del polimero. La struttura interna dell'idrogel al variare della struttura chimica del polimero che lo compone è stata studiata tramite microscopia confocale.

Il **capitolo 5** investiga un metodo alternativo di formazione dei legami crociati dell'idrogel, che si avvale dell'uso di un agente per l'addizione di Michael. Acido ialuronico, un polisaccaride naturale presente in molti tessuti dell'organismo e conosciuto per le sue favorevoli proprietà fisiche e biologiche, è stato chimicamente modificato con gruppi tiolici ed usato in combinazione con un polimero a triblocchi molto simile a quello descritto precedentemente, modificato con gruppi acrilici o metacrilici. I gruppi tiolici sono in grado di reagire con quelli acrilici o metacrilici in condizioni fisiologiche senza bisogno di catalizzatori (tossici) o di stimoli esterni (es. luce UV) a formare ponti crociati. L'inovativa combinazione di questi due polimeri presenta due vantaggi principali: migliorata biocompatibilità, dovuta alla presenza di un polimero naturale e le simultanee gelificazioni fisica e chimica, che assicurano la prima un'immediata stabilizzazione dell'idrogel a temperatura corporea e la seconda la stabilizzazione a lungo termine, con maggiore resistenza alla degradazione idrolitica

Le cinetiche di formazione dei legami crociati covalenti, il comportamento alla degradazione a pH fisiologico e la capacità di rilasciare peptidi in maniera controllata, sono stati investigati.

Il **capitolo 6** studia l'applicazione dell'idrogel termosensibile e fotopolimerizzabile per l'ingegneria della cartilagine, utilizzando una tecnologia emergente chiamata "bioprinting". Il bioprinting è una tecnica di preparazione di strutture tridimensionali basata sulla deposizione strato su strato di fibre di idrogel caricato con cellule. Tale tecnica si avvale dell'uso di un computer che guida la deposizione delle fibre da una siringa pneumatica al fine di mimare la forma della cartilagine da rigenerare e la distribuzione naturale delle sue cellule. I materiali da poter essere utilizzati per il bioprinting devono rispondere a precisi requisiti, quali viscosità adeguata a poter essere estrusi ed al contempo capacità di mantenere la propria struttura tridimensionale in seguito alla deposizione, compatibilità cellulare e abilità di promuovere la differenziazione e la formazione del tessuto artificiale. La termosensitività del materiale utilizzato in questa tesi si dimostra particolarmente adatto al bioprinting, in quanto il semplice cambiamento di temperatura riesce a modulare la viscosità dell'idrogel, in modo tale da renderlo estrudibile a temperatura ambiente e da mantenere stabilità strutturale in seguito alla deposizione per innalzamento della temperatura a valori corporei. Successivamente, l'esposizione alla luce UV conferisce al costrutto stabilità alla degradazione a lungo termine. Il capitolo in discussione presenta l'analisi meccanica, reologica e la sopravvivenza di condrociti equini in strutture porose tridimensionali di idrogel termosensibile e fotopolimerizzato.

Infine, il **capitolo 7** tratta il tema della biocompatibilità dell'idrogel in topi Balc/c, in seguito a somministrazione sottocutanea. Come osservato con altri materiali sintetici bioriassorbibili, una reazione infiammatoria localizzata e di moderata entità, con presenza di macrofagi infiltranti, è stata analizzata e correlata alla progressiva degradazione dell'idrogel ed alla sua digestione da parte delle citate cellule infiammatorie. Associata all'infiltrazione di macrofagi, è stata osservata la formazione di microcapillari all'interno dell'idrogel, che ha prodotto un perfetto innesto del biomateriale nel tessuto in cui esso è impiantato. Complessivamente, l'idrogel oggetto di questa tesi risulta possedere una buona biocompatibilità in topi.

Concludendo, questa tesi descrive un innovativo idrogel termosensibile e fotopolimerizzabile, che ha dimostrato buona compatibilità con proteine, cellule e tessuti L'efficace applicazione di questo idrogel nei campi del rilascio controllato di farmaci biotecnologici e dell'ingegneria tissutale, proiettano questa tecnologia un passo in avanti verso la loro applicazione clinica.

List of Abbreviations

3DF	three dimensional fiber deposition
4EDMAB	4-*N*,*N*-dimethylaminobenzoate
α/βCD	α/β-cyclodextrin
δ	diffusional distance
ρ	polymer concentration [g/m^3]
AA	acrylic acid
ABCPA	4,4'-azobis(cyanopentanoic acid)
ADA	4,4'-azodibenzoic acid
ACN	acetonitril
AIBN	α,α'-azoisobutyronitrile
AUC	area under the curve
AZOB	azobenzene
bFGF	basic fibroblst growth factor
BDA	butane-1,4-diol diacrylate
BIS	*N*,*N*'-methylenebisacrylamide
BK	bradykinin
BMA	butyl methacrylate
BSA	bovine serum albumin
C	polymer concentration (wt%)
CD	circular dichroism
CDCl$_3$	deuterated chloroform
CLSM	confocal laser scanning microscopy
CP	cloud point
CQ	camphorquinone
CTA	chain transfer agent
D	diffusion coefficient
DA	degree of acrylation
D$_2$O	deuterated water
DCC	*N*,*N*-dicyclohexyl carbodiimide
DCM	dichloromethane
DCU	dicyclourea
Dex-HEMA	dextran-hydroxyethyl methacrylate
Dex-HEMA-DMAE	dex-HEMA-dimethylaminoethyl
d$_h$	hydrodynamic diameter
DM	degree of methacrylation
DMA	dynamic mechanical analysis
DMAEMA	*N*,*N*-dimethyl aminoethyl methacrylate

DMAP	dimethyl amino pyridine
DMEM	Dulbecco's modified eagle's medium
DMF	dimethylformamide
DMSO-d_6	deuterated dimethyl sulfoxide
DNA	deoxyribonucleic acid
DPTS	4-(dimethylamino)pyridinium-4-toluenesulfonate)
DS	degree of substitution
DSC	differential scanning calorimetry
DTP	dithiobis(propanoic dihydrazide)
DTT	dithiothreitol
E	elastic modulus
EDC	1-ethyl-3[3-(dimethylamino)propyl]carbodiimide
EPO	erythropoietin
FDA	Food and Drug Administration
FGF-2	basic fibroblast growth factor 2
FITC	fluorescein isothiocyanate
FRAP	Fluorescence Recovery After Photobleaching
FTIR	fourier transform infrared spectroscopy
G′	storage modulus
G′$_\infty$	storage plateau modulus
G″	loss modulus
GI	gastro-intestinal
GLP-1	incretin hormone glucagon-like peptide-1
GMHA	glycidyl methacrylate-hyaluronic acid
GPC	Gel Permeation Chromatography
GyrB	gyrase sub-unit B
HA	Hyaluronic acid
HA-ADH	adipic acid dihydrazide grafted hyaluronic acid
HA-MA	methacrylated hyaluronic acid
HAse SD	hyaluronidase from Streptococcus dysgalactiae
HA-SH	thiolated HA
hGH	human growth hormone
HMDI	hexamethylene diisocyanate
HPLC	High Performance Liquid Chromatography
HPMAm	*N*-(2-hydroxypropyl)methacrylamide
HPMAm-lac$_{(1\ or\ 2)}$	HPMAm esterified with (mono or di)lactoyl lactate
IDA	iminodiacetic acid
IGF-I	insulin-like growth factor I

IgG   immunoglobulin G

IleOEt   L-isoleucine ethyl ester

i.m.   intramuscular

IPN   interpenetrating network

ITS-X   insulin-transferrin-selenium mixture

i.v.   intravenous

k   release kinetics constant

kDa   kilo Dalton

LCST   Lower Critical Solution Temperature

LeuOEt   D,L-leucine ethyl ester

MA   methacrylic anhydride

MAA   methacrylic acid

M_c molecular weight between cross-links

ML/DL   ratio $HPMAm\text{-}lac_1$/$HPMAm\text{-}lac_2$

MMP   matrix metalloprotein

M_n number average molecular weight

MPEG   mono methoxy PEG

M_t/M_∞ fractional release

MSC   mesenchymal stem cell

M_w weight average molecular weight

$M_x(P_y)$ p(HPMAM-lac)-PEG-p(HPMAm-lac) triblock copolymer, having DM

                          (%) of x (and PEG M_w (kDa) of y)

n   diffusional exponent

NASI   *N*-acryloxysuccinimide

NIH   National Institute of Health

NIPAAm   *N*-isopropylacrylamide

NMR   nuclear magnetic resonance spectroscopy

NR   Nile red

OSM   carboxylic acid terminated sulfamethazine oligomers

PA   poly(L/DL alanine)

p(AA)   poly(acrylic acid)

p(AAm)   poly(acrylic amide)

PAE   poly(β-aminoester)

PAU   poly(amino urethane)

PBS   phosphate buffered saline

PCL   poly(ε-caprolactone)

PCLA   poly(ε-caprolactone-*co*-lactic acid)

PDGF-BB   platelet-derived growth factor-1

PDI   polydispersity

PDLA	poly(D-lactic acid)
PEA	poly(ethylene adipate)
PEG	poly(ethylene glycol)
PEGDA	poly(ethylene glycol) diacrylate
PEG-VS	poly(ethylene glycol) vinyl sulfone
PEO	poly(ethylene oxide)
PES	poly(ethylene succinate)
PHA	poly(hexamethylene adipate)
PHB	poly((R)-3-hydroxybutyratel)
P(HEMA)	poly(2-hydroxyethyl methacrylate)
p(HPMAm)	poly(*N*-(2-hydroxypropyl)methacrylamide)
p(HPMAm-lac$_{(1 \text{ or } 2)}$)	poly(HPMAm esterified with (mono or di)lactoyl lactate)
PL	poly(d-lysine)
PLA	poly(lactic acid)
PLHMGA	poly(lactic-*co*-hydroxymethyl glycolic acid)
PLLA	poly(L-lactic acid)
PLGA	poly(lactic-*co*-glycolic acid)
PLX	poly(propylene glycol)-poly(ethylene glycol)-poly(propylene glycol)
p(MAA)	poly(methacrylic acid)
PMPC	poly(2-methacryloyloxyethyl phosphorylcholine)
pNIPAAm	poly(*N*-isopropylacrylamide)
pNHPt(m)a	(meth)acrylated poly(NIPAAm/HPMAm-lac$_2$-PEG-poly(NIPAAm/HPMAm-lac$_2$)
p(NVP-PBA)	poly(*N*-vinyl-2-pyrrolidone-*co*-phenylboronic acid)
PPF	poly(propylene fumarate)
PPG	poly(propylene glycol)
PPODA	poly(propylene glycol) diacrylate
PVA	poly(vinyl alcohol)
PVE	poly(vinyl ether)
PVL	poly(δ-valerolactone)
PVP	poly(*N*-vinyl pirrolidone)
QT	pentaerythritol tetrakis 3'-mercaptopropionate
R	molar gas constant
RAFT	reversible addition fragmentation chain tranfer
rhIL-2	recombinant human interleukin 2
RI	refractive index
s.c.	subcutaneous
SDF-1	stromal cell-derived factor-1

SLS	static light scattering
SR	swelling ratio
STZ	streptozotocin
t	time
T	absolute temperature
TA	pentaerythritol triacrylate
Tan (δ)	tangent delta
TDA	triple detector array
TEA	triethanolamine
TFAA	trifluoroacetic acid
TGF-β1/2	transforming growth factor β1/2
THF	tetrahydrofuran
TMDP	4,4-trimethylene dipiperidine
UPLC	ultra performance liquid chromatography
UCST	Upper Critical Solution Temperature
UV	ultra violet
ValOEt	L-valine ethyl ester
VEGF	vascular endothelial growth factor
vis	visible
W_0	weight of the gel at time 0
W_t	weight of the gel at time t
wt%	weight percentage

Curiculum Vitae

Roberta Censi was born in Fermo, Italy, on April 7th, 1980. She attended the secondary school Liceo Scientifico T. C. Onesti in Fermo, where she was awarded as best student of 1995/'96 and obtained her graduation in 1999. In the same year she started her study in Industrial Pharmacy at the University of Camerino, Italy. During the course of her academic studies, she did interniships at the Community Pharmacy of P. S. Giorgio, Italy and at the Division of Drug Delivery of the University of Camerino, where she worked for one year on a master thesis project, aimed at the physico-chemical characterization of complexes between aryl propionic acid derivatives and poly(vinylpyrrolidone) K30, under the supervision of Prof. Piera Di Martino. In 2005 she graduated cum laude from the University of Camerino and became a licensed pharmacist in the following year. In 2006, she was employed as a formulation scientist at the University of Camerino, carrying out a project on polymorphic forms of anti-inflammatory drugs, before starting, in February 2007, her PhD on a joint project between the Department of Pharmaceutics of Utrecht University, The Netherlands and the Department of Chemical Sciences of the University of Camerino. This thesis describes the major findings of her PhD studies on novel thermosensitive hydrogels for protein delivery and tissue engineering, performed under the supervision of Prof. dr. ir. Wim E. Hennink, Prof. dr. Piera Di Martino, Dr. ir. Tina Vermonden and Dr. Cornelus F. van Nostrum. During her PhD studentship, she was lecturer in "Delivery and Targeting of Biotechnological Drugs" (40 hours course) at the faculty of Pharmaceutical Biotechnology of the University of Camerino, attended several educational courses, participated in international conferences and received an award for the best research idea for business (University of Camerino) and a grant for industrial valorization of thermosensitive hydrogels, funded by IMPAT (an italian consortium between ENEA (Italian national agency for novel technologies, energy and sustainable economic development), Tecnopolis and University of Ferrara).

At present, Roberta is working as a postdoctoral researcher on the project funded by IMPAT, assessing the feasibility of the industrial exploitation of thermosensitive hydrogels.

List of Publications

From this thesis

Censi R, Vermonden T, van Steenbergen MJ, Deschout H, Braeckmans K, De Smedt SC, van Nostrum CF, di Martino P & Hennink WE (2009), Photopolymerized thermosensitive hydrogels for tailorable diffusion-controlled protein delivery. *Journal of Controlled Release* 140(3):230-236

Censi R, Vermonden T, Deschout H, Braeckmans K, Di Martino P, De Smedt SC, Van Nostrum CF & Hennink WE (2010), Photopolymerized thermosensitive poly(HPMAlactate)-PEG-based hydrogels: Effect of network design on mechanical properties, degradation, and release behavior. *Biomacromolecules* 11(8):2143-2151

Censi R, Fieten PJ, Di Martino P, Hennink WE & Vermonden T (2010), In situ forming hydrogels by tandem thermal gelling and Michael addition reaction between thermosensitive triblock copolymers and thiolated hyaluronan. *Macromolecules* 43(13):5771-5778

Censi R*,* Schuurman W*,* Malda J*,* di Dato G*,* Burgisser PE*,* Dhert WJA*,* van Nostrum CF*,* Di Martino P*,* Vermonden T & Hennink WE, Printable Photopolymerizable Thermosensitive p(HPMA-lactate)-PEG Hydrogel as Scaffold for Tissue Engineering. *Submitted for publication*

Censi R, van Putten S, Vermonden T, Di Martino P*,* van Nostrum CF*,* Harmsen MC, Bank RA & Hennink WE, *In Vivo* Biocompatibility and Biodegradability of Photopolymerized PEG-p(HPMAm-lactate)-based Hydrogels. *In Preparation*

Vermonden T, **Censi R** & Hennink WE, Hydrogels for protein delivery.
 Chemical Reviews, In Preparation

Other Publications

Di Martino P, **Censi R**, Barthélémy C, Gobetto R, Joiris E, Masic A, Odou P & Martelli S (2007), Characterization and compaction behaviour of nimesulide crystal forms. *International Journal of Pharmaceutics* 342(1-2):137-144

Di Martino P, **Censi R**, Malaj L, Capsoni D, Massarotti V & Martelli S (2007), Influence of solvent and crystallization method on the crystal habit of metronidazole. *Crystal Research and Technology* 42(8):800-806

Di Martino P, Malaj L, **Censi R** & Martelli S (2008), Physico-chemical and technological properties of sodium naproxen granules prepared in a high-shear mixer-granulator. *Journal of Pharmaceutical Sciences* 97(12):5263-5273

Gashi Z, **Censi R**, Malaj L, Gobetto R, Mozzicafreddo M, Angeletti M, Masic A & Di Martino P (2009), Differences in the interaction between aryl propionic acid derivatives and poly(vinylpyrrolidone) K30: A multi-methodological approach. *Journal of Pharmaceutical Sciences* 98(11):4216-4228

Hoti E, **Censi R**, Ricciutelli M, Malaj L, Barboni L, Martelli S, Valleri M & Di Martino P (2008), Validation of an HPLC-MS method for rociverine tablet dissolution analysis. *Journal of Pharmaceutical and Biomedical Analysis* 47(2):422-428

Joiris E, Martino PD, Malaj L, **Censi R**, Barthélémy C & Odou P (2008), Influence of crystal hydration on the mechanical properties of sodium naproxen. *European Journal of Pharmaceutics and Biopharmaceutics* 70(1):345-356

Malaj L, **Censi R** & Di Martino P (2009), Mechanisms for Dehydration of Three Sodium Naproxen Hydrates. *Crystal Growth and Design* 9(5):2128-2136

Malaj L, **Censi R**, Gashi Z & Di Martino P (2010), Compression behaviour of anhydrous and hydrate forms of sodium naproxen. *International Journal of Pharmaceutics* 390(2):142-149

Malaj L, **Censi R**, Mozzicafreddo M, Pellegrino L, Angeletti M, Gobetto R & Di Martino P (2010), Influence of relative humidity on the interaction between different aryl propionic acid derivatives and poly(vinylpyrrolydone) K30: Evaluation of the effect on drug bioavailability. *International Journal of Pharmaceutics* 398(1-2):61-72

Martino PD, **Censi R**, Malaj L, Martelli S, Joiris E & Barthélémy C (2007), Influence of metronidazole particle properties on granules prepared in a high-shear mixer-granulator. *Drug Development and Industrial Pharmacy* 33(2):121-131

Martino PD, Malaj L, **Censi R**, Martelli S, Joiris E & Barthélémy C (2007), The role of several L-HPCs in preventing tablet capping during direct compression of metronidazole. *Drug Development and Industrial Pharmacy* 33(12):1308-1317

Vermonden T, Jena SS, Barriet D, **Censi R**, Van Der Gucht J, Hennink WE & Siegel RA (2010), Macromolecular diffusion in self-assembling biodegradable thermosensitive hydrogels. *Macromolecules* 43(2):782-789

Malaj L, **Censi R**, Pellegrino L ,Gobetto R & Di Martino P, Characterization of nicergoline polymorphs crystallyzed in several organic solvents. *Submitted for publication*

Pescosolido L, Vermonden T, Malda J, **Censi R**, Dhert WJA, Alhaique F, Hennink W E, Matricardi P, In situ forming IPN Hydrogels of Calcium Alginate and Dextran-HEMA for Biomedical Applications. *Submitted for publication*

Selected abstracts

<u>Oral Presentations</u>

Censi R, Vermonden T, van Nostrum CF, Di Martino P & Hennink WE, Thermosensitive Hydrogels for Protein Delivery. 17^ Conference of the Dutch Society for Biomaterials and Tissue Engineering. Noordwijkerhout, November 2008

Censi R, Vermonden T, Di Martino P, Hennink WE, Thermosensitive triblock copolymer hydrogels for controlled protein release. Spring Meeting of the Belgian-Dutch Biopharmaceutical Society. Leuven, May 2008

Censi R, Vermonden T, van Nostrum CF, Di Martino P, Hennink WE, Photopolymerizable Thermosensitive Hydrogels for Protein Delivery. Dutch Polymer Days (DPD), Lunteren, February 2009

Censi R, Fieten PJ, Di Martino P, Hennink WE, Vermonden T, Tandem thermal gelling and Michael addition cross-linking as a tool for the preparation of injectable hydrogels, Xth Dutch Polymer Days (DPD),Veldhoven, February 2010.

Censi R, Di Martini P, Vermonden T, Hennink WE, In Situ Forming Hydrogels for Protein Delivery and Tissue Engineering, ADELBIOTECH: Advanced drug delivery of Biotechnological drugs, Camerino,   June 2010

<u>**Poster presentations**</u>

Censi R, Vermonden T, Di Martino P, Hennink WE, Thermosensitive triblock copolymer hydrogels for the controlled release of lysozyme*,* 10^ European Symposium on Controlled Drug Delivery. Noordwijk, April 2008

Censi R, Vermonden T, Di Martino P, Hennink WE, Synthesis, Characterization and Protein Release Behavior of Thermosensitive Triblock Copolymer Hydrogels, 6th World Meeting on Pharmaceutics Biopharmaceutics and Pharmaceutical Technology. Barcelona, April 2008

Censi R, Vermonden T, van Steenbergen MJ, Deschout H, Braeckmans K, De Smedt SC, van Nostrum CF, Di Martino P, Hennink WE, Photopolymerized thermosensitive hydrogels for tailorable diffusion-controlled protein delivery, 36th Annual Meeting and Exposition of the Controlled Release Society. Copenhagen, July 2009

Censi R, Fieten PJ, Di Martino P, Hennink WE, Vermonden T, In situ forming hydrogels by simultaneous thermal gelling and Michael Addition reaction between methacrylate bearing thermosensitive triblock copolymers and thiolated hyaluronan, 11^ European Symposium on Controlled Drug Delivery, Egmond aan Zee, April 2010

Censi R, Fieten PJ, Di Martino P, Hennink WE, Vermonden T,   Simultaneous thermal gelling and Michael addition cross-linking for the preparation of injectable hydrogels, 37th Annual Meeting and Exposition of the Controlled Release Society. Portland, July 2010

Award and grant

- First prize *"Research Ideas for Business"*, Camerino 2009

- Italian national grant *"IMPAT: PROGETTO IMPRESA 2010"*, Project; *"Gennex DS: Next Generation Delivery Systems - Improving therapeutic responses"*

Acknowledgements

A hundred times every day I remind myself that my inner and outer life depend on the labours of other men, living and dead, and that I must exert myself in order to give in the same measure as I have received.

A. Einstein

This thesis has not been a lonesome journey. Along the way a number of remarkable people have given me enormous support and contribution to overcome the obstacles that this challenging but fascinating run was hiding at every turn. I owe my gratitude to all those people who have walked with me and because of whom my PhD experience has been one that I will cherish forever.

First and foremost, I would like to thank my research supervisors, who guided me through a process of progressive learning and intellectual maturing, shared their knowledge with me, supported and believed in me in all my undertakings. My deepest gratitude goes to Prof. Wim E. Hennink. Dear Wim, thanks for your tireless, decisive and energetic support in all the stages of my PhD. Our work-discussions, your pragmatic advice and constructive criticism cleared the path towards thesis completion. Your dedication and passion for science, along with care for your graduate students, have been and will always be a source of inspiration for further development of my career. Thanks also for your "continuous delivery of the right dose of pressure", which enabled me to do my utmost to the thesis and for your exceptional sense of humor, which helped me overcoming my shyness.

During my PhD, another extraordinary scientist, Dr Tina Vermonden, perfectly complemented the supervision of Prof. Wim E. Hennink. Dear Tina, thanks for keeping your door always open to me. Thanks for your patience, honesty, trust, insightful advice and capacity to combine critique with immediate empathy and commitment. Thanks also for being the early reader of all my draft manuscripts – your comments helped tremendously to shape this work.

I am grateful to Prof. Piera Di Martino, whose guidance and encouragement helped me, always, even from far away. My dearest Piera, you initiated me into research, at the time of my undergraduate thesis, and gave me the confidence I needed to start doing research seriously. Thanks for providing me tutelage and for giving me a chance when I had none, for always showing full approval and unceasing appreciation for my work and for allowing me to grow as a scientist with freedom of choice.

This thesis is a small tribute to these three irreplaceable people from a young scientist still anxious to learn from them.

I wish to thank also my co-promotor Dr. Cornelus van Nostrum, whose interest in my project and ideas during work-discussions contributed to give a sense of direction to my PhD.

I cannot forget Jeroen, Peter, Francesca S. and Giorgio, whom I guided during my PhD and to whom I dedicate my hearty acknowledgements for their work and cheerful moments in the lab. *A Francesca va un grazie dal profondo del cuore, anche per la bella amicizia che ci lega...mi mancano molto le nostre chiacchierate sulle "croccantelle" del giorno, che spero poter tornare a fare presto!*

A special mention goes to Mies van Steenbergen, a fine technician always willing to provide technical support, who taught me that in research problems do not exist…they are just challenges.

Thank you, Barbara and Lidija, for your kind assistance in all the paperwork and administrative issues.

This thesis grew out of a number of collaborations with other research groups and I would like to gratefully acknowledge their valuable contribution to this work. I am indebted to Hendrik Deschout, Dr Kevin Braeckmans and and Prof. Stefaan De Smedt from the Laboratory of General Biochemistry and Physical Chemistry of Gent University for their help with FRAP experiments; Wouter Schuurman, Petra Burgissen, Dr Jos Malda and Prof. Wouter Dhert from the Department of Orthopaedics of University Medical Center Utrecht for the tissue engineering studies and Sander van Putten, Dr Marco Harmsen and Prof. Ruud Bank from the Department of Pathology and Medical Biology of University Medical Center Groningen for their comments and experiments on in vivo biocompatibility studies.

The sense of my PhD goes beyond mere research. Life blessed me with the opportunity to meet incomparable friends, whose warm support enabled me to complete this thesis and have a wonderful time along the way.

My immense gratitude to Emmy and Hajar for being my "paraninfen", for their good listening, kind hearts, generosity, emotional support, all the meaningful moments, laughers and fun we had together. You definitely became friends for life and wherever we will end up in the future, you will always be with me, in my heart. Dear Emmy, talking to someone has never been so easy and enjoyable as with you, thanks for sharing with me all the ups and downs of these years, for your cheery cards, calls and texts and the unforgettable "cappuccino

moments" in the lab. Hajar, I have the feeling I have always known you – in a short time you became one of those people I can certainly count on forever. Thanks for all the dinners and holiday together, the surprise party and our chats…I truly hope these are only some of the many common experiences to come.

Another special person to me has been Lise, who started as a colleague and became one of my closest friends. Dear Lise, your friendship immensely contributed to animate my PhD years. Your presence made the lab a very pleasant and stimulating environment, where the work routine was turned into fun. We have been very supportive to each other and thinking of all the memories we share – shopping at Albert Heijn by Twingo, body shaping lessons, dinners, holidays in France and Italy… - will always bring a smile to my face! In many of these memories, Nicolas was also present and I would like to express to him my sincere gratitude for his nice company.

My special thanks to all the helpful colleagues at the Department of Pharmaceutics who opened their doors and hearts to me and to only some of whom it is possible to give particular mention here. Back in time I remember, with great pleasure, Sophie, Marion, Sabrina, Najim, Niels, Manuela, Aldo, Chiara, Frank, Evelyn… and the present colleagues Marina, Rolf, Amir G, Amir V, Neda, Afrouz, Sima, Maryam, Negar, Cristianne, Alex, Naushad, Maria, Sylvia, Filis, Luis, Albert, Isil, Roy, Pieter, Agnes, Audrey…

A heart-felt thank you goes to Kimberley and Helena for their friendship. I had very pleasant moments and talks with you girls, both in the lab and outside work. I am so very happy you both were back to the Went building!

I miei anni in Olanda non sarebbero stati gli stessi se la vita non mi avesse fatto incontrare Francesca P., Laura, Eleonora ed Elena. L'amicizia e la complicità che sono sorte immediatamente con ognuna di voi, facilitate dalla condivisione di un'esperienza comune in un altro paese, sono certamente cresciute al di là di ciò e sono diventate per me un bene irrinunciabile, che spero coltiveremo negli anni. Grazie per aver fatto parte delle mie gioie, frustrazioni, risate, coffee-breaks, il cui tema di discussione principale era quanto disgustoso fosse il caffè...lo stesso caffè che sono sicura mi mancherà per tutti i momenti insieme che pur ci ha regalato.

Devo molta della serenità con la quale ho affrontato questa parte della mia vita agli amici di sempre che ho lasciato in Italia e che, malgrado la frequentazione sporadica, mi hanno sempre fatto sentire come se nulla fosse mai cambiato. Silvia, Giulio e Sofia, voi siete l'essenza della vera amicizia, grazie per non averci mai mollato in questi anni, per la vostra generosità di sentimenti e per gli innumerevoli tasselli di vita che condividiamo e che sono

certa continueranno a rendere sempre più prezioso e colorato il mosaico della nostra esistenza. Grazie anche a Roberta e Michele per l'affetto che sempre ci dimostrano...ad altri amici di vecchia data: Elena, Emilie, Silvia D., Ledijan, Ela...e a quelli acquisiti più di recente: Monia, Ernestina, Roberto, Alessandro, Tiziana, Massi, Laura...

To **all** my friends, a big **thanks** for understanding that I could not always be there for them and that I needed time away from everyone, especially during the last phase of my PhD, to complete this work.

Quest'ultima parte dei ringraziamenti è dedicata a chi, più di chiunque altro, mi ha sostenuto con amore nel percorso del dottorato e della vita in genere.

Alla mia meravigliosa ed allargata famiglia, cui devo tutto ciò che sono oggi, voglio dedicare questo mio lavoro per il loro incessante incoraggiamento e sostegno, nonostante la sofferenza nell'avermi lontano. Ringrazio mamma e papà, i miei zii ed i miei nonni, incluso chi non è più tra noi, ma sicuramente mi guarda da lassù. Grazie per aver da sempre creato intorno a me un ambiente unico - il solo che mi faccia sentire a casa - e per avermi trasmesso l'importanza dell' onestà, dell'umiltà e dell'impegno nella vita. Proprio questi valori, che cerco costantemente negli altri, hanno determinato, sopra ogni altra cosa, il successo delle piccole conquiste di questi anni. Grazie per la vostra fiducia e stima nei miei confronti, che spero solo di riuscire a ripagare. Grazie a mia sorella Daniela ed alla mia cugina-praticamente-sorella Federica, per la loro contagiosa gioia di vivere, capace di rendere briosa ed esuberante anche la più grigia delle vite...ed a Marco, per il quale nutro moltissimo affetto, come se facesse da sempre parte della nostra famiglia – le nostre lunghe chiacchierate in edicola sulla vita mi mancano spesso, quando sono lontana!

Sono stata baciata dalla vita quando ho incontrato Romano, che non finirò mai di ringraziare per aver sempre camminato al mio fianco, stringendomi la mano – sempre, senza eccezioni. Anche a lui questa tesi è dedicata. Sei certamente la persona che ha dato significato e completezza a questi anni in Olanda, come pure al resto della mia vita. La lista delle cose per cui vorrei ringraziarti sarebbe interminabile e preferisco che i miei occhi ed il mio cuore ti parlino personalmente. Dunque, mi limito a dirti grazie per l'amore, l'empatia e la comprensione di questi anni, per avermi dimostrato che darsi fiducia l'un l'altra è un modo per crescere e costruire, per essere il perfetto punto di equlibrio tra le sfere personale e professionale della mia vita. Grazie per credere nei nostri sogni, malgrado tutto, e per avermi regalato così tanti momenti speciali, che hanno contribuito alla costruzione di una storia comune senza eguali, le cui pagine colorate ci portano ora verso nuovi capitoli. As long as I have you in my life, I have no worries.

I wish I could mention everyone, but I am sure there are people, contributing to this unforgettable experience, who will not find their names in these pages. For them I will throw a party, instead. Then, **I** want to celebrate **YOU all**, who led me towards the future hand-in-hand. This future is starting now and it feels as a new journey, that I will undertake confidently, with a luggage full of all the moments you have been given me throughout these years.

Thanks! Bedankt! Grazie!

Roberta